Quantification of molecular and isotopic alterations in biodegraded crude oils

vorgelegt von
Dipl.-Geol. Rouven Elias
aus Köln

von der Fakultät VI – Planen Bauen Umwelt
der Technischen Universität Berlin
zur Erlangung des akademischen Grades

Doktor der Naturwissenschaften
- Dr. rer. nat. -

genehmigte Dissertation

Promotionsausschuss:

Vorsitzender: Prof. Dr. G. Franz
Berichter: PD Dr. H. Wilkes
Berichter: Prof. Dr. B. Horsfield
Berichter: Prof. Dr. W. Dominik

Tag der wissenschaftlichen Aussprache: 18. Juli 2008

Berlin 2008
D 83

CONTENTS

ABSTRACT

The present study is part of the industry project **Mechanisms and Effects of Petroleum Biodegradation** between the GFZ Potsdam, Germany and Eni-Agip Milan, Italy. The study aims at contributing to a better understanding of microbially caused alterations of the hydrocarbon composition in petroleum reservoirs.

Microbial activity in the deep biosphere causes volumetrically important changes in the hydrocarbon composition of crude oils, which lead to a significant deterioration of the petroleum quality. Because crude oil quality mainly declines during the early stages of biodegradation, the study focuses on effects that occur within light to moderate alteration levels. A suite of 55 crude oils from five different petroleum systems is investigated to decipher the quantitatively most important compositional alterations that are due to in-reservoir biodegradation. For this purpose, all samples were measured by thermovaporisation gas-chromatography (GC-FID) to investigate the quantitatively most important crude oil constituents. Hereafter, samples were separated by Medium-Pressure-Liquid-Chromatography (MPLC) to obtain aliphatic, aromatic and polar fractions. The individual fractions were analysed by GC-FID, GC-MS and GC-MS-MS experiments. Additionally, the crude oil samples were characterised by compound-specific stable carbon and hydrogen isotopic compositions.

Based on a comprehensive geochemical characterisation, five biodegradation sequences are defined where the compositional variability within each subset is mainly due to microbial activity in the reservoir. The study illustrates that conventional molecular biodegradation parameters are not suitable to define the extent of biodegradation in a petroleum reservoir. To improve such an assessment, a new molecular biodegradation parameter is suggested that can be used to quantify depletions for individual crude oil constituents. The discussed approach also enables an improved assessment of the degree of biodegradation in a single

crude oil sample. It is shown that the quantitative abundance of individual crude oil constituents affects relative degradation rates in petroleum reservoirs. Using the example of the aromatic hydrocarbon fraction, it is discussed that specific conventional molecular parameters cannot be used for biodegraded crude oils because the compounds that define the parameters are affected by microbial activity. It is also elucidated how stable carbon isotopic compositions of crude oils can be used to quantify the depletion of specific petroleum substrates. Further it is demonstrated that the petroleum quality, as indicated by the API gravity, can be predicted directly from the molecular composition of crude oils. The obtained results give rise to the interpretation that microbial communities in individual reservoirs are different and therefore generate varying molecular degradation patterns.

ZUSAMMENFASSUNG

Die vorliegende Arbeit ist Teil des Industrie-Projektes **Mechanismen und Effekte des biologischen Erdölabbaus** zwischen dem GeoForschungsZentrum Potsdam und der Firma Eni-Agip Mailand, Italien. Ein wichtiges Ziel dieser Arbeit ist das bessere Verständnis von biologisch verursachten Veränderungen in der Erdölzusammensetzung.

Mikrobielle Aktivität in der tiefen Biosphäre verursacht quantitativ wichtige Veränderungen in der Kohlenwasserstoff-Zusammensetzung von Erdölen, die zu einer signifikanten Verschlechterung der Erdölqualität führen. Im Wesentlichen verschlechtert sich die Erdölqualität während der frühen Stadien der mikrobiellen Aktivität. Daher konzentriert sich diese Arbeit auf die Effekte, die während der frühen bis mittleren Abbaustadien auftreten. Hierfür wurden zunächst bei insgesamt 55 Erdölen, die von fünf verschieden Erdölsystemen stammen, mittels der Thermovaporisations-Gaschromatographie (GC-FID) die quantitativ wichtigsten Erdölbestandteile untersucht. Anschließend wurden mit Hilfe der Mittel-Druck-Flüssigkeits-Chromatographie (engl.: MPLC) alle Ölproben in aliphatische, aromatische und polare Fraktionen aufgetrennt. Die Bestandteile dieser Fraktionen wurden mit gaschromatographischen und/oder massenspektrometrischen Methoden (GC-FID, GC-MS und GC-MS-MS) quantifiziert. Zusätzlich wurden bei den Erdölproben die Komponenten-spezifischen Kohlenstoff- und Wasserstoff- Isotopen-Signaturen untersucht.

Basierend auf einer umfangreichen geochemischen Charakterisierung der Erdöle wurden fünf Abbau-Sequenzen bestimmt, bei denen die kompositionellen Unterschiede im Wesentlichen auf mikrobielle Aktivitäten in der Erdöllagerstätte zurückzuführen sind. Anhand dieser Probensätze wird illustriert, dass konventionelle molekulare Parameter nicht geeignet sind um das Ausmaß des biologischen Abbaus in einem Erdölreservoir zu bestimmen. Für eine verbesserte Beurteilung wird in dieser Arbeit ein neuer molekularer Parameter vorgeschlagen, der die durch mikrobielle Prozesse verursachten Abreicherungen quantifiziert. Der

diskutierte Quantifizierungsansatz ermöglicht ebenso eine verbesserte Beurteilung des Ausmaßes der molekularen Veränderungen in einer Ölprobe. Die vorliegende Arbeit zeigt auch, dass die relativen Abbauraten einzelner Erdölbestandteile im Wesentlichen von der jeweiligen Substratmenge in der Lagerstätte abhängen. Am Beispiel der aromatischen Kohlenwasserstoffe wird gezeigt, dass einzelne konventionelle molekulare Parameter nicht genutzt werden sollten, da die Komponenten auf denen diese Parameter basieren durch die mikrobielle Aktivität abgereichert werden. Des Weiteren wird gezeigt, wie die Signaturen der stabilen Kohlenstoffisotope genutzt werden können, um das Ausmaß des biologischen Abbaus von einzelnen Erdölbestandteilen zu quantifizieren. Anhand der API-Dichte wird demonstriert, dass die Erdölqualität von der molekularen Zusammensetzung abgeleitet werden kann. Die Ergebnisse dieser Arbeit geben Anlass zur Interpretation, dass in verschiedenen Erdöllagerstätten unterschiedliche mikrobielle Gemeinschaften verschiedene molekulare Abbaumuster verursachen.

LIST OF FIGURES (in the Text)

LIST OF FIGURES (in the Appendix)

LIST OF TABLES (in the Text)

LIST OF TABLES (in the Appendix)

LIST OF PUBLICATIONS AND PRESENTATIONS

JOURNALS

ELIAS, R., VIETH, A., RIVA, A., HORSFIELD, B.; WILKES, H. (2007): Improved assessment of biodegradation extent and prediction of petroleum quality. - *Organic Geochemistry, 38, 2111-2130.*.

CONFERENCE PAPER

ELIAS, R., MÜLLER, A., VIETH, A., RIVA, A., WILKES, H. (2005): Compositional alteration of crude oils from different petroleum systems during initial biodegradation. *22nd International Meeting on Organic Geochemistry, Seville/Spain, 12–16/09/05.*

VIETH, A., ELIAS, R., KÜHNER, S., RABUS, R., WILKES, H. (2006): Using carbon and hydrogen isotopic compositions of hydrocarbons to decipher biodegradation effects in petroleum reservoirs. *EGU General Assembly, Vienna/Austria, 02-07/04/06.*

ELIAS, R., VIETH, A., RIVA, A., HORSFIELD, B.; WILKES, H. (2006): Improved assessment of biodegradation extent and prediction of petroleum quality for crude oils from the Gullfaks area, offshore Norway. *10th Norwegian Meeting on Organic Geochemistry, Bergen/Norway, 07-08/09/06.*

WILKES, H., VIETH, A., ELIAS, R., KÜHNER, S., RABUS, R. (2006): Carbon and hydrogen isotope fractionation during biodegradation: From laboratory studies to petroleum reservoirs. *10th Norwegian Meeting on Organic Geochemistry, Bergen/Norway, 07-08/09/06.*

VIETH, A., ELIAS, R., WILKES, H. (2006): Carbon and hydrogen isotope fractionation of light hydrocarbons in crude oils to characterize in-reservoir alteration processes. *29. Annual Convention of the German Association for Stable Isotope Research (GASIR), Freiberg/Germany, 04-06/10/06.*

WILKES, H., VIETH, A., ELIAS, R., KÜHNER, S., RABUS, R. (2006): Carbon and Hydrogen Isotope Fractionation during Biodegradation: from Laboratory Studies to Petroleum Reservoirs. *10th Latin American Association of Organic Geochemistry Conference, Salvador/Brazil, 05-09/11/06.*

ELIAS, R., VIETH, A., RIVA, A., HORSFIELD, B.; WILKES, H. (2006): Improved assessment of biodegradation extent and prediction of petroleum quality for crude oils from the South Atlantic margin. *10th Latin American Association of Organic Geochemistry Conference, Salvador/Brazil, 05-09/11/06.*

ORAL PRESENTATIONS (*internal*)

ELIAS, R., VIETH, A., WILKES, H. (2005): Compositional alteration of initially biodegraded crude oils from various petroleum systems. *Group Seminar Talk GFZ/Pb 4.3, Potsdam, 18/05/05.*

ELIAS, R., VIETH, A., WILKES, H. (2005): Geochemical characterisation and compositional alterations in initially biodegraded crude oils. *Talk at 1st IPP Meeting Potsdam, 31/08/06.*

ELIAS, R., VIETH, A., WILKES, H. (2005): Assessment of biodegradation in initially altered crude oils and it`s correlation to the API gravity. *Talk at 1st IPP Meeting Potsdam, 31/08/06.*

ELIAS, R., VIETH, A., WILKES, H. (2005): Impact of microbial activity in the „Deep Biosphere" on composition and quality of crude oils in petroleum reservoirs. *Talk at PhD-Day at GFZ, Potsdam, 20/12/06.*

ELIAS, R. (2006): Petroleum Biodegradation in Reservoirs. *Talk at a Meeting of the Scientific Advisory Council of GFZ, Potsdam, 31/03/06.*

ELIAS, R., VIETH, A., RIVA, A., HORSFIELD, B. WILKES, H. (2006): Improved Assessment of Biodegradation Extent and Prediction of Petroleum Quality. *Talk at the 2nd IPP Meeting in Milan/Italy, 19/09/06.*

ELIAS, R., VIETH, A., WILKES, H. (2006): Compound-specific carbon and hydrogen isotope ratios in biodegraded crude oils from West Africa. *Talk at the 2nd IPP Meeting in Milan/Italy, 19/09/06.*

ELIAS, R., VIETH, A., RIVA, A., HORSFIELD, B.; WILKES, H. (2006): Improved assessment of biodegradation extent for crude oils from diverse petroleum systems. *Industry Meeting at GFZ, Potsdam, 31/11/06.*

INTERNAL REPORTS for the Project Partner *(not published)*

1st Activity Report (Oct 2004)
2nd Activity Report (Oct 2005)
3rd Activity Report (Oct 2006)

1st Annual Report (Apr 2005)
2nd Annual Report (Apr 2006)
3rd & Final Report (August 2007)

ACKNOWLEDGEMENTS

I am grateful to Dr. Heinz Wilkes who supervised this study and who is thanked for his helping support, many discussions and his patience in explaining me a part of the world of chemistry. Many thanks to Dr. Andrea Vieth for several discussions and her very helpful suggestions on various drafts for reports, presentations and publications. Thoughtful reviews and critical comments by Prof. Dr. Brian Horsfield supported the success of this study. This work has benefited from discussions with and help of many colleagues within the Organic Geochemistry Section at GFZ Potsdam. The entire team at GFZ provided an excellent working environment. Thanks to all of you!

Many thanks to my Italian colleagues at Eni-Agip in Milan for the pleasant co-operation. The possibility to present the results of this study at conferences and to publish parts of the work is gratefully acknowledged. Many thanks to Dr. Angelo Riva who always supported the study by several discussions and his patience in collecting background data.

Special thanks to Bent Barman Skaare for critical discussions on petroleum biodegradation and for rebooting my motivation for academia by exploring several breweries.

Infinite thanks to my wife Mamke who supported me throughout the whole PhD thesis by finding many different ways how to keep me going on.

1 INTRODUCTION

1.1 FORMATION OF PETROLEUM

Petroleum is ultimately derived from the degradation products of prehistoric organic matter, which was primarily buried in the ancient mud of swamps, lakes and oceans. Over geological times, layers of inorganic particles and organic debris are buried to greater depths during progressive subsidence and are compacted to sedimentary rocks. If the organic matter content is high these accumulations are potential source rocks for petroleum which is formed when high temperature promotes the thermal transformation of bio- and geomacromolecules to liquid oil and/or gas. Following TISSOT AND WELTE (1984) this transformation process of organic matter to petroleum can be divided into the three stages of maturation, termed diagenesis, catagenesis and metagenesis. A generalized scheme of petroleum generation is shown in Figure 1.

The diagenesis comprises the biological, physical and chemical alterations of the organic matter nearest the surface and in the subsiding sediment succession up to a few hundred or even thousands of meters. The dominant form of organic matter from which petroleum is derived are the microscopic, photosynthetic organisms known as phytoplankton that live at or near the surface of lakes and oceans. In addition to phytoplankton the residues of zooplankton and terrestrial organic matter (higher plants) can also contribute to the pool of hydrocarbons which are capable to be transferred to petroleum (PETERS ET AL., 2005). During diagenesis organic matter in the form of biomacromolecules is preserved and/or condensed to geopolymers: In the classical theory of geopolymer formation, kerogen was believed to derive from organic substances, where biopolymers like proteins, cellulose and lipids, are converted into biomonomers such as amino acids, sugars and fatty acids (TISSOT AND WELTE, 1984). Nowadays, it is thought that kerogen

is formed by a combination of geopolymer formation and the selective preservation of resistant biopolymers. It is believed that highly aliphatic, insoluble and non-hydrolysable biomacromolecules (e.g., algaenan, cutan and lignin) that resist microbial decomposition significantly contribute to kerogen. In contrast, amino acids, low molecular weight peptides and carbohydrates are water-soluble and can be directly assimilated by microorganisms during diagenesis. However, also less or insoluble organic molecules, like proteins, polysaccharides, lipids and lignin can be hydrolysed by extracellular enzymes of fungi and bacteria into water-soluble compounds, and hence, can also be recycled. As a result, the initial biological input is strongly decomposed in the upper layers of the sediment (KILLOPS AND KILLOPS, 2005).

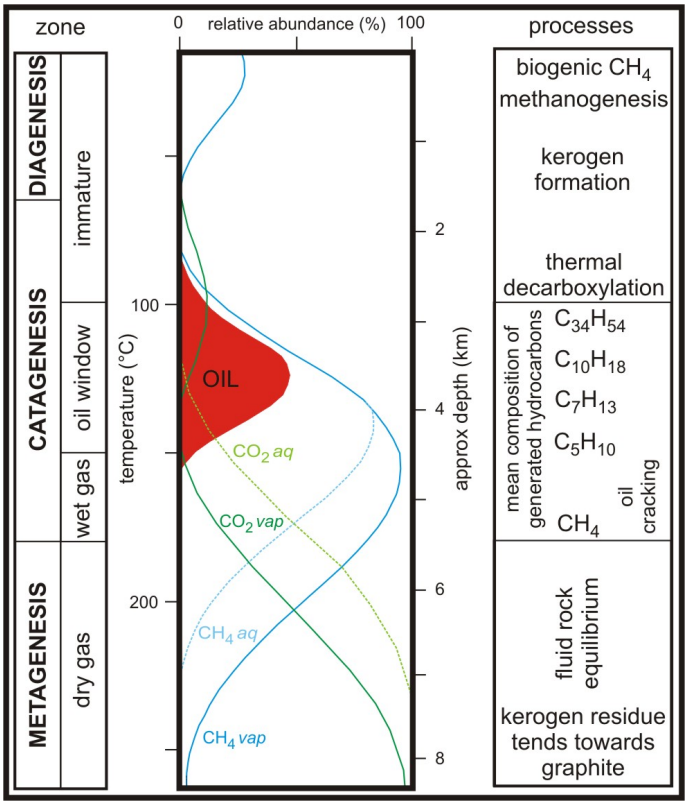

Fig. 1: Generalized scheme of hydrocaron generation. The Figure illustrates relative abundances of hydrocarbons, which are generated from sapropelic sources with incraesing temperature. Methane (CH_4) and carbon dioxide (CO_2) distributions are shown for separate vapor and aquaeous phases in equilibrium with crustal rocks. The diagenesis-catagenesis boundary is variable and can be placed between ~50°C and the onset of oil generation at ~100°C. An average surface temperature of 15°C and a geothermal gradient of 30°C/km have been assumed (modified from KILLOPS AND KILLOPS, 2005).

During diagenesis the organic derivates become progressively engaged in new polycondensed structures. Irreversible condensation reactions, e.g., between sugars and amino acids, lead to the formation of brown polymeric humic substances called melanoidins. The extent of condensation increases during diagenesis yielding to geomolecules which are incorporated in the sediment. At the end of diagenesis the polycondensed organic residue is called kerogen, which likely contains a mixture of preserved refractory biopolymers and geopolymers (KILLOPS AND KILLOPS, 2005). During diagenesis the sediment is progressively compacted which goes along with a drastic reduction of the water content.

The following zone of catagenesis is dominated by the thermal alteration of kerogen. With proceeding subsidence temperatures increase until the thermal energy is sufficient to crack hydrocarbons from the kerogen structure and previously generated asphaltenes and waxes. With increasing thermal maturity the size of the generated hydrocarbon structures decreases (KILLOPS AND KILLOPS, 2005). Therefore, the catagenesis is divided into the zone of liquid oil generation (oil window) and the wet gas zone. Within the main phase of liquid petroleum generation, which occurs mainly between 100-150°C, predominantly hydrocarbons with low and intermediate molecular weights are generated. Here, predominantly C-C and C-O bonds are cracked and biomarker hydrocarbons which were previously bound within or at the kerogen structure are progressively diluted by thermally generated hydrocarbons (TISSOT AND WELTE, 1984). The first liquid hydrocarbons expelled are characterised by relative high molecular weights (~ $C_{34}H_{54}$), but with increasing maturity more and more hydrocarbons with lower molecular weights are generated. Petroleum is generated because the kerogen structure attempts to attain thermodynamic equilibrium as temperature and pressure increase during burial (KILLOPS AND KILLOPS, 2005). The main modification of the inorganic fraction of the sediment during catagenesis is compaction as water is progressively expelled while the porosity and permeability are further reduced (PETERS ET AL., 2005).

The generation of gas occurs throughout the entire burial of the organic matter. First, methane is generated due to microbial degradation processes near the sediment surface. In greater depths methane and other hydrocarbon gases are produced by the thermal fragmentation of the kerogen (KILLOPS AND KILLOPS, 2005). During the late phase of catagenesis the cleavage of C-C bounds becomes progressively important and between 150-180°C a mixture of C_1-C_5 gases is produced, designated as the "wet gas" zone. The relative amount of generated methane increases with ongoing maturation of the kerogen until only this "dry gas" is generated during the metagenesis (TISSOT AND WELTE, 1984). The whole zone of gas generation is sometimes called the cracking zone, because previously generated hydrocarbons are also thermally cracked into smaller gaseous products (KILLOPS AND KILLOPS, 2005).

Time and temperature are thus mainly responsible for transforming organic matter derived from decaying organisms to petroleum and gas. The original chemistry of the organic matter, the environment of deposition, and the temperature history imposed on the organic matter control the type of crude oil or gas formed. The chemistry of the oil and gas can be used to reconstruct the source of the original organic matter and temperature of hydrocarbon generation, because individual derivates of the original biopolymers are preserved as biomarkers or are transformed to geopolymers in response to thermal exposure during the hydrocarbon generation process. However, the bio- and geomarker signatures of petroleum are also preserved during the transport of the petroleum into the reservoirs. This process is divided into primary and secondary migration with the primary being designated as the expulsion of the petroleum from the source into the carrier rock. The secondary migration describes the process of transport within the carrier rock to the petroleum reservoir. This migration is a relatively fast process compared to the time necessary for formation or even storage in the trap. As soon as the hydrocarbons enter a petroleum reservoir secondary alteration processes such as biological activity may affect the composition of crude oil (TISSOT AND WELTE, 1984, KILLOPS AND KILLOPS, 2005, PETERS ET AL., 2005).

1.2 COMPOSITION OF PETROLEUM

Most abundant elements in unaltered crude oils are carbon (~ 80 - 87 %), hydrogen (~ 12 - 15 %), sulphur (~ 0,1 - 5 %), oxygen (0,1 - 4,5 %) and nitrogen (0,1 - 1,5 %). Much of the nitrogen, sulphur and oxygen is associated with the resins and asphaltenes and therefore these compounds are often termed the NSO-compounds. Other elements in crude oils include various metals, in particular nickel and vanadium, which are generally present only in trace amounts. The composition of crude oils is often described by four major compound classes termed as saturated hydrocarbons, aromatic hydrocarbons, resins and asphaltenes (SARA). The average crude oil contains 57% saturated hydrocarbons, 29% aromatic hydrocarbons and 14% resins and asphaltenes (KILLOPS AND KILLOPS, 2005). However, this average composition can vary significantly due to, e.g., the origin of organic matter, the thermal history and secondary alterations.

Saturated hydrocarbons, which are also known as aliphatic hydrocarbons, comprise various compounds such as acyclic, cyclic and branched alkanes. Quantitative important saturated hydrocarbons in unaltered crude oils are represented by the acyclic normal alkanes (*n*-alkanes, $C_nH_{(n+2)}$). Among the aromatic hydrocarbons alkylbenzenes are generally most abundant (KILLOPS AND KILLOPS, 2005). However, also alkylnaphthalenes and alkylphenanthrenes are quantitatively important aromatic crude oil constituents. In addition, petroleum contains various preserved lipid components, which are termed biomarkers. Such biomarkers can often be unambiguously linked with biological precursor compounds, because their basic skeletons are preserved throughout diagenesis and much of catagenesis. Many biomarkers originally have oxygen-containing functional groups and undergo a defunctionalisation process. Important biomarker compounds can be found among the saturated and the aromatic hydrocarbon fractions, such as the saturated steranes and hopanes and the aromatic steroids. However, biomarkers generally represent less than 1% by weight of unaltered crude oils (KILLOPS AND KILLOPS, 2005).

Following TISSOT & WELTE (1984), crude oils can be classified according to the relative amounts of acyclic alkanes (paraffins), cyclic alkanes (naphthenes) and summed aromatic and NSO compounds. This classification can be illustrated by a ternary plot (Fig. 2), and is used to distinguish between marine and terrestrially sourced oils. The main classes of crude oils resulting from this classification are (I) paraffinic oils that mainly contain acyclic alkanes with less than 1% sulphur, (II) paraffinic-naphthenic oils that are characterised by acyclic and cyclic alkanes with less than 1% sulphur, and (III) aromatic-intermediate oils which contain more than 50% aromatic hydrocarbons and more than 1% sulphur (TISSOT AND WELTE, 1984; KILLOPS & KILLOPS, 2005).

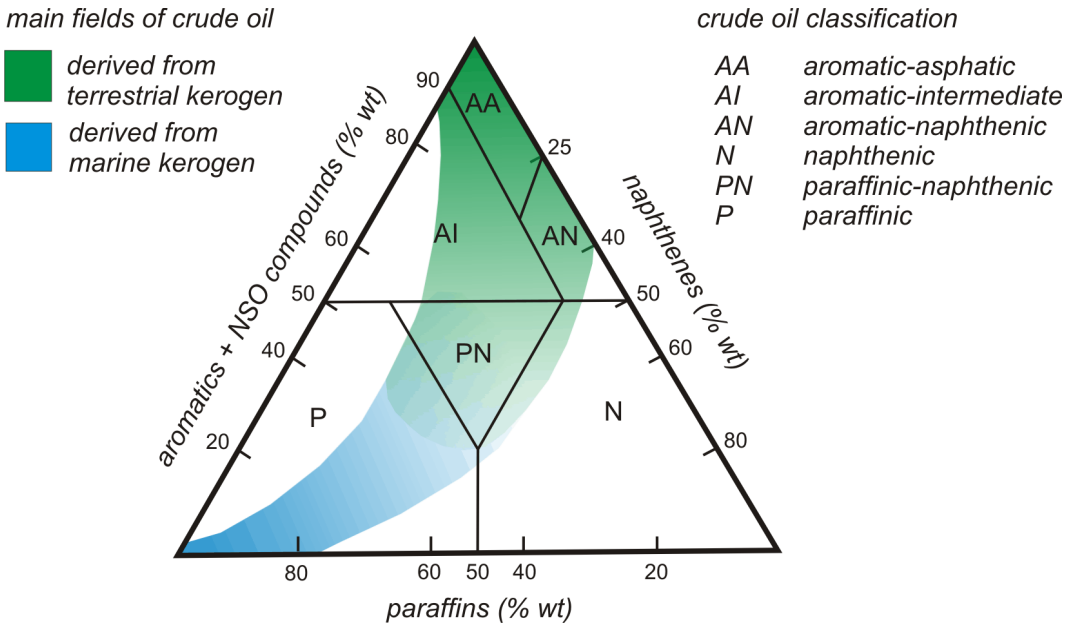

Fig. 2: Classification of crude oils based on distribution of paraffins, naphthenes and aromatic plus NSO compounds (after TISSOT & WELTE, 1984).

However, the petroleum composition can significantly be altered by post-generation processes, such as migration, de-asphalting, water-washing, thermal alteration, thermochemical sulphate reduction, gas diffusion, evaporative fractionation, tertiary migration and biodegradation (KILLOPS AND KILLOPS, 2005). In the following paragraph well-known effects of biodegradation on the petroleum composition are summarised.

1.3 BIODEGRADATION OF PETROLEUM

Biodegradation of petroleum is defined as the alteration of crude oil by living organisms (e.g. MILNER ET AL., 1977; CONNAN, 1984; PALMER, 1993; BLANC AND CONNAN, 1994). Biological degradation of crude oil in reservoirs is already known since the 1930`s when BASTIN ET AL. (1926) isolated sulphate-reducing bacteria from oil field waters. Although this publication as well as studies by e.g. NOVELLI AND ZOBELL (1944), ROSENFELD (1947) and DAVIS AND YARBROUGH (1965) clearly documented that anaerobic bacteria are capable of oxidising hydrocarbons, most studies published within the last 30 years focussed on biodegradation processes occurring under aerobic conditions (BAILEY ET AL., 1973; GOODWIN ET AL., 1981). However, it has been shown by numerous recent studies (e.g. AECKERSBERG ET AL., 1991; ZENGLER ET AL., 1999; WIDDEL AND RABUS, 2001; WILKES ET AL., 2000 AND 2002) that a great variety of different strains of anaerobic microorganisms is capable of utilizing crude oils as growth substrates. Such organisms use specific hydrocarbons as energy and / or carbon sources for their metabolic processes and to build up biomass. Petroleum biodegradation is assumed to be a hydrocarbon oxidation process (PETERS ET AL., 2005), which leads to the formation of carbon dioxide (CO_2) and partially oxidised residues, such as organic acids. Generally it is supposed (WENGER ET AL., 2001; PETERS ET AL., 2005) that individual crude oil constituents are degradable to different extents leading to a relative enrichment of the more recalcitrant species with proceeding biodegradation. The alteration of the crude oil composition caused by biological activity predominantly occurs within the reservoir and is accompanied by a decrease in the net volume of petroleum and a significant deterioration of the crude oil quality.

Biodegraded petroleum systems are often located in foreland basins which can be up to thousands of kilometres long and hundreds of kilometres wide. When organic-rich sediments with hydrocarbon source potential are present in the basin sediments, these troughs develop large elongated hydrocarbon source kitchens,

which may produce vast volumes of oil. The oil migrates laterally up the slope strata from the source rocks for up to several hundred kilometres to structural and stratigraphic traps at the margins of the basin. Viable petroleum traps occur throughout the foreland basins, and light oils may be trapped along the migration pathway, in reservoirs which are found deeper in the basin. At the flanks of such basins, reservoir sediments, which are typically represented by sandstones, lay on the older basement rocks and produce petroleum reservoirs that are shallow, cool and locally may have active meteoric water circulation (BARSON ET AL., 2001), conditions ideal for biological activity. An idealized foreland basin is shown in Figure 3 summarizing relevant geological processes, which lead to the generation, migration and accumulation of petroleum, which in turn can be biodegraded, if trapped in shallow reservoirs.

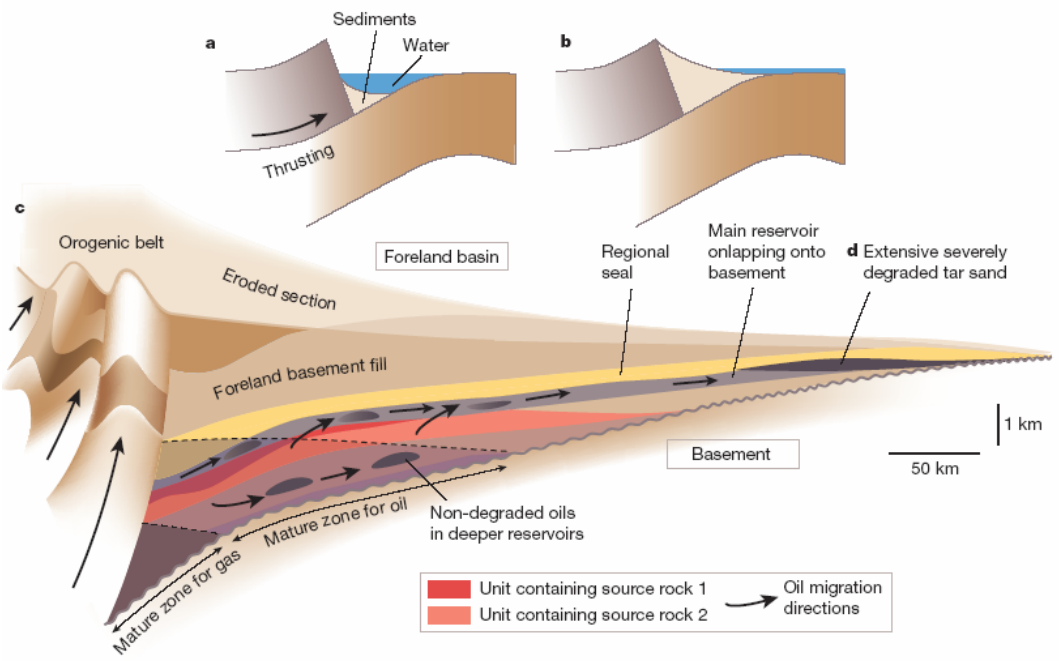

Fig. 3: An idealized foreland basin petroleum system with source rocks, reservoir sandstone and seal. a, b, The foreland basin is formed during the period of active deformation and the source rocks are buried. c, Oil migrates to the shallow cool basin flanks over distances of several hundred kilometres, where the oil is biodegraded. (Figure adopted from HEAD ET AL., 2003)

The occurrence of biodegraded oil in the subsurface is bound to specific geological and geochemical conditions that enable and enhance microbial life. A crucial prerequisite for the existence of microorganisms in the geosphere is ready

access to abundant water supplies. Microbes are thought to live in the so-called water leg located beneath the oil column and utilize the hydrocarbons of the petroleum within the water phase or near the oil-water contact in the reservoir (LARTER ET AL., 2006). According to HUANG ET AL. (2004) the diffusion of hydrocarbons from the oil column to the oil-water contact zone may control and limit degradation processes. Another requirement for microbial activity in the deep biosphere is a sufficient porosity and permeability in the rock fabric which enables the diffusion of nutrients and sufficient bacterial motility (PETERS ET AL, 2005). Empirical observations dictate that petroleum biodegradation can occur up to reservoir temperatures of ~80°C. Assuming typical geothermal gradients (25-30°C/km), such temperatures are reached in ~2-3 km depth below the sediment surface. HEAD ET AL. (2003) have also mentioned that the salinity of the formation water should not exceed 100-150 parts per thousand. Oils in petroleum reservoirs with higher salinity are typically non-biodegraded (PETERS ET AL., 2005). The schematic mechanisms within a biodegrading petroleum reservoir are summarized in Figure 4.

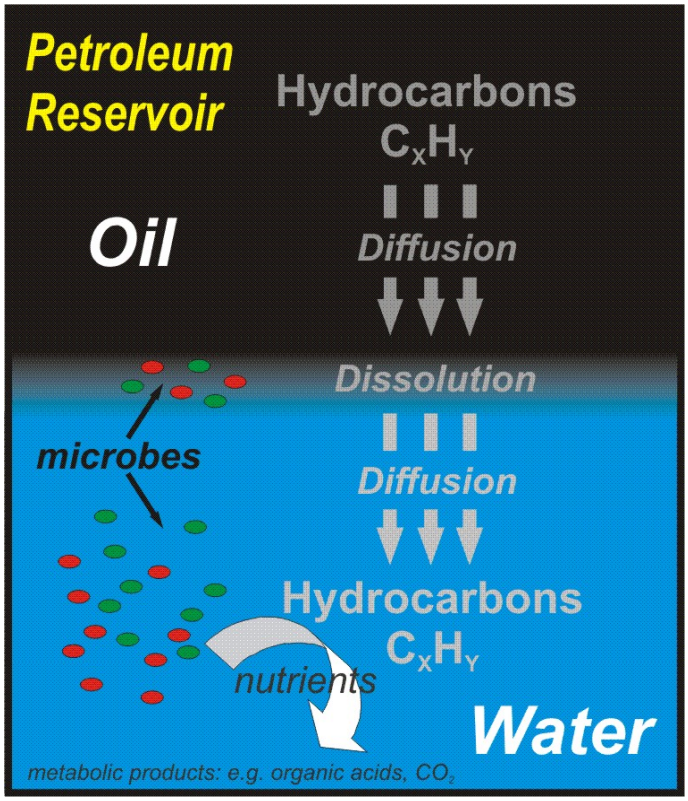

Fig. 4: Schematic mechanisms of biodegradation within a petroleum reservoir. Hydrocarbons are utilized by microorganisms as energy suppliers (electron donors) for their metabolic processes. Nutrients, such as molecular oxygen, nitrates, sulphates or ferric iron are required as electron acceptors for microbial activity. Biodegradation is a process where hydrocarbons are transformed to metabolites, such as organic acids and/or CO_2.

Under suitable conditions of temperature and salinity viable microorganisms can degrade large volumes of oil in relatively short times, especially when compared with geologic and geochemical processes (CONNAN, 1984; PALMER, 1993, BLANC AND CONNAN, 1994). It was estimated by HEAD ET AL. (2003) and LARTER ET AL. (2003) that hydrocarbon degradation at the base of the oil column can attain up to 10^{-4} kg m^{-2} y^{-1} for petroleum reservoirs at 40-70°C. However, the exact rates of petroleum biodegradation are not well known and likely depend on e.g., the degradation mechanisms such as aerobic or anaerobic biodegradation with the latter being significantly slower (PETERS ET AL., 2005).

During the last 20 years it has been shown by several studies that biodegradation in petroleum reservoirs is likely always anaerobic (e.g., AITKEN ET AL., 2004 and references therein). Even conservative mass balances which were calculated for the volumes of water that are required to transport sufficient oxygen to the oil in a reservoir are unrealistically large (HORSTAD ET AL., 1992). It appears also rather unlikely that, where meteoric water may have penetrated a basin, oxygenated waters could reach the deep reservoirs, because oxygen in the meteoric water is likely to be completely removed by reactive organic matter and pyrite in shallow sediments. Further, some biodegraded oils have been shown to contain metabolic markers for anaerobic petroleum degradation, such as specific reduced naphthoic acids, indicating that anaerobic metabolism is the likely mechanism by which biodegraded petroleum accumulations are formed in the deep subsurface (HEAD ET AL., 2003, 2006; AITKEN ET AL., 2004). It was discussed by MAGOT ET AL. (2000) that diverse anaerobic microorganisms commonly occur in oilfields. They concluded from laboratory and field studies that anaerobes are responsible for most subsurface hydrocarbon degradation processes. In recent years, several anaerobic degradation pathways for specific hydrocarbons have been proposed (e.g., AECKERSBERG ET AL., 1991; ANNWEILER ET AL., 2000, 2001; FRITSCHE AND HOFRICHTER, 2000; WIDDEL AND RABUS, 2001, WILKES ET AL, 2002). Among these, it was also demonstrated that *n*-alkanes can be degraded under strictly anaerobic conditions (WILKES ET AL., 2002). Most of the suggested degradation pathways assume that sufficient amounts of electron acceptors such as sulphate,

nitrate or ferric iron are present in the biodegrading system. However, it was also proposed that methanogenesis (ZENGLER ET AL., 1999) is capable of oxidising hydrocarbons, which only react with water to methane and carbon dioxide. The methanogenic degradation of hydrocarbons could explain why biodegraded petroleum reservoirs do not always contain significant amounts of carbon dioxide. It also implies that anaerobic biodegradation of hydrocarbons is even possible in deep buried sedimentary systems, which likely contain no molecular oxygen for aerobic processes, and, which are often depleted in nutrients. These results, together with the geological time frame in which biodegradation can proceed makes it likely that rather anaerobic than aerobic hydrocarbon degradation is common in most petroleum reservoirs (AITKEN ET AL., 2004).

Biodegradation of petroleum alters the molecular composition of crude oils because specific constituents are consumed while others are not degraded to the same extent or even are produced, such as organic acids, carbon dioxide or methane. It is assumed that biodegradation leads to a selective removal of specific types of crude oil constituents as it proceeds (PETERS AND MOLDOWAN, 1993; WENGER ET AL., 2001), with saturated hydrocarbons being degraded first. Typically, it is accepted that the selective removal of *n*-alkanes indicates the onset of petroleum biodegradation in crude oils, and that normal alkanes degrade at faster rates than mono- or polymethylated alkanes (PETERS ET AL., 2005). Light aromatic hydrocarbons, such as benzene and toluene are the first of the aromatic compounds which are depleted either by biodegradation and/or water washing. Considering the compositional changes, various classification systems describing different degradation stages have been proposed. The most commonly applied scheme was suggested by PETERS AND MOLDOWAN (1993). This model (PM scale) proposes a systematic and sequential removal of individual compound classes with proceeding biodegradation. The authors suggest that biodegradation should be ranked on a scale from 1-10, with rank 1 indicating a slight extent of biodegradation while rank 10 denotes to severe effects on the composition of crude oils. A modified biodegradation scheme that is based on the PM scale, was

published by WENGER ET AL. (2001) and modified by HEAD ET AL. (2003), and is shown in Figure 5.

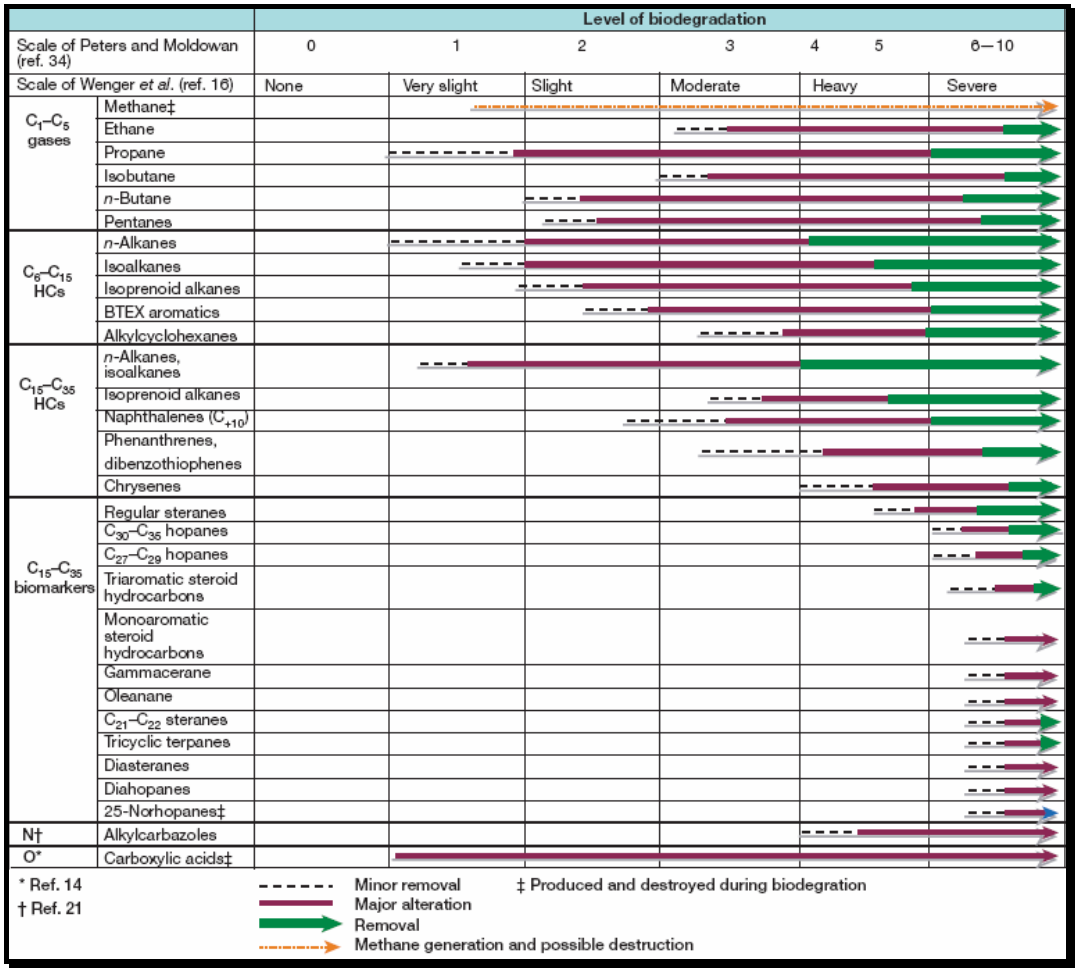

Fig. 5: Schematic diagram showing the chemical changes occurring during crude oil and natural gas biodegradation as suggested by Wenger et al. (2001) and republished by Head et al. (2003).

Both models (PETERS AND MOLDOWAN, 1993; WENGER ET AL., 2001) propose a sequential degradation of individual crude oil constituents with proceeding extents of biodegradation. The latter scheme describes a sequential removal of compound groups as follows: *n*-alkanes > *i*-alkanes > alkylbenzenes > alkylnaphthalenes > alkylcyclohexanes, alkylphenanthrenes and alkyldibenzothiophenes > isoprenoids (C_{15+}) > regular steranes > hopanes > aromatic steranes. Both schemes are based on a qualitative assessment of biodegradation and describe a quasi-stepwise alteration process which is thought to be ubiquitous. PETERS ET AL. (2005) elucidated that these biodegradation scales are based mostly on empirical field

observations. The authors also noted that the scale must be used with caution, because numerous exceptions are known. It was put up for discussion that different degradation patterns may reflect different in-reservoir conditions and specific microbial communities.

Due to the microbial degradation of specific oil constituents major changes in the bulk chemical and physical properties of petroleum occur. Some of the most important alterations occurring with proceeding biodegradation are shown in Figure 6.

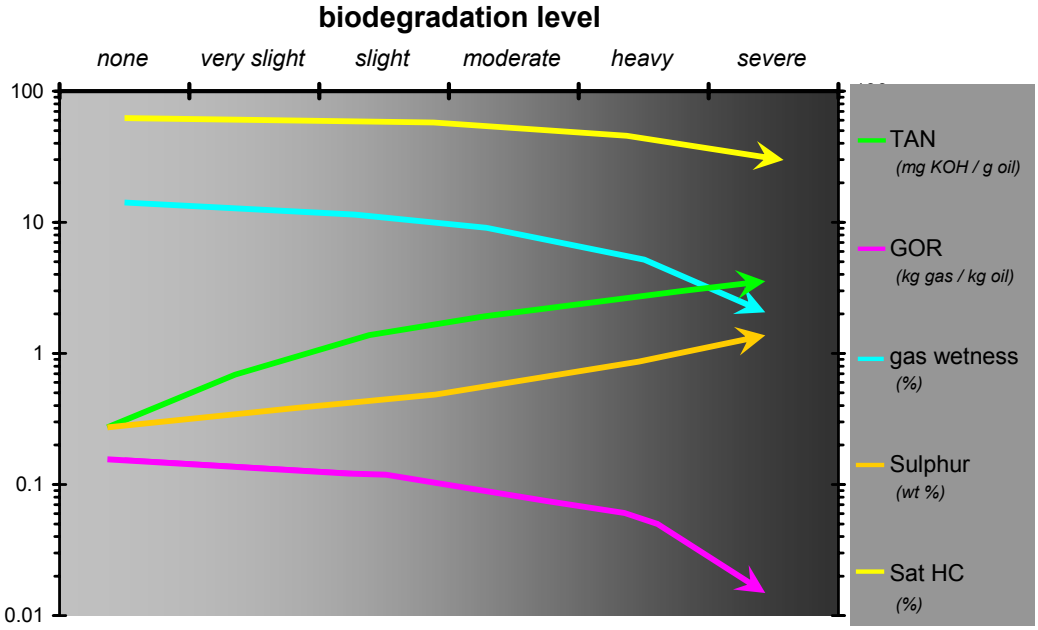

Fig. 6: Biodegradation leads to the change of various important crude oil properties, such as the API gravity, acidity (TAN – total acid number) and sulphur content. Other parameters shown are the gas / oil ratio (GOR), the gas wetness defined as % = ($\sum C_2$-C_5)*100/($\sum C_1$-C_5); and the content of saturated hydrocarbons (Sat HC). Data are adopted from HEAD ET AL. (2003).

Based on data published by HEAD ET AL. (2003) Figure 6 displays on a logarithmic scale that the acidity (TAN) and sulphur content in crude oils increase during biodegradation, and that the gas : oil ratio (GOR), the amount of saturated hydrocarbons (Sat HC) and gas wetness are clearly reduced. Biodegradation leads to a preferential degradation of hydrocarbons *sensu stricto* and therefore the residual oil becomes relatively enriched in nitrogen, sulphur and oxygen (NSO) bearing compounds as represented by polar and asphaltene fractions. Moreover,

microbial alterations induce an increase of the oil viscosity, and a relative enrichment of metal contents (e.g. Ni and V) in the residue. As a consequence of these compositional changes the environmentally relevant properties of biodegraded crude oils are adversely affected, where increased sulphur and metal contents could result in the formation of iron sulphide coatings in production and refining pipelines, which could also be corroded by the increased acidities. Interestingly, the compositional effects of biodegradation are in turn used to remediate oil contaminated sites, where microbes are technically employed to degrade hydrocarbons. However, a very important indicator for the oil recovery is the API gravity, which is significantly reduced with proceeding biodegradation making the oils pastier (Figure 7). The API gravity, established by the American Petroleum Institute, is a measure of how heavy or light a crude oil liquid is, as compared to water.

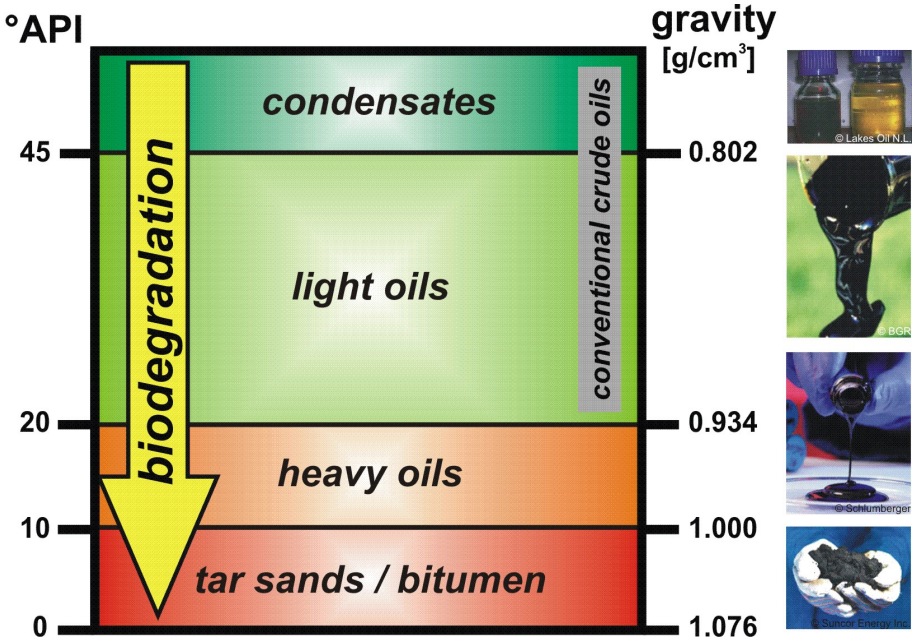

Fig. 7: Biodegradation leads to the deterioration of crude oil quality as indicated by the API gravity. The API gravity is based on the specific gravity at the given temperature of 60°F (15.6°C) calculated by the formula: °AP I= (141.5 / specific gravity at 60°F) - 131.5.

The world's largest single petroleum accumulations can be found in sandstones that are saturated with biodegraded oil. Figure 8 illustrates the volumetric importance of biodegraded crude oil in the worlds petroleum inventory by

comparison of the two largest single reservoirs for conventional and biodegraded crude oil, respectively. The biggest deposit of such biodegraded hydrocarbon reservoirs is located in the Orinoco Belt in eastern Venezuela with an estimated oil volume of more than 1.2 X 10^{12} barrels of oil. Another volumetrically important reservoir with comparable amounts (0.9 X 10^{12} barrels) of biodegraded hydrocarbons are the Athabasca tar sand deposits in western Canada. In contrast, the largest single accumulation of non-biodegraded petroleum, the supergiant oil field of Ghawar in Saudi Arabia contains only 1.9 X 10^{11} barrels of conventional light crude oil (HEAD ET AL., 2003).

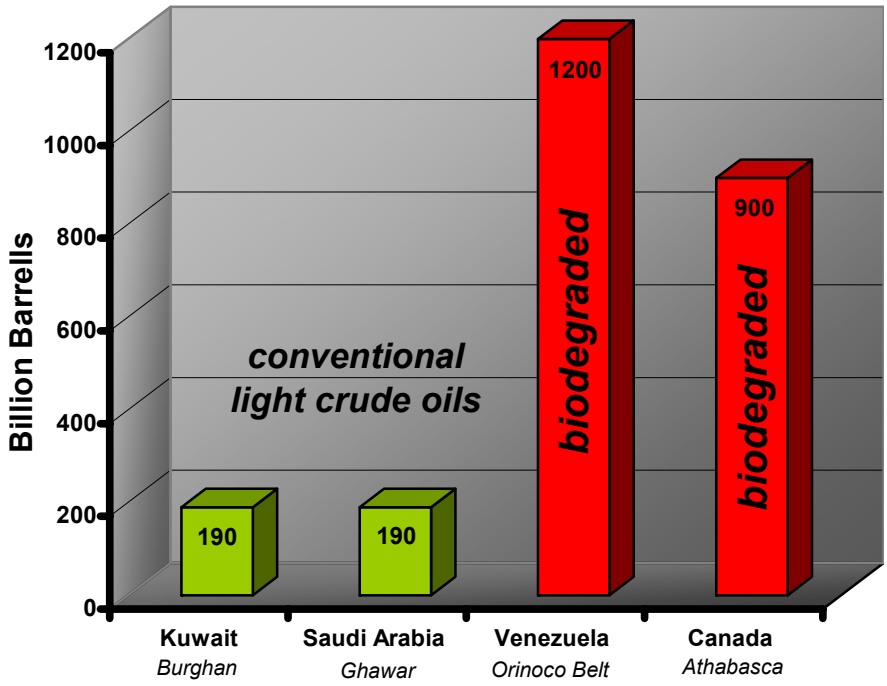

Fig. 8: Comparison of the largest single petroleum accumulations of conventional and biodegraded crude oils. Data adopted from HEAD ET AL. (2003) and PETERS ET AL. (2005).

Biodegraded petroleum accumulations are not limited to the two reservoirs in Venezuela and Canada, and are common in the subsurface throughout the world. The amount of biodegraded oil worldwide may exceed that of conventional oil (e.g. TISSOT AND WELTE, 1984, ROADIFER, 1987; HEAD ET AL., 2003) and therefore biologically altered hydrocarbon accumulations are of enormous economic importance for the petroleum industry.

2 Motivation, Goals and Approach

Microbial activity in the deep biosphere causes significant compositional changes in crude oils within petroleum reservoirs. These alterations induce a clear deterioration of petroleum quality and, hence, also negatively affect oil recovery and refining. Therefore, the ability to assess and predict the extent of biodegradation is of particular interest for the petroleum industry in order to evaluate future prospects and exploration developments.

The most common biodegradation models (PETERS AND MOLDOWAN, 1993; WENGER ET AL., 2001) applied to assess the extent of compositional changes focus on qualitative alterations occurring at heavy to severe biodegradation levels. Interestingly, the volumetrically most important crude oil constituents, which define petroleum quality (PETERS ET AL., 2005), are already more or less completely lost at such pronounced biodegradation levels. Until now it has not been studied in much detail how the depletion of volumetrically important crude oil constituents, such as normal and branched alkanes, leads to the observed deterioration of chemical and physical petroleum properties. Only little is known about the influence of initial biodegradation on the molecular composition of crude oil in petroleum reservoirs and its impact on the crude oil quality. Therefore, the current study concentrates on the effects of biodegradation on bulk oil composition and the related deterioration of petroleum quality occurring during the initial to moderate alteration levels.

With these considerations in mind, the study was designed to determine even slight differences in the abundance of the volumetrically important oil constituents, such as normal and branched alkanes. These oil constituents constitute ~35-50% of a non-biodegraded crude oil (PETERS ET AL., 2005) and therefore also may reflect the petroleum quality. Furthermore, it was decided that oil samples from different petroleum systems should be evaluated in order to

determine if relationships between the chemical composition and physical properties were always the same.

The central objective of this study is to better understand the influence of light to moderate biodegradation on the composition and quality of crude oil. The specific goals of the study, as agreed with the project partner ENI-AGIP, are listed below:

- Determination of biodegradation effects on oil quality prior to production
    - Detailed molecular characterization of biodegradation sequences
    - Definition of new molecular parameters to assess biodegradation effects
    - Correlation of molecular parameters with the crude oil quality
- Differentiation of biodegradation and water washing effects
- Quantification of biodegradation extent in crude oils

The approach used in this study is based on the assumption that compositional differences due to biodegradation can be assessed, if other factors which are also known to cause compositional variability in crude oils are not contributing to the chemical heterogeneity of crude oils. Therefore, the study starts with a detailed organic geochemical characterisation of all selected crude oils in order to assess geological factors like facies, depositional environment and thermal maturity. Having done so, compositional differences within each subset could be predominantly related to biodegradation. Hereafter, it is intended to assess and to quantify the microbially caused alterations in the different sequences and to define the impact of specific oil constituents on the crude oil quality. Furthermore, the study should discuss the effects of biodegradation on selected geochemical crude oil parameters, which are often applied in the literature in order to assess the geological frame. Finally, the discussion should evaluate the reliability and practicability of such widely applied parameters for light to moderately biodegraded crude oils.

3 SAMPLES AND GEOLOGICAL BACKGROUND

The investigated sample set comprises 55 crude oils (drill stem tests) from offshore and onshore hydrocarbon provinces in Angola, Norway, Canada, Egypt and Nigeria. Within each study area crude oils were sampled from different wells penetrating several oil fields (Table 1).

Table 1: Origins of crude oils investigated in this study with sample numbers used in the text and respective GFZ laboratory identifications (GFZ sample no.). Different letters and numbers assign individual oil fields and wells for samples from Angola and Nigeria. Due to confidentiality, sampling depth and reservoir formation can not be provided.

sample no.	GFZ sample no.	country	oil field	well	depth [m]	reservoir formation	°API
A1	G002029	Angola	A	1			19.8
A2	G002030	Angola	B	2			15.2
A3	G002031	Angola	B	2			17.6
A4	G002032	Angola	C	3			24.2
A5	G002033	Angola	C	3			34.8
A6	G002034	Angola	C	3			35.2
A7	G002035	Angola	D	4			32
A8	G002036	Angola	D	4			32.8
A9	G002037	Angola	A	5			19.2
A10	G002038	Angola	A	5			23.2
A11	G002039	Angola	E	6			36.1
A12	G002040	Angola	E	6			36.3
A13	G002041	Angola	A	7			19
A14	G002042	Angola	A	7			21.5
A15	G002043	Angola	A	7			24.6
A16	G002044	Angola	F	8			n.a.
A17	G002045	Angola	G	9			n.a.
G1	G000017	Norway	Gullfaks	34/10-3	1895-1900	Brent Group	28.8
G2	G000018	Norway	Gullfaks	34/10-8	1845-1848	Brent Group	28.6
G3	G000019	Norway	Gullfaks	34/10-9	1906-1910	Brent Group	31.1
G4	G000020	Norway	Gullfaks	34/10-14		Brent Group	28.9
G5	G000021	Norway	Gullfaks	34/10-A-1H		Brent Group	30.9
G6	G000022	Norway	Gullfaks	34/10-1	1839-1844	Brent Group / Etive-Fm.	28.6
G7	G000023	Norway	Gullfaks Sør	34/10-32R	3368-3374	Statfjord-Fm.	31.5
G8	G000024	Norway	Gullfaks Vest	34/10-34			31.7
G9	G001327	Norway	Rimfaks	34/10-17	2880-2890	Brent Group / Ness-Fm.	36.1
G10	G001328	Norway	Gullfaks Sør	34/10-30	3297-3318	Statfjord Fm.	31.7
G11	G001329	Norway	Gullfaks Gamma	34/10-35	4015-4025	Dunlin Group / Cook-Fm.	43.5
G12	G001374	Norway	Gullfaks	34/10-3	1936-1948	Brent Group	28.4
G13	G001385	Norway	Gullfaks	34/10-7	1835-1865	Dunlin Group / Cook-Fm.	37.2
C1	G001609	Canada	Tuktuk	221	943-950	Reindeer-Fm.	16
C2	G001610	Canada	Tuktuk	221	1368-1375	Reindeer-Fm.	23
C3	G001611	Canada	Tuktuk	221	1460-1465	Reindeer-Fm.	32
C4	G001612	Canada	Tuktuk	221	1470-1483	Reindeer-Fm.	38
C5	G001613	Canada	Tuktuk	212	1498-1508	Reindeer-Fm.	24
C6	G001614	Canada	Kumak	71	2148-2154	Reindeer-Fm.	n.a.
C7	G001615	Canada	Kumak	71	2306-2313	Reindeer-Fm.	n.a.
C8	G001616	Canada	Arnak	230	2924	Reindeer-Fm.	n.a.
C9	G001617	Canada	Arnak	230	3065	Reindeer-Fm.	n.a.
C10	G001618	Canada	Arnak	230	3209	Reindeer-Fm.	n.a.
C11	G001619	Canada	Mayogiak	27	1155-1182	Reindeer-Fm.	n.a.
C12	G001620	Canada	Mayogiak	27	2864-2921	Husky-Fm./Parsons-Fm.	n.a.
E1	G001865	Egypt	Sudr	26	569-629	Asl Upper Layer	22.3
E2	G001866	Egypt	Sudr	27	453-463	Ayun Mussa (Kareem-Fm.)	15.7
E3	G001867	Egypt	Sudr	30	680-706	Asl Medium Layer	22.4
E4	G001868	Egypt	Sudr	36	801-828	Nukhul Fm.	22.8
E5	G001869	Egypt	Sudr	34	834-846	Thebes Fm.	19.7
E6	G001871	Egypt	Issaran	1	300-378	South Gharib-Belayim eq.	16.1
E7	G001872	Egypt	Issaran	7	613-665	Nukhul Fm.	21.1
N1	G002351	Nigeria	X	1			35
N2	G002352	Nigeria	X	2			19
N3	G002353	Nigeria	X	2			40
N4	G002354	Nigeria	Y	3			30
N5	G002355	Nigeria	Y	4			28
N6	G002356	Nigeria	Y	4			35

3.1 ANGOLA

Angolan crude oils were drilled offshore of Cabinda, an exclave of Angola (Figure 9). The sampling area is part of the Lower Congo Basin, and hence, part of the Late Jurassic/ Early Cretaceous rifting zone which led to the continental break-up of Pangaea. These tectonic movements resulted in the separation of South America from Africa and the formation of the South Atlantic Ocean (PENDENTCHOUK ET AL., 2004). The Congo Basin was formed north of the Walvis ridge, a barrier which initially isolated this area from marine influence and thus led to continental sedimentation until the Lower Cretaceous (Aptian). This lacustrine-dominated sedimentation was succeeded by a marine facies. These accumulations are of enormous economic importance, both as reservoir strata and highly prolific hydrocarbon source rocks (COLE ET AL., 2000). A generalized stratigraphic column of the Lower Congo Basin is shown in Figure 10.

Fig. 9: Location of Angola in West Africa. Crude oils samples are derived from well sites in the Lower Congo Basin, which is located offshore Cabinda, an exclave of Angola.

Major tectonic phases associated with the evolution of the South Atlantic Ocean have been divided by BRICE ET AL. (1982) into four stages from oldest to youngest in prerift, synrift I, synrift II and postrift stages. Accumulations of the prerift stage

were deposited on a faulted metamorphic basement and comprise up to 1000 m thick sediments which consist primarily of sandy fluvial-lacustrine strata. Subsequently, during the synrift I stage, a range of graben and half-graben troughs evolved along the early rifted margins and formed the depocenters for organic-rich sediments (COLE ET AL., 2000).

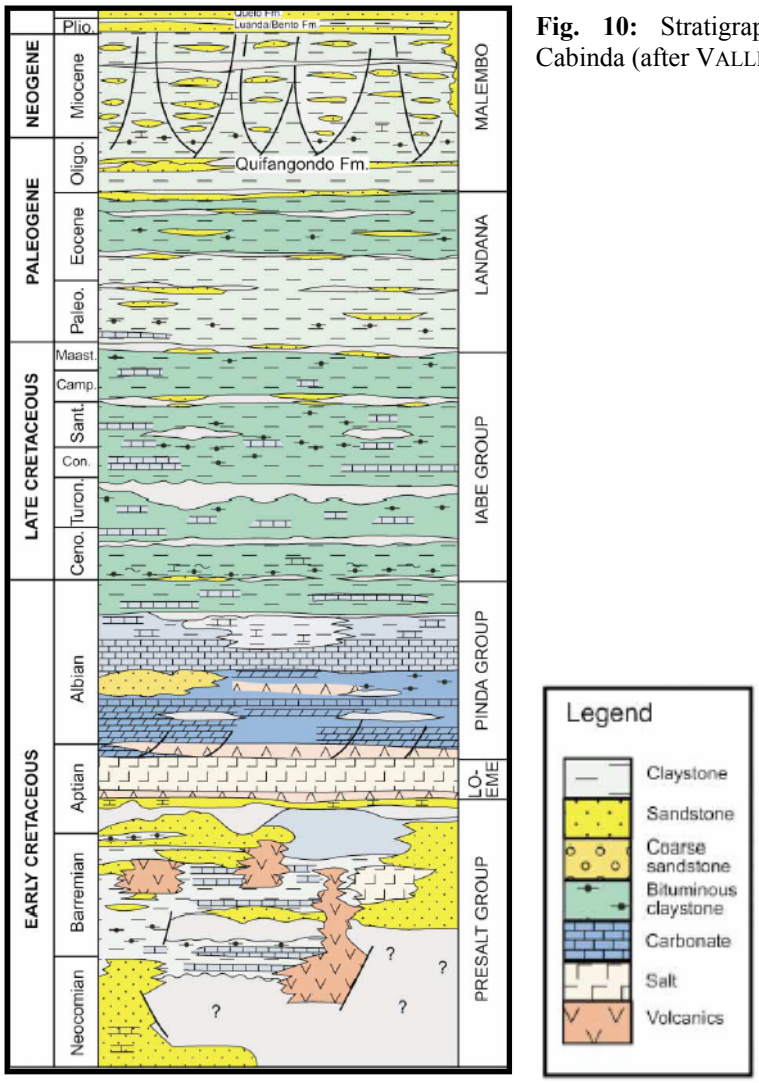

Fig. 10: Stratigraphic column for offshore Cabinda (after VALLE ET AL., 2001)

These grabens were progressively filled by turbidites that graded laterally and upward into organic-rich shales. During the rifting stage the bituminous Bucomazi Formation was formed, which is the primary hydrocarbon source facies of Lower Cretaceous age. These shales can attain a maximum thickness of 1800 m (MCHARGUE, 1990). The synrift I stage continued until the Upper Barremian and

was followed by a period of regional subsidence (synrift II), which led to numerous marine incursions. The entire sequence consists of lacustrine carbonates, sandstones and alluvial clastics followed by the transition to a marine regime. Marine waters initially entered the Lower Congo Basin from the South whereas the ongoing transgression culminated in the deposition of the Loeme Salt. This regional to subregional seal between the lacustrine synrift I and II sediments and the overlying marine postrift sediments were deposited in Aptian times (SCHOELLKOPF & PATTERSON, 2000; COLE ET AL., 2000).

The following postsalt units are characterized by permanent marine conditions and carbonate-dominated sedimentation accompanied by evaporitic depositions. First accumulations are Albian to early Cenomanian continental clastics to marine shaly marls of the Pinda Group with minor source potential (COLE ET AL., 2000). These deposits are followed by three major source strata. The first unit, the Iabe Group accumulated from the Cenomanian to Maastrichtian and consists of marine clastic sediments. The two following major assemblages consist of turbiditic sandstones and marine shales with the older unit deposited in the Early Tertiary.

Sediments of the Paleocene to Eocene Landana Formation consist primarily of deep-water shales. They generally have TOC contents as high as 3 to 5 percent characterised as Type II kerogen. The Malembo Formation as the younger unit accumulated in the Oligocene and Miocene representing an overall fining upward sequence which was deposited in a deepwater slope environment characterised by hemipelagic shales and interbedded channel sands. The sandstone packages represent debris-flow and turbidite units (VALLE ET AL., 2001). Generally TOC contents vary between 1 to 2 percent, but lower and upper parts of the formation can attain up to 5 percent TOC in form of Type II and Type II/III kerogens (SCHOELLKOPF AND PATTERSEN, 2000). Extensive faulting movements throughout Tertiary times formed effective conduits for hydrocarbon migration. Periodic halokinesis caused by tectonic activity resulted in the formation of significant salt diapirs which encapsulated potential reservoir sandstones in their vicinity. These

structures increase in size and frequency westward into the deep-water areas of the sediment basin (COLE ET AL., 2000).

3.2 NORWAY

All 13 crude oils from Norway were collected from the Gullfaks fields, offshore Norway. This area is situated approximately 175 km northwest of Bergen within Block 34/10 at 61°N and 2°E (OLAUSSEN ET AL., 1992). Most samples are derived from the Gullfaks field, but some were also collected from the surrounding satellites Gullfaks Vest, Gullfaks Sør, Rimfaks and Gullfaks Gamma (Table 1, Figure 11).

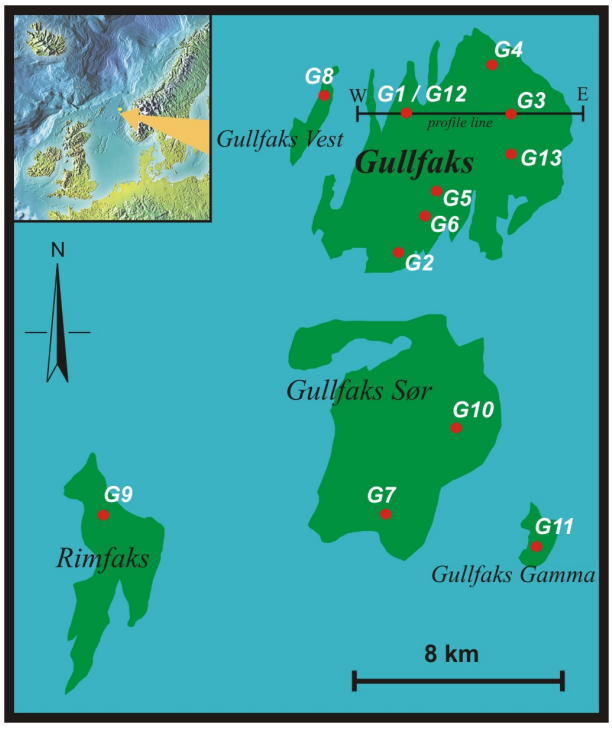

Fig. 11: Map of the Gullfaks area with sampling wells. The small map in the upper left corner shows the location of the Gullfaks area offshore Norway. Also shown is the profile line for the cross section displayed in Figure 13.

The Gullfaks area is part of the central East Shetland Basin and represents the shallowest structure in the Tampen Spur, which is located on the western shoulder of the NNE-SSW trending Viking Graben. (HORSTAD ET AL., 1992, OLAUSSEN ET AL., 1992). This area was affected by at least two major rift phases (ROBERTS ET

AL., 1990). First significant tectonic movements started in the Permian and Early Triassic and affected the total width of the northern North Sea and resulted in the formation of the proto-Viking Graben. In the East Shetland Basin, syndepositional tectonic movements determined facies and thickness of the Triassic and Jurassic depositions (OLAUSSEN ET AL., 1992). A generalized stratigraphic column for the Gullfaks area and a cross section through the Gullfaks field are shown in Figure 12 and 13, respectively.

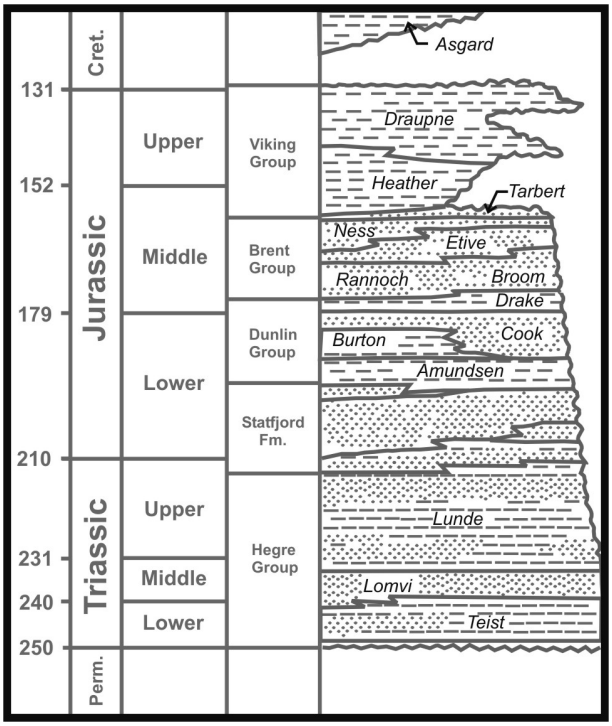

Fig. 12: Stratigraphy in the Gullfaks area (modified after HORSTAD ET AL., 1995)

The lowermost strata in the Gullfaks area penetrated by wellsis the Late Triassic Lunde Formation, which represents the upper part of the Hegre Group. This continental sequence deposited on a wide alluvial floodplain comprises alternating sandstones, oxidized claystones and shales (HORSTAD ET AL., 1995; HEESTHAMMER & FOSSEN, 2001). One important reservoir lithology in the Gullfaks area is represented by alluvial sandstones of the uppermost Triassic (Rhaetian) - Early Jurassic Statfjord Formation. From this reservoir formation the two samples drilled in the Gullfaks Sør oil field (G7 & G10) were collected. The Statfjord Formation deposited in a braided river regime was transgressed by the Early Jurassic (Sinemurian – Toarcian) Dunlin Group, which comprises different

stratigraphic units whereas the marine, silty claystones, muddy sandstones and sands of the Cook Formation represent the major reservoir lithology (HORSTAD ET AL., 1995; ROBERTS ET AL., 1990; FOSSEN AND HEESTHAMMER, 1998 & 2000). From this reservoir unit the sample from the Gullfkas Gamma field (G11) and one crude oil from the Gullfaks field (G13) were collected. The next younger part in the stratigraphic sequence in the Gullfaks area is formed by the Bajocian – Early Bathonian (Middle Jurassic) Brent Group. These deltaic sandstones hosted all other crude oils collected from the Gullfaks field (G1 – G6, G12) as well as the sample derived from the Rimfaks oil field (G9). The Brent Group was transgressed by the Upper Jurassic Viking Group with marine accumulations of the Heather Formation and the 200 – 400 m thick Draupne Formation. Generally, the Draupne Formation is quoted as the major source facies in the Tampen Spur area (e.g., OLAUSSEN ET AL., 1992; HORSTAD ET AL., 1995). Locally, also the underlying Heather Formation generated hydrocarbons, however, a higher terrestrial input causes a lower kerogen quality (HORSTAD ET AL., 1995). Alternative source rocks of secondary importance for the oils reservoired in the Gullfaks area are the black shales of the Dunlin Group and some Cretaceous shales in the Viking Graben (OLAUSSEN ET AL., 1992).

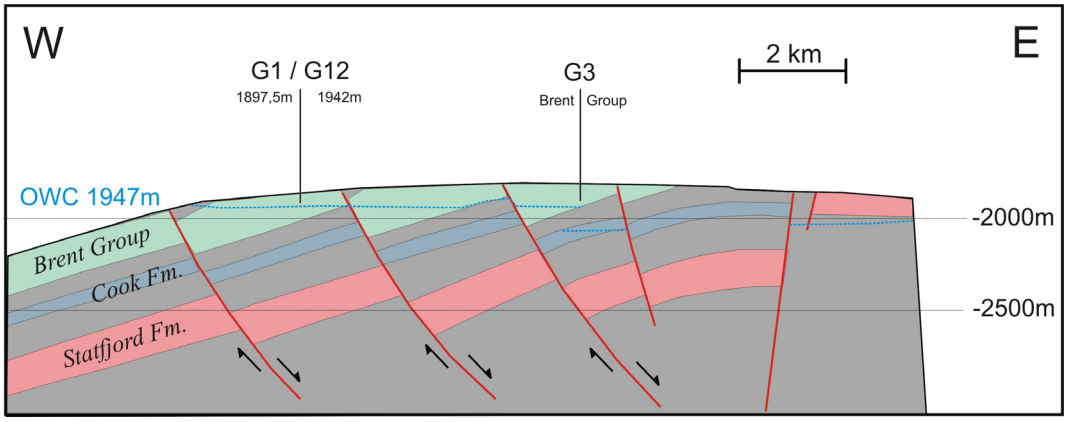

Fig. 13: Cross section through the Gullfaks Field with the location of two wells and sampling depths where 3 of the 8 samples from the Gullfaks Field are derived from (modified after HORSTAD ET AL., 1989). The blue dashed line indicates the level of the oil water contact (OWC) in the subsurface.

During the Kimmerian orogeny (Upper Jurassic) the whole area was uplifted and structural elements with westerly tilted fault blocks developed. In general, faults are dipping with 25 - 30° to the east while strata show a 10 - 20° westerly-dipping bedding (HEESTHAMMER ET AL., 2001). The amount of uplift increases to the North and to the East within each major fault block. This led to the complete erosion down to the Brent Formation in the eastern part of the Gullfaks Field (HORSTAD ET AL., 1989 & 1992). Downflank deposition of the eroded sandstones in structurally low positions formed prospective stratigraphic traps (HORSTAD ET AL., 1995). Locally, up to 100 m of the Upper Jurassic Heather Fm. are preserved in the Gullfaks Field and can exceed up to 1000 m in the Gullfaks Sør area (HEESTHAMMER & FOSSEN, 2001). The second major rifting phase caused the late Kimmerian unconformity, representing a time gap of up to 100 My and defines the base of the Cretaceous shales and siltstones which are considered to be effective seal rocks (OLAUSSEN ET AL., 1992).

3.3 CANADA

Another sample set investigated in this study comprises 12 crude oils from Canada. These samples are derived from the Beaufort-Mackenzie-Basin in north-western Canada. The investigated oils, both onshore and offshore, originate from five different wells located in the Mackenzie-Delta. Samples were collected from the oil fields Tuktuk (C1- C5), Kumak (C6 – C7), Arnak (C8 - C10) and Mayogiak (C11 – C12). A well location map for crude oils collected in the Mackenzie Delta is shown in Figure 14.

On the basis of lithology, facies distributions and thickness variations DIXON ET AL. (1985) divided the accumulations of the Mackenzie Delta into five tectono-stratigraphic assemblages (TANG AND LERCHE, 1992). A stratigraphic coloumn for the Beaufort-Mackenzie-Basin is shown in Figure 15. The lowermost unit was deposited from Jurassic to early Cretaceous (Hauterivian) on an epicontinental

shelf, whereas the Husky Formation is considered to be a hydrocarbon source lithology and the overlying Parsons sandstone is the corresponding reservoir formation (DIXON ET AL., 1985). A regional unconformity separates the strata of this first unit from the deposition of the following second period which were accumulated from the late Hauterivian to the Albian (mid Cretaceous) and represent a low energy shelf and deep water flysch. At the end of the first major extensional phase a significant unconformity marks the base of the Upper Cretaceous to Pleistocene strata (LANE, 2002). These accumulations have been subdivided into three tectono-stratigraphic assemblages, again separated by unconformities in the Late Eocene and Late Miocene. The first of these three units comprises six formations deposited from the Upper Cretaceous to the Eocene. The Late Cretaceous Boundary Creek and Smoking Hills sequences consist of dark grey to black, organic rich shales (TANG AND LERCHE, 1992). These depositions represent a low energy anoxic marine environment deposited in an outer shelf to slope setting (DIXON ET AL., 1985).

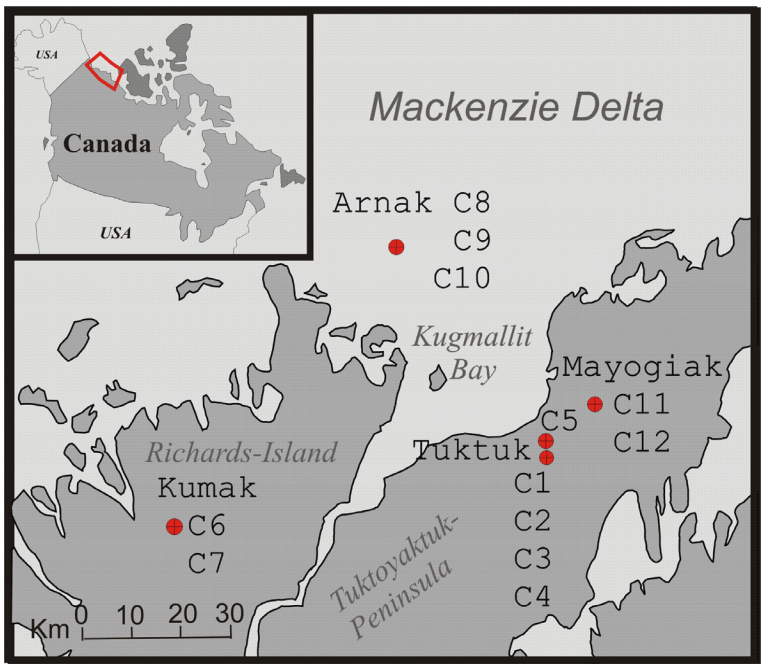

Fig. 14: Well location map of crude oils collected in the Mackenzie Delta. The small map in the upper left corner shows the location of the Mackenzie Delta in north-western Canada. Red dots indicate the 5 different wells, which penetrate 4 different oil fields Arnak, Kumak, Tuktuk and Mayogiak.

The uppermost Cretaceous Fish River sequence represents the first complex deposited in a fluvio-deltaic regime and therefore indicates a regressive trend. In

the Early – Middle Paleocene to Late Eocene sediments were deposited in a deltaic regime. These accumulations, the Reindeer and Richards Formations, comprise the younger Aklak, Taglu and Richards sequence. In this assemblage the Richards sequence is cited as the prolific hydrocarbon source (e.g. SNOWDON, 1987) with the Fish River sequence and Reindeer Formation as the associated reservoir strata (DIXON ET AL., 1985). The second tectono-stratigraphic unit consists of the Oligocene Kugmallit sequence and the Late Miocene Mackenzie Bay and Apkak sequence (TANG AND LERCHE, 1992). The Kugmallit sequence was deposited on a delta plain to slope distal basin plain environment and represents a major reservoir in the Beaufort-Mackenzie region (DIXON ET AL., 1985). It is sealed by the Mackenzie and Akpak sequence. These latter deposits represent mud dominated deep water accumulations beneath the outer shelf (TANG AND LERCHE, 1992). The third and youngest tectono-stratigraphic unit described by DIXON ET AL. (1985) consists of the Late Miocene to Pleistocene Iperk sequence which rests discordantly on the older strata and was deposited in a fluvio-deltaic regime (TANG AND LERCHE, 1992).

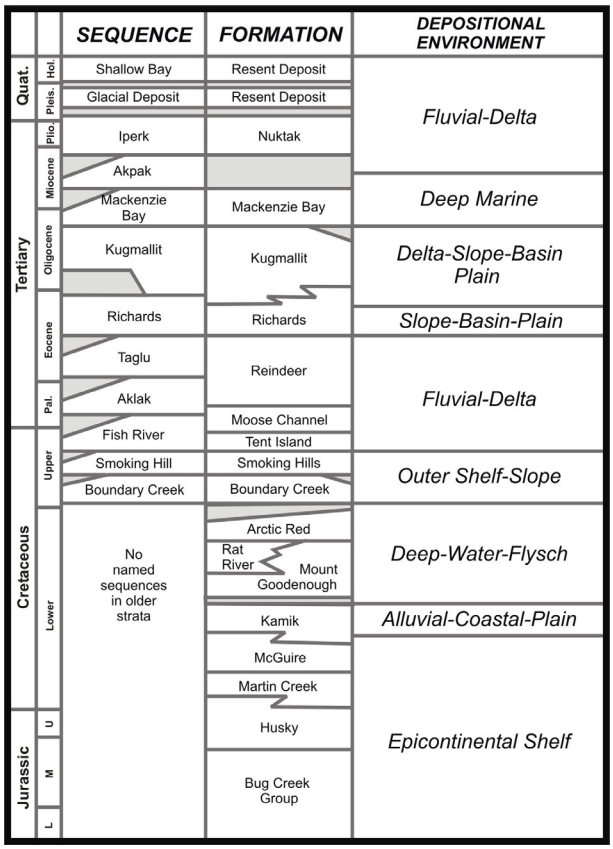

Fig. 15: Stratigraphic column for the Beaufort-Mackenzie Basin (MODIFIED FROM TANG AND LERCHE, 1992).

3.4 EGYPT

The Egyptian crude oil samples originate from the Gulf of Suez. The area is separated into three structural sub-provinces that are divided by ENE-WSW trending hinge zones (Figure 16). The tectonic units of the northern and southern provinces dip towards the southwest whereas the strata of the central province dip to the northeast (PATTON ET AL., 1994). Due to the rifting movements, typical fault blocks have been formed bearing numerous oil accumulations (BAKR AND WILKES, 2002).

Fig. 16: Crude oil samples from Egypt originate from two wells penetrating the Issaran and Sudr oil fields in the Gulf of Suez. (modified after BAKR AND WILKES, 2002).

The stratigraphic sequence in the Gulf of Suez can be divided into two grand units, a prerift sequence and a synrift sequence (Figure 17). Throughout the prerift stage two major lithologies were deposited on top of the Precambrian basement. Palaeozoic to Late Cretaceous sandstones of the Nubia formations are followed by accumulations of Upper Cretaceous (Cenomanian) to Eocene carbonate successions which are interrupted by minor clastics. The overlying synrift stage is represented (a) by a clastic sequence mainly deposited in the Lower Miocene and (b) by the Upper Miocene evaporitic succession (SCHULTZ, 1994). Source rocks are mainly abundant in the carbonatic strata of the prerift sequence but can also be

found in a few clastic Lower Miocene units (SHAHIN AND SHEHAB, 1984). Hydrocarbon traps exist in the entire stratigraphic succession. Evaporitic deposits of Middle Eocene age seal these stratigraphic and structural hydrocarbon traps which were formed during the rifting movements. Important migration pathways are located along the vertical dislocation lines corresponding to the fault blocks emerged by rifting movements. Important oil reservoirs exist in the sandy deposits of Miocene, Cretaceous and Carboniferous age. Further commercial hydrocarbon accumulations are located in the limestones of Miocene, Eocene and Upper Cretaceous age (BAKR AND WILKES, 2002).

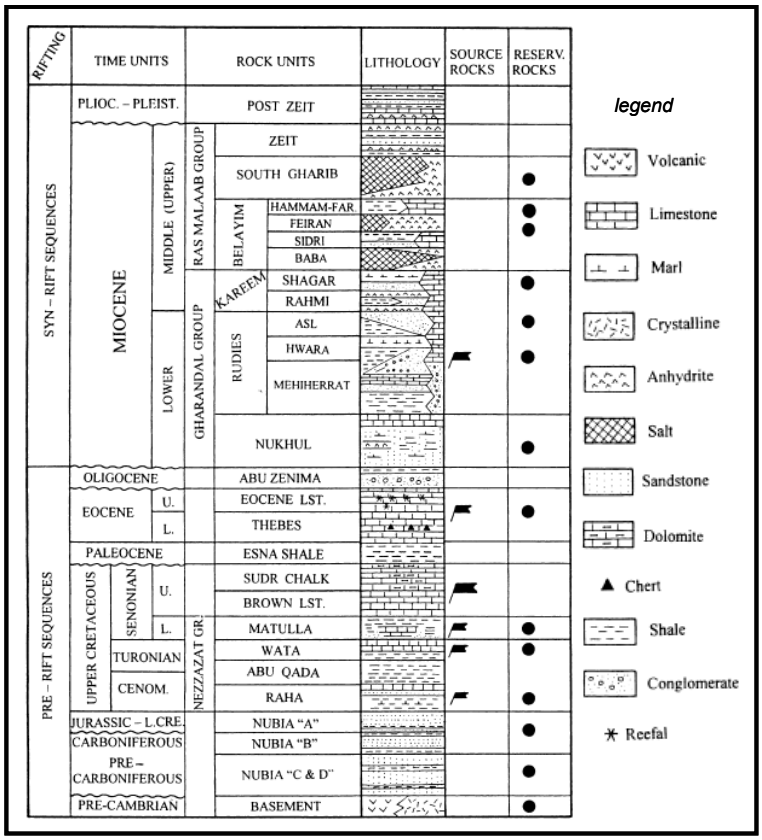

Fig. 17: Stratigraphic column for the Gulf of Suez (adopted from BAKR AND WILKES, 2002).

The seven Egyptian crude oils originate from the Sudr (E1 – E5) and Issaran (E6 – E7) fields in the Gulf of Suez. The Sudr oil field is located in the Northern Province, where oils were characterised as mixtures derived from sources of carbonate/marl with little shale rocks deposited in an anoxic to suboxic environment (BAKR AND WILKES, 2002). SHAHIN ET AL. (1994) suggested the

Cenomanian rocks of the Raha Formation as the main source rock. This lithology is composed of fossiliferous massive limestones, marls and shales, which were deposited in a restricted, shallow-marine environment (SCHULTZ, 1994). The two crude oils from the Issaran field originate from the Central Province, where the upper Senonian Brown Limestone and the Lower Eocene Thebes Formation have been considered to be potential source rocks (ROBISON, 1995). The Miocene organic-rich Brown Limestone, deposited in an open marine environment with limited circulation causing dysaerobic to anaerobic conditions, has generated economically significant amounts of oil in the Gulf of Suez (BAKR AND WILKES, 2002).

3.5 NIGERIA

Crude oils from Nigeria were drilled offshore in the Gulf of Guinea, being part of the Niger Delta. Figure 18 shows the location of the Gulf of Guinea, offshore Nigeria.

Fig. 18: Location of Nigeria in West Africa. Crude oils samples are derived from offshore well sites in the Gulf of Guinea.

Here, sediments accumulated from Cretaceous to Recent. Following the Mesozoic rifting of the Atlantic, sedimentation began with Lower Cretaceous (Albian) drift deposits. Sediments filled the Benue Trough and from Late Eocene accumulation prograded across the existing continental slope into the deep sea. Continuing seaward progradation since the Eocene has extended the continental margin to its present position (ZIEGLER, 2003). A generalized stratigraphic column for the Gulf of Guinea is shown in Figure 19.

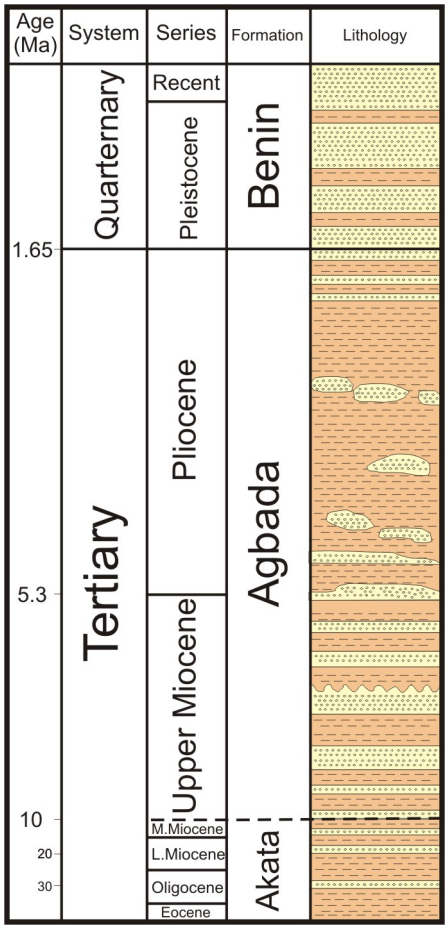

Fig. 19: Generalized stratigraphic column for the Niger Delta in the Gulf of Guinea, offshore Nigeria. Stratigraphy and lithology are adopted and modified from ZIEGLER (2003).

Tertiary sediments in the Niger delta are divided into three diachronous units of Eocene to Recent age. The Akata, Agbada and Benin Formations form a major regressive cycle and represent prograding depositional facies which are predominantly distinguished on the basis of sand-shale ratios. The oldest sediment package, the Akata Formation, comprises up to 6500 m of marine shales, turbidite sands with minor amounts of clay and silt. These sediments are overpressured and

have been deformed in response to delta progradation. The Akata Formation represents the major source rock for the offshore petroleum systems in the Gulf of Guinea. The overlying Upper Miocene to Pliocene deltaic Agbada Formation consists of paralic, brackish to marine, coastal and fluvio-marine deposits and hosts the major petroleum reservoirs offshore Nigeria. Within this nearly 2 km thick sediment succession five erosionally bounded sequences can be distinguished. Generally each sequence becomes progressively thinner and changes from upward-coarsening deltaic sediments to channel sandstones which are interbedded with paralic mudstones. The youngest sequence, overlying the Akata and Agbada Formations is represented by the continental Benin Formation, which dominantly consists of sand-rich fluvial deposits (OWOYEMI AND WILLIS, 2006). The primary seal rock in the Niger Delta is represented by the interbedded shales within the Agbada Formation. On the flanks of the delta early to middle Miocene erosion formed canyons that are now clay-filled. These clays form the top seals for some important offshore fields (DOUST AND OMATSOLA, 1990).

4 METHODOLOGY

All 55 crude oils were characterised by analytical techniques described below. The chromatographic separation via MPLC (RADKE ET AL., 1980) was carried out in order to produce enriched compound classes fractions which are suitable for detailed molecular analysis using gas chromatography (GC) and gas chromatography-mass spectrometry (GC-MS). The detection of compound-specific isotopic signatures (IRM-GC-MS) was carried out for both carbon and hydrogen isotopes. Technical specifications for the various analytical methods are described in the following chapters.

4.1 THERMOVAPORISATION GAS CHROMATOGRAPHY

The crude oils were analysed by thermovaporisation gas chromatography (GC) in order to gain the distribution of light hydrocarbons and *n*-alkanes. This method enables the analysis of samples which are too viscous for injection with a syringe into a conventional whole-oil-GC instrument. For thermovaporisation runs, a GC system (6890A, Agilent Technologies, USA) equipped with a Quantum MSSV-2 thermal analyser system and a FID, operating at 310°C, was used. The GC was fitted with a HP Ultra 1 fused silica capillary column (50 m x 0.32 mm i.d., f.t. = 0.52 µm), using Helium as the carrier gas. For the NSO-1 crude oil from Norway, which is used as the reference sample, all identified light and saturated hydrocarbons are shown in Figure 20.

The injected sample volume was 0.5 µl with variable split ratios between 1:10 and 1:50. The crude oils were weighed onto quartz wool within small glass vials which were sealed by heating according to the MSSV method established by HORSFIELD ET AL. (1989). The closed glass tubes were stored in the pyrolysis oven that was heated up to 300°C for 5 minutes. Hereafter, the glass tube was cracked

by a piston and the thermally mobilized products were held in a nitrogen-cooled cryogenic trap at -196°C. By heating up the trap to 300°C, the products were subsequently released to the GC. The GC oven temperature was set to initial 30°C and held for 13 min. Next, a heating rate of 5°C/min increased the temperature to 320°C which was then held for 35 min.

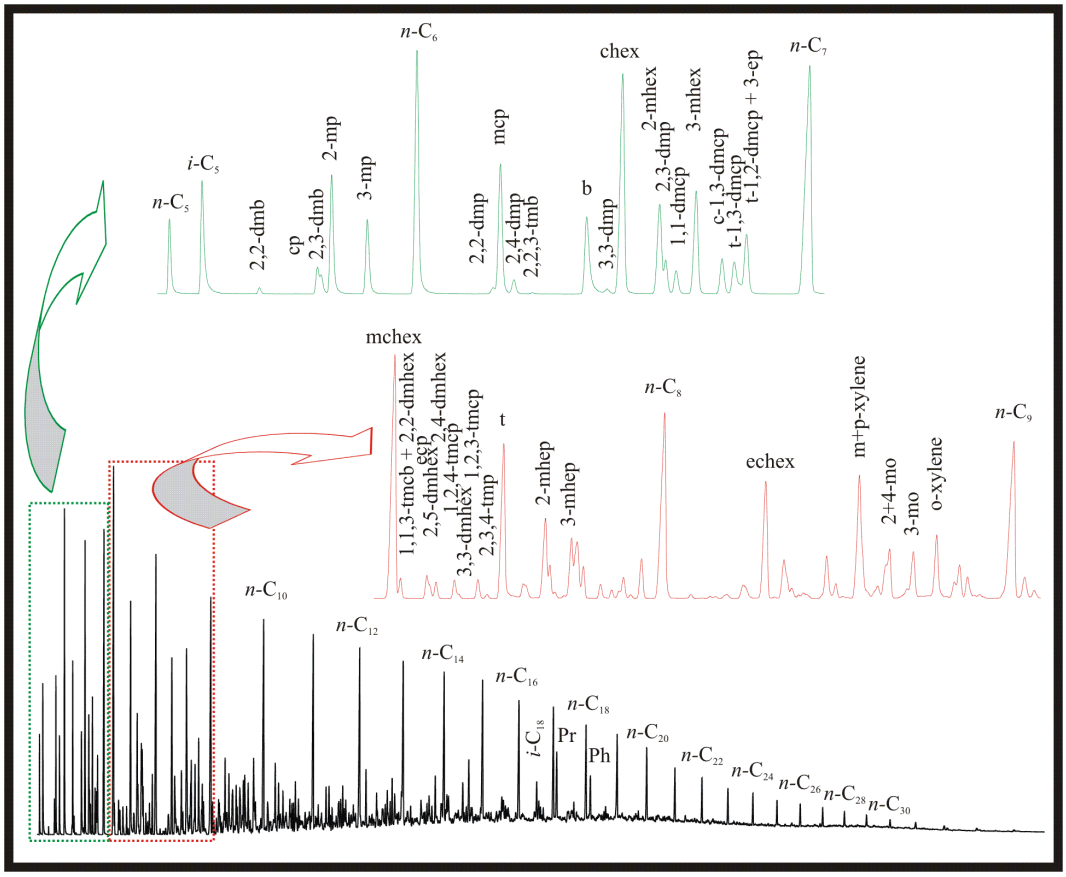

Fig. 20: Thermovaporisation-GC of the NSO-1 crude oil. Full compound names for abbreviations used here are listed in Table X- 1 in the Appendix.

4.2 GC-FID

All 55 samples were separated by an automated medium pressure liquid-chromatography procedure (MPLC) to obtain aliphatic, aromatic and polar fractions (RADKE ET AL., 1980). The GC-FID measurements on the aliphatic

fraction were carried out for the detection and quantification of saturated compounds in the *n*-C_{15} to *n*-C_{30} range. Analyses were performed with a GC-FID (6890A, Agilent Technologies, USA) which was equipped with a HP Ultra 1 capillary column (50 m x 0.32 mm i.d., f.t. = 0.52 µm). The injector temperature was set to 40°C with a rate of 700°C/min heating up to 300°C held for 3 minutes. The GC oven was programmed from 40°C (2 min isothermal) to a final temperature of 300°C (65 min isothermal) at a heating rate of 5°C/min with a constant flow rate. The injected aliphatic fraction, diluted in *n*-hexane, was detected by a FID operating at 310°C.

Quantification of the resolved compounds in the aliphatic fraction was carried out using 5α-androstane as internal standard. The concentration (µg/g oil) obtained for phytane using this method was then assigned to the peak area of phytane in the thermovaporisation measurements which served as the reference value to determine the concentrations for all other compounds detected by the latter method. A GC-FID chromatogram of the aliphatic fraction is shown in Figure 21.

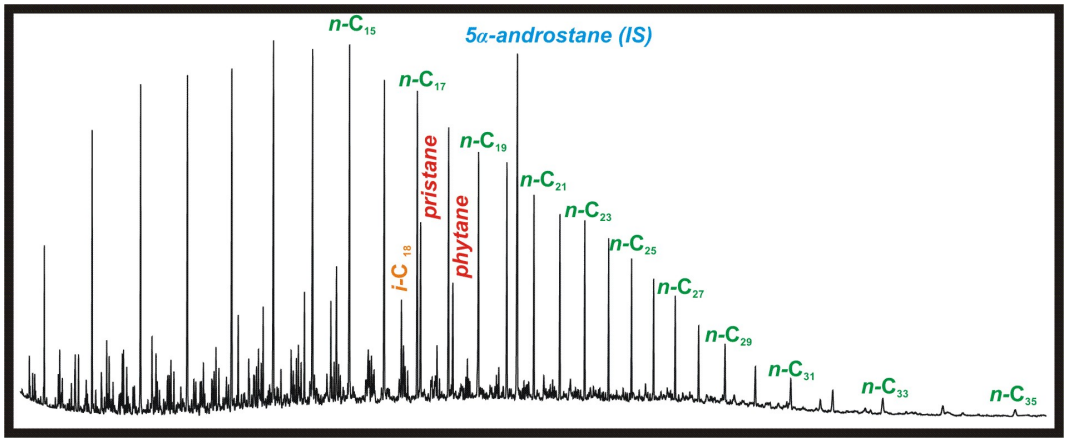

Fig. 21: GC-FID measurement of the aliphatic fraction yielded by MPLC for the NSO-1 crude oil from Norway showing saturated hydrocarbons. Due the separation technique (MPLC), quantities for *n*-alkanes eluting prior to *n*-C_{15} are not accurate and therefore these compounds are not assigned in the figure and were not used to determine the concentrations for the investigated samples.

4.3 GC-MS

The aromatic hydrocarbon fractions yielded by MPLC separation and the combined low- plus medium-polarity NSO compound fractions yielded by combined H-MPLC and MPLC separation were analysed by gas chromatography-mass spectrometry (GC-MS). Analyses were performed using a Finnigan MAT 95XL mass spectrometer that was coupled to a HP 6890A gas chromatograph. The GC was equipped with a BPX5 fused silica capillary column (50 m x 0.22 mm i.d; f.t. = 0.25 µm). The injector temperature was set to 52°C, subsequently heated up with 720°C/min to 300°C. The oven temperature started at 50°C with a 1 min isothermal stage, then heating up with 3°C/min to 310°C final temperature which was held for 20 min. Helium was used as the carrier gas with a constant flow of 1 ml/min. The MS unit operated in the EI mode at an electron energy of 70eV and a source temperature of 260°C. For the aromatic hydrocarbon fractions, full scan mass spectra were recorded over the mass range of 100-330 Da at a scan rate of 1 s per decade, an inter scan time of 0.2 s and a scan cycle time of 0.719 s. For the combined low- plus medium-polarity NSO compound fractions, full scan mass spectra were recorded over the mass scan range of 50-600 Da.

GC-MS measurements were used to evaluate several alkylated benzenes, naphthalenes, phenanthrenes and dibenzothiophenes as well as mono- and triaromatic steroids. Identification of each compound class was carried out using respective *m/z* values displayed in Figures 22-27. The summed chromatogram of each subgroup including *m/z* 215 & 230 for ethylpyrene as the internal standard for alkylated benzenes, naphthalenes, phenanthrenes and dibenzothiophenes were used to calculate the concentrations in µg/g oil. All calculated concentrations for individual compounds are given in the Appendix. Identification of individual alkylbenzenes was carried out by comparison with HARTGERS ET AL. (1992). Alkylnaphthalenes were identified by comparison with BUDZINSKI ET AL. (1998), HUANG ET AL (2004) and VAN AARSSEN ET AL. (1999). By comparison with HUANG ET AL. (2004), individual alkylphenanthrenes were assessed and the

identification of dibenzothiophenes was carried out by comparison with CHAKHMAKHCHEV AND SUZUKI (1995); CHAKHMAKHCHEV ET AL. (1997); DEPAUW AND FROMENT (1997) and MÖSSNER ET AL. (1999). Aromatic steroids were identified by comparison with PETERS AND MOLDOWAN (1993).

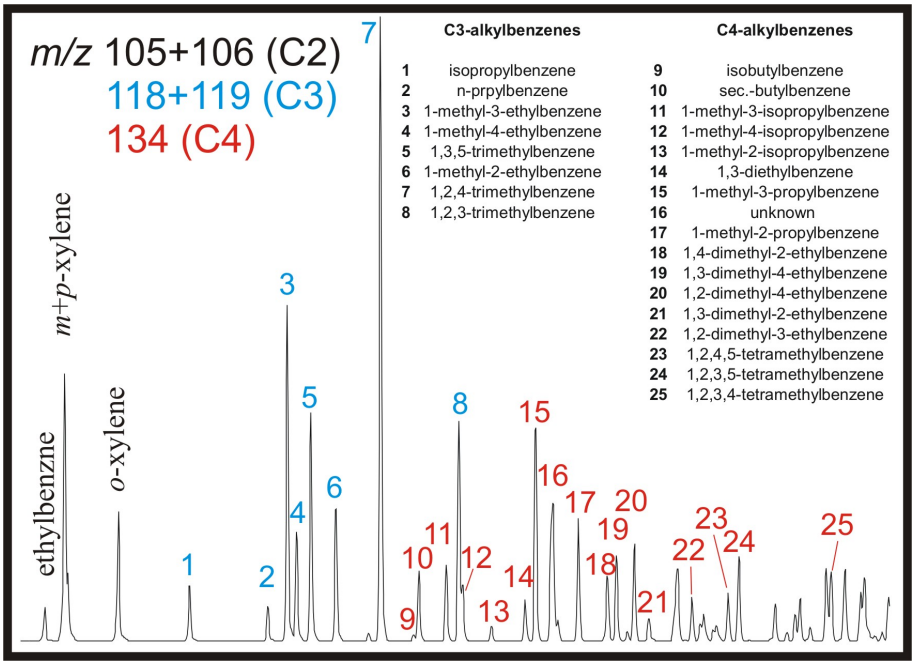

Fig. 22: Partial mass chromatogram of alkylbenzenes in the reference sample (NSO-1).

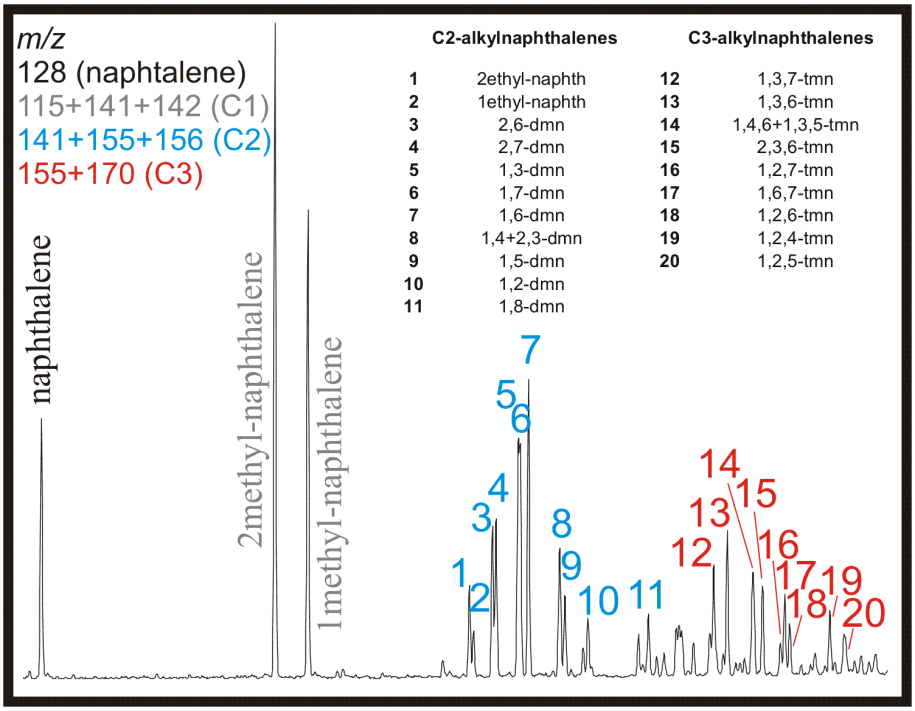

Fig. 23: Partial mass chromatogram of alkylnaphthalenes in the reference sample (NSO-1).

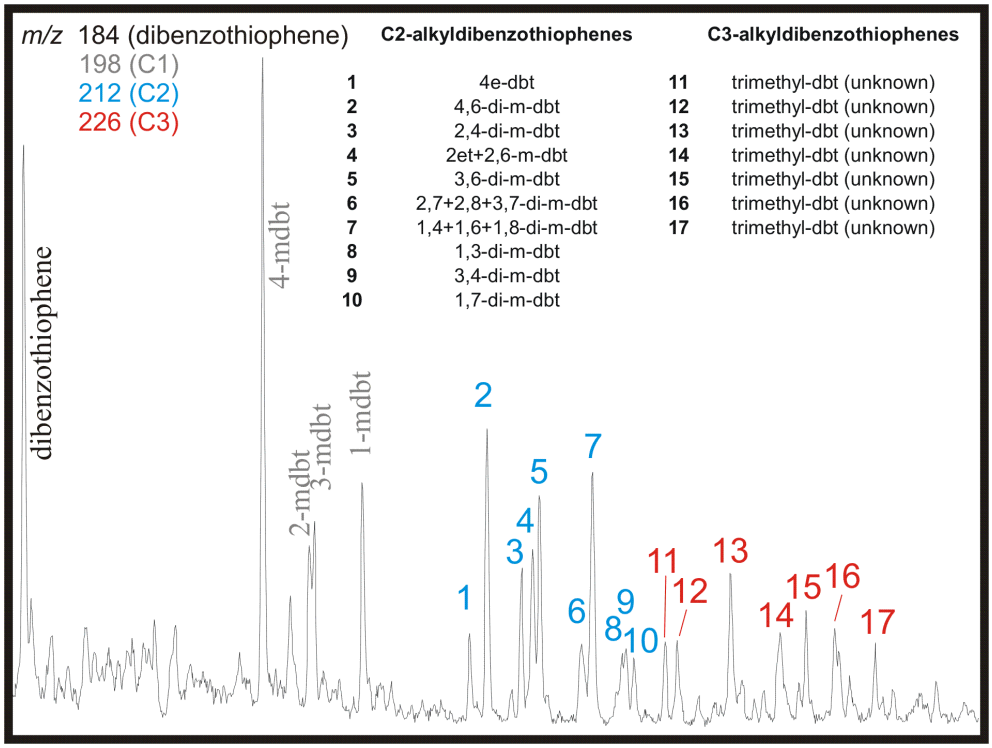

Fig. 24: Partial mass chromatogram of alkyldibenzothiophenes in the reference sample (NSO-1).

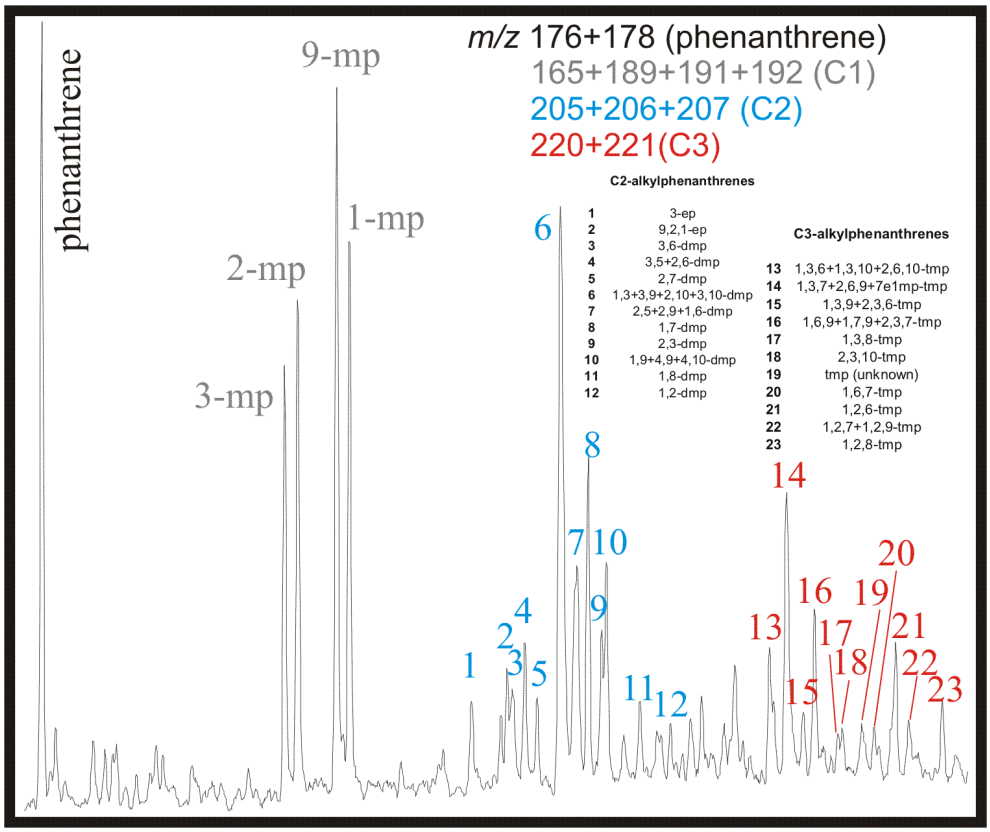

Fig. 25: Partial mass chromatogram of alkylphenanthrenes in the reference sample (NSO-1).

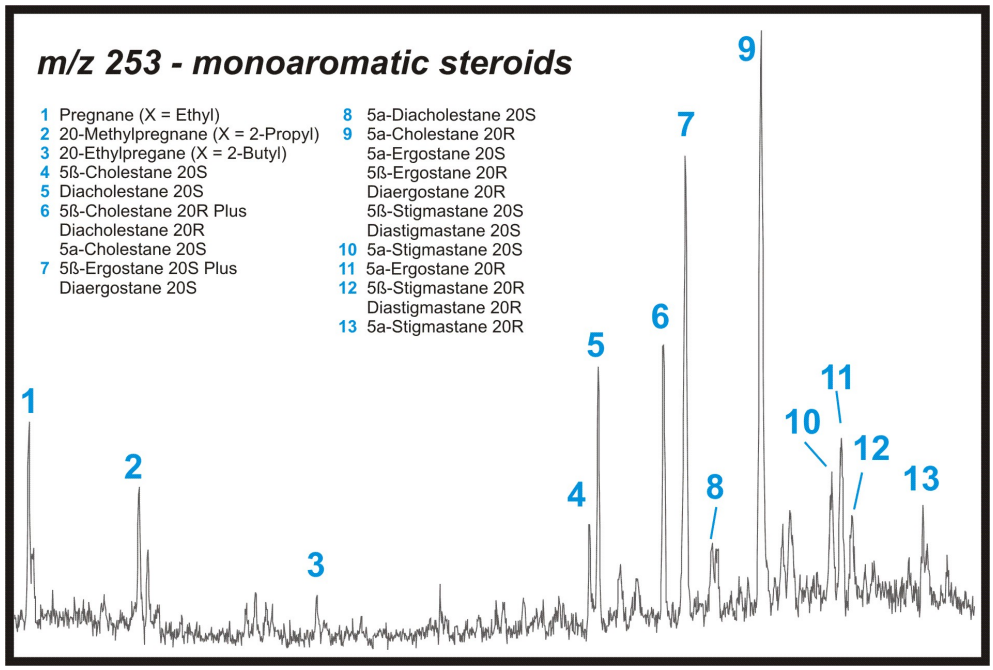

Fig. 26: Partial mass chromatogram showing monoaromatic steroids in the reference sample (NSO-1).

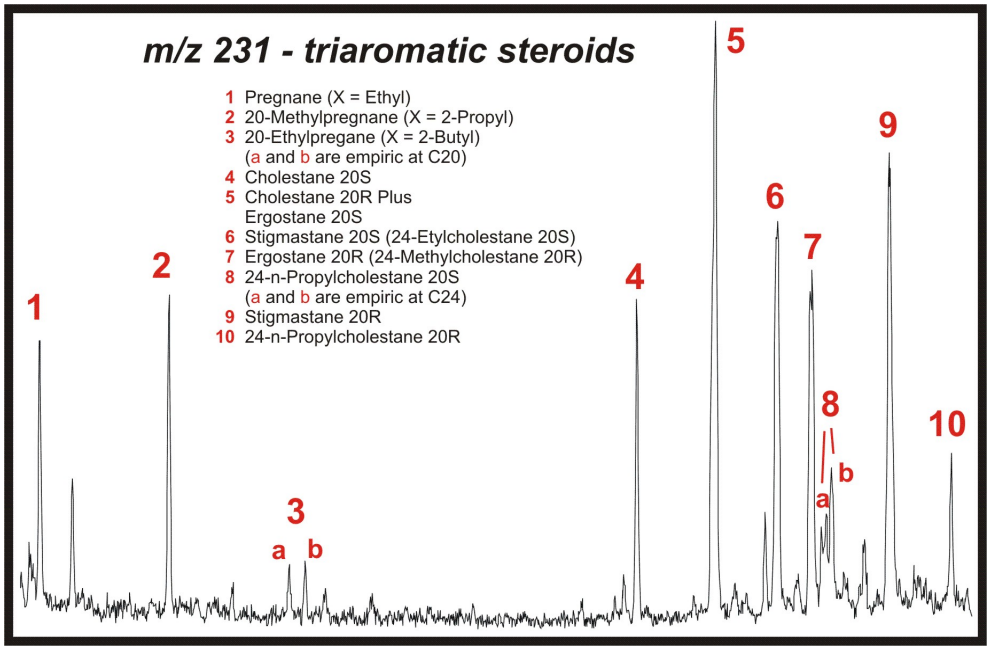

Fig. 27: Partial mass chromatogram showing triaromatic steroids in the reference sample (NSO-1)

4.4 GC-MS-MS

GC-MS-MS measurements were applied to the aliphatic fractions for evaluation of saturated biomarker compounds. For these analyses, the GC-MS unit described above with identical technical specifications was used. The saturated hydrocarbon biomarkers were recorded in the Multiple Reaction Monitoring (MRM) mode with a dwell time of 21 ms and an inter dwell time of 20 ms per metastable transition resulting in a scan cycle time of 0.984 s for the detection of 24 metastable transitions. Evaluations of hopanes (*m/z* 191) and steranes (*m/z* 217) were carried out using these daughter fragments with corresponding parent ions *m/z* 370, 398, 412, 426 for hopanes and *m/z* 372, 386, 400, 414 for steranes.

The evaluation of hopane and sterane distributions in crude oils investigated in this study was carried out by relative abundances of peak areas. Contrary to the light, saturated and aromatic hydrocarbons the total concentrations in µg/g oil were not determined. Figure 28 displays hopanes listed in Table 2 using a GC-MS-MS chromatogram for the NSO-1 reference oil. Figure 29 displays steranes listed in Table 3 using a GC-MS-MS chromatogram for the NSO-1 reference oil.

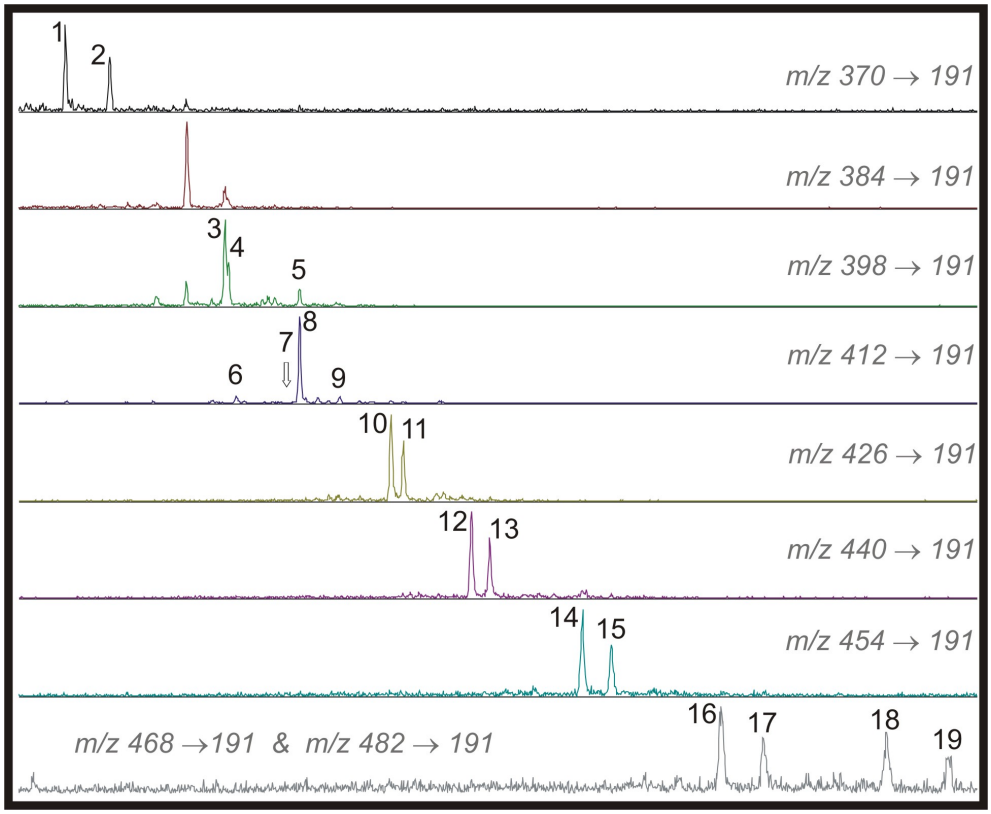

Fig. 28: GC-MS-MS chromatogram showing hopanes listed in Table 2 detected in the reference oil (NSO-1).

no.	compound name	synonym	formula	mass
1	18α(H)-22,29,30-Trinorneohopane	Ts	$C_{27}H_{46}$	370
2	17α(H)-22,29,30-Trinorhopane	Tm	$C_{27}H_{46}$	370
3	17α(H),21β(H)-30-Norhopane		$C_{29}H_{50}$	398
4	18α(H)-Norneohopane	C_{29}-Ts	$C_{29}H_{50}$	398
5	17β(H),21α(H)-30-Norhopane	Normoretane	$C_{29}H_{52}$	398
6	17α(H)-Diahopane	X-C_{30}	$C_{30}H_{52}$	412
7	Oleanane		$C_{30}H_{52}$	412
8	17α(H),21β(H)-Hopane	Hopane	$C_{30}H_{52}$	412
9	17β(H),21α(H)-Hopane	Moretane	$C_{30}H_{52}$	412
10	(22*S*)-17α(H),21β(H)-29-Homohopane		$C_{31}H_{54}$	426
11	(22*R*)-17α(H),21β(H)-29-Homohopane		$C_{31}H_{54}$	426
12	(22*S*)-17α(H),21β(H)-29-Dihomohopane		$C_{32}H_{56}$	440
13	(22*R*)-17α(H),21β(H)-29-Dihomohopane		$C_{32}H_{56}$	440
14	(22*S*)-17α(H),21β(H)-29-Trihomohopane		$C_{33}H_{58}$	454
15	(22*R*)-17α(H),21β(H)-29-Trihomohopane		$C_{33}H_{58}$	454
16	(22*S*)-17α(H),21β(H)-29-Tetrahomohopane		$C_{34}H_{60}$	468
17	(22*R*)-17α(H),21β(H)-29-Tetrahomohopane		$C_{34}H_{60}$	468
18	(22*S*)-17α(H),21β(H)-29-Pentahomohopane		$C_{35}H_{62}$	482
19	(22*R*)-17α(H),21β(H)-29-Pentahomohopane		$C_{35}H_{62}$	482

Table 2: Individual hopanes identified in the aliphatic fraction analysed by GC-MS-MS.

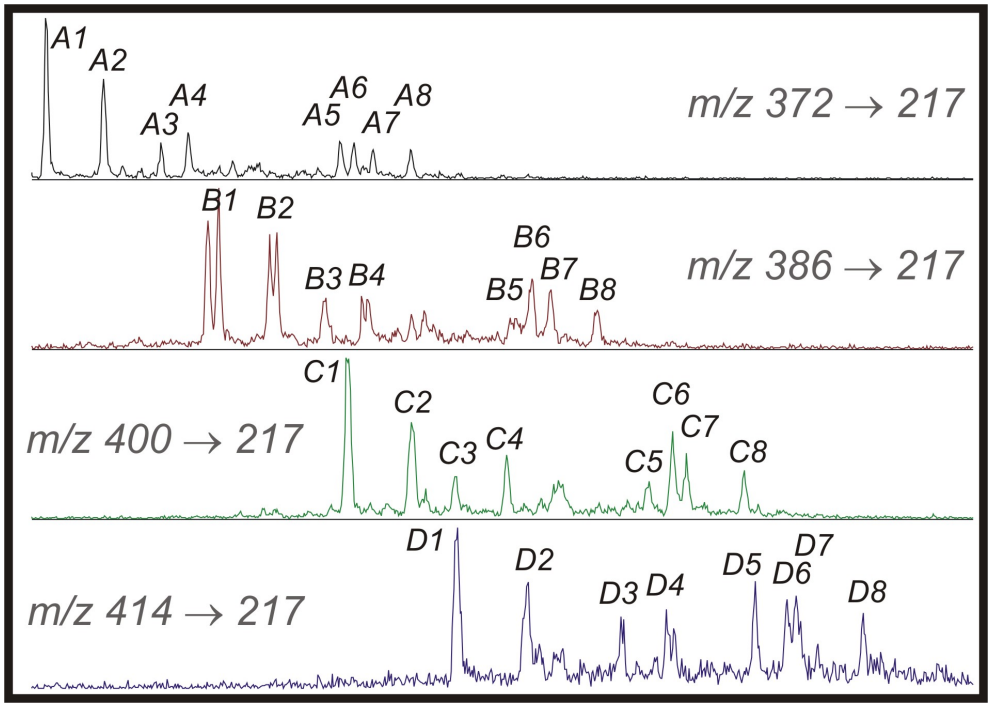

Fig. 29: GC-MS-MS chromatogram showing steranes listed in Table 3 detected in the reference oil (NSO-1).

no.	compound name	configuration	formula		mass
A1	(20*S*)-13β(H),17α(H)-Diacholestane	βα20*S*	$C_{27}H_{48}$	R=H	372
A2	(20*R*)-13β(H),17α(H)-Diacholestane	βα20*R*	$C_{27}H_{48}$	R=H	372
A3	(20*R*)-13α(H),17β(H)-Diacholestane	αβ20*R*	$C_{27}H_{48}$	R=H	372
A4	(20*S*)-13α(H),17β(H)-Diacholestane	αβ20*S*	$C_{27}H_{48}$	R=H	372
A5	(20*S*)-5α(H),14α(H),17α(H)-Cholestane	ααα20*S*	$C_{27}H_{48}$	R=H	372
A6	(20*R*)-5α(H),14β(H),17β(H)-Cholestane	αββ20*R*	$C_{27}H_{48}$	R=H	372
A7	(20*S*)-5α(H),14β(H),17β(H)-Cholestane	αββ20*S*	$C_{27}H_{48}$	R=H	372
A8	(20*R*)-5α(H),14α(H),17α(H)-Cholestane	ααα20*R*	$C_{27}H_{48}$	R=H	372
B1	(20*S*)-24-Methyl-13β(H),17α(H)-Diacholestane	βα20*S*	$C_{28}H_{50}$	R=Me	386
B2	(20*R*)-24-Methyl-13β(H),17α(H)-Diacholestane	βα20*R*	$C_{28}H_{50}$	R=Me	386
B3	(20*R*)-24-Methyl-13α(H),17β(H)-Diacholestane	αβ20*R*	$C_{28}H_{50}$	R=Me	386
B4	(20*S*)-24-Methyl-13α(H),17β(H)-Diacholestane	αβ20*S*	$C_{28}H_{50}$	R=Me	386
B5	(20*S*)-24-Methyl-5α(H),14α(H),17α(H)-Cholestane	ααα20*S*	$C_{28}H_{50}$	R=Me	386
B6	(20*R*)-24-Methyl-5α(H),14β(H),17β(H)-Cholestane	αββ20*R*	$C_{28}H_{50}$	R=Me	386
B7	(20*S*)-24-Methyl-5α(H),14β(H),17β(H)-Cholestane	αββ20*S*	$C_{28}H_{50}$	R=Me	386
B8	(20*R*)-24-Methyl-5α(H),14α(H),17α(H)-Cholestane	ααα20*R*	$C_{28}H_{50}$	R=Me	386
C1	(20*S*)-24-Ethyl-13β(H),17α(H)-Diacholestane	βα20*S*	$C_{29}H_{52}$	R=Et	400
C2	(20*R*)-24-Ethyl-13β(H),17α(H)-Diacholestane	βα20*R*	$C_{29}H_{52}$	R=Et	400
C3	(20*R*)-24-Ethyl-13α(H),17β(H)-Diacholestane	αβ20*R*	$C_{29}H_{52}$	R=Et	400
C4	(20*S*)-24-Ethyl-13α(H),17β(H)-Diacholestane	αβ20*S*	$C_{29}H_{52}$	R=Et	400
C5	(20*S*)-24-Ethyl-5α(H),14α(H),17α(H)-Cholestane	ααα20*S*	$C_{29}H_{52}$	R=Et	400
C6	(20*R*)-24-Ethyl-5α(H),14β(H),17β(H)-Cholestane	αββ20*R*	$C_{29}H_{52}$	R=Et	400
C7	(20*S*)-24-Ethyl-5α(H),14β(H),17β(H)-Cholestane	αββ20*S*	$C_{29}H_{52}$	R=Et	400
C8	(20*R*)-24-Ethyl-5α(H),14α(H),17α(H)-Cholestane	ααα20*R*	$C_{29}H_{52}$	R=Et	400
D1	(20*S*)-24-Propyl-13β(H),17α(H)-Diacholestane	βα20*S*	$C_{30}H_{54}$	R=n-Pr	414
D2	(20*R*)-24-Propyl-13β(H),17α(H)-Diacholestane	βα20*R*	$C_{30}H_{54}$	R=n-Pr	414
D3	(20*R*)-24-Propyl-13α(H),17β(H)-Diacholestane	αβ20*R*	$C_{30}H_{54}$	R=n-Pr	414
D4	(20*S*)-24-Propyl-13α(H),17β(H)-Diacholestane	αβ20*S*	$C_{30}H_{54}$	R=n-Pr	414
D5	(20*S*)-24-Propyl-5α(H),14α(H),17α(H)-Cholestane	ααα20*S*	$C_{30}H_{54}$	R=n-Pr	414
D6	(20*R*)-24-Propyl-5α(H),14β(H),17β(H)-Cholestane	αββ20*R*	$C_{30}H_{54}$	R=n-Pr	414
D7	(20*S*)-24-Propyl-5α(H),14β(H),17β(H)-Cholestane	αββ20*S*	$C_{30}H_{54}$	R=n-Pr	414
D8	(20*R*)-24-Propyl-5α(H),14α(H),17α(H)-Cholestane	ααα20*R*	$C_{30}H_{54}$	R=n-Pr	414

Table 3: Identified steranes in the aliphatic fraction determined by GC-MS-MS.

4.5 COMPOUND-SPECIFIC ISOTOPE ANALYSIS

4.5.1 STABLE CARBON ISOTOPE ANALYSIS

The carbon isotopic composition of specific petroleum components was measured by gas chromatography/combustion/isotope-ratio mass spectrometry (GC–C–IRMS). The GC–C–IRMS system consisted of a GC unit (6890 Series, Agilent Technology, USA) which was connected to a Finnigan MAT GC combustion III device coupled via open split to a Finnigan MAT 253 mass spectrometer (Thermo, Germany). For carbon isotopic measurements the organic components of the GC effluent stream were oxidised to CO_2 in the combustion furnace operating at 940 °C on a CuO/Ni/Pt catalyst. CO_2 was transferred on-line to the mass spectrometer to determine carbon isotope ratios. Crude oil (0.5 µl) was injected to the programmable temperature vaporisation inlet (PTV, Agilent Technology, USA) with a septumless head, working in split/splitless mode. The injector was held at a variety of split ratios ranging from 1:5 to 1:40, depending on the compound concentrations in individual oils. The initial temperature of the injector was set to 50 °C. With injection, the injector temperature increased to 300 °C at a programmed rate of 700 °C min^{1} and held at this temperature for the rest of the analysis time. Carrier gas flow of helium was set at a rate of 1 ml min^{1}. Petroleum constituents were separated on a HP Ultra 1 fused silica capillary column (50 m · 0.32 mm i.d. · 0.52 µm film thickness, Agilent Technology, USA). The temperature of the GC oven was initially held at 30 °C for 10 min, followed by a 2 °C min^{1} ramp to 60 °C, then at a rate of 4 °C min^{1} to 300 °C and held there for a further 30 min. All oil samples were measured in triplicate with a standard deviation of ≤0.5‰ for most of the compounds and samples. The quality of the carbon isotope measurements was checked regularly by measuring *n*-alkane standards (*n*-C_{15}, *n*-C_{20}, *n*-C_{25}) with known isotopic composition (provided by Campro Scientific, Germany).

4.5.2 STABLE HYDROGEN ISOTOPE ANALYSIS

The hydrogen isotopic compositions of hydrocarbons were measured using nearly the identical GC–C–IRMS –system described before. 0.5 µl of the crude oils were injected with varying split ratios of 1:5 and 1:10, depending on the concentration of hydrocarbons in the samples. After passing the GC (6890 Series, Agilent Technology, USA), hydrocarbons were reduced to H_2 and elemental carbon in the pyrolysis reactor held at 1450°C. H_2 was transferred on line to the mass spectrometer to determine hydrogen isotope ratios. All other instrument specifications are identical to the system described for carbon isotopic measurements. The H_3^+-factor was determined daily by measuring 10 reference gas peaks with increasing amplitude. This factor had an average value of 9.28 ± 0.14 ppm/nA. The quality of the hydrogen isotope measurements was checked regularly by measuring *n*-alkane standards (*n*-C_{17}, *n*-C_{19}, *n*-C_{21}, *n*-C_{23}, *n*-C_{25}) with known isotopic composition (provided by A. Schimmelmann, Biogeochemical Laboratories, Indiana University).

5 RESULTS AND DISCUSSION

5.1 PART I: GENERAL GEOCHEMICAL CHARACTERISATION

5.1.1 Light and saturated hydrocarbon parameters

Light and saturated hydrocarbons are widely used for various applications, e.g., oil/source rock correlations, maturity assessment, determination of source lithofacies and alteration processes (e.g., THOMPSON, 1983 & 1988; MANGO, 1990A, 1990B; HALPERN, 1995; TEN HAVEN, 1996; ODDEN ET AL., 1998; WEVER, 2000; GEORGE ET AL., 2002). Within this first part of chapter 5.1.1, several of these established light and saturated hydrocarbon parameters are used to characterise the crude oils. The calculations of concentrations are based on thermovaporisation and GC-FID measurements for *i*-C_5 to *n*-C_{14} and *n*-C_{15} to *n*-C_{30}, respectively. A list of individual light and saturated hydrocarbons whose summed concentrations are given in Figure 30 are provided in Table X-1 of the Appendix.

Highest summed concentrations were calculated for crude oil G11 and G13 from Norway and for sample C7 from the Tuktuk reservoir in Canada. For these three crude oils concentrations of up to 385 mg / g oil were determined. For all other crude oils the summed concentrations for light and saturated hydrocarbons are below 250 mg/g oil. Interestingly, the calculated concentrations vary significantly within all subsets from the different petroleum systems giving a first indication that the extent of biodegradation could be variable. For crude oils A2 and A3 from Angola, C1 from Canada and N2 from Nigeria no light and saturated hydrocarbons could be determined which might indicate that these samples have already reached alteration levels beyond moderate stages on the PM scale (PETERS AND MOLDOWAN, 1993).

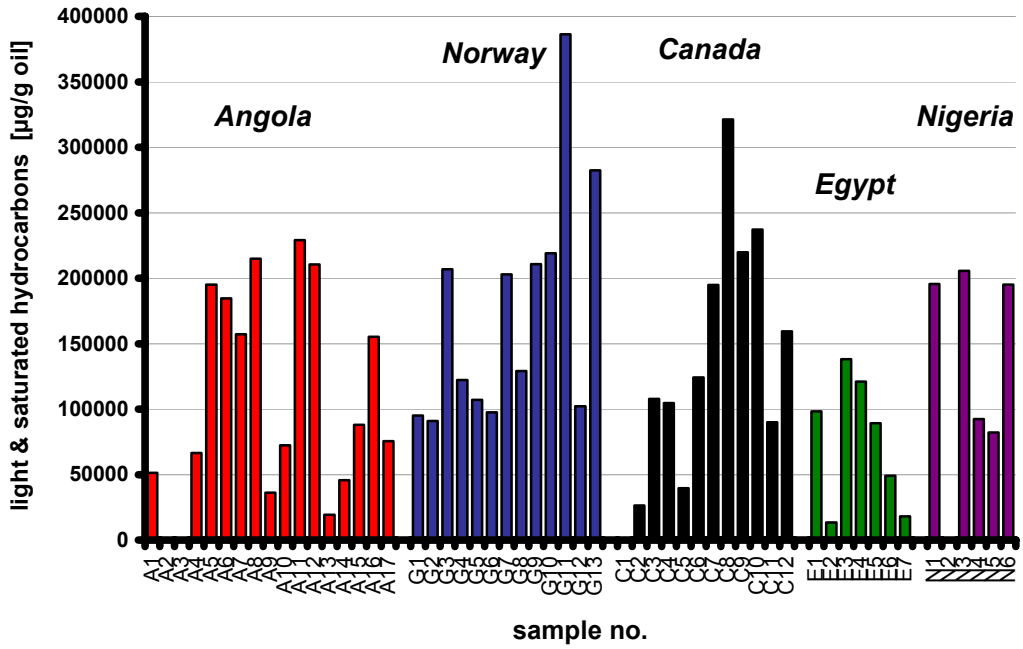

Fig. 30: Summed concentrations [µg/g oil] for light hydrocarbons and *n*-alkanes. In samples A2 and A3 from Angola as well as in sample C1 from Canada none of the compounds which are shown in Figure 20 were detected. Sample N2 from Nigeria contains light hydrocarbons, but no mid- and long-chain saturates (chromatogram shown in Figure X- 3 in the Appendix). Hence, the determination of concentrations which is based on the calculation via phytane was not possible.

All thermovaporisation chromatograms for the studied crude oils and the calculated concentrations [µg/g oil] for each resolved compound are provided in the Appendix (Part I). As indicated by the chromatograms in the Appendix, for 3 of the 55 investigated crude oils (A2, A3 and C1), light hydrocarbon and *n*-alkane parameters could not be determined because these petroleum constituents are absent in the samples. The lack of low molecular weight components and *n*-alkanes is due to pronounced biodegradation. These three crude oils would be marked as moderately to severely biodegraded. In contrast, all other crude oils contain significant amounts of light and saturated hydrocarbons indicating that these samples are either non-biodegraded or only slightly to moderately biodegraded (PETERS ET AL., 2005).

Although extensive literature on the effects of biodegradation has been published (e.g., PETERS ET AL., 2005), only little is known about the alterations of volumetrically important crude oil constituents occurring within initial stages of

biodegradation. Especially the impact of biodegradation on the distribution of low molecular weight hydrocarbons is not well understood even though biodegradation often results in a complete loss of these components. WELTE ET AL. (1982) used light hydrocarbons to describe different extents of biodegradation. They suggested that the preferential depletion of low molecular weight *n*-alkanes relative to branched and cyclic alkanes indicates ongoing biodegradation. The ratios *i*-pentane/*n*-pentane (*i*-C_5/*n*-C_5) and 3-methylpentane/*n*-hexane (3-mp/*n*-C_6) were proposed to illustrate proceeding extents of biodegradation by increasing values.

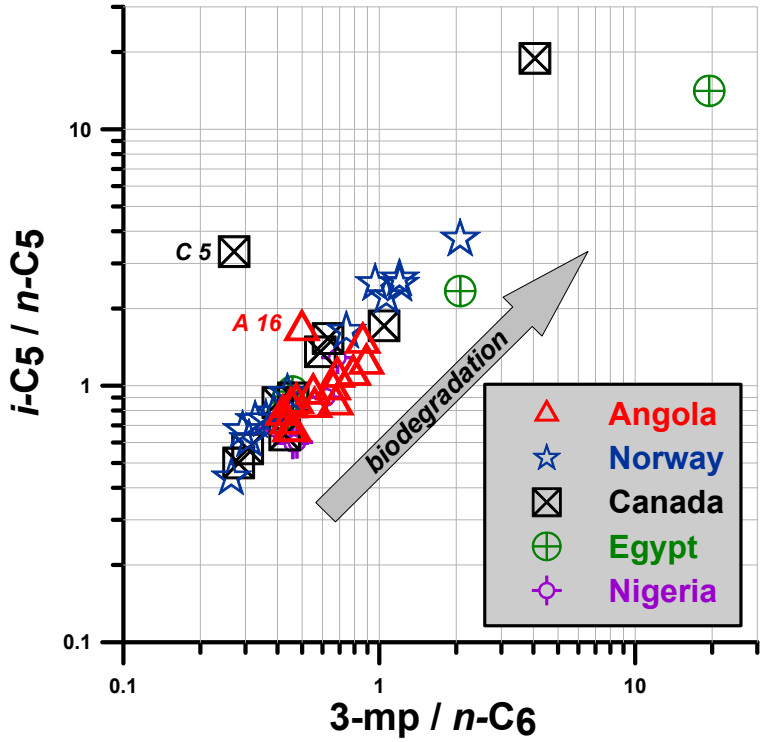

Fig. 31: Light hydrocarbon ratios displayed on a logarithmic scale indicating a preferential depletion of regular alkanes relative to branched alkanes (after WELTE ET AL., 1982) with increasing biodegradation.

Calculation of these two ratios for the crude oils investigated in this study reveals such a systematic increase of branched alkanes relative to normal alkanes and thus denotes various extents of biodegradation within each of the five individual sample sets (Figure 31). Highest concentration ratios for *i*-C_5/*n*-C_5 and 3-mp/*n*-C_6

were determined for crude oils from Egypt (E6, E7), Norway (G12) and Canada (C6) with values above 2.0 for both parameters. Generally, the ranges of concentration ratios shown in Figure 31 vary within each of the five subsets. These variable ranges for every subset describe individual slopes but differ only slightly. Interestingly, crude oils C5 from Canada and A16 from Angola do not follow the general trends of the slopes within the respective subsets. By comparison of the two largest sample sets from Angola (15 oils) and Norway (13 oils) the parameters shown in Figure 31 indicate that the crude oils from Norway cover the much broader range of biodegradation extent than the samples from Angola.

Another parameter which is based on light hydrocarbons and is used to characterise crude oils was suggested by THOMPSON (1978, 1983). In these publications the heptane and *iso*-heptane ratios (for definition of the ratios see description of Figure 32) were established. The parameters were originally used to evaluate thermal maturities. The author stated that increasing values could indicate higher oil generation temperatures. In addition to the application as maturity indicators GEORGE ET AL. (2002) suggested that the heptane and *iso*-heptane ratios could also be used as biodegradation parameters. They suggested that lower values may indicate higher alteration extents, which again is based on the assumption that normal alkanes are more susceptible to biodegradation than branched and cyclic alkanes and that the latter compounds are more recalcitrant to microbial processes than branched alkanes.

The heptane vs. *iso*-heptane ratios for crude oils investigated in this study are shown in the crossplot of Figure 32. The values indicate a brought range of maturities and/or biodegradation extents in the different sample sets. Crude oils from Angola and Norway as the two subsets with highest numbers of samples show a linear evolution for both ratios, however, with different slopes. In contrast, the oils from Canada are distributed more erratically. Interestingly, the samples from Egypt denote different trends for the two oil fields. Contrary to the biodegradation parameters suggested by WELTE ET AL. (1982) the heptane and *iso*-

heptane values indicate, following GEORGE ET AL. (2002), that at least three of the crude oils from Angola are more strongly biodegraded than any of the samples from Norway.

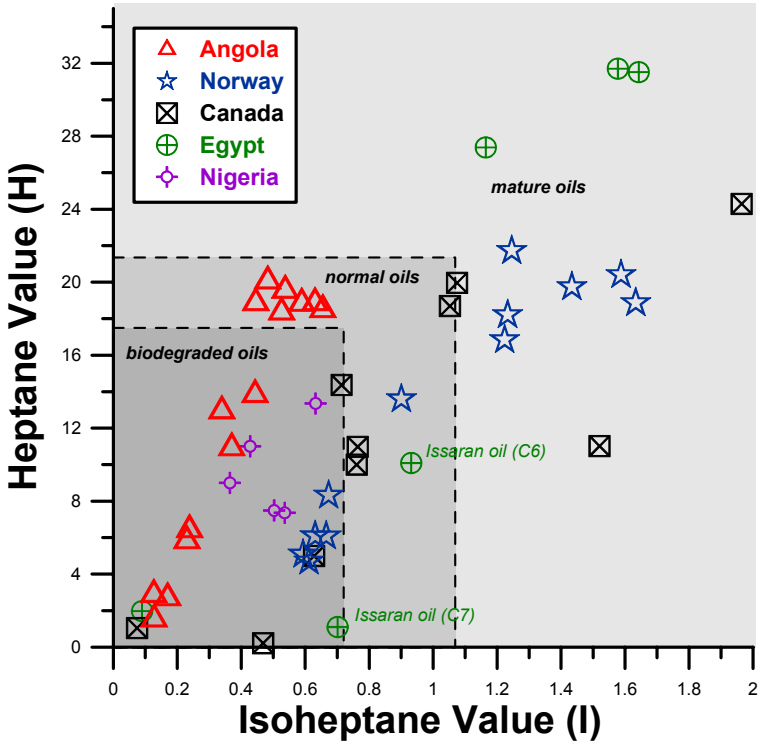

Fig. 32: Thompson (1983) Isoheptane Value (I) versus Heptane Value (H). I= (2mhex + 3mhex) / (c13dmcp + t13dmcp + t12dmcp); H= (100 x *n*-C_7) / (chex + 2mhex + 23dmp + 11dmcp + 3mhex + c13dmcp + t13dmcp + t12dmcp + 3ep + 224tmp + *n*-C_7 + mchex). See Table X- 1 for definition of abbreviations. Dashed boundaries and classifications in italics are adopted from GEORGE ET AL. (2002).

THOMPSON (1988) suggested the paraffinicity and aromaticity ratios to describe in-reservoir evaporative fractionation processes. Modified by TALUKDAR AND DOW (1990) the crossplot for both values can be used to describe several alteration processes in crude oils (see Figure 33). For samples investigated in this study the plot would suggest that a significant number of oils are affected by evaporative fractionation. Especially the samples from Norway show a significant increase of the aromaticity value indicating strong in-reservoir evaporative fractionation (THOMPSON, 1988).

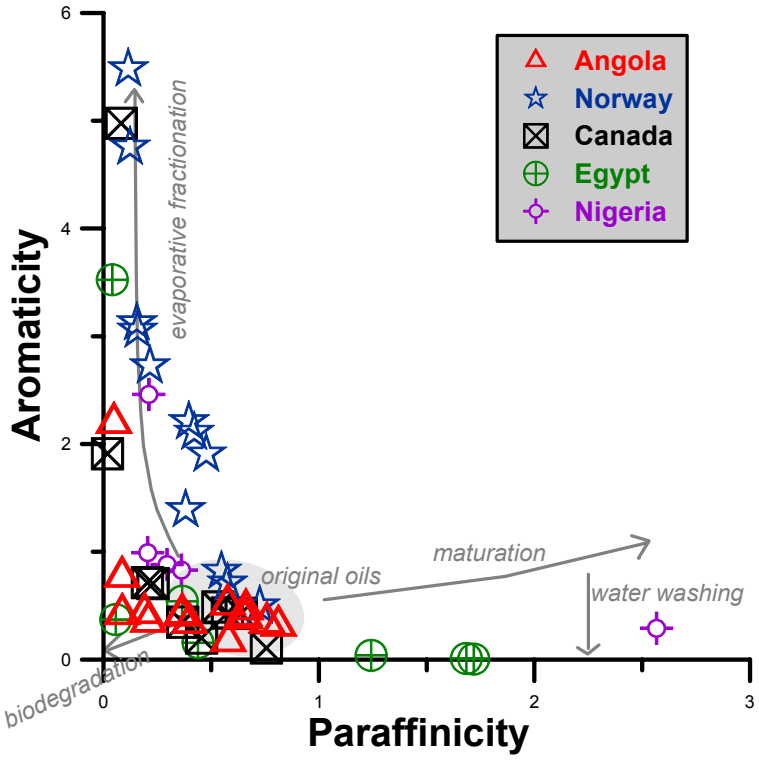

Fig. 33: Aromaticity (toluene/*n*-heptane) vs. paraffinicity (*n*-heptane/methylcyclohexane) plot (after THOMPSON, 1988); indicating several alteration processes (after TALUKDAR AND DOW, 1990)

However, this appears rather unlikely, because several studies (e.g. HORSTAD ET AL. 1992; VIETH AND WILKES, 2006) have proven that the crude oils from the Gullfaks area, offshore Norway are not significantly affected by other in-reservoir alteration processes than biodegradation. This may indicate that this type of plot with the assigned areas, which were established for crude oils from Trinidad (TALUKDAR AND DOW, 1990) is not suitable to characterise biodegraded oils from other petroleum systems.

As mentioned before, it is believed that microbial degradation affects preferentially regular alkanes relative to branched compounds (WELTE ET AL., 1982). Among several parameters which are based on this assumption, the most commonly used biodegradation indicator for initial to moderate alteration levels is the crossplot of Pr/*n*-C_{17} vs. Ph/*n*-C_{18}. These ratios are shown in the following

logarithmic plot which was also used by PETERS ET AL. (1999) for evaluations concerning oxicity and depositional environment of the source rock (Figure 34).

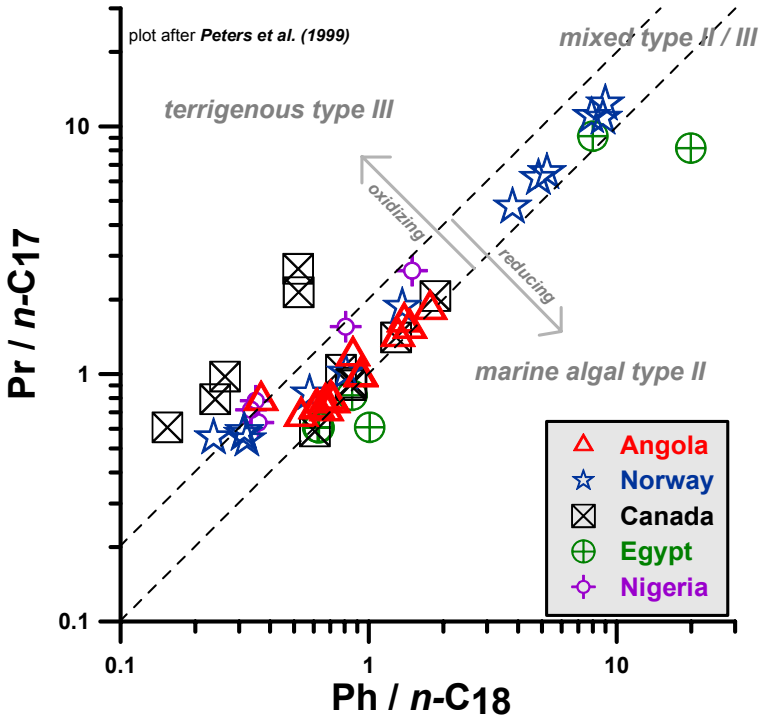

Fig. 34: Crossplot of the ratios Pr/*n*-C_{17} vs. Ph/*n*-C_{18} for crude oils of the entire sample set. Increasing values are commonly interpreted as indication for ongoing biodegradation. Following PETERS ET AL. (1999) the plot can be used to infer oxicity and organic matter type in the source rock depositional environment.

Figure 34 illustrates that the entire sample set covers a broad range of different alteration levels in terms of initial to moderate biodegradation. In particular the crude oils from Norway represent a biodegradation sequence with a broad variability of values. Moreover, the plot displays that the crude oils are probably derived from various depositional environments. Especially the oils from Canada obviously show a minimum of two different sources. In this plot Canadian samples from the Kumak and Arnak oil fields are clearly differentiated from those of the Tuktuk and Mayogiak reservoirs. Referring to the classification of PETERS ET AL. (1999), these samples (C6-C10) could be termed as terrestrially sourced oils while the samples from Tuktuk (C1-5) and Mayogiak (C11-C12) probably have source rock depositional environments with stronger marine influences.

Based on Figure 34 samples from the Issaran oil field in Egypt seem to have the strongest input of marine organic matter in their source rock depositional environments. All other investigated crude oils plot between these two areas, and hence are generated from mixed sources. Interestingly, only crude oil A16 from Angola does not fit to the general trend which is obvious for the other samples of this sequence. Based on Figure 34 this crude oil was likely generated from a source rock which contains enhanced amounts of terrestrial organic matter. Norwegian samples derived from the Brent Group show consistently higher Ph/*n*-C_{18} values than oils from other North Sea reservoir formations. This indicates that there is indeed a strong correlation of origin and Ph/*n*-C_{18} values. Evaluations concerning the oxicity of the depositional environment of the sourced organic matter are mainly based on the pristane and phytane amounts and can therefore also be described by the conventional Pr/Ph ratio.

Pristane and phytane are primarily derived from phytyl side chains of chlorophyll in phototrophic organisms. Under anoxic conditions predominantly phytane is formed, while oxic conditions favour the conversion of the phytyl side chain to pristane (DIDYK ET AL., 1978). Therefore, Pr/Ph ratios of oils or bitumens were also used to indicate the redox potential of source sediments (PETERS AND MOLDOWAN, 1993). Oxic conditions are indicated by Pr/Ph ratios >1, while values less than unity notify an anoxic deposition of the organic matter.

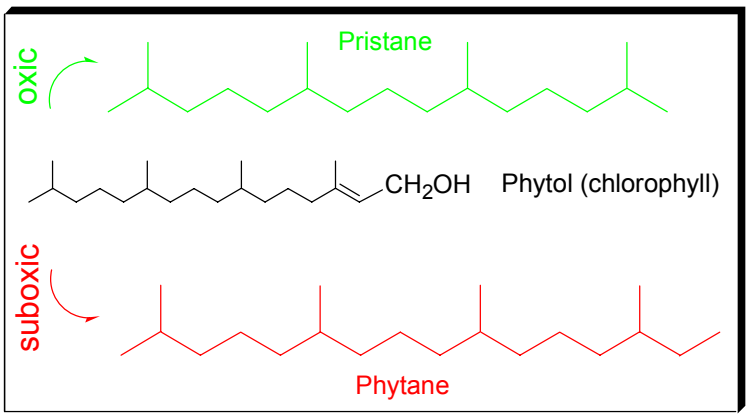

Fig. 35: Phytol is derived from the side chain of chlorophyll a and is a possible precursor for pristane and phytane. However, acyclic isoprenoids with 20 carbon atoms or less can also be derivatives of chlorophyll b, bacteriochlorophyll a, tocopherols, archaeal membrane components and other biomolecules.

But it has also to be mentioned that the application of this parameter should be used cautiously, because pristane and phytane are not only derived from the chlorophyll a side chain. It was shown that phytane could also be derived from methanogenous and halophile phytanyllipid sources and that zooplankton and tocopherol (Vitamin E) could be precursors for pristane (GOOSSENS ET AL., 1984, TEN HAVEN ET AL., 1987, FRIMMEL ET AL., 2004). Moreover TEN HAVEN ET AL. (1987) showed that thermal maturity could affect the Pr/Ph ratio. However, the Pr/Ph ratio is a widely applied parameter and therefore also used in this study to estimate possible differences in the oxicity of the accumulation regime of the organic matter in the source rocks. The Pr/Ph ratio for crude oils investigated in this study is displayed in Figure 36.

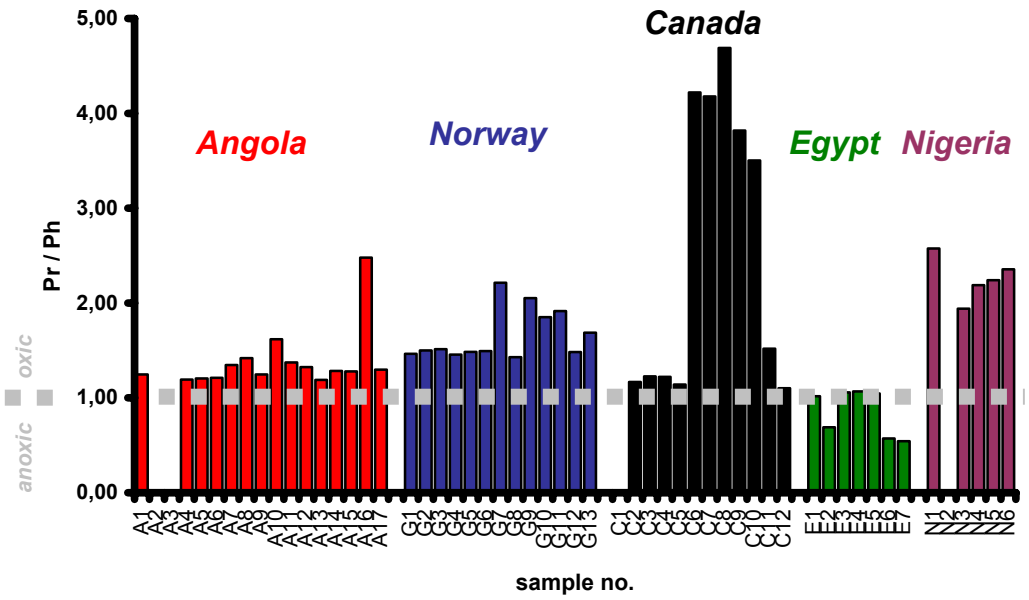

Fig. 36: Pristane/Phytane ratios for the investigated crude oils from Angola (red), Norway (blue), Canada (black), Egypt (green) and Nigeria (purple). The dashed grey horizontal line delineates redox potentials of the source sediments. In broad terms, values >1 indicate oxic conditions, ratios less than unity notify anoxic regimes. Due to a high biodegradation level and the lack of isoprenoids no values for samples A2, A3, C1 and N2 can be displayed.

Only three samples show ratios <1 indicating an anoxic regime. In accordance with Figure 34 these samples are again the crude oils from the Issaran oil field in Egypt (E6-E7) plus one oil from the Sudr field (E2). Highest values (>3.5) have

been determined for samples from the Kumak and Arnak oil fields in Canada (C6-C10). These samples also plot clearly in the terrigeneous zone of Figure 34. The Norwegian oils derived from the Brent Formation are separated from those of other reservoir formations by slightly reduced Pr/Ph values. A relatively low phytane value in sample A16 from Angola is responsible for the high Pr/Ph ratio, which separates this oil from the remaining sample set and indicates a higher terrestrial input. Relatively high Pr/Ph ratios indicating higher percentages of continentally derived organic matter were also observed for the oils from Nigeria. Due to the pronounced biodegradation extent in samples A2, A3 from Angola, C1 from Canada and N2 from Nigeria no Pr/Ph ratio could be determined because the isoprenoids are absent.

5.1.2 Aromatic hydrocarbon parameters

Aromatic hydrocarbons are a class of organic compounds which have been widely used to characterise the thermal maturity of source rock bitumens and oils (ALEXANDER ET AL., 1985; RADKE, 1988; BUDZINSKI ET AL., 1995). Especially, the distribution of different isomers of alkylnaphthalenes and alkylphenanthrenes have been used to assess maturities. The abundance and distribution of this compound class in crude oils and rock extracts is also indicative for the origin of the organic matter (HUGHES ET AL., 1995; HUANG AND PEARSON, 1999). Moreover, numerous authors stated that the distribution of aromatic hydrocarbons depends on the extent of biodegradation (CONNAN, 1984; VOLKMAN ET AL., 1984, ROWLAND ET AL, 1986; FISHER ET AL., 1998; BUDZINSKI ET AL., 1998).

This chapter describes the occurrence of aromatic hydrocarbon in the investigated crude oils. It is illustrated that alkylbenzenes, alkylnaphthalenes, alkylphenanthrenes and alkyldibenzothiophenes are volumetrically relevant petroleum compounds and therefore important targets within this study. Some selected aromatic hydrocarbon parameters which are discussed in the literature

mentioned above are used to further characterise the crude oils. However, the detailed consideration of biodegradation effects on the individual aromatic hydrocarbons is discussed in chapter 6. The calculations of concentrations [µg/g] are based on GC-MS measurements of the aromatic fraction seperated by MPLC. In total, 103 individual aromatic hydrocarbons were identified belonging to the 4 different subgroups of alkylbenzenes, alkylnaphthalenes, alkylphenanthrenes and alkyldibenzothiophenes. Summed concentrations for all identified aromatic hydrocarbons in all investigated crude oils are shown Figure 37.

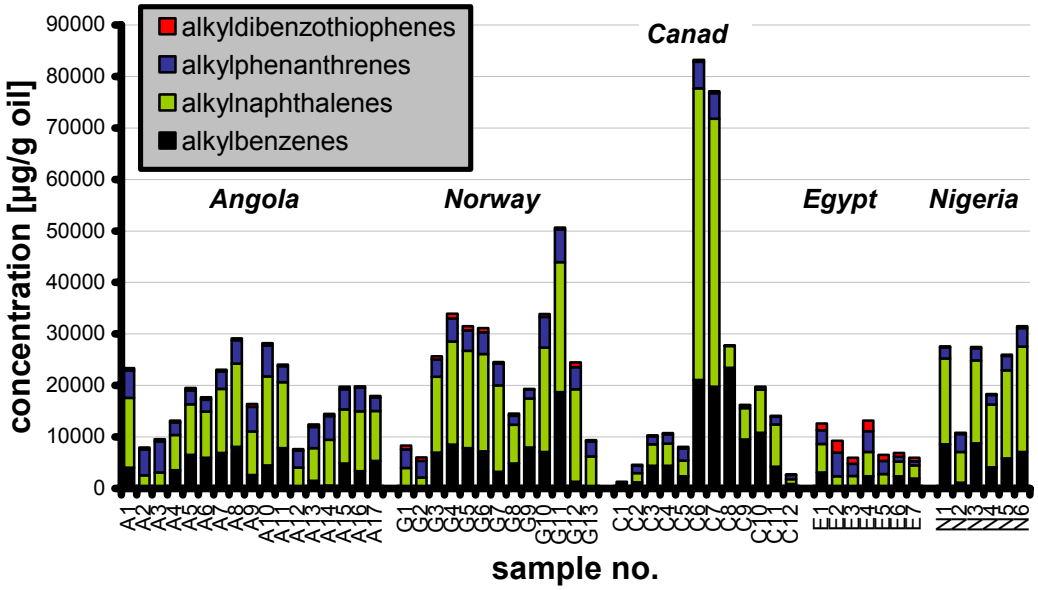

Fig. 37: Summed concentrations of the four volumetrically most important aromatic hydrocarbons subgroups in crude oils from Angola, Norway, Canada, Egypt and Nigeria. For each sample the concentrations of alkylbenzenes, alkylnaphthalenes, alkylphenanthrenes and alkyldibenzothiophenes are shown by the stacked bars.

Highest concentrations were measured for the crude oils C6 and C7 from the Kumak oil field in Canada with 85 and 79 mg/g oil, respectively. Also the condensate sample G11 from Norway is characterised by a relative high amount of aromatic hydrocarbons with 53 mg/g oil. For all other crude oils the concentrations are below 35 mg/g oil. Lowest concentrations were determined for crude oils C1, C2 and C12 from Canada with 1.3, 4.6 and 2.8 mg/g oil, respectively. As it was already shown for light and saturated hydrocarbons also the concentrations of aromatics vary significantly within each of the five

petroleum systems. Interestingly, these variations are not exclusively attributed to the different oil fields within each petroleum system.

The most commonly used parameter to assess thermal maturities in crude oils and source rocks which is based on aromatic hydrocarbons is the Methylphenanthrene Index (MPI) established by RADKE AND WELTE (1981). The distribution of methylphenanthrenes in the source is controlled by the thermal maturity in the approximate range of 0.6 % - 1.7 % vitrinite reflectance. MPI-1 values in crude oils increase with increasing maturity, because the thermally less stable α-isomers 1-methylphenanthrene (1-MP) and 9-methylphenanthrene (9-MP) are in the denominator, while the intermediately stable β-isomers 2-methylphenanthrene (2-MP) and 3-methylphenanthrene (3-MP) are in the numerator of the equation (PETERS ET AL., 2005) which is shown in Figure 38. In this plot MPI-1 values and calculated vitrinite reflectances for all investigated crude oils are shown. Due to the lack of methylphenanthrenes in sample C1 from Canada no values for MPI-1 and $\%R_C$ can be given. The highest inferred vitrinite reflectance with $\%R_C = 1.6$ was calculated for the condensate sample G11 from the Gullfaks Gamma field in Norway. Within the Norwegian sample set $\%R_C$ values show variations with a total range from 0.74 to 1.60. For the eight samples from the Gullfaks field (G1-G6; G12 –G13) only very slight variances for calculated vitrinite reflectances with values ranging from $\%R_C = 0.83$ to 0.86 were defined. This indicates a high similarity of thermal maturities in the source rock for oils sampled in the Gullfaks field. Only slight differences of thermal maturities as indicated by calculated vitrinite reflectances were also observed for crude oils from Angola ($\%R_C = 0.86$ - 1.00), Egypt ($\%R_C = 0.92$ - 0.99) and Nigeria ($\%R_C = 0.92$ - 1.00). In contrast, crude oils from Canada are characterised by the broadest range in calculated vitrinite reflectances with $\%R_C$ values in the range of 0.66 up to 1.17. Even within the different Canadian reservoirs, the crude oils show clear differences for the MPI-1 and the corresponding inferred vitrinite reflectances, e.g. the Tuktuk oils (C1-C5) have $\%R_C$ values in the range of 0.75 – 1.17.

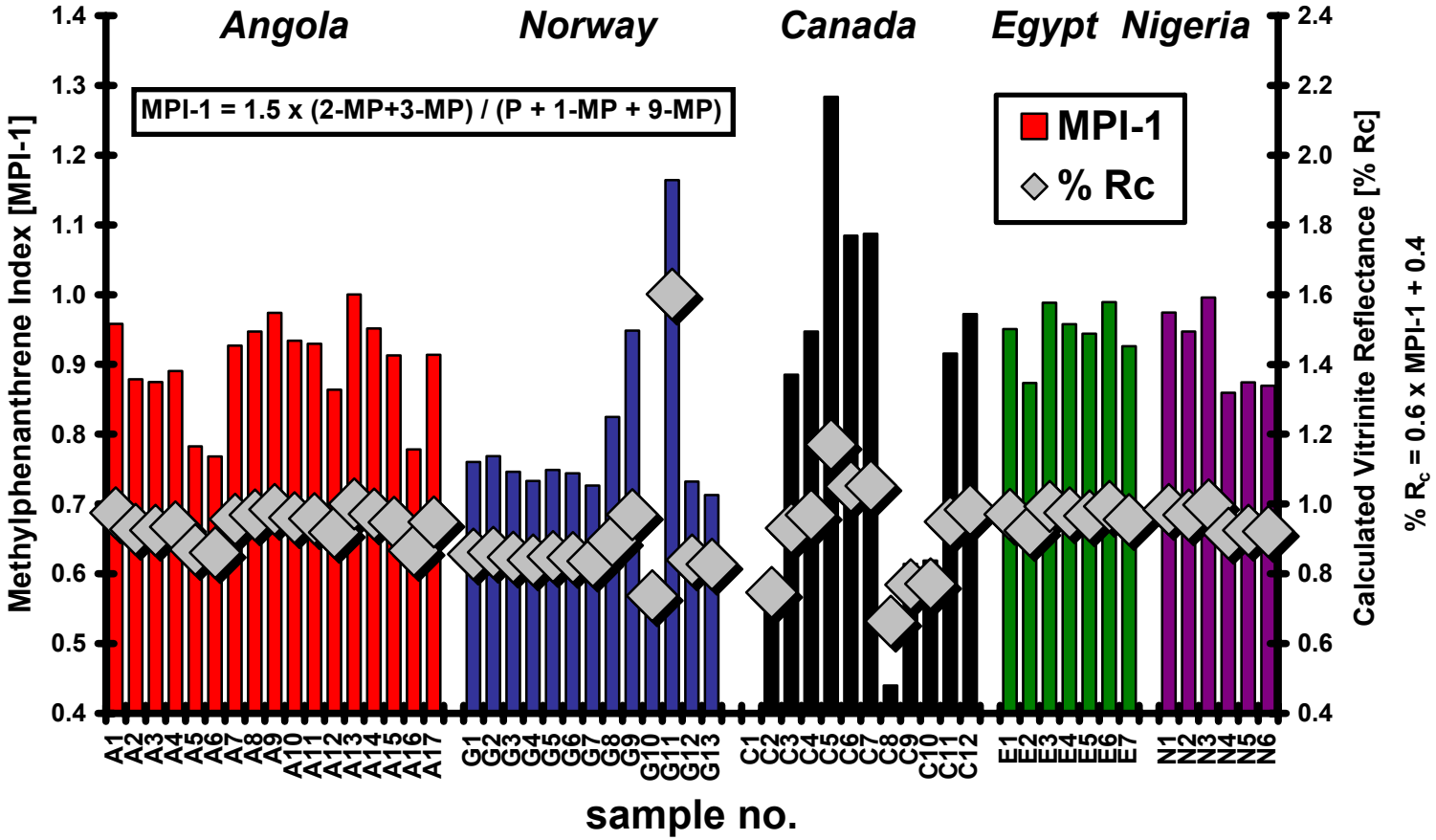

Fig. 38: The coloured bars display values of the Methylphenanthrene Index [MPI-1] in all investigated crude oils. The MPI-1 is calculated by the formula given in the plot. Grey diamonds indicate calculated Vitrinite Reflectances [% R_C] which are inferred from MPI-1 values by the formula given beside the 2nd y-axis. The R_C value for the condensate sample from (G11) from Norway was calculated using R_C=-0.6xMPI+2.3 relevant for condensates and wet gases as described in PETERS ET AL. (2005). For the sample C1 from Canada no value can be displayed because all four isomers of methylphenanthrenes lack in this oil.

Another widely applied molecular parameter which is based on hydrocarbons which eluted in the aromatic fraction is the dibenzothiophene to phenanthrene ratio (DBT/Phen). This parameter plotted versus the pristane to phytane ratio (Pr/Ph) was used by HUGHES ET AL. (1995) to infer source rock depositional environments and lithologies by analysing crude oils. This study showed that the DBT/Phen ratio is an excellent indicator of source rock lithology, with carbonates having ratios > 1 and shales showing ratios < 1. The DBT/Phen ratio portrays the availability of reduced sulphur for incorporation into the organic matter. Consequently, increased dibenzothiophene amounts represent relatively high sulphur incorporation. Following HUGHES ET AL. (1995) the crossplot of DBT/Phen versus Pr/Ph can be used to classify crude oils into the 5 different depositional environment / lithology groups: marine carbonate; marine carbonate/mixed and lacustrine sulphate-rich; lacustrine sulphate-poor; marine and lacustrine shale; and fluvial/deltaic carbonaceous shale and coal.

The crossplot of DBT/Phen versus Pr/Ph applied for crude oils investigated in this study is shown Figure 39. The Pr/Ph ratio was already discussed before and shows highest values for crude oils from the Tuktuk and Arnak reservoirs in Canada indicating a significant input of terrestrial organic matter in source rock depositional environment. This correlates to the classification suggested by HUGHES ET AL. (1995) which suggests that the organic matter from which these 5 crude oils were expelled was deposited in a fluvial/deltaic environment typically being terrestrially influenced. Lowest Pr/Ph ratios with values < 1 were determined for crude oils from Egypt denoting to an anoxic depositional regime. These samples show also the highest DBT/Phen ratios with values close to unity or > 1 for the two crude oils from the Issaran reservoir. This correlates to the general petroleum system geology which was described in chapter 4.3. Here it was already mentioned that the crude oils from Egypt were likely generated from marine carbonate source rocks, which are typically characterised by high sulphur contents. Such high sulphur contents are generally accompanied by increased alkyldibenzothiophene concentrations. As mentioned before this type of aromatic hydrocarbons bear a sulphur atom in their aromatic structure ($C_{12}H_8S$). For all

other samples DBT/Phen ratios were determined with values clearly below unity. This may indicate (HUGHES ET AL., 1995) that these oils were generated from shaly source rocks.

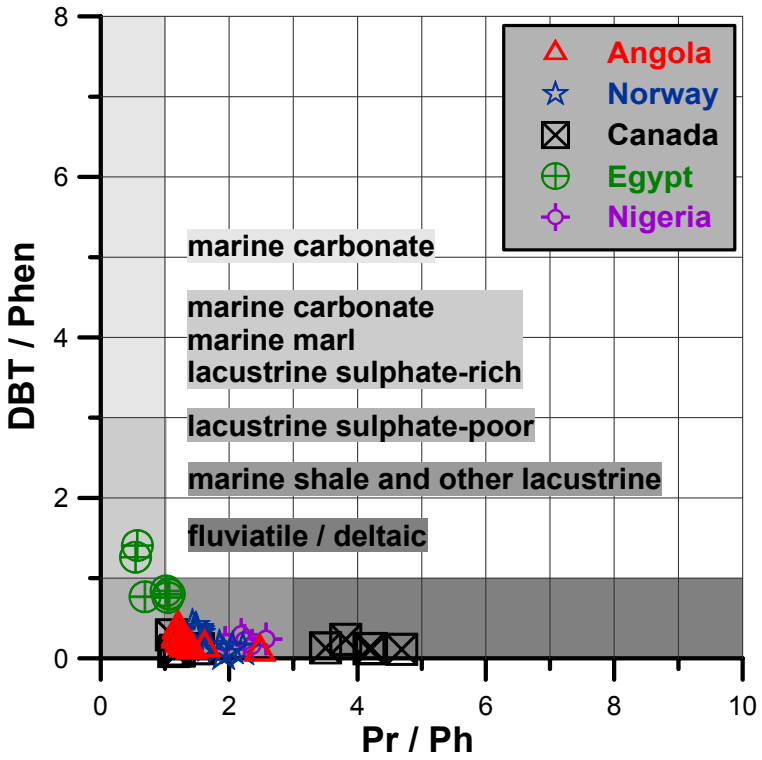

Fig. 39: Dibenzothiophene to phenanthrene (DBT/Phen) plotted vs. the pristane/phytane (Pr/Ph) ratio. The crossplot was suggested by HUGHES ET AL. (1995) to distinguish source rock depositional environments.

Aromatic hydrocarbons are also used to assess the extent of biodegradation in crude oils. Various publications (e.g., CONNAN, 1984; VOLKMAN ET AL., 1984, ROWLAND ET AL, 1986; BUDZINSKI ET AL., 1998) used different aromatic compounds to describe microbially caused alterations in petroleum reservoirs. In addition to these studies FISHER ET AL. (1998) suggested that, e.g., the distribution of different alkylnaphthalene isomers characterises the alteration level in crude oils, even within the very initial stages of biodegradation. Hence, this type of aromatic compounds may also be used to assess the extent of biodegradation in the crude oils investigated in this study. The authors showed that in crude oils from Australia 1,6-dimethylnaphthalene is more susceptible to microbial attack than 1,5-dimethylnaphthalene. Consequently, decreasing values of the ratio 1,6- /

1,5- dimethylnaphthalene (DBR) may indicate higher extents of biodegradation. In the same study it was also proposed that individual isomers of trimethylnaphthalenes are biodegraded to different extents. The authors showed that in the Australian samples the isomer 1,2,4-trimethylnaphthalene is more recalcitrant to biodegradation than 1,3,6-trimethylnaphthalene. Consequently, the ratio 1,3,6- / 1,2,4- trimethylnaphthalene (TBR) also decreases with ongoing biodegradation. The crossplot of both ratios suggested by FISHER ET AL. (1998) applied for the sample set investigated in this study is shown in Figure 40.

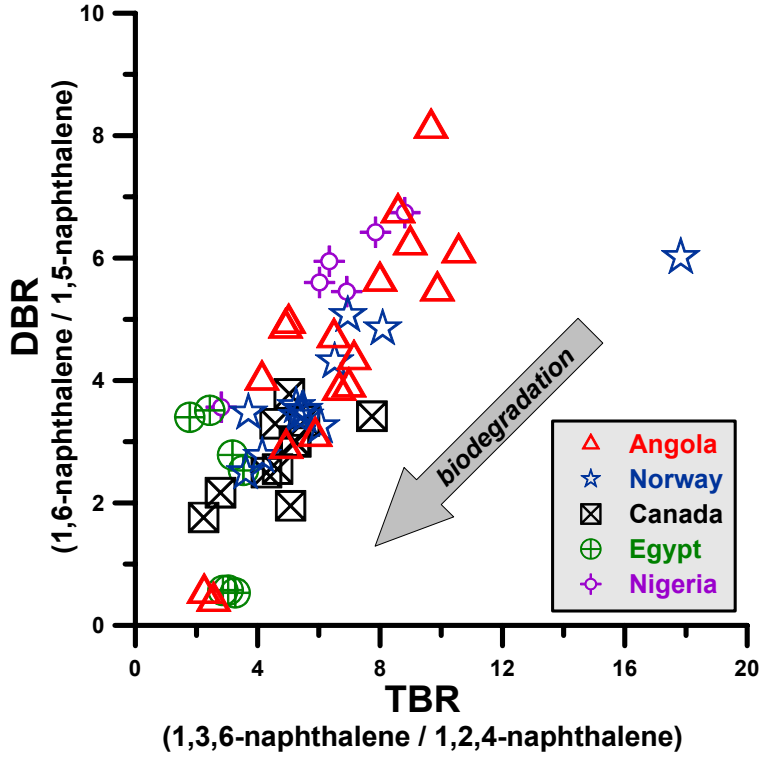

Fig. 40: The crossplot shows the DBR vs. the TBR ratios suggested by FISHER ET AL. (1998). Decreasing values may indicate ongoing biodegradation.

The DBR plotted over the TBR ratio shows a good correlation and a significant shift for both ratios in the investigated samples. Only the condensate sample from Norway (C11), represented by the highest TBR does not follow the general trend of all other crude oils. The broad shift of DBR and TBR values implies that these specific individual isomers of alkylnaphthalenes are altered to different extents in all samples from the 5 petroleum systems. However, crude oils from Egypt show

a clear shift only for the DBR, which is based on dimethylnaphthalenes. In contrast, the TBR shows no significant variations in these oils. Interestingly, the broadest range of DBR and TBR values is determined for samples from Angola. Hence, it would be assumed that crude oils from Angola cover the broadest range of biodegradation extents in the five sample sets. This is contrary to the biodegradation parameters based on light and saturated hydrocarbons (*i*-C_5/*n*-C_5; 3-mp/*n*-C_6 and Pr/*n*-C_{17}; Ph/*n*-C_{18}) discussed in chapter 5.1.1 which suggest that the Norwegian crude oils show the broadest shift of alteration extents. However, it has to be mentioned that maturity differences may have an impact on the distribution of aromatic hydrocarbons. Therefore, it can not be excluded that especially for the crude oils from Canada, which are characterised by the highest variations in MPI-1 values, biodegradation is not the only factor controlling the abundance of aromatic hydrocarbons.

Another parameter inferred from GC-MS measurements which is based on aromatic hydrocarbons is the ratio of triaromatic steroids (TA) over monoaromatic steroids (MA). This ratio is used to assess crude oil maturities. Increasing thermal exposure causes an aromatization of C-ring monoaromatic steroids to ABC-ring triaromatic steroids. The catagenetic process involves the loss of a methyl group at the A/B ring junction. Thus, maturation of monoaromatic steroids leads to the generation of triaromatic steroids with one less carbon atom (PETERS ET AL., 2005) as illustrated in Figure 41.

The TA / (TA+MA) ratio increases from 0 to 100% during thermal maturation. Among several different definitions of the TA / (TA+MA) ratios reported in the literature, PETERS ET AL. (2005) suggested that the parameter should include the major C_{29} monoaromatic steroids which are labelled in Figure 26 with the peak numbers 9, 10, 12 and 13. The same study also proposed that triaromatic steroids should be represented in the ratio by compounds labelled in Figure 27 with the peak numbers 6 and 9. The calculated TA / (TA+MA) ratios for crude oils investigated in this study are shown in Figure 42.

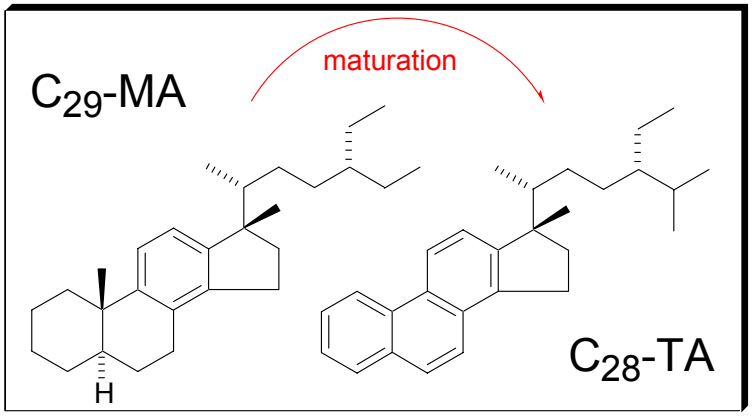

Fig. 41: During thermal maturation C_{29}-monoaromatic (MA) steroids are converted to C_{28}-triaromatic steroids.

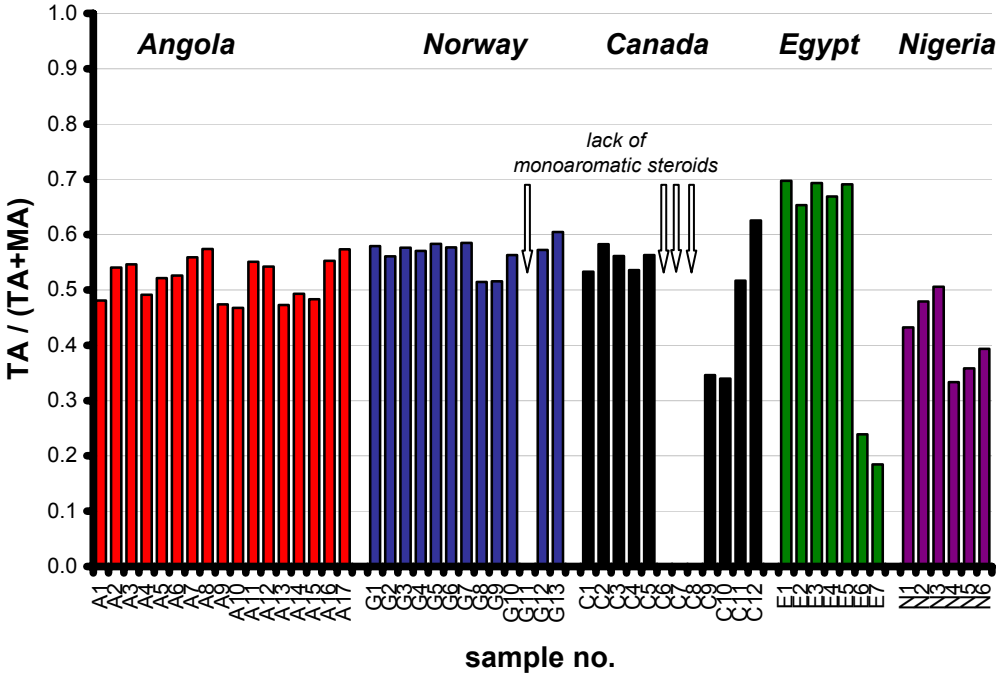

Fig. 42: The ratio of triaromatic steroids (TA) over monoaromatic steroids (MA) indicates increasing thermal maturity by higher values.

The thermal maturities indicated by aromatic steroids do not change significantly within the subsets from Angola and Norway. Especially crude oils from the Gullfaks field (G1-G6, G12-G13) in Norway show very slight differences in the TA / (TA+MA) ratio. For samples from Canada the aromatic steroids suggest that thermal maturities are rather constant within each of the different reservoirs. Contrary to the MPI-1 discussed earlier the TA / (TA+MA) ratio indicates that

oils from the Tuktuk reservoir (C1-C5) are characterised by only slight differences in thermal maturities. Concentrations for monoaromatic steroids in samples C6-C8 are below the detection limit and therefore no TA / (TA+MA) ratios can be displayed. The samples from Egypt are clearly separated by the two reservoirs. Here, samples from the Issaran field (E6-E7) show clearly lower TA / (TA+MA) ratios than the crude oils from the Sudr field (E1-E5). The sample set from Nigeria is also characterised by slightly higher TA / (TA+MA) ratios for crude oils from reservoir X (N1-3) compared to values for the samples derived from reservoir Y (N4-N6).

5.1.3 Terpane biomarker parameters

Terpanes are derived from the acyclic squalene ($C_{30}H_{50}$) present in lipids of living organisms. Important subgroups of such triterpanes are the tetracyclic steranes and the pentacyclic hopanes. PETERS AND MOLDOWAN (1993) and WENGER ET AL. (2001) have discussed that hopanes and steranes are not altered prior to heavy stages of biodegradation. As shown in chapter 5.1.1 in 51 of the 55 investigated crude oils light hydrocarbons and n-alkanes are abundant. Therefore, these 51 crude oil samples have not exceeded moderate alteration levels. Hence, the distributions of terpane biomarkers are likely not affected in the great majority of the investigated crude oils and thus can be used as reliable indicators for, e.g., facies/depositional environment and thermal maturity. The measurements of hopanes and steranes were performed by GC-MS-MS experiments on the aliphatic fraction yielded by MPLC separation. Due to the detection mode (MRM) for hopanes and steranes the total concentrations [µ/g oil] were not determined; therefore evaluations are based on relative abundances.

5.1.3.1 Hopanes

Hopanes are pentacyclic triterpanes generally derived from membrane lipids of bacteria. Such bacterial derivatives reflect source rock depositional environments, type of organic matter input and thermal maturities. This group of biomarkers can easily be identified by the molecular fingerprint *m/z* 191. The molecular structure of hopanes is shown in Figure 43.

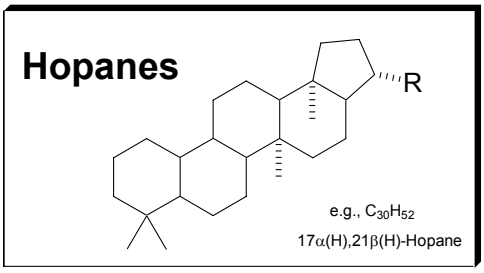

Fig. 43: Molecular structure of hopanes

According to VOLKMAN ET AL. (1984) and PHILP AND GILBERT (1986), 17α(H)-diahopane (X-C_{30}) is a possible terrestrial marker because of its presence in coals and terrestrially sourced oils. Although PETERS AND MOLDOWAN (1993) stated that this compound is also derived from bacterial input into sediments rich in clays and deposited under oxic to suboxic conditions, they also mentioned that source rocks rich in terrestrial organic matter are often accumulated in exactly these depositional environments. They suggested the ratio 17α(H)-diahopane/18α(H)-norneohopane (X-C_{30}/C_{29}Ts) to distinguish oils which originate from shales deposited under oxic-suboxic conditions from those derived from source rocks accumulated in anoxic regimes. The molecule structure for 17α(H)-diahopane and 18α(H)-norneohopane are shown in Figure 44.

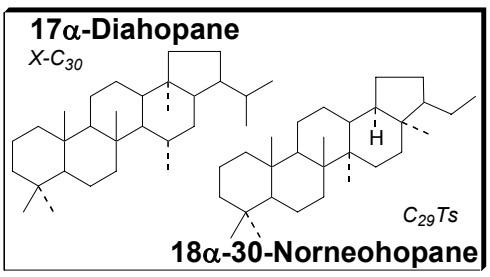

Fig. 44: Molecule structures for 17α(H)-diahopane (X-C_{30}) and 18α(H)-norneohopane (C_{29}Ts).

It was also pointed out that the ratio possibly increases with increasing thermal maturities, particularly for oils generated at high temperatures. However, in general lower ratios of X-C_{30}/C_{29}Ts may indicate stronger anoxic conditions. Figure 45 shows the X-C_{30}/C_{29}Ts ratio to differentiate depositional environments in the investigated sample sets.

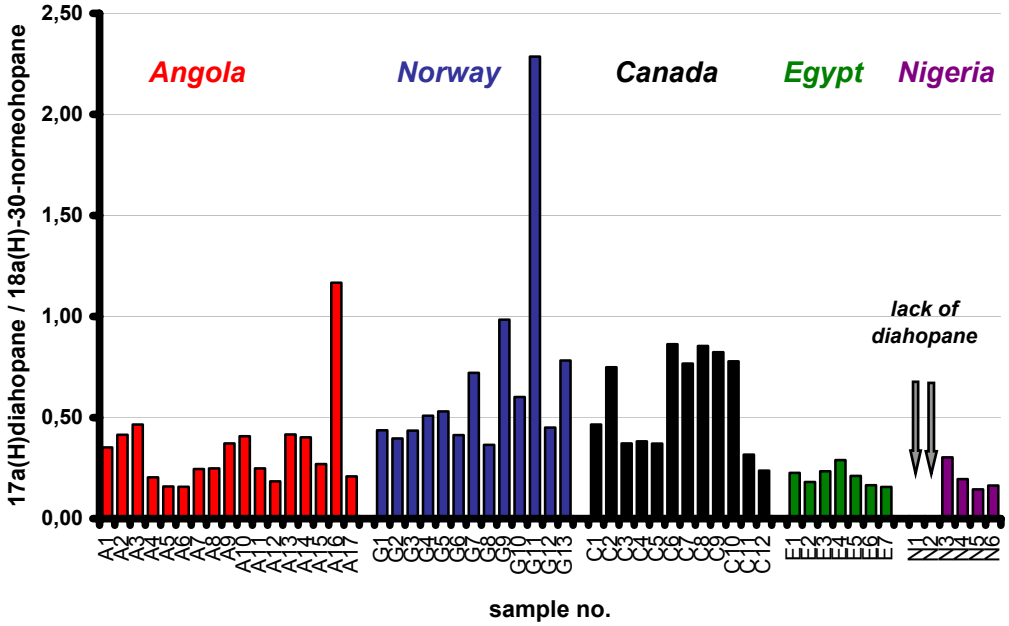

Fig. 45: Plot displaying the 17α(H)-diahopane/18α(H)-norneohopane (X-C_{30}/C_{29}Ts) ratios which were suggested by PETERS AND MOLDOWAN (1993) in order to distinguish different depositional environments. Oils derived from source rocks deposited under anoxic conditions show lower values than those accumulated under oxic-suboxic conditions often accompanied by high terrestrial inputs. Due to the absence of 17α(H)-diahopane no values can be displayed for samples N1 and N2 from Nigeria.

Highest X-C_{30}/C_{29}Ts ratios were calculated for one crude oil from Angola (A16) and the condensate from Norway (G11). These two samples are clearly separated from the rest of the respective subsets, which could refer to a deviant source. However, the condensate sample is characterised by a high thermal maturity, as indicated by the MPI-1, which might have also affected the X-C_{30}/C_{29}Ts ratio. Lowest values are determined for crude oils from Egypt and Nigeria denoting to an anoxic regime of the depositional environment. Interestingly, samples from the Kumak and Arnak oil fields in Canada show enhanced X-C_{30}/C_{29}Ts ratios compared to those from the other oil fields in the Mackenzie-Delta. Only sample

C2 shows a relative enrichment of 17α(H)-diahopane relative to the other oils from the Tuktuk (C1-C5) and Mayogiak (C11-C12) reservoirs. Interestingly, the values for Norwegian crude oils derived from the reservoirs located in the Statfjord Formation (G7, G10) and the Dunlin Group (G11, G13) are higher compared to the samples which originate from reservoirs in the Brent Formation, suggesting a higher terrestrial input to the source rocks of the satellites.

Another often applied hopane parameter is the Ts/(Ts+Tm) ratio which is thought to be both maturity- and source-dependent (PETERS AND MOLDOWAN, 1993). The stability of Tm (17α(H)-22,29,30-trinorhopane) during catagenesis is lower compared to Ts (18α(H)-22,29,30-trinorneohopane) and therefore the ratio may indicate different source rock maturities. The molecular structures of these hopanes are shown in Figure 46. An overview of the Ts/(Ts+Tm) ratios in the samples under study is given in Figure 47.

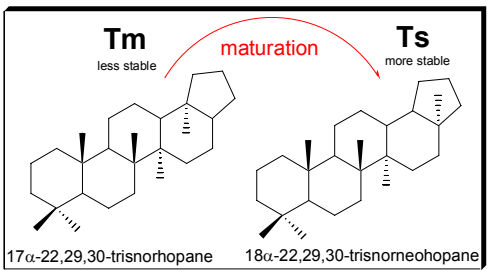

Fig. 46: Molecular structures of 17α(H)-22,29,30-trinorhopane (Tm) and 8α(H)-22,29,30-trinorneohopane (Ts).

Considering the different reservoirs within the five sample sets no significant differences in Ts/(Ts+Tm) can be observed. The highest value was observed for the condensate from Norway (G11) which originates from a drilling depth of 4020 m. Crude oils derived from reservoirs in the Brent Formation show almost constant values indicating similar depositional regimes and thermal maturities. This is also noticeable for the entire sample set from Angola where no significant changes in Ts/(Ts+Tm) values are obvious. Crude oils from Egypt show a difference between the samples from the Issaran (E6-E7) and oils from the Sudr oil field (E1-E5) with higher values for the latter reservoir. This observation is adaptable to the samples from Canada where crude oils from Arnak (C6-C8) and Kumak (C9-C10) reservoirs have lower Ts/(Ts+Tm) values than those from

Tuktuk (C1-C5) and Mayogiak (C11-C12). Except the condensate from Norway, it seems that differences in this parameter are due to the origin of the crude oil but not to significant differences of maturities within a sample set.

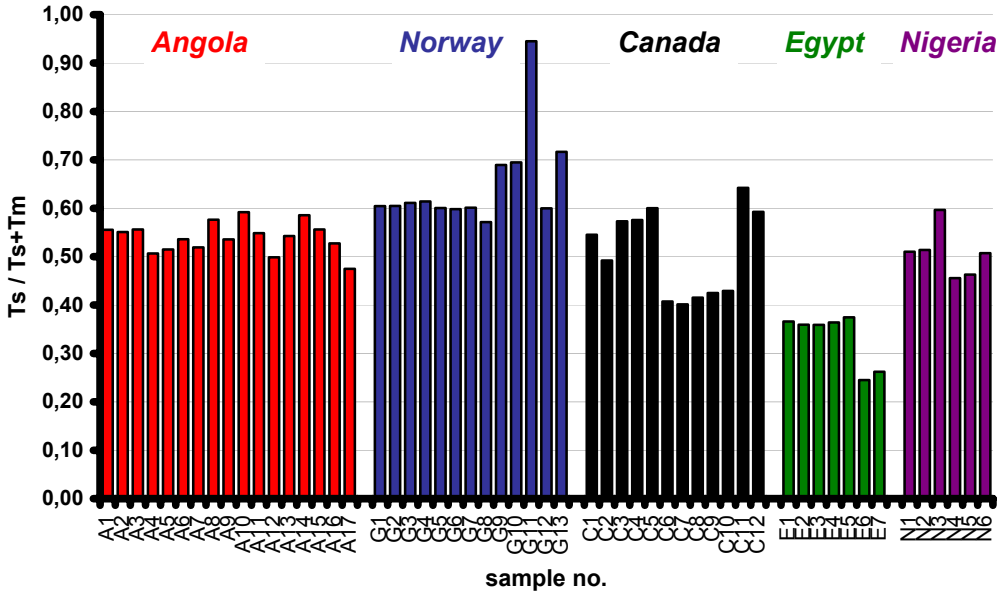

Fig. 47: Plot displays the Ts/(Ts+Tm) ratio for all investigated crude oils. The parameter is thought to be rather source than maturity-dependent (BAKR AND WILKES, 2002).

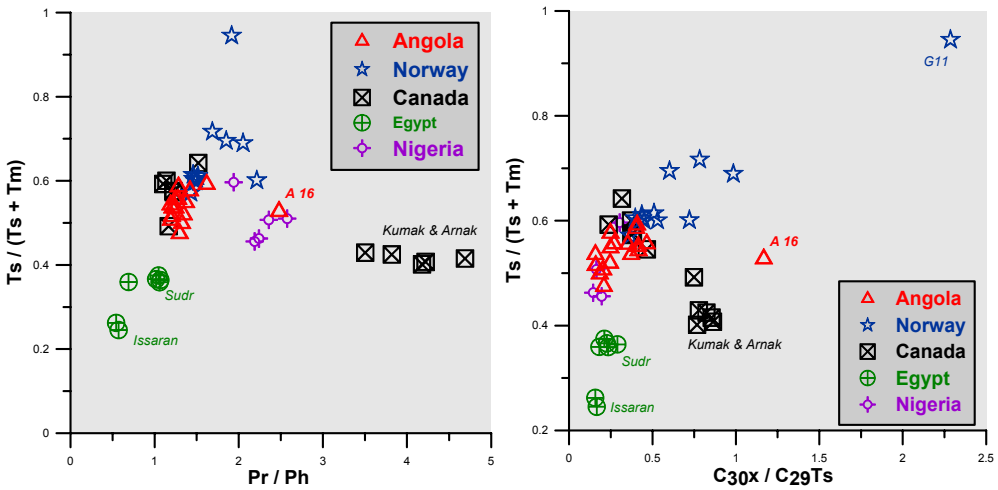

Fig. 48 (left): Crossplots of Ts/(Ts+Tm) vs. the Pr/Ph ratio. Low values indicate anoxic conditions in the depositional environment of the source rocks. **Fig. 49 (right):** Crossplots of Ts/(Ts+Tm) vs. 17α(H)-diahopane/18α(H)-norneohopane (X-C_{30}/C_{29}Ts). Low values indicate anoxic conditions in the depositional environment of the source rocks.

This observation was also made by BAKR AND WILKES (2002) who stated that the biomarker parameter (Ts/Ts+Tm) is controlled by variations of facies and

depositional environment but not by variances of petroleum maturities in the petroleum systems of the Gulf of Suez. The dependence of the Ts/(Ts+Tm) to the depositional environment is also approved by a crossplot of Ts/(Ts+Tm) versus Pr/Ph (Figure 48) and the crossplot of Ts/(Ts+Tm) versus X-C_{30}/C_{29}Ts (Figure 49). In these plots lowest Ts/(Ts+Tm) ratios for oils from Egypt correlate to lowest Pr/Ph and X-C_{30}/C_{29}Ts values likely indicating anoxic conditions in the depositional environment.

The ratio 17β(H),21α(H)-hopane (moretane) to 17α(H),21β(H)-hopane (hopane) decreases with increasing thermal maturity. Both moretanes and hopanes are formed during diagenesis, but the more labile moretane decreases faster during catagenesis relative to its αβ-equivalent (PETERS AND MOLDOWAN, 1993). Values usually vary from 0.8 in immature bitumens to 0.15 in mature source rocks and oils to a minimum of 0.05. In Figure 50 the moretane/hopane ratio is shown on a logarithmic scale for 54 crude oils. Due to the absence of moretane no value is displayed for the condensate sample G11 from Norway.

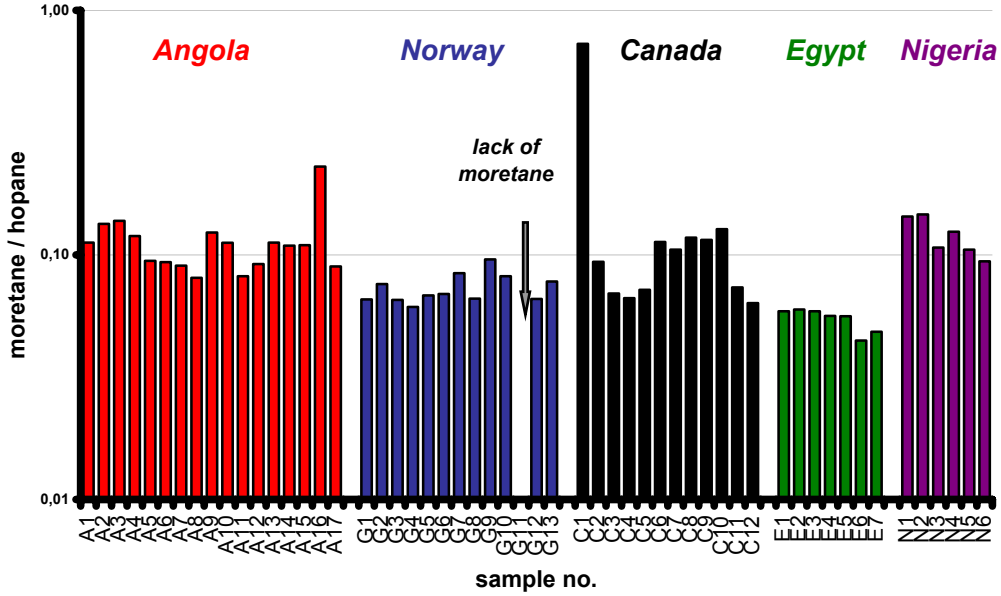

Fig. 50: Plot showing the ratio **17β(H),21α(H)-hopane (moretane) / 17α(H),21β(H)-hopane (hopane)** on a logarithmic scale. Due to the absence of 17β(H),21α(H)-Hopane (moretane), no value for the condensate G11 from Norway is displayed. Values decrease with increasing maturity of the source rock.

PETERS AND MOLDOWAN (1993) discussed that the moretane/hopane ratio is only partly dependent on source input or depositional environment. It was noted that higher values may indicate a hypersaline regime but this observation was made for bitumens of source rocks and not for crude oils. Only two crude oils of the investigated sample set show significantly increased values. Highest values were calculated for samples A16 from Angola and C1 from Canada. Interestingly, the origin of the crude oils seems to have only minor impact on the moretane/hopane ratio. Again, samples from the Issaran oil field (E6-E7) show slightly reduced values compared to the oils from the Sudr reservoir (E1-E5). Additionally Canadian crude oils from Kumak (C6-C8) and Arnak (C9-C10) show slightly higher values than those from Tuktuk (C1-C5) and Mayogiak (C11-C12) oil fields. Only sample C1 which may have reached a pronounced alteration level at which even the hopanes are affected is characterised by a clearly increased moretane/hopane ratio.

5.1.3.2 Steranes

Another important class of triterpanes is represented by the tetracyclic steranes, which are commonly used to distinguish crude oils generated from different organic matter type. Additionally, such tetracyclic terpanes can give reliable information about thermal maturities in petroleum systems (PETERS AND MOLDOWAN, 1993). This group of biomarkers can easily be identified by the molecular fingerprint *m/z* 217. The molecule structure of steranes is shown in Figure 51.

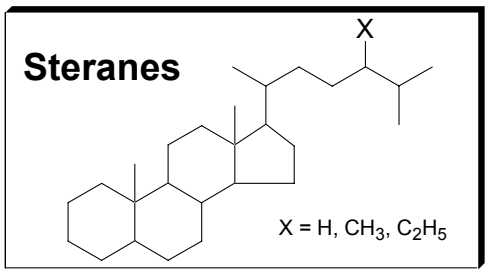

Fig. 51: Molecule structure of steranes.

A study on recent marine and terrigeneous sediments performed by HUANG AND MEINSHEIN (1979) showed that the distribution of C_{27}, C_{28} and C_{29} sterols displayed on a ternary diagram can be used to differentiate depositional settings. PETERS AND MOLDOWAN (1993) stated that the corresponding sterane ternary diagrams do not change significantly throughout the oil-generative window. Generally, high concentrations of C_{29} steranes (24-ethylcholestanes) compared to C_{27} and C_{28} steranes indicate a clearly terrestrial input. Various authors (e.g., MOLDOWAN ET AL., 1985, RULLKÖTTER ET AL., 1986) also noticed that C_{29} steranes are abundant components in crude oils derived from carbonate source rocks with no or only little higher plant input (PETERS AND MOLDOWAN, 1993). Furthermore it was discussed that the applicability of the ternary sterane plot for crude oils and source rocks is limited, because of broad overlaps of different depositional environments in the diagram (MOLDOWAN ET AL., 1985; PETERS ET AL., 2005). However, ternary sterane diagrams are used extensively to assess relationships between oils and / or source rock bitumens (PETERS ET AL. 2005). Figure 52 displays the ternary diagram for C_{27} – C_{29} steranes (sum of regular cholestanes and diacholestanes) in crude oils investigated in this study.

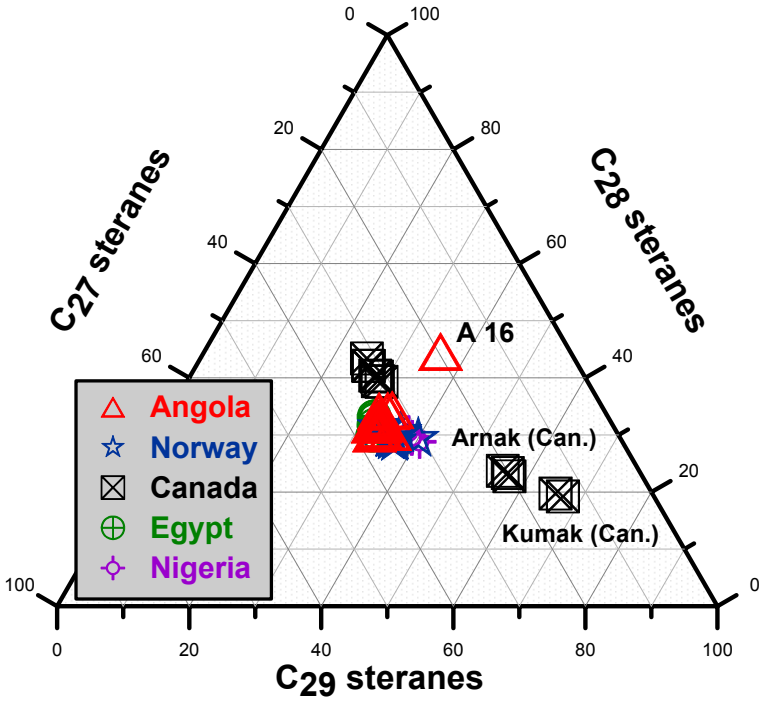

Fig. 52: Ternary diagram showing relative abundances of C_{27}, C_{28} and C_{29} steranes in the aliphatic fractions of all studied crude oils.

Lowest relative concentrations of C_{27} steranes with less than 25% were detected for sample A16 from Angola and for the crude oils derived from Kumak (C6-C7) and Arnak (C8-C9) reservoirs in Canada. Crude oils from other petroleum systems show only minor variances of less than 10% in C_{27} steranes. Highest relative abundances of C_{28} steranes with more than 35% were calculated for crude oils from Tuktuk (C1-C5) and Mayogiak (C11-C12) reservoirs in Canada and for sample A16 from Angola. Lowest values were observed for the Kumak and Arnak oils with less 25% of C_{28} steranes.

Highest relative C_{29} sterane contents (>50%) were detected for the Canadian Kumak and Arnak samples. In contrast, lowest relative C_{29} steranes amounts with less than 30% were determined for crude oils from the Tuktuk and Mayogiak oil fields. Generally, the great majority of samples are concentrated in middle of the ternary diagram indicating similar sources of the organic matter. Only the Kumak and Arnak oils as well as sample A16 from Angola are clearly separated from the other oils of the respective petroleum systems.

To distinguish crude oils generated from carbonate and clastic source rocks commonly the diasterane/sterane ratio is used. Low ratios may indicate anoxic, clay-poor, carbonate source rocks, whereby high ratios are typical for crude oils derived from source rocks rich in clay (PETERS ET AL., 2005). However, severe biodegradation can also affect the diasterane/sterane ratio by a selective destruction of steranes relative to diasteranes (PETERS AND MOLDOWAN, 1993). Figure 53 shows the diasterane / (diasterane + regular sterane) ratio [D/(D+R)] for crude oils investigated in this study.

Lowest values were determined for oil samples from the Issaran oil field in Egypt (E6-E7) and for three samples from Nigeria (N4-N6), which may denote to a clay-poor lithology of the source rocks. Highest relative amounts of diasteranes are found in sample A16 from Angola and in sample C1 from the Tuktuk reservoir in Canada. For the latter sample a preferential depletion of regular steranes due to severe biodegradation cannot be excluded. Especially the crude oils from Angola

show a rather broad range of D/(D+R) sterane ratios, which indicates some variability in the source rock lithology for this subset. In contrast, crude oil samples from Norway, which were sampled from the reservoirs in the Brent Formation of the Gullfaks field (G1-G6, G12) are characterised by rather constant values. Only the Norwegian samples from the Gullfaks satellites (G9-G11) and crude oil G13 from the Cook Formation in the Gullfaks field show increased ratios. No significant differences are obvious for samples from the Kumak (C6-C7) and the Arnak (C8-C10) oil fields in Canada.

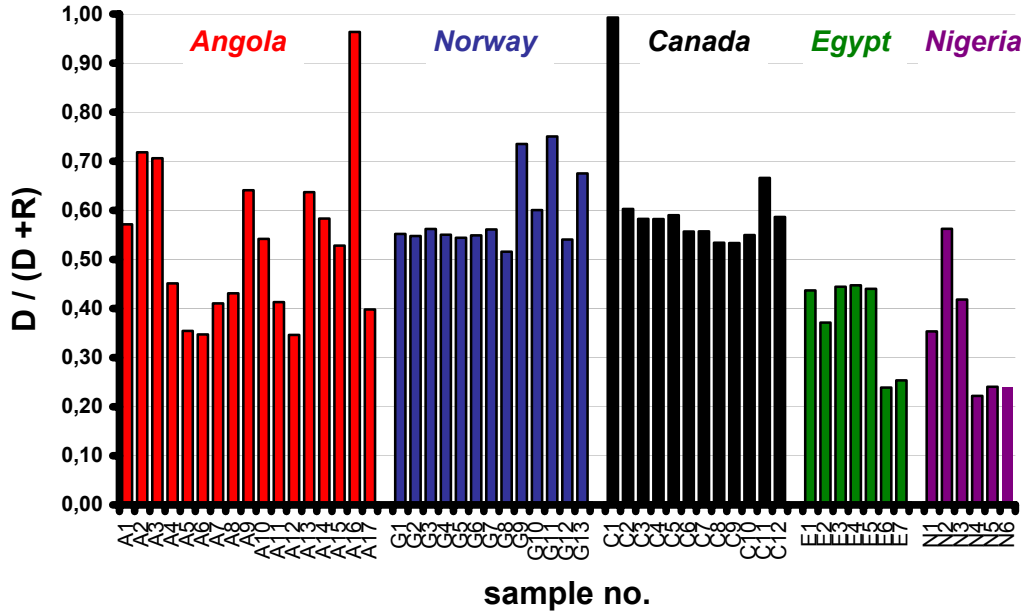

Fig. 53: Diagram showing diasterane / (diasterane + regular sterane) ratios [D/(D+R)] for all investigated crude oils. Low values are typical for a clay-poor source rock lithology. High values may indicate petroleum derived from clay-rich sources but can also be produced by a preferential depletion of regular steranes due to heavy biodegradation as it may be relevant for sample C1 from Canada.

The distribution of individual steranes is also widely used to assess crude oil maturities (e.g., SOFER ET AL., 1993). Thermal stress causes an isomerization at the C-14 and C-17 positions in the 20*S* and 20*R* C_{29} regular steranes and leads to an increase in the ratio ββ / (ββ + αα). The isomerization reaction reaches equilibrium for the latter ratio at 0.7 and is supposed to be independent of source organic matter input (PETERS ET AL., 2005). With increasing maturity

isomerization at C-20 in the C_{29} 5α,14α,17α(H)-steranes causes also a shift of the 20*S* / (20*S* + 20*R*) ratio from 0 to ~0.5. The *R* configuration at the C-20 position in the C_{29} steroid molecule occurs only in living organisms. During diagenesis and catagenesis of the organic matter this *R* configuration is gradually converted into a mixture of the *R* and *S* steranes until equilibrium at 0.52 -0.55 for the ratio 20*S* / (20*S* + 20*R*) is reached (PETERS ET AL., 2005). The 20*S* and 20*R* isomers were also used by SOFER ET AL. (1993) to infer vitrinite reflectances (%R_C) from C_{29} ααα sterane distributions. The authors showed in a case study for crude oils from Argentina, that the vitrinite reflectance can be inferred from sterane distributions by the formula %R_C = 0.5 * (20*S* / 20*R*) + 0.35.

Figure 54 and 55 display the sterane parameters discussed above for all investigated crude oils. The crossplot of ββ / (ββ + αα) versus 20*S* / (20*S* + 20*R*) in Figure 54 indicates lowest maturities for two crude oils from Nigeria (N1, N4). Inferred vitrinite reflectances (Figure 55) calculated by the approach of SOFER ET AL. (1993), denote a moderate diversity (%R_C = 0.55 - 068) for thermal maturities in this sample set. The lowest variance of sterane ratios was determined for the sample set from Egypt. Here, inferred vitrinite reflectances have a range of %R_C = 0.75 - 0.81 indicating similar thermal maturities. Norwegian samples from the Gullfaks field (G1-G6, G12-G13) are also characterised by only slight differences for sterane ratios. For these samples %R_C values between 0.71 and 0.78 were calculated. Crude oils from Angola show some differences within the sample set, with inferred %RC values between 0.66 and 0.78. Greatest differences for ratios displayed Figure 54 and 55 were determined for oils from Canada. Here, calculated vitrinite reflectances vary from 0.61 to 0.81 %R_C. However, the cholestanes indicate that the maturities for the Canadian sample set are clearly assigned to the different oil fields. Oils derived from the Kumak (C6-C7) and Arnak (C8-C10) field show lowest values with R_C = 0.67-0.69 and 0.61-063, respectively. In contrast, highest ratios were detected for the Tuktuk (C1-C5) and Mayogiak (C11-C12) oils with %R_C = 0.74-0.81 for both reservoirs. Because of low concentrations for C_{29} cholestanes in samples A16 from Angola and C1 from Canada no values are displayed.

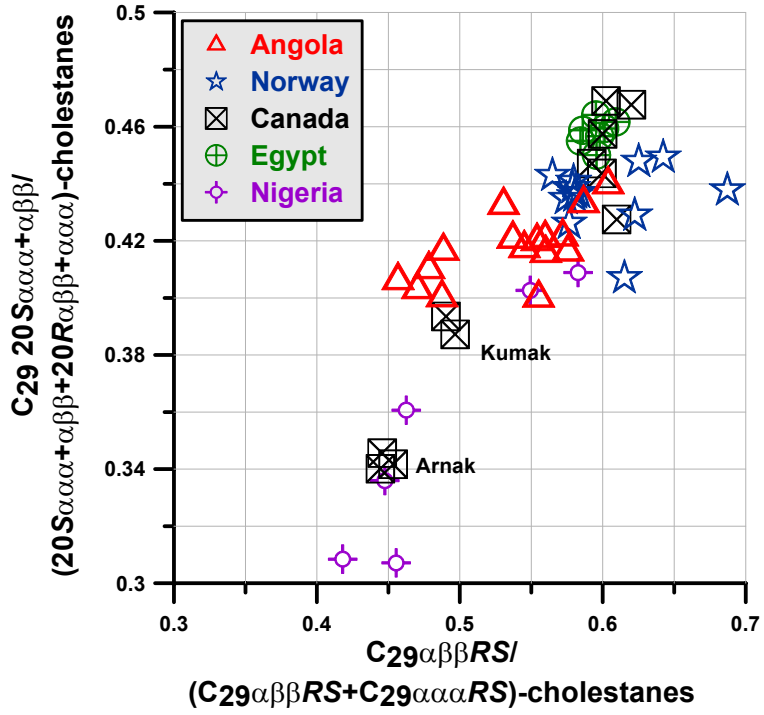

Fig. 54: Crossplot of maturity parameters described by PETERS AND MOLDOWAN (1993). Due to the absence of C_{29} regular steranes no data can be displayed for sample C1 from Canada.

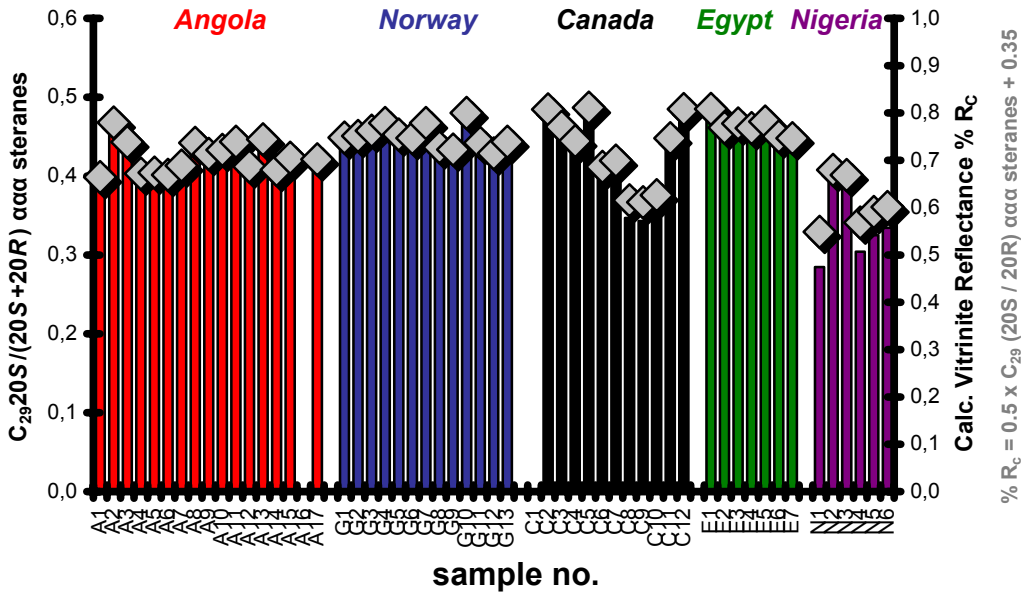

Fig. 55: The coloured bars display values of 20*S* / (20*S*+20*R*) C_{29} ααα sterane ratio. The 20*S*/20*R* ratio was used by SOFER ET AL. (1993) to infer vitrinite reflectances by the formula given beside the right y-axis. Grey diamonds indicate the calculated values for inferred vitrinite reflectances [% Rc].

5.1.4 Summary

For a valid assessment of biodegradation effects geological factors like facies, depositional environment and maturity, which are known to cause compositional variability in crude oils, have to be well-constrained. Evaluations of these geological parameters for crude oils under study are basically carried out by interpreting the tetra- and pentacyclic terpane distributions which were discussed before. These high molecular weight hydrocarbons are thought to be recalcitrant against initial to moderate biodegradation (WENGER ET AL., 2001; PETERS ET AL., 2005). Consequently, terpane distributions should not be affected by microbially induced alterations for the investigated crude oils, which predominantly have not exceeded moderate alteration levels.

ANGOLA

Source-dependent geochemical parameters indicate that samples from Angola show only slight differences in the molecular composition of the source rock. Only sample A16 is clearly separated from the rest of the Angolan subset. This crude oil is characterised by a relatively high concentration ratio for the D/(D+R) sterane ratio (Figure 53) indicating that this oil was generated from a clay-rich source. It was also shown that sample A16 contains a relatively high C_{29} sterane concentration (Figure 52) compared to all other crude oils from this subset. This may indicate that the oil was generated from a source rock which is significantly influenced by terrestrial organic matter. This assumption is also supported by the 17α(H)-diahopane/18α(H)-norneohopane (X-C_{30}/C_{29}Ts) ratio (Figure 45) which is clearly higher for this particular oil. PETERS AND MOLDOWAN (1993) reported that high X-C_{30}/C_{29}Ts values could be indicative for organic matter accumulated under oxic-suboxic conditions. A further indication that sample A16 was generated from a source rock deposited in a terrestrially influenced suboxic to oxic regime is given by the clearly increased Pr/Ph ratio (Figure 36). All other crude oils from

Angola show only minor differences in the source-related biomarkers. Only the D/(D+R) sterane ratio suggests some variability for the depositional environment of the source rock. As mentioned before this proxy denotes to a clay-rich facies by higher values and may differentiate the Angolan samples into two subsets by ratios above and below 0.5. Hence, crude oils A1-A3, A9-10 and A13-A15 would be generated from a source lithology relatively enriched in clay compared to samples A4-A8, A11-A12 and A17.

Maturity-related biomarker parameters for crude oils from Angola like Ts/(Ts+Tm), moretane/hopane, C_{29} αββ/(αββ+ααα)-cholestanes and C_{29}*S*/(*S*+*R*)-cholestanes (Figures 47, 50, 54) indicate only moderate variability for the thermal maturity. This relative homogeneity of maturity is also revealed by aromatic steroids as indicated by the TA/(TA+TM) ratio (Figure 42), which ranges, on a scale of 0-100% from 47% to 57%. Moreover, calculated vitrinite reflectances (R_C) derived from the MPI-1 (RADKE AND WELTE, 1981) and C_{29} sterane distributions (SOFER ET AL., 1993) show relatively small differences for $\%R_C$ with 0.86-1.00 and 0.66-0.78, respectively.

As a result of the geochemical characterisation it appears likely that 16 of the 17 crude oils from Angola are characterised by comparable compositions in the organic matter of the source rocks. Obviously, the source rock organofacies is rather similar for these samples, although the D/(D+R) sterane ratio indicates some variability's in the lithology of the source rock. In contrast, sample A16 is derived from a source rock which is clearly different in the composition of the organic matter. It was shown that the biomarker parameters also indicate comparable thermal maturities for oils of this sample set. Consequently, it can be concluded that the compositional variability in 16 of the 17 samples, which was observed especially within the distribution of light, saturated and aromatic hydrocarbons is predominantly due to in-reservoir alteration processes.

NORWAY

Although sterane distributions shown in the triangular plot of Figure 52 suggest similar sources for all investigated samples from Norway, other molecular ratios indicate some compositional differences between oils sampled in the Gullfaks field and those produced from the Gullfaks satellites. While samples from the surrounding oil fields Gullfaks Vest, Gullfaks Sor, Rimfaks and Gullfaks Gamma show clear variances in, e.g., the D/(D+R) sterane ratio, X-C_{30}/C_{29}Ts, and Ts/(Ts+Tm) are oils derived from the Brent Formation reservoirs characterised by rather constant values for these parameters. The data are in agreement with HORSTAD ET AL. (1992), who identified the Draupne Formation as the source rock for crude oils from the Gullfaks field, while oils from the satellites were predominantly generated from the Heather Formation. Only sample G13 which was sampled in the eastern part of the Gullfaks field shows some minor compositional differences compared to the other 7 oils from this reservoir. Here, slightly increased values for Ts/(Ts+Tm), D/(D+R) steranes and Pr/Ph ratios indicate a minor contribution from a second source. Increased values for the latter ratio in sample G13 may suggest the Heather Fm., being characterised by higher terrestrial input, as the contributing second source for hydrocarbons in this area of the Gullfaks field.

Based on the sterane maturity parameters C_{29}αββ/(αββ+ααα)-cholestanes and C_{29}*S*/(*S*+*R*)-cholestanes invariant thermal maturities for crude oils from the Gullfaks field (G1-G6, G12-G13) can be assumed. Only the hopane ratio Ts/(Ts+Tm), which is thought to be both maturity and source dependent shows slightly increased values for sample G13. Some minor differences in maturity-related biomarkers can also be observed for crude oils from the Gullfaks satellite reservoirs. However, for the 8 crude oils from the Gullfaks field calculated vitrinite reflectances inferred from sterane distributions (R_C = 0.71-0.78) as well as deduced from the MPI-1 (R_C = 0.83-0.86) clearly illustrate a rather narrow range for thermal maturities.

Crude oils from the Gullfaks area have already been extensively characterised in various studies (e.g., GORMLY ET AL., 1994; HORSTAD ET AL., 1995, VIETH AND WILKES, 2006). In these studies samples from the Gullfaks field are described as a biodegradation sequence generated from the same source rock showing comparable maturities. Only crude oil G13 is thought to have received a minor contribution from a second source. These observations are supported by the present geochemical investigations. Therefore, the 8 crude oils from the Gullfaks field are defined as a biodegradation sequence; with the constraint that sample G13 has received some minor contributions from a second source.

CANADA

Based on the various molecular parameters discussed in chapter 5.1 the samples from Canada can be divided into two oil families. As it is shown in the ternary plot of Figure 52 crude oils from the Mackenzie Basin are clearly separated by sterane distributions. Here, samples derived from Kumak and Arnak reservoirs show relatively higher amounts of C_{29} steranes compared to the crude oils produced from the Tuktuk and Mayogiak wells. With respect to the sterane distribution and high X-C_{30}/C_{29}Ts values, which are thought to be indicative for high wax oils sourced from lithofacies deposited under oxic to suboxic conditions (PETERS AND MOLDOWAN, 1993), it appears likely that these oils were generated from a terrestrially influenced source rock. BROOKS (1986) and SNOWDON (1987) also assumed that crude oils from Arnak and Kumak reservoirs were sourced from a terrestrially influenced facies, which is represented in the Mackenzie Basin by the pro-deltaic clays of the Eocene Richards Formation. Crude oils from Arnak and Kumak reservoirs are also characterised by highest Pr/Ph values within the Canadian sample set (Figure 36), which again denote to a terrestrially influenced source facies. In contrast, biomarker parameters for crude oils from Tuktuk and Mayogiak reservoirs indicate that the source rock was deposited in a stronger marine influenced regime. These oils are generally correlated to the source rocks of the Cretaceous Smoking Hills- and Boundary Creek- sequences (DIXON ET AL.,

1985). This implies that crude oils from Canada are derived from two clearly different sources splitting the Canadian sample set into two oil families representing a marine and a terrestrial facies.

Maturity-related parameters for crude oils from Canada show a high variability within the different subsets from Tuktuk, Arnak, Kumak and Mayogiak. A clear difference of thermal maturities between Arnak and Kumak oils and samples from Tuktuk and Mayogiak is indicated by the $C_{29}\alpha\beta\beta/(\alpha\beta\beta+\alpha\alpha\alpha)$-cholestanes and $C_{29}S/(S+R)$-cholestanes. Both ratios suggest clearly lower thermal maturities for the terrestrial oil family from the Arnak and Kumak reservoirs. This assumption is also supported by the Ts/(Ts + Tm) ratio which again indicates lower thermal maturities for Arnak and Kumak samples. In contrast, the distribution of cholestanes denotes to rather similar thermal maturities for crude oils derived from the Tuktuk field. For these oils also the inferred vitrinite reflectances (R_C = 0.74-0.81) and the aromatic steroids parameter TA/(TA+TM) with values ranging from 0.53 to 0.58 support the assumption of rather slight differences of thermal maturities.

With respect to the different reservoirs, sources and variable maturities the Canadian samples are separated into 4 individual subsets corresponding to the respective oil fields. Therefore, the subset with highest numbers of samples, 5 crude oils from the Tuktuk wells (C1-C5), was chosen for further investigations which are related to microbially caused alterations in the reservoir.

EGYPT

Geochemical investigations for the samples from Egypt show strong indications of an anoxic marine depositional environment. For Egyptian oils lowest Pr/Ph ratios were determined (Figure 36) within the entire sample set. In accordance with literature data (BAKR AND WILKES, 2002), oils derived from the Issaran field show stronger evidence of a marine algal type II source rock than those drilled in

the Sudr field. This assumption is supported by hopane parameters Ts/(Ts+Tm) and X-C_{30}/C_{29}Ts, because both ratios indicate anoxic marine depositional conditions by low values (PETERS AND MOLDOWAN, 1993). A differentiation of crude oils generated from clay-rich rocks and clay-poor carbonate sources is also revealed by the D/(D+R) sterane ratios displayed in Figure 53. Here, again crude oils from the Issaran field in Egypt are characterised by lowest values typical of anoxic, clay-poor, carbonateous depositional environments.

Maturity parameters based on sterane distributions (Figure 54 & Figure 55) indicate very similar values for all crude oils from Egypt. Slight differences for samples collected in the Sudr field and for oils derived from the Issaran reservoir are suggested by the hopane parameters moretane/hopane and Ts/(Ts+Tm). Additionally, the aromatic steroid parameter TA/(TA+MA) indicates lower maturities for oils from the Issaran field. This is confirmed by the calculated vitrinite reflectances (R_c) which are derived from sterane distributions (SOFER ET AL., 1993). Here, crude oils from the Sudr field are characterised by R_C values between 0.77 and 0.81, while the two oils from Issaran both have R_C values of 0.75.

As a result of the geochemical characterisations which were described in the literature (BAKR AND WILKES, 2002) and the parameters discussed before, only the 5 samples from the Sudr field (E1-E5) can be regarded as a biodegradation sequence and thus were selected for further investigations which are related to microbially induced alterations.

NIGERIA

For crude oils from Nigeria similar sterane distributions as displayed in Figure 52 denote to comparable origins of the organic matter in the source rock. The Ts/(Ts+Tm) ratio, which is thought to be both maturity and source dependent (PETERS ET AL., 2005), also illustrates rather constant values, although a slight

difference for oils produced in oil fields X (N1-N3) and Y (N4-N6) can be observed with lower values for the latter one. Slight variability in the depositional environments for the source organic matter is further indicated by the Pr/Ph values (1.94 – 2.58). However, the values clearly suggest an oxic regime for all samples from Nigeria and are not systematically related to the oil fields from which the samples were collected. The D/(D+R) sterane ratio which is commonly applied to distinguish crude oils generated from carbonate or clastic source rocks again shows some minor differences within the sample set with higher values for oils produced from reservoir X. However, pronounced biodegradation probably relevant for sample N2, which shows the highest value, can also affect the D/(D+R) sterane ratio by a selective destruction of regular steranes relative to diasteranes (PETERS ET AL., 2005).

Constant moretane/hopane ratios, which decrease with increasing maturity, indicate a relative homogeneity for thermal maturities within the samples from Nigeria. Although this sequence covers a relatively broad range for the maturity-dependent parameters $C_{29}\alpha\beta\beta/(\alpha\beta\beta+\alpha\alpha\alpha)$-cholestanes and $C_{29}S/(S+R)$-cholestanes compared to all other investigated subsets, inferred R_C values (0.55-0.68) illustrate rather comparable thermal maturities for samples from Nigeria. This is corroborated by aromatic steroids, which indicate only slight variances for the TA/(TA+TM) ratio from 0.52 – 0.67.

Consequently, the sample set from Nigeria can be designated as a sequence with slight to moderate differences for source rock organofacies and thermal maturities. However, it can be concluded that possible compositional differences within this subset were not exclusively but predominantly caused by in-reservoir alteration processes.

5.2 Part II: Molecular alterations in biodegraded crude oils

5.2.1 Biodegradation effects on light and saturated hydrocarbons

5.2.1.1 Introduction

Various classification systems describing different biodegradation stages have been proposed. The most commonly applied scheme is that suggested by PETERS AND MOLDOWAN (1993). This model describes a systematic and sequential removal of individual compound classes with increasing microbial degradation, focussing on moderate to severe biodegradation levels. A modified scheme was published by WENGER ET AL. (2001), who proposed a sequential degradation scheme with a slightly stronger emphasis on initial, slight and moderate alteration levels. This scheme describes the quasi-sequential removal of compound groups as follows: *n*-alkanes > *i*-alkanes > alkylbenzenes > alkylnaphthalenes > alkylcyclohexanes, alkylphenanthrenes and alkyldibenzothiophenes > isoprenoids (C_{15+}) > regular steranes > hopanes > aromatic steranes. Both schemes are based on the qualitative assessment of a generalized pattern of compositional alteration due to biodegradation, although it has been pointed out that the biomarker biodegradation scale must be used cautiously (PETERS ET AL., 2005). These widely applied biodegradation models focus on compositional changes during moderate to severe alteration stages, although the most significant decrease in oil quality (e.g. API gravity) takes place during depletion of volumetrically relevant compounds during the early stages of biodegradation (HEAD ET AL., 2003).

The volumetrically most important crude oil constituents in unaltered crude oils are light hydrocarbons, which make up about 30% of the whole oil (HUNT ET AL., 1980). This implies that information derived from these petroleum constituents is more representative of the bulk composition than that from oil constituents, which are less abundant, such as biological markers (ODDEN ET AL., 1998). However, most studies use light hydrocarbons and *n*-alkanes only on a qualitative basis, e.g., to assess the extent of biodegradation (WELTE ET AL., 1982, MASTERSON ET AL., 2001, GEORGE ET AL., 2002). In addition, numerous field studies showed that light hydrocarbons and *n*-alkanes in crude oils are useful to asses, e.g., the thermal history of petroleum (THOMPSON, 1983, MANGO, 1987). Also, the differentiation of in-reservoir alteration processes, such as evaporative fractionation, water washing and biodegradation have been elucidated using light hydrocarbons by, for example, THOMPSON (1988), HALPERN (1995) and GEORGE ET AL. (2002). Other authors (TEN HAVEN, 1996, ODDEN ET AL., 1998, WEVER, 2000) have used light hydrocarbons for oil correlation studies.

Despite this extensive literature about light hydrocarbons and *n*-alkanes, their abundance was not rigorously linked to the deterioration of petroleum quality. It is clear that the bulk composition of petroleum controls its quality in terms of physicochemical properties, such as API gravity (e.g., BEMENT ET AL., 1996). A rational approach to a better quantitative assessment of biodegradation therefore needs to consider the volumetrically important oil constituents as a starting point. Several studies suggested approaches to predict petroleum quality on the basis of, e.g., sulphur content or Rock-Eval pyrolysis in reservoir rocks (BASKIN AND JONES, 1993), basin modelling with individual thermal and charging histories (YU ET AL., 2002) and mixing reconstructions in the reservoir (KOOPMANS ET AL., 2002). More recently, BEHAR ET AL. (2006) introduced a more quantitative approach to assess the extent of biodegradation among crude oil samples from the Potiguar Basin in Brazil. However, to date, it has not been shown in detail how ongoing biodegradation influences the specific molecular composition in a petroleum reservoir or the extent to which compositional alteration, even within the early stages of biodegradation, affects the deterioration of crude oil quality.

Therefore, this study concentrates on the effects of light to moderate biodegradation on molecular petroleum composition and the related deterioration in crude oil quality.

5.2.1.2 Conventional evaluation of petroleum biodegradation

On the basis of the geochemical characterisation discussed before, 5 different biodegradation sequences were identified, where the compositional differences can be traced back to processes caused by in-reservoir alteration. Most of the samples are covered by biodegradation levels 0 - 3 on the PETERS AND MOLDOWAN (1993) scale (PM scale). Only two samples from Angola and one each from Nigeria and Canada show higher alteration levels (see chapter 5.1.1). Consequently, the sample set comprises 36 light to moderately altered crude oils among the five biodegradation sequences.

Generally, light to moderate microbial alteration of crude oils can be assessed by ratios of branched and cyclic alkanes over *n*-alkanes (WELTE ET AL., 1982). It is assumed that *n*-alkanes are more susceptible to biodegradation than branched and cyclic alkanes. Hence, concentration ratios, such as *i*-pentane/*n*-pentane (*i*-C_5/*n*-C_5) and 3-methylpentane/*n*-hexane (3-mp/*n*-C_6), increase with extent of biodegradation. Among these widely accepted parameters, pristane/*n*-heptadecane (Pr/*n*-C_{17}) and phytane/*n*-octadecane (Ph/*n*-C_{18}) are most commonly used to describe the extent of microbial alteration in light to moderately biodegraded crude oils. In general, it is believed (PETERS AND MOLDOWAN, 1993, WENGER ET AL., 2001) that isoprenoids, such as pristane and phytane, are not depleted by initial to moderate biodegradation, while *n*-alkanes are clearly affected. Consequently, increasing values of *i*-C_5/*n*-C_5, 3-mp/*n*-C_6, Pr/*n*-C_{17} and Ph/*n*-C_{18} indicate increasing biodegradation (Figures 56 and 57).

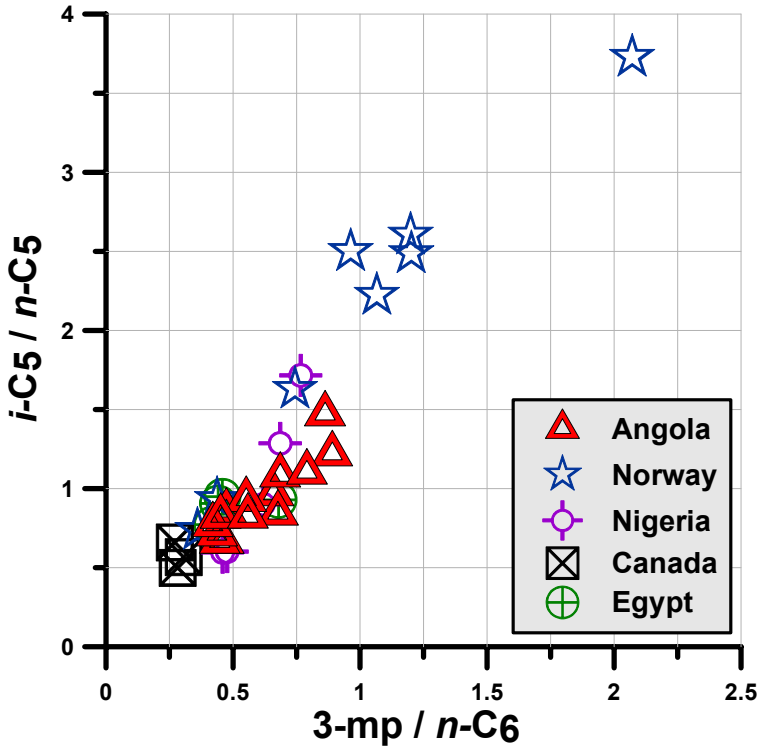

Fig. 56: Crossplot of the conventional biodegradation parameters *i*-C_5/*n*-C_5 vs. 3-mp/*n*-C_6 suggested by WELTE ET AL. (1982). Data are only shown for crude oils of the five biodegradation sequences.

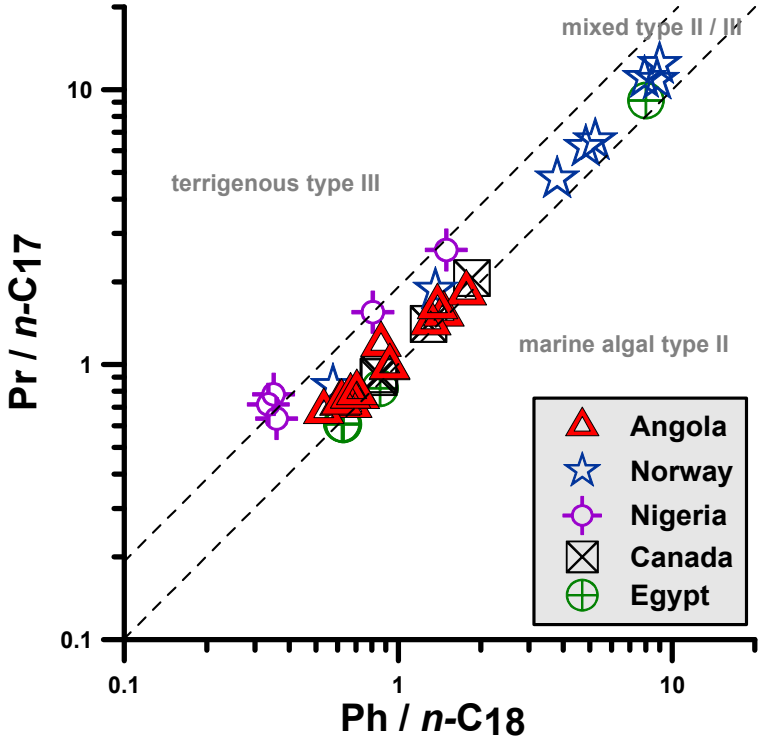

Fig. 57: Crossplot of the conventional biodegradation parameters Pr/*n*-C_{17} vs. Ph/*n*-C_{18} for crude oils from biodegradation sequences. Following PETERS ET AL. (1999) the plot can also be used to infer oxicity and organic matter type in the corresponding source rock depositional environment.

The logarithmic plot in Figure 57 shows a range of Pr/*n*-C_{17} and Ph/*n*-C_{18} values for samples from the five petroleum systems of 0.6 to 12.3 and 0.3 to 9.0, respectively. Following PETERS ET AL. (1999) this plot can also be used to characterise the organic matter type in the source rock, indicated by the dashed lines. The light to moderately degraded oil samples from Angola show an increase in Pr/*n*-C_{17} from 0.7 to 1.8, while values for Ph/*n*-C_{18} range from 0.6 to 1.8. The eight oil samples from the Gullfaks field show Pr/*n*-C_{17} values of 0.8 to 12.3 and Ph/*n*-C_{18} values of 0.6 to 9.0 suggesting a more extensive range of biodegradation. The same assessment would be made using the biodegradation ratios in Figure 56. Thus, biodegradation appears to be more extensive for most of the crude oils from Norway than for any of the samples from Angola.

API gravity is an important bulk parameter to describe crude oil quality. As oil density increases with increasing biodegradation, the numerical value of the API gravity decreases. One would therefore expect a systematic relationship between molecular biodegradation parameters and API gravity. However, our data show no consistent correlation between Ph/*n*-C_{18} and the API gravity (Figure 58) in the samples from Angola and Norway.

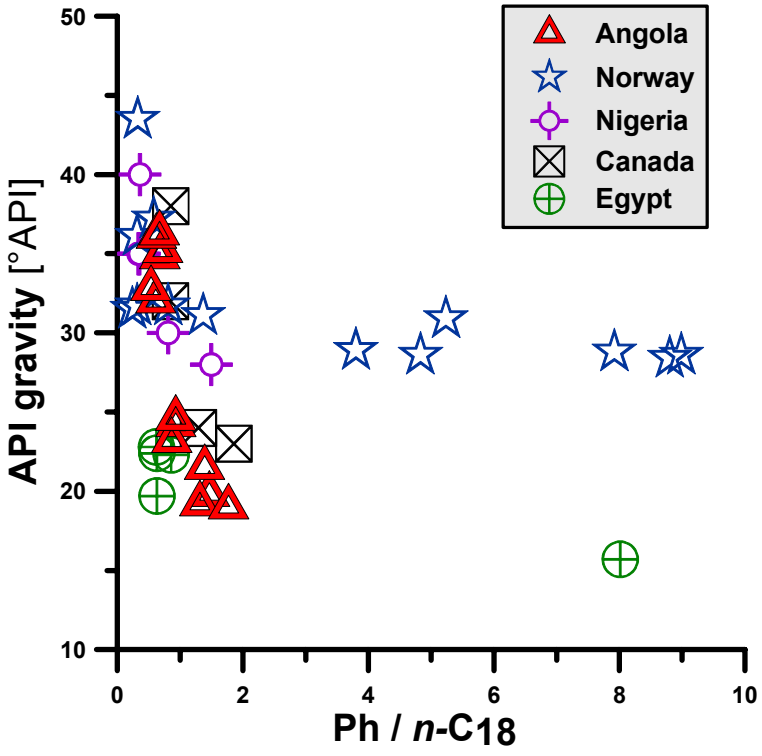

Fig. 58: Correlation of crude API gravity and the conventional bio-degradation parameter Ph/*n*-C_{18}. Samples from Norway show the broadest range for the extent of biodegradation, although crude oils from West Africa (A) have the grater range of API gravities.

Moreover, there is a discrepancy between the two parameters. As mentioned above, the oils from Norway show a broader range of Ph/*n*-C_{18} than those from Angola. In contrast, oils from Angola cover a much wider range of API gravity (36.3° – 19.0°) than those from Norway (37.2° – 28.4°). Here, it should be mentioned that the API gravities in crude oils from Angola, which are apparently separated into groups with °API higher and lower than 30°API, do not correlate to the D/D+R ratio, which was shown to differentiate the Angolan samples into two subsets.

To overcome the inconsistency between the assessment of biodegradation by conventional qualitative parameters and the API gravity this paper suggests and discusses a new concept to evaluate and quantify alteration extents. As mentioned above, conventional biodegradation models (PETERS AND MOLDOWAN, 1993, WENGER ET AL., 2001) propose no depletion in isoprenoids, such as pristane and phytane, prior to moderate alteration. In contrast, our data in Figure 59 clearly illustrate that the total amount [µg/g oil] of phytane is strongly reduced in the Angolan samples, even during the early stages of biodegradation.

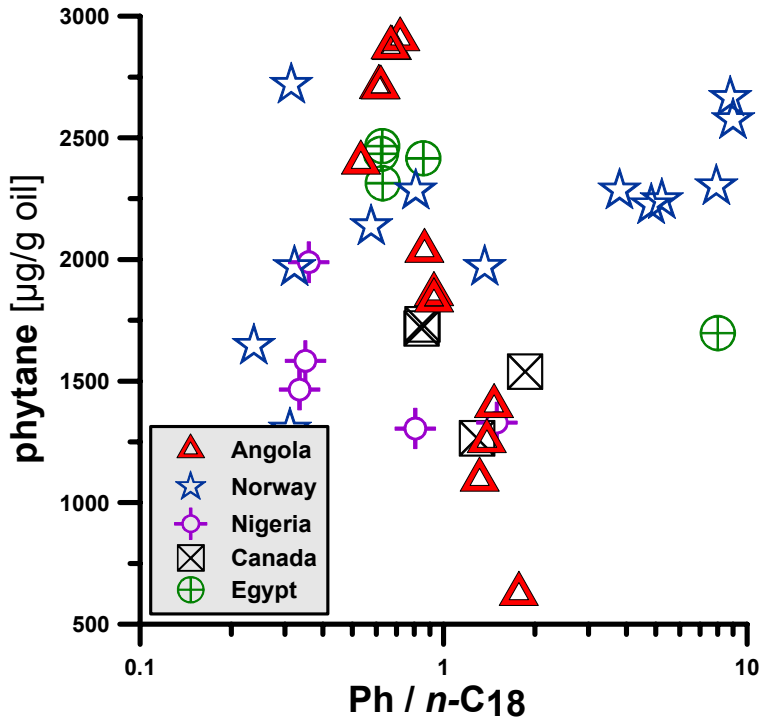

Fig. 59: Crossplot of the concentrations [µg/g oil] for phytane vs. Ph/*n*-C_{18}. Concentrations for phytane decrease in crude oils from Angola but not in the samples Norway, although Ph/*n*-C_{18} indicate stronger alterations for samples from Norway.

A similar behaviour, although less pronounced, is observed for the samples from Nigeria, Canada and Egypt. Only the samples from Norway show no decrease of phytane with increasing biodegradation, although the extent of alteration is apparently greater in this petroleum system, as indicated by the conventional biodegradation parameters in Figures 56 and 57.

As shown in Figure 60, the decrease in concentration of phytane in the oil samples from Angola and Norway is not due to the slight variance in maturity. Therefore, it is supposed that the quantitative depletion of phytane is controlled by in-reservoir biodegradation. In the sample sets, pristane exhibits the same general behaviour as phytane (data not shown).

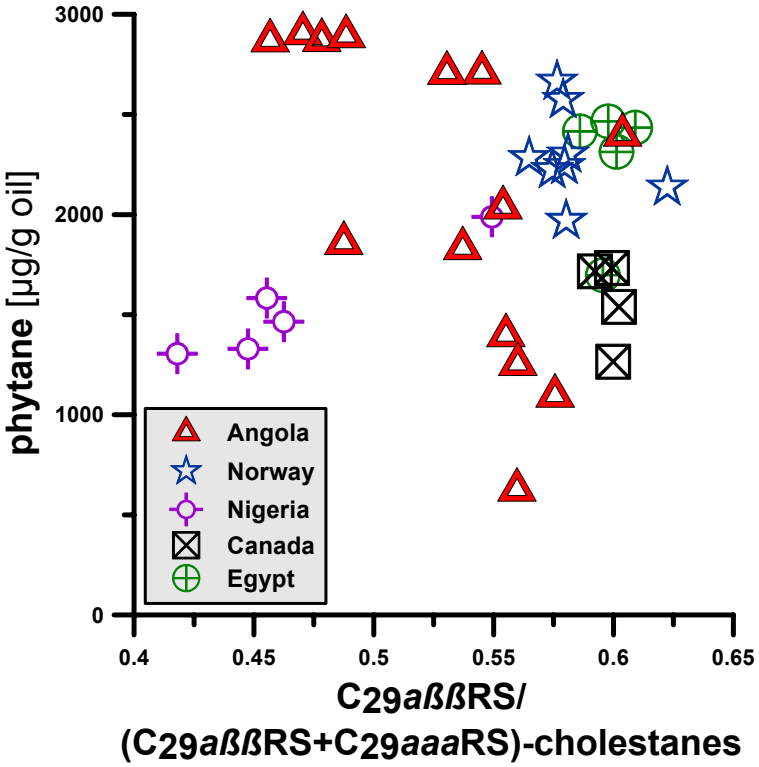

Fig. 60: Correlation of concentrations for phytane [µg/g oil] vs. a widely applied maturity parameter suggested by PETERS AND MOLDOWAN (1993). The crossplot indicates that the depletion of phytane in crude oils from Angola is not correlated to the slight variances of oil generation temperatures.

5.2.1.3 Improved assessment of biodegradation extent in petroleum reservoirs

A new concept to assess biodegradation is discussed for the sample sets from Gullfaks and Angola, while the other three sample sets are used mainly to further illustrate the general applicability of the concept. Compositional changes in crude oils due to biodegradation can easily be investigated by comparison of the molecular "fingerprints", the chromatograms from whole-oil-GC or thermovaporisation-GC. Thermovaporisation GCs are shown in Figure 61 for four crude oil samples from Angola.

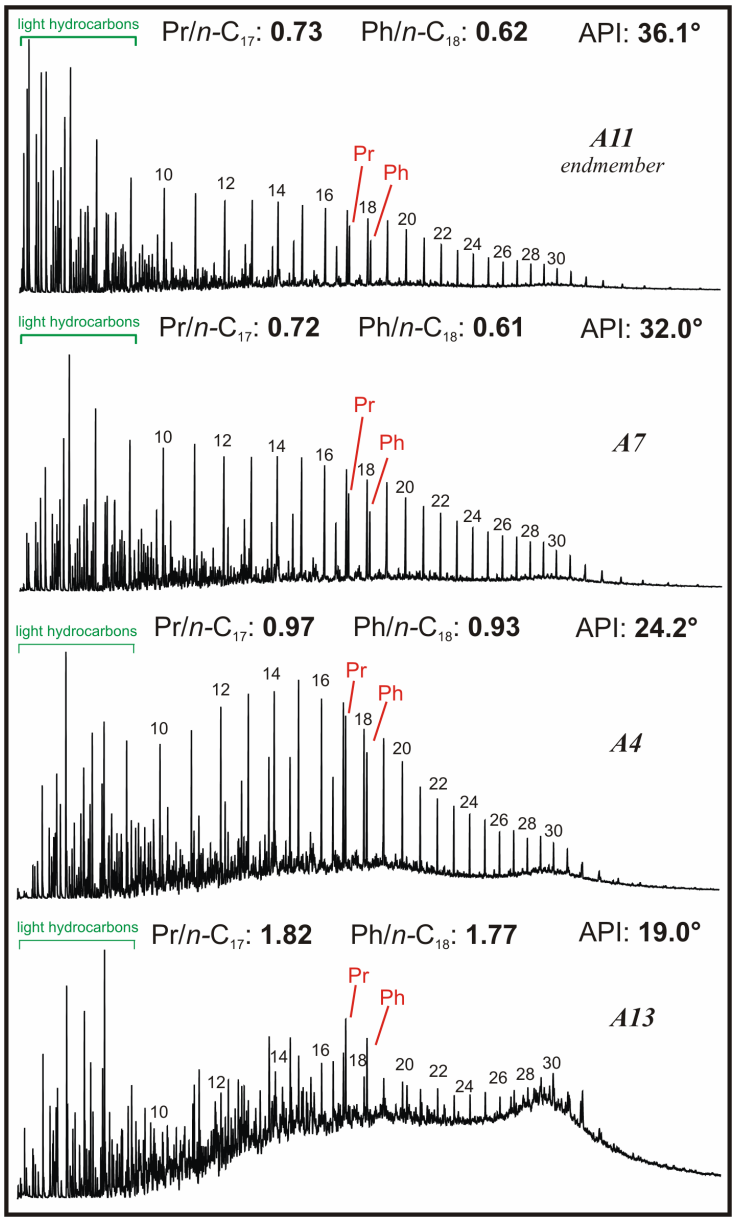

Fig. 61: Thermo-vaporisation chromatograms for crude oil samples (A11, A7, A4 and A13) from Angola. The least degraded crude oil A11 is labelled as the local endmember of this petroleum system.

With regard to the PM scale, no differences in extent of biodegradation are apparent between the chromatograms for samples A11 and A7. Additionally, the conventional biodegradation parameters Pr/*n*-C_{17} and Ph/*n*-C_{18} indicate the same level (PM 0) of biodegradation for these two oil samples. Interestingly, crude oil quality, indicated by API gravities, decreases from 36.1° for sample A11 to 32.0° for sample A7. On closer examination, some rather minor differences between the two chromatograms can be observed. Detailed analysis indicates some slight compositional changes for the low molecular-weight hydrocarbons in sample A7. From comparison of the two samples, the light hydrocarbons in sample A7 are slightly depleted relative to the mid- and long chain *n*-alkanes. These slight compositional differences between the two crude oil samples cannot be illustrated by conventional biodegradation parameters, which only describe qualitative differences in molecular composition. Accordingly, we propose a model to assess light to moderate biodegradation that is based on a quantitative evaluation of individual compounds.

First, total amounts [µg/g oil] for 66 crude oil constituents representing resolvable peaks in whole-oil-GC or thermovaporisation-GC traces (Table X- 1) were determined. The least degraded sample within each set, representing the crude oil with the highest summed concentration [µg/g oil] of compounds listed in Table X-1, was identified. For these end members within the five individual biodegradation sequences, the concentrations [µg/g oil] for each of the 66 compounds were set to 100%. Thereafter, individual concentrations for the 66 constituents in the other oil samples from the same sample set were calculated as a percentage relative to the respective compound concentration in the least degraded oil. Using the following equation (1) the DEGRADATIVE LOSS for each individual compound can be calculated:

$$\textbf{DEGRADATIVE LOSS [\%]} =$$

$$\textbf{100 – [(Conc. } \textit{(comp.)}_{\textbf{sample}} \textbf{ * 100) / (Conc. } \textit{(comp.)}_{\textbf{endmember}}\textbf{)]} \qquad \textbf{(1)}$$

The DEGRADATIVE LOSS for each of the 66 individual crude oil constituents is shown in Figure 62 for three Angolan samples. It should be noted again that conventional biodegradation parameters indicated no significant compositional alteration for this sample, although the API gravity is 4.1° lower than in the least degraded crude oil from this sample set. In contrast, the DEGRADATIVE LOSS illustrates significant compositional alteration, especially in the light hydrocarbon range of sample A7.

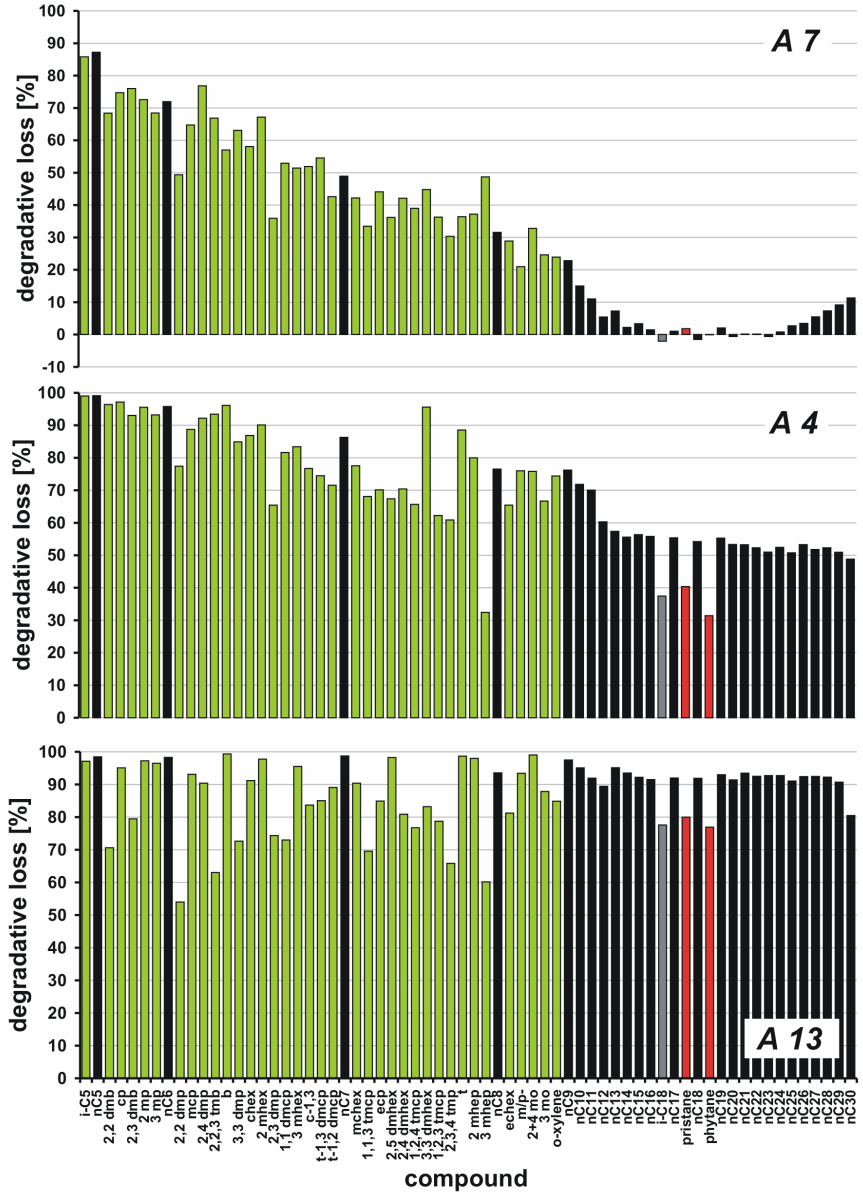

Fig. 62: Calculated DEGRADATIVE LOSSESS [%] for 66 quantitively important crude oil constituents in three samples from Angola.

Interestingly, the extent of degradation for individual crude oil constituents decreases with complexity of molecule structure. In particular, the susceptibility of *n*-alkanes to microbial alteration decreases with increasing carbon number. Note that a depletion of up to 85% for individual compounds (e.g., *n*-C_5) occurred in the very lightly biodegraded sample A7, which would have been labelled as a non-biodegraded crude oil using conventional biodegradation parameters. It is important to recognise that in various cases compounds of lower volatility are depleted to a stronger extent than other compounds of higher volatility, e.g. compare 2,3-dimethylpentane and 3-methylheptane. This rules out that the observed difference in composition might be the result of simple evaporative loss.

Another two samples from the Angola sequence were chosen to illustrate increasing DEGRADATIVE LOSS during light to moderate biodegradation. Figure 61 also shows a chromatogram for sample A4, a slightly biodegraded (PM 1) crude oil with 24.1° API gravity. Here, conventional biodegradation parameters indicate initial depletions by way of slightly increased Pr/*n*-C_{17} and Ph/*n*-C_{18} values of 1.0 and 0.9, respectively. Contrary to these rather minor indications of biodegradation, the DEGRADATIVE LOSS for this sample A4 shown in Figure 62 displays significant compositional alterations. All of the crude oil constituents investigated were clearly affected by in-reservoir alteration. Again, the extent of depletion seems to be reduced for higher molecular-weight components. It is important to note that none of the compounds is completely degraded, although a significant DEGRADATIVE LOSS for e.g., acyclic isoprenoids has occurred. A depletion of up to 40% for pristane and phytane in this slightly biodegraded (PM 1) crude oil again contradicts conventional biodegradation models, which postulate no susceptibility to biodegradation of acyclic isoprenoids prior to PM level 3.

Figure 61 also shows the chromatogram of the most strongly degraded sample (A13) from the Angolan data set which still exhibits the 66 individual oil constituents as resolvable peaks in the GC. This sample has an API gravity of 19.0° and the DEGRADATIVE LOSS increased to more that 90% for the majority of

individual constituents (Figure 62). Again, none of the 66 compounds is degraded completely, although pristane and phytane are heavily depleted (80%). This indicates that the onset of depletions for specific compounds in samples from Angola does not occur at different biodegradation levels, as suggested by conventional biodegradation scales (WENGER ET AL., 2001; PETERS ET AL., 2005). Additionally, the data for the three samples shown in Figure 62 give rise to the interpretation that the relative degradation rates for individual oil constituents change throughout ongoing biodegradation. The degradative losses indicate that in the very early biodegradation stage (A7) *n*-alkanes are degraded more strongly than e.g. pristane and phytane. However, at higher extents of biodegradation (A4 and A13) the loss of *n*-alkanes is slower than that of e.g., pristane and phytane. This suggests that biodegradation is a process where individual components are degraded simultaneously with different rates at various degradation levels. This is in agreement with PETERS ET AL. (2005), who stated, that the quasi-sequential degradation of hydrocarbons does not occur in a true stepwise fashion but reflects differences in the rates of catabolism under varying conditions. Thus, our results support that the published ranking schemes for biodegradation have to be used very cautiously.

In addition to the determination of losses of individual oil constituents, our quantitative approach to evaluate the extent of biodegradation can also be applied to assess the DEGRADATIVE LOSS in a whole crude oil. Thus, summed concentrations [µg/g oil] for the 66 quantitatively important crude oil constituents (Table X- 1) were used to calculate the MEAN DEGRADATIVE LOSS for a single crude oil relative to the local end member of the respective subset (equation 2).

$$\textbf{MEAN DEGRADATIVE LOSS [\%]} =$$

$$100 - [(\sum \text{Conc. } (i\text{-}C_5\text{–}n\text{-}C_{30})_{sample} * 100) / (\sum \text{Conc. } (i\text{-}C_5\text{–}n\text{-}C_{30})_{endmember})] \quad (2)$$

Calculated MEAN DEGRADATIVE LOSS and measured API gravity for samples from the five biodegradation sequences are listed in Table 4. Crude oils with a MEAN

DEGRADATION of 100% have already reached alteration levels above moderate biodegradation, i.e., the 66 oil constituents used here to assess biodegradation are generally below detection level. Samples with 0% represent local end members of the different subsets.

Angola	mean degradative loss [%]	API gravity [°API]	Norway	mean degradative loss [%]	API gravity [°API]
A11	**0.0**	36.1	**G8**	**0.0**	37.2
A8	**6.3**	32.8	**G3**	**26.8**	31.1
A12	**8.2**	36.3	**G4**	**56.7**	28.9
A5	**14.8**	34.8	**G5**	**62.1**	30.9
A6	**19.5**	35.2	**G7**	**63.8**	28.4
A7	**31.4**	32.0	**G6**	**65.5**	28.6
A15	**61.6**	24.6	**G1**	**66.3**	28.8
A16	**67.0**	n.a.	**G2**	**67.8**	28.6
A10	**68.5**	23.2			
A4	**71.0**	24.2			
A1	**77.6**	19.8			
A14	**80.0**	21.5	**Canada**		
A9	**84.2**	19.2	**C3**	**0.0**	32.0
A13	**91.5**	19.0	**C4**	**2.8**	38.0
A3	**100.0**	17.6	**C5**	**63.2**	24.0
A2	**100.0**	15.2	**C2**	**75.6**	23.0
			C1	**100.0**	16.0
Nigeria					
N3	**0.0**	40.0	**Egypt**		
N1	**4.9**	35.0	**E3**	**0.0**	22.4
N6	**5.1**	35.0	**E4**	**12.4**	22.8
N4	**55.0**	30.0	**E1**	**28.9**	22.3
N5	**60.0**	28.0	**E5**	**35.4**	19.7
N2	**100.0**	19.0	**E2**	**90.2**	15.7

Table 4: MEAN DEGRADATIVE LOSS [%] for 40 crude oil samples from five biodegradation sequences. Samples with a value of 0% are the least degraded; those with 100% have reached alteration levels above moderate biodegradation and so contain none of the 66 compounds shown in the chromatogram of Figure 20 and listed in Table X- 1 in the Appendix.

Interestingly, the MEAN DEGRADATIVE LOSS indicates the strongest alteration, in terms of light to moderate biodegradation, for a crude oil from Angola, with a total depletion of more than 90% relative to the least degraded oil in this sequence. In contrast, the maximum degradation for a sample from Norway is only 67.8%. This is contrary to the values indicated by the conventional biodegradation parameters, such as Pr/*n*-C_{17} and Ph/*n*-C_{18}, which denote stronger extents of alteration for samples from Norway. Based on our approach, six crude oils from Angola are more strongly degraded than any of the samples from Norway. Figures 59 and 63 substantiate this assumption, because the isoprenoid

phytane is clearly depleted in these most degraded samples from Angola but not in any of the samples from Norway.

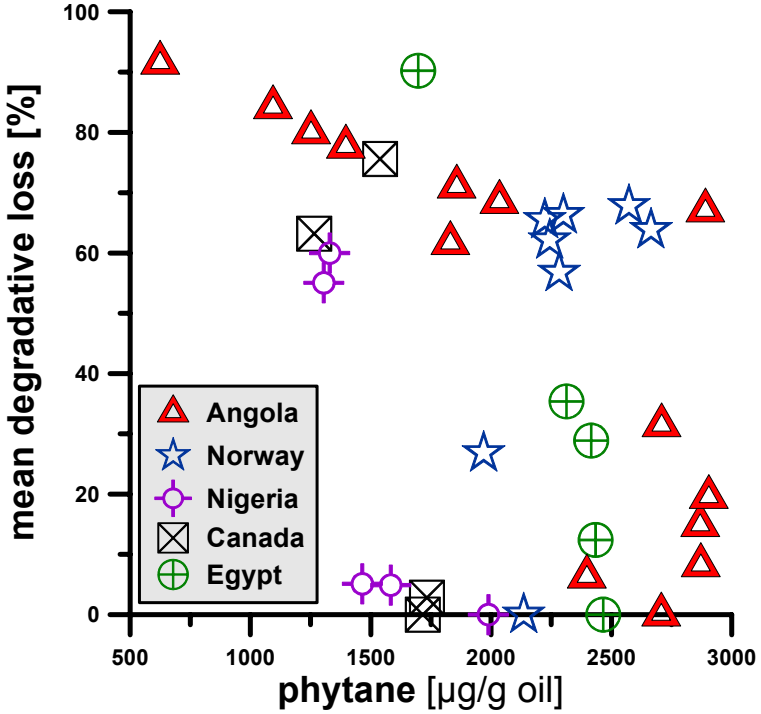

Fig. 63: Crossplot of the MEAN DEGRADATIVE LOSS [%] vs. the concentrations [µg/g oil] of the isoprenoid phytane.

Consequently, we conclude that the extents of biodegradation for samples from Norway are too low for a significant depletion of phytane. As displayed in Figure 64, our quantitative approach also illustrates compositional alteration within very early stages of biodegradation. In samples from Angola, conventional biodegradation parameters do not change significantly, although in-reservoir alteration processes have clearly affected the petroleum composition as indicated by the MEAN DEGRADATIVE LOSS. Obviously, the conventional parameters Pr/*n*-C_{17} and Ph/*n*-C_{18} do not document adequately the compositional changes occurring within early stages of biodegradation. In contrast, the MEAN DEGRADATIVE LOSS provides the opportunity to assess in-reservoir alterations, which are based not only on four crude oil constituents (i.e., Pr/*n*-C_{17} and Ph/*n*-C_{18}), but on 66 volumetrically important petroleum components. Hence, the

reliability for a proper assessment of biodegradation is greater by use of the MEAN DEGRADATIVE LOSS.

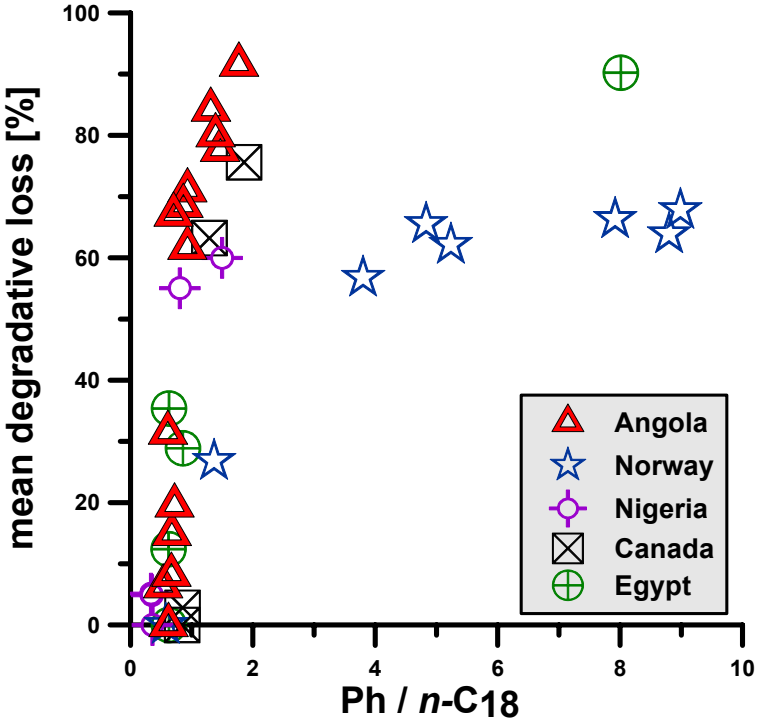

Fig. 64: Crossplot of the MEAN DEGRADATIVE LOSS [%] vs. the conventional biodegradation parameter Ph/*n*-C_{18}.

It should be noted that other in-reservoir processes like water washing or evaporative fractionation may be expected to affect the MEAN DEGRADATIVE LOSS if they contribute significantly to the depletion of volumetrically relevant oil constituents. However, we believe that this would not principally obscure the integrity of our above described approach, which in such cases would allow quantifying the combined effect of different alteration processes. This might be tested using suitable sample sets, where such processes are known to have influenced the oil composition. However, it appears unlikely that water washing has a major impact on oil composition for the samples analysed in this study. Benzene and toluene, as highly water soluble crude oil constituents, are not the most depleted compounds as shown in Figure 62. Based on simulation experiments LAFARGUE AND LE THIEZ (1996) had concluded that over geological time, compounds such as benzene and toluene should be completely absent in an

oil column if water washing had a significant influence on oil composition. In addition, the analysis of compound-specific carbon isotopes for samples from the Gullfaks field already showed that water washing and evaporative fractionation do not significantly affect the crude oil composition (VIETH AND WILKES, 2006). Because carbon isotope ratios of light hydrocarbons in samples from the other four petroleum systems (data not shown) also show fractionation, which cannot be explained by water washing and evaporative fractionation (MANSUY ET AL., 1997; SMALLWOOD ET AL., 2002), it appears likely that biodegradation is the main control on the crude oil composition in these samples as well. Thus, we conclude that water washing and evaporative fractionation in the reservoir had a negligible impact on the MEAN DEGRADATIVE LOSS for crude oil samples investigated in this study.

Furthermore, it should be noted that molecular biodegradation parameters, such as Pr/*n*-C_{17} and Ph/*n*-C_{18}, may still be used for a relative assessment of alteration within a single reservoir, but appear not to be appropriate to compare the extent of compositional alterations in various petroleum systems where the degradation mechanisms and effects might be different. This assumption is supported by the data shown in Figure 65, which indicate different degradation patterns for five crude oils, one from each investigated petroleum system. Here, samples with comparable extent of biodegradation, as indicated by the MEAN DEGRADATIVE LOSS and the API gravity, are shown. Only from the Egyptian sample set no crude oil with a comparable alteration extent was available. Figure 65 also illustrates that only in the crude oil from Norway, the isoprenoids pristane and phytane are not significantly depleted. It must be pointed out again that all five samples represent light to moderately altered crude oils based on conventional biodegradation tools (PETERS AND MOLDOWAN, 1993, WENGER ET AL., 2001), which propose that pristane and phytane should not be affected in such oils. In contrast, our results clearly show that these compounds are significantly affected by in-reservoir alteration processes in four of the five investigated petroleum systems. The variable degradation patterns illustrated in Figure 65 give rise to the

interpretation that different petroleum systems may host different microbial communities exhibiting different degradative capabilities.

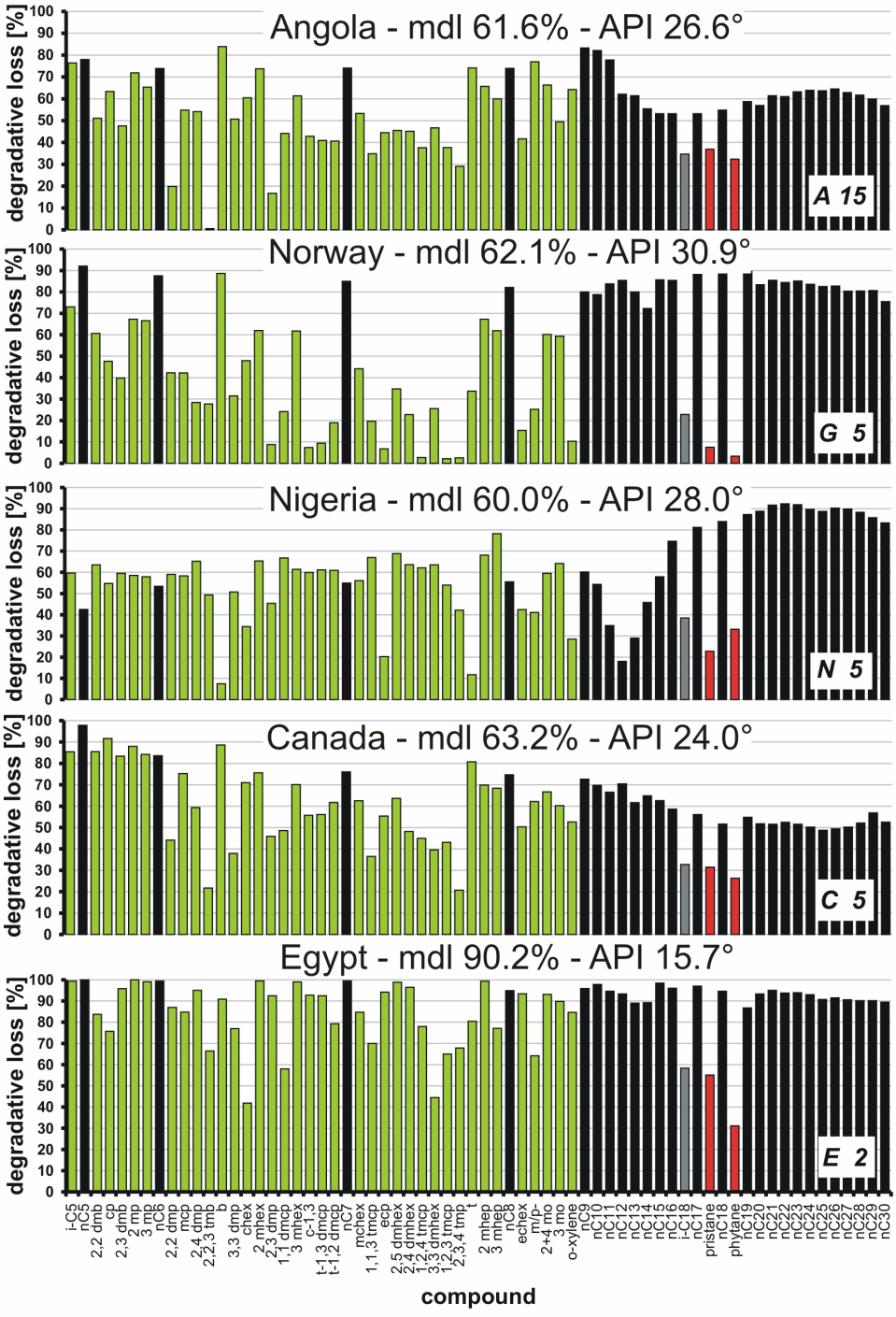

Fig. 65: Bar charts showing DEGRADATIVE LOSSES for crude oil samples from each investigated petroleum system representing comparable extents of biodegradation. The diverse degradation patterns indicate that compositional alteration is highly individual in each petroleum system.

This interpretation is in agreement with results published by PETERS ET AL. (1996), who provided evidence that the demethylation of extended hopanes to 25-norhopanes is a selective process that occurs only in certain reservoirs. However, the enrichment of 25-norhopanes is generally assumed to be restricted to severe biodegradation levels. Our results provide more general evidence for the relevance of individual degradative capabilities of different hydrocarbon-degrading microorganisms in different petroleum reservoirs with respect to the loss of volumetrically important crude oil constituents, such as light hydrocarbons and *n*-alkanes. Thus, the extent of in-reservoir alteration should be assessed by tools which are based on a wide variety of crude oil constituents. Such a comprehensive evaluation is possible by using the MEAN DEGRADATIVE LOSS.

5.2.1.4 Correlation of API gravity and molecular composition

It was shown above that conventional biodegradation parameters (Ph/*n*-C_{18}) show no consistent correlation with the API gravity (Figure 58). In contrast, the MEAN DEGRADATIVE LOSS is in good accordance with the API gravity of all the sample sets (Figure 66 A & B). Within the individual sub-sets linear correlation coefficients vary from R^2 = 0.97 for Angola to R^2 = 0.85 for Norway. This indicates a clear dependence of API gravity on molecular composition. Consequently, the MEAN DEGRADATIVE LOSS can be used to calculate the API gravity of crude oil from its molecular composition. Linear regression lines of every biodegradation sequence describe individual slopes for each petroleum system. Applying the linear regression equation, unknown API gravity values can be calculated for oil samples from a known petroleum system. A comparison of measured and calculated API gravity (Fig. 67) shows a good correlation for these parameters, with a linear regression slope of b = 0.9995 and a coefficient of determination R^2 = 0.96. A mean deviation of 1.2 ° API for the calculated API

gravity relative to the measured API gravity also illustrates that the MEAN DEGRADATIVE LOSS enables a reliable assessment of petroleum quality.

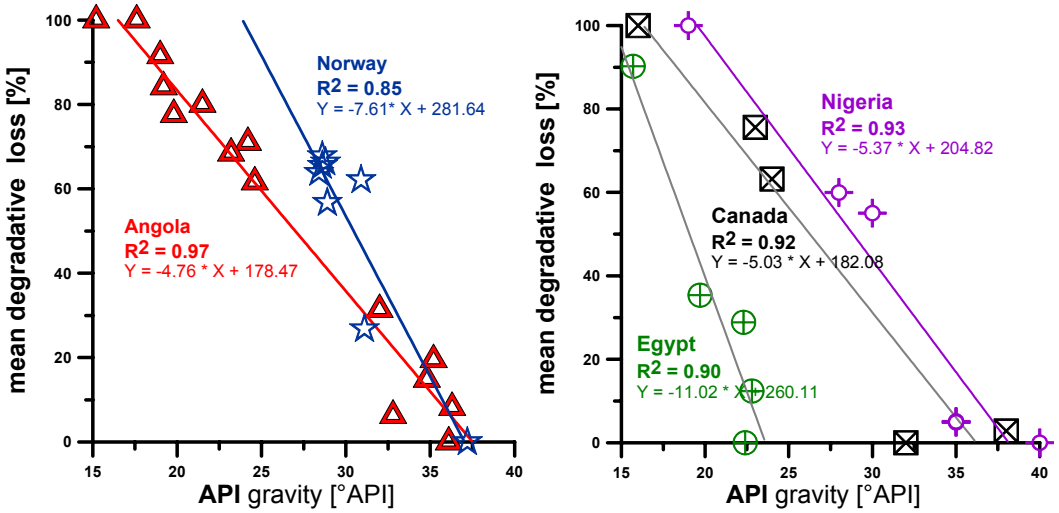

Fig. 66A & B: Crossplots of MEAN DEGRADATIVE LOSSESS [%] vs. the measured API gravities for crude oils from Angola and Norway. Also shown are the slopes for calculated linear regression lines with determination coefficients and y-axis intercepts.

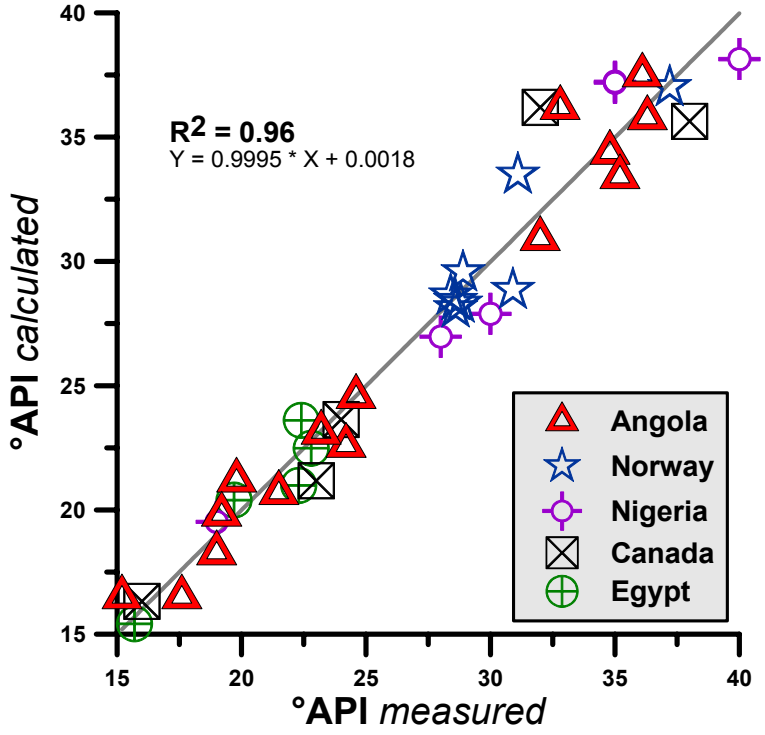

Fig. 67: Crossplot of measured and calculated API gravity. The determination coefficient of R^2 = 0.96 illustrates a good linear correlation.

Our results clearly show that an adequate prediction of crude oil quality is only possible when specific geochemical signatures within individual petroleum systems are evaluated precisely. Moreover, it is shown that crude oil quality, indicated by API gravity, predominantly depends on the quantitative abundance of light hydrocarbons and *n*-alkanes. Obviously, our quantitative approach provides the opportunity for a more detailed consideration of compositional alteration during light to moderate biodegradation compared to biodegradation tools based on qualitative observations.

5.2.1.5 Conclusions

The approach discussed in chapter 5.2.1 enables a quantitative evaluation of molecular changes associated with biodegradation in petroleum reservoirs. It was shown that volumetrically relevant petroleum constituents, such as light hydrocarbons and *n*-alkanes, can be used to assess the quantitative effects of light to moderate biodegradation. Our results indicate that the use of conventional alteration parameters may lead to a misinterpretation of the intensity in petroleum biodegradation. Such an improper assessment occurs predominantly because of the underestimated depletions in, e.g., branched alkanes. Such previously unexpected, but obviously relevant depletions of isoprenoids during light to moderate biodegradation levels cause the increase of Pr/*n*-C_{17} and Ph/*n*-C_{18} ratios to be lower than expected. The relative degradation rates of regular alkanes decrease compared to isoprenoids with ongoing biodegradation. Based on crude oil samples from various petroleum systems, it was clearly shown that biodegradation causes volumetrically important changes within light hydrocarbons, *n*-alkanes and the isoprenoids pristane and phytane. However, the depletion extents for these crude oil constituents are not ubiquitous and therefore have to be calibrated individually in each petroleum system.

5.2.2 Biodegradation effects on aromatic hydrocarbons

5.2.2.1 Introduction

It has been shown in several laboratory studies (e.g., RABUS ET AL., 1996; COATES ET AL., 1996 & 2002; HARMS ET AL., 1999; WILKES ET AL., 2000) that aromatic hydrocarbons are not only highly degradable in aerobic habitats but also susceptible to biodegradation under strictly anoxic conditions. It is therefore expected that biodegradation should lead to significant changes in the aromatic fractions of crude oils from petroleum reservoirs. Aromatic hydrocarbons contribute up to 50% of unaltered crude oils and are degradable within light to moderate stages of biodegradation (e.g., WENGER ET AL., 2001; GEORGE ET AL., 2002). Therefore, this compound class is of particular interest within this study.

Generally, it is believed that the susceptibility of aromatic hydrocarbons to bacterial attack depends on the number of aromatic rings (HUANG ET AL., 2004). The rate of biodegradation is thought to be relatively lower for compounds with a higher number of aromatic rings present in the molecule. It has also been suggested that the degree of alkylation controls the rate of degradation, i.e., decreasing with increasing number of alkyl substituents (e.g., FISHER ET AL., 1996; GEORGE ET AL., 2002). However, it was not shown quantitatively to which extent aromatic hydrocarbons are affected by light to moderate stages of biodegradation.

Therefore, this chapter describes the quantitative abundances of individual aromatic hydrocarbon subgroups and discusses their individual susceptibilities to biodegradation. It is also discussed whether conventional geochemical parameters, which are based on aromatic hydrocarbons, are still reliable for light to moderately biodegraded crude oils.

It was already discussed in chapter 4 that the compositional variability in 40 of the 55 investigated crude oils can predominantly be attributed to in-reservoir alteration processes. Therefore, the considerations of biodegradation effects on aromatic hydrocarbons are discussed only for these 40 crude oils.

5.2.2.2 Quantitative variabilities in the aromatic fraction of biodegraded oils

The quantitatively most important aromatic hydrocarbons in nonbiodegraded crude oils are represented by alkylated benzenes, naphthalenes, phenanthrenes and dibenzothiophenes (PETERS ET AL., 2005). Summed concentrations for 103 identified individual aromatic hydrocarbons of these four quantitatively most relevant subgroups are displayed in Figure 68. In the following, concentrations are given in parts per million (ppm), which can also be expressed as microgram compound per gram crude oil (µg/g oil).

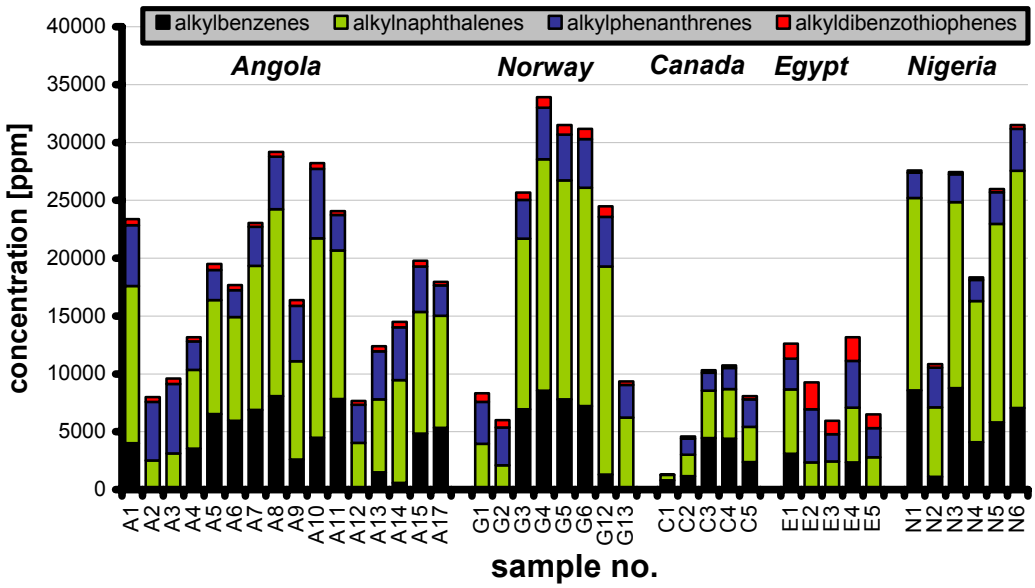

Fig. 68: Summed concentrations [ppm] of alkylbenzenes, alkylnaphthalenes, alkylphenanthrenes and alkyldibenzothiophenes in crude oils from the five biodegradation sequences.

In total, the summed aromatic hydrocarbon concentrations vary from 33,900 ppm in sample G4 from Norway to 1,300 ppm in sample C1 from Canada. The greatest

difference of concentrations within a single subset was calculated for the crude oils from Norway. Here, total concentration shifts of nearly 28,000 ppm were determined. The lowest difference of aromatic hydrocarbon concentrations within a single subset was calculated for oils from Egypt with a total shift of about 9,400 ppm. However, the calculation of concentrations clearly illustrates that within each of the five different petroleum systems the abundances of aromatic hydrocarbons vary significantly. Figure 69 A-D illustrates the correlation between the extent of biodegradation as indicated by four different parameters and the total amount of aromatic hydrocarbons.

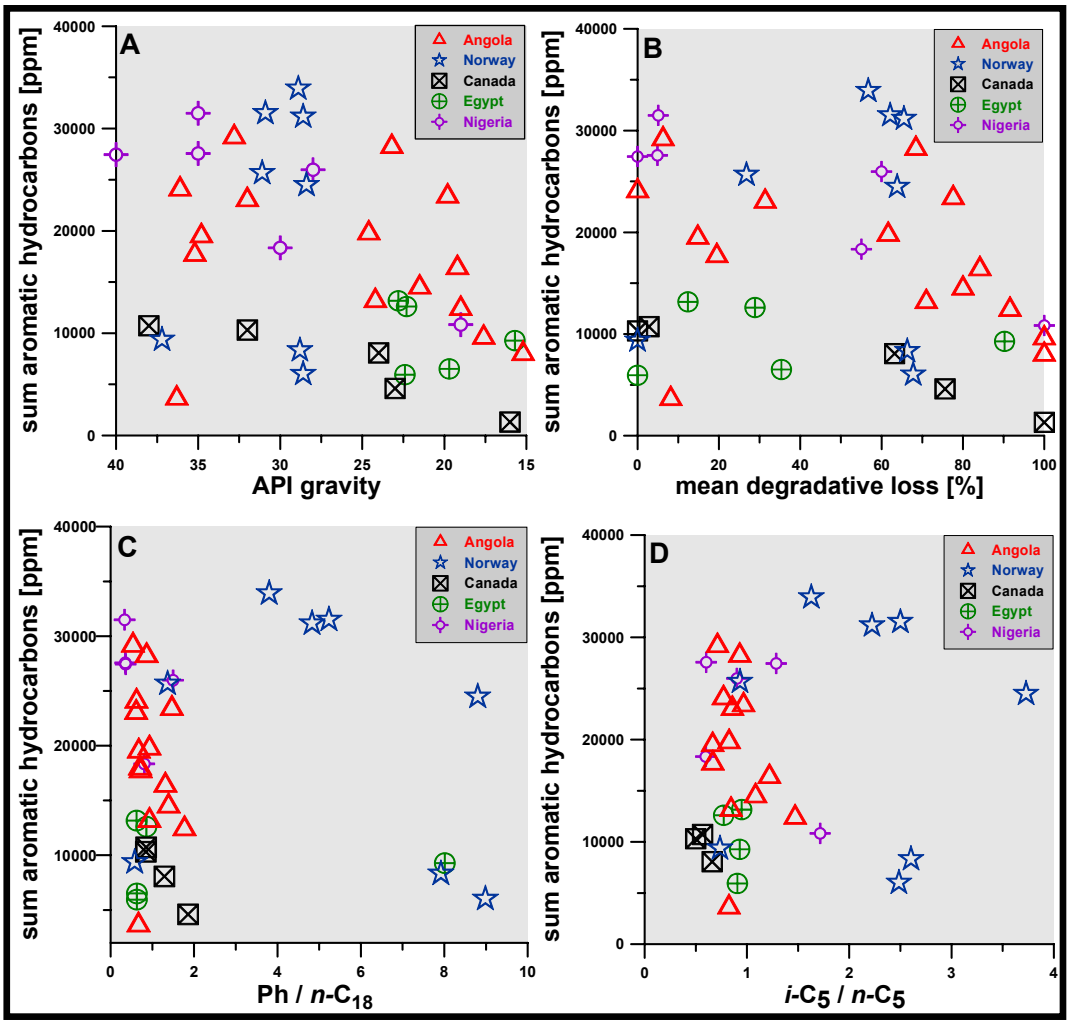

Fig. 69 A-D: The crossplots show the sum of aromatic hydrocarbons [µg/g oil = ppm] vs. API gravity, mean degradative loss [%], Phytane / *n*-C_{18} and *iso*-pentane / *n*-pentane ratios which may indicate increasing extents of biodegradation on the x-axis from the left to right.

Figure 69 A-D illustrates that in crude oils from Angola each of the four displayed biodegradation parameters shows a fair correlation with the summed concentrations of aromatic hydrocarbons. This implies that in Angolan crude oil samples the concentrations of aromatic hydrocarbons are clearly affected by light to moderate biodegradation. Only sample A12 from this petroleum system, which is characterised by the lowest amount of aromatic hydrocarbons (7,700 ppm), does not follow the general trend obvious for the other oils of the subset. In total, the concentrations in the Angolan samples vary between ~29,000 ppm and ~9,000 ppm, which represents a relative decrease for aromatic hydrocarbons of 72.6%. In accordance with the Angolan oils, the summed concentrations of aromatic hydrocarbons in crude oils from the Tuktuk reservoirs in Canada also show a clear correlation to the extent of biodegradation, as indicated by the API gravity, the mean degradative loss [%] and the Ph/*n*-C_{18} ratio. In total, summed aromatic hydrocarbons in crude oils from Canada vary between ~10,700 ppm and ~1,300 ppm, representing an overall shift of 87.8%. A weak correlation between the extent of biodegradation and the concentration of aromatic hydrocarbons is also obvious for crude oil samples from Nigeria. Here, the concentrations shift from ~31,500 to 10,800 ppm, reflecting a decrease of almost 66%. As already mentioned before, the greatest total concentration shift of ~28,000 ppm was calculated for crude oils from Norway, representing a percentage decrease of 82.3%. Interestingly, this significant concentration shift does not clearly correlate to three of the four biodegradation parameters shown in Figure 69A-D. Only the Ph/*n*-C_{18} ratio shows for six of the eight crude oils from Norway a fair correlation to the summed amounts of aromatic hydrocarbons. However, it should be noted again (see chapter 5.2.1.3) that the sample set from Norway is the only investigated sequence where phytane (Ph) is clearly less depleted than *n*-octadecane (*n*-C_{18}). This may explain the unique applicability of the Ph/*n*-C_{18} ratio as a biodegradation indicator and its correlation to the aromatic hydrocarbon concentrations in the Norwegian sample set. The four biodegradation parameters shown in Figure 69 A-D also show a weak correlation to the summed concentrations of aromatic hydrocarbons in crude oils from Egypt. The concentration shift in the Egyptian oils reflects a percentage decrease of almost

55% between highest and lowest calculated concentrations. Interestingly, the sample sets from Angola, Canada and Nigeria, where the concentrations of aromatic hydrocarbons clearly correlate to the extent of biodegradation, are characterised by maximum differences in API gravities of 21°, 22° and 21°, respectively. In contrast, crude oils from Norway and Egypt, which show no clear correlation between the amount of aromatic hydrocarbons and the extent of biodegradation, cover only maximum API gravity ranges of ±9° and ±7°, respectively.

The clear variability of total aromatic hydrocarbon concentrations can also be observed within each of the four individual subgroups of alkylated benzenes, naphthalenes, phenanthrenes and dibenzothiophenes. Figure 70 shows the percentage amounts of the four aromatic hydrocarbon subgroups relative to the total sum of aromatic hydrocarbons.

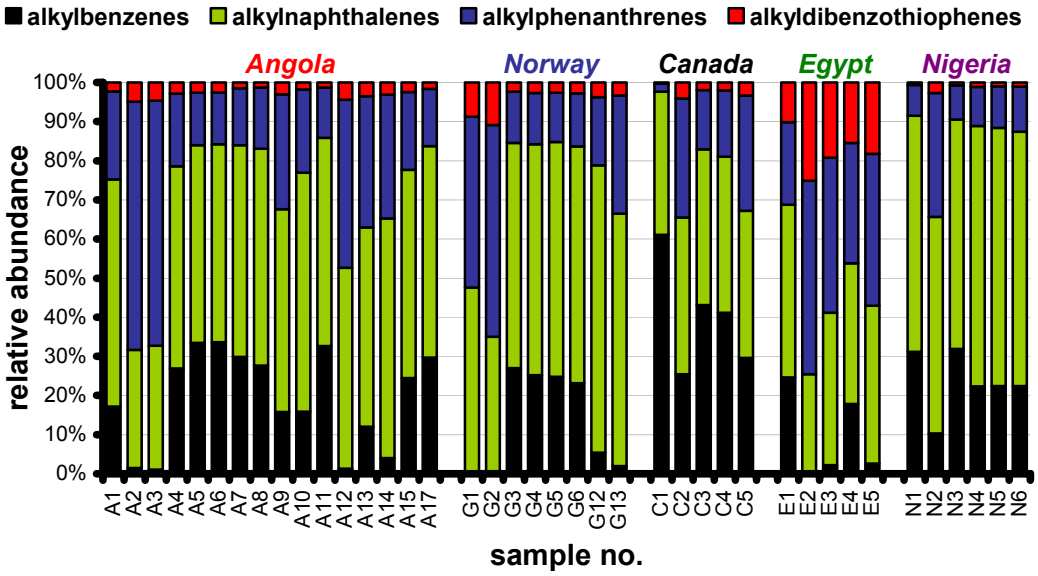

Fig. 70: Amounts of alkylbenzenes (black), alkylnaphthalenes (green), alkylphenanthrenes (blue) and alkyldibenzothiophenes (red) given as a percentage relative to the total sum of aromatic hydrocarbons.

In each of the five petroleum systems relatively highest abundances were calculated for alkylnaphthalenes with an average of nearly 50% of the sum of all four aromatic hydrocarbon subgroups. After this, averaged alkylbenzene and

alkylphenanthrene abundances contribute each with 22% to the aromatic fraction. Lowest averaged relative concentrations were calculated for the sum of alkylated dibenzothiophenes, which make up about 6% of the sum of all four subgroups. It should be mentioned again (see chapter 5.1), that the total concentrations for alkylated benzenes might be too low due to the GC-MS instrument settings. However, relative considerations within the alkylbenzene subgroup are not affected and can still be used to evaluate quantitative variability's for the different petroleum systems. The large quantitative differences give rise to the assumption that biodegradation also affected the individual aromatic hydrocarbon subgroups. Consequently, in the following the study also discusses the effects of biodegradation on the individual aromatic hydrocarbon subgroups. Figure 71 A & B displays the relative quantitative variabilities of alkylated benzenes, naphthalenes, phenanthrenes and dibenzothiophenes in the five biodegradation sequences.

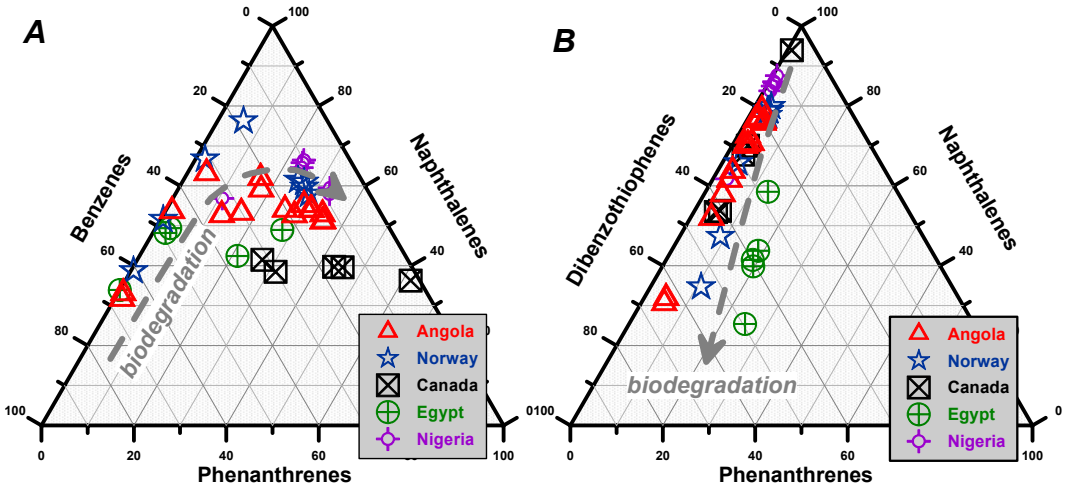

Fig. 71 A & B: The ternary plots show relative abundances for alkylated benzenes, naphthalenes, phenanthrenes and dibenzothiophenes. Grey arrows indicate changes in the distribution of aromatic hydrocarbons subgroups with increasing extent of biodegradation.

HUANG ET AL. (2004) discussed that the susceptibility of aromatic hydrocarbons to microbial attack depends on the number of aromatic rings. It was suggested the higher the number of aromatic rings in a molecule the more recalcitrant is the compound to biodegradation. With regard to this assumption, Figure 71 A may indicate that with increasing extent of biodegradation the relative amounts of

benzenes (1 aromatic ring) decrease during biodegradation. The triangular plot suggests that during early biodegradation naphthalenes (2 aromatic rings) are relatively enriched, while the concentrations of phenanthrenes (3 aromatic rings) remain unaffected. However, the plot further shows that with proceeding biodegradation the naphthalenes are depleted while phenanthrenes become relatively enriched. According to the assumption that hydrocarbons with less aromatic rings are more biodegradable (HUANG ET AL., 2004), the triangular plot of Figure 71 B may suggest that biodegradation leads to a relative depletion of naphthalenes, while the relative amounts of phenanthrenes slightly increase and the relative concentration of dibenzothiophenes clearly increase with ongoing biodegradation.

These general trends as indicated in Figure 71 A and B by the grey arrows are in particular obvious for crude oil samples from Angola and Norway. Compared to these two sample sets crude oils from Canada and Egypt show less variability in the distribution of aromatic hydrocarbon subgroups. No clear trend in the two triangular plots can be observed for crude oils from Nigeria, which can be attributed to the slight variability of concentrations for individual aromatic hydrocarbon subgroups (see Figure 70). However, the quantitative and relative variabilities shown before illustrate that aromatic hydrocarbons can be affected by light to moderate levels of biodegradation. Obviously, individual hydrocarbon subgroups are affected to different extents by microbial processes. Hence, it appears appropriate to assess the effects of biodegradation on individual aromatic subgroups and specific aromatic compounds in more detail. In the following it is discussed to which extent light to moderate biodegradation affects individual aromatic hydrocarbon subgroups and specific aromatic crude oil constituents.

Alkylbenzenes

In total, 29 individual benzenes with 2, 3 and 4 carbon atoms in the alkyl substituents were identified. A partial mass chromatogram for the C_2-C_4

alkylbenzenes is shown in Figure 22. Summed concentrations for identified alkylbenzenes of the 3 different subgroups are given in Figure 72.

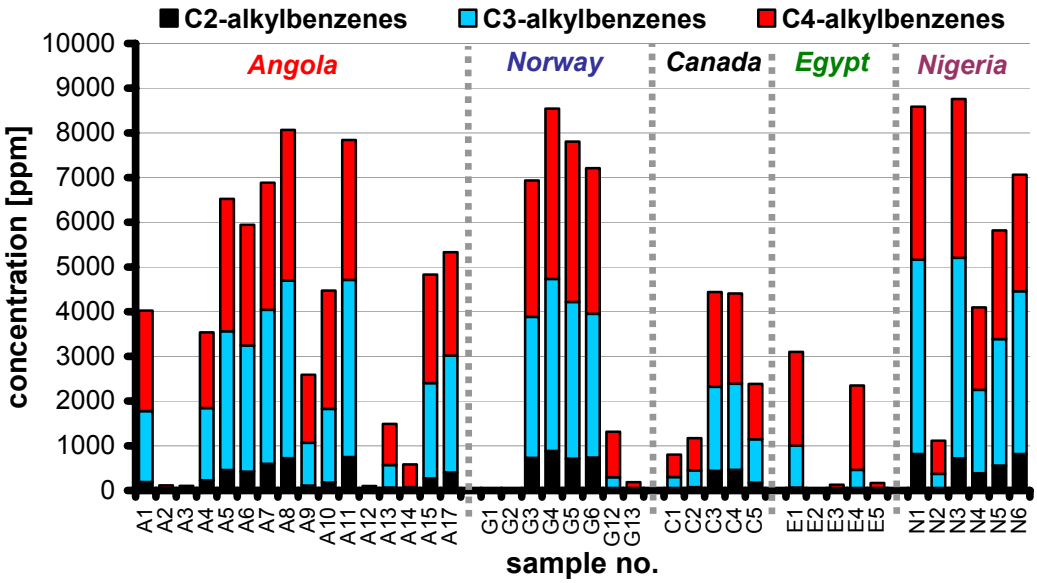

Fig. 72: Summed concentrations for all identified C_2-C_4 alkylbenzenes in light to moderate biodegraded crude oils from Angola, Norway, Canada, Egypt and Nigeria. For each sample the concentrations for C_2, C_3 and C_4 alkylbenzenes are shown by the stacked bars.

Highest relative alkylbenzene concentrations within the five biodegradation sequences were determined for samples N1 and N3 from oil field X in Nigeria with 8,600 to 8,800 ppm, respectively. Also the sample G4 from the Gullfaks oil field in Norway and sample A7 from Angola are characterised by alkylbenzene concentrations > 8,000 ppm. All other investigated crude oils have alkylbenzene amounts lower than 8,000 ppm. Lowest alkylbenzene concentrations with less than 500 ppm were measured for crude oils A2, A3 and A12 from Angola and G1, G2 and G13 from Norway as well as for E3 and E5 from Egypt. In crude oil E2 from the Sudr field in Egypt, which was characterised as the most biodegraded sample from this petroleum system, none of the identified alkylbenzenes shown in Figure 22 was detected. Figures 73 A-D illustrate that the variability of alkylbenzene concentrations correlates in most of the samples to the extent of biodegradation as indicated by the API gravity, mean degradative loss, Ph/*n*-C_{18} and *i*-C_5/*n*-C_5.

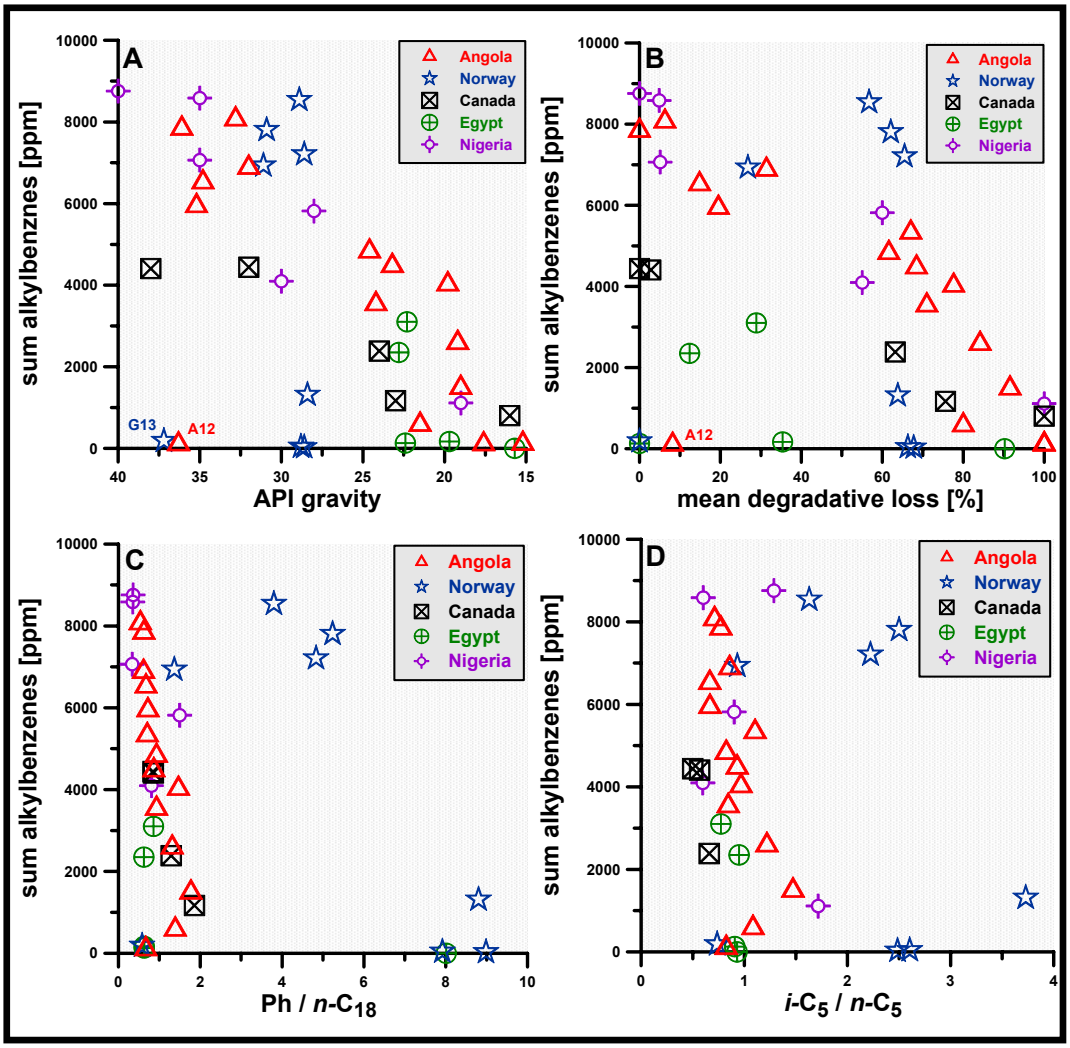

Fig. 73 A - D: The crossplots show the summed concentrations of alkylbenzenes [ppm] vs. API gravity, mean degradative loss, Ph/*n*-C_{18} and *i*-C_5/*n*-C_5 ratios which all indicate increasing extents of biodegradation on the x-axis from the left to right.

In crude oils from Angola, Canada and Nigeria the sum of alkylbenzene concentrations shows a good correlation to an increasing extent of biodegradation as indicated by the parameters shown on the x-axes in Figure 73 A-D. In contrast, the alkylbenzene concentrations in samples from Norway and Egypt show no clear correlation to the extent of biodegradation. This observation was already described for the total amounts of aromatic hydrocarbons and obviously corresponds to the limited variability of API gravities in the petroleum systems from Norway and Egypt. However, Figure 73 A-D clearly illustrates that alkylbenzenes can be significantly depleted in light to moderately biodegraded

crude oils. This raises the question as to whether individual alkylbenzenes, such as C_2-, C_3- and C_4- alkylbenzenes, are biodegraded to different extents.

The triangular plot of Figure 74 illustrates the relative amounts of C_2- C_3- and C_4-alkylbenzenes. HUANG ET AL. (2004) suggested that compounds with higher number of carbon atoms in the substituent(s) are more recalcitrant to biodegradation. Accordingly, the triangular plot indicates that C_2- and C_3-alkylbenzenes are depleted, while C_4- alkylbenzenes are relatively enriched in the investigated crude oil samples. This trend, as indicated by the grey arrow in Figure 74, is in particular obvious for crude oils from Angola, which cover the broadest variety of C_2-, C_3- and C_4- alkylbenzene distributions.

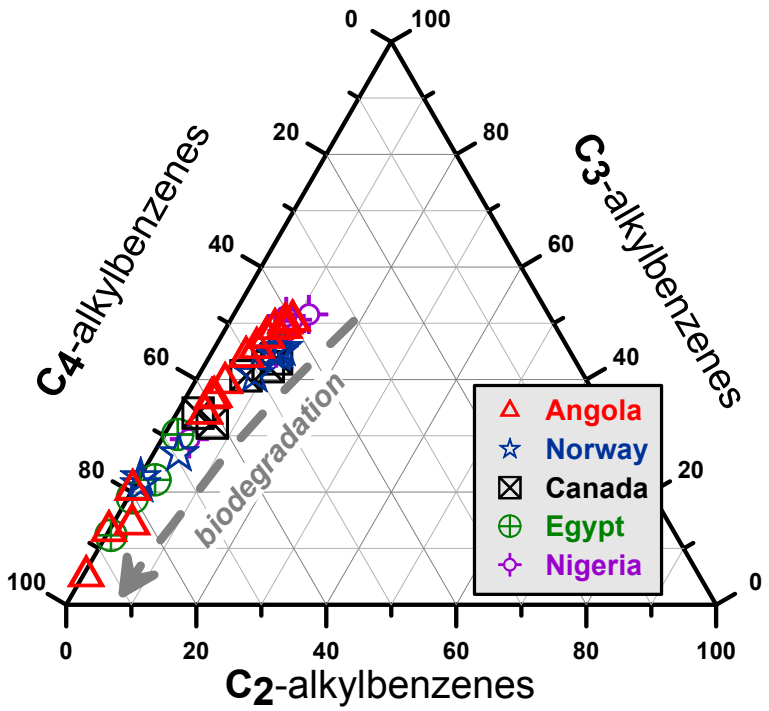

Fig. 74: Triangular plot shows relative abundances of C_2-, C_3- and C_4-alkylbenzenes. Obviously, the relative amounts of C_2- and C_3-alkylbenzenes are significantly depleted within the different petroleum systems. In contrast, relative amounts of C_4-alkylbenzenes increase. The grey arrow indicates increasing extents of biodegradation.

The triangular plot (Figure 74) indicates that in Angolan crude oils the strongest relative changes are obvious for C_3- and C_4- alkylbenzenes. In this sample set C_3-alkylbenzenes are reduced from ~50% to ~5%, while the percentage amounts of

C_4 –alkylbenzenes increase from ~40% to ~95%. In contrast, the relative concentration for C_2-alkylbenzens decreases only between ~10% and ~1%. Based on these relative changes C_2- and C_3- alkylbenzenes would be both depleted about 90%, while C_4- alkylbenzenes are enriched about 137% relative to least degraded sample.

Contrary to these relative concentration changes, the crossplot shown in Figure 75 indicates that in Angolan crude oils not only C_2- and C_3- alkylbenzenes are depleted by light to moderate biodegradation, but also the concentrations of C_4-alkylbenzenes are significantly reduced.

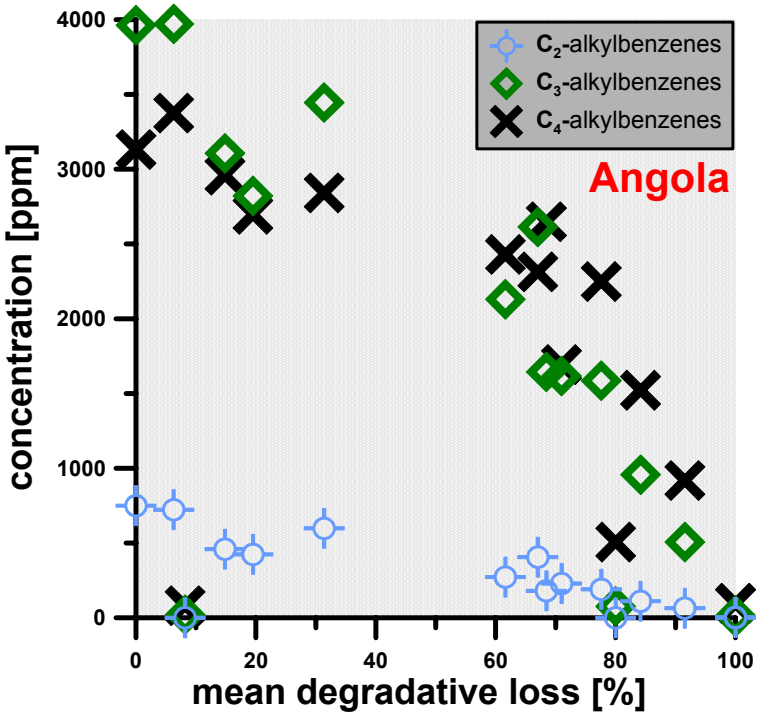

Fig. 75: Crossplot of calculated concentrations for C_2-, C_3- and C_4-alkylbenzenes in crude oils from Angola vs. the biodegradation parameter mean degradative loss, which was suggested earlier in this study.

In Angolan crude oils the calculated concentrations decrease for C_2-, C_3- and C_4 –alkylbenzenes from 750 to 0 ppm, 4000 to 5 ppm and 3400 to 80 ppm, respectively. Based on these concentration changes C_2- would be depleted about 100 %, C_3- alkylbenzenes about 99.9 % and C_4- alkylbenzenes about 97.7 %

relative to the highest concentration of the respective subgroups with the Angolan sample set. This clearly shows that all three alkylbenzene subgroups are significantly depleted in the light to moderately biodegraded crude oils from Angola. It also implies that the relative concentrations, as indicated by the triangular plot of Figure 74 may evoke a misinterpretation of the biodegradability of specific crude oil constituents. Here, it should be noted again that the calculated total concentrations of C_2- alkylbenzenes are too low due to the detection mode of GC-MS instrument. Nevertheless, in Angolan crude oils C_2 -alkylbenzenes are the most biodegraded compounds (100 %) among the three subgroups, which is in agreement with HUANG ET AL. (2004). It appears also reasonable that C_3-alkylbenzenes with 99.9 % are more degraded than the C_4-alkylbenzens (97.7 %). These data clearly show that the calculation of compound specific concentrations (ppm) enables the quantification of depletions. Hence, this approach enables a better assessment of the biodegradability of individual crude oil constituents than by relative considerations.

The specific susceptibility of individual aromatic hydrocarbons is not limited to compounds with different numbers of aromatic rings and to a different degree of alkylation of the molecule, but the compound-specific biodegradability is also likely to be relevant for different isomers of the same compound. In this context, it was shown by WILKES ET AL. (2000) that individual C_2-alkylbenzenes can be degraded to variable extents by sulphate-reducing bacteria. These laboratory experiments showed that, depending on the bacterial strain, the different isomers of, e.g., dimethylbenzenes decrease to variable extents. It was also reported by WIDDEL AND RABUS (2001) that among the three xylenes (*para*-, *meta*- and *ortho*-*xylene*) the *para*-isomer is most recalcitrant to biodegradation under anoxic conditions. For crude oils investigated in this study Figure 76 illustrates the relative amounts of the three isomers of dimethylbenzene in a triangular plot.

According to WIDDEL AND RABUS (2001), who reported that *para*-xylene is most recalcitrant to biodegradation, the triangular plot apparently indicates that *para*- and *ortho*- xylene are relatively enriched while *meta*- xylene is relatively depleted.

This trend, as indicated by the grey arrow in Figure 76, is in particular obvious for crude oils from Angola, which cover the broadest variety of individual xylene distributions. In crude oils from Angola the relative concentrations shift for *meta-xylene* from ~60% to ~30%, for *ortho*-xylene from ~30% to ~40% and for *para*-xylene from ~10% to ~35%. This apparently indicates a relative depletion of -50 % for *meta*-xylene and a relative enrichment of +25 % and +350 % for *ortho*- and *para*- xylenes, respectively.

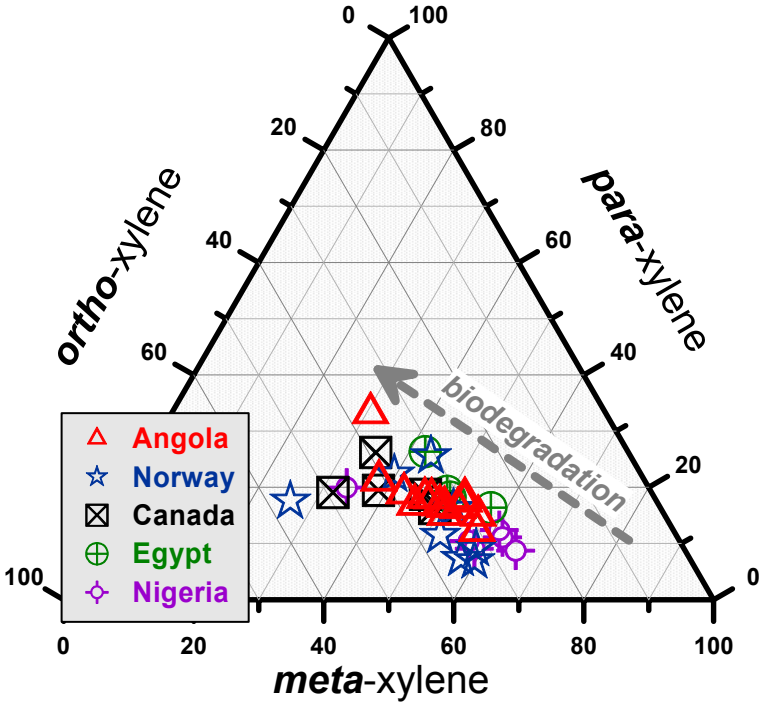

Fig. 76: Triangular plot showing relative abundances for dimethylbenzenes. Following WIDDEL AND RABUS (2001) *para*-xylene is most recalcitrant to biodegradation among the three dimethylbenzene isomers. Accordingly, the grey dashed arrow indicates increasing extents of biodegradation.

Contrary to these relative considerations, the crossplot of calculated concentrations vs. the biodegradation indicator mean degradative loss shown in Figure 77 clearly illustrates that in the crude oils from Angola all three xylenes are significantly depleted. Here it is shown that in Angolan crude oils the calculated concentrations for *meta*-, *ortho*- and *para*- xylenes decrease from 380ppm, 200ppm and 125 ppm, respectively, to zero ppm in all three dimethylbenzenes. Hence, a depletion of 100% of the initial amount of each isomer documents the

high susceptibility of this compound class within light to moderate biodegradation levels.

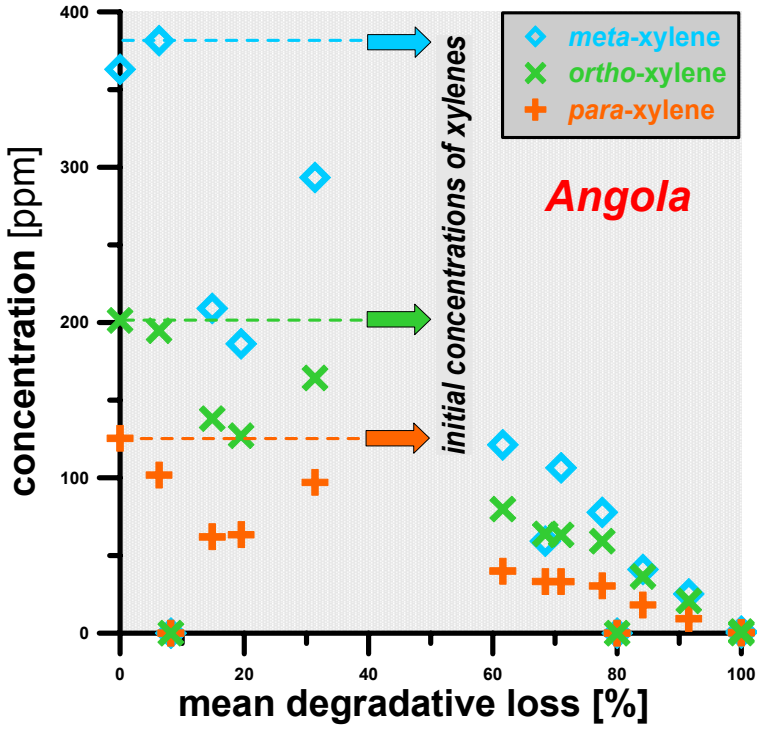

Fig. 77: Crossplot of calculated concentrations for the 3 isomers of dimethylbenzenes in crude oils from Angola vs. the biodegradation parameter mean degradative loss, which was earlier suggested in this study.

The triangular plot of Figure 76 indicates that *meta*- xylene is most depleted, while ortho- xylene is slightly and para- xylene is clearly enriched. This corresponds to the extent of concentration decreases as illustrated by Figure 77. It is shown in Figure 77 that *meta*-xylene is the isomer with the highest concentration in least degraded sample and that its total decrease is most pronounced, because the less abundant *ortho*- and *para*- xylene are also degraded to 100% in the most biodegraded sample. This raises the questions as to whether the extent of depletion of a specific crude oil constituent depends on its quantitative abundance. It might be speculated that the higher the concentration of a specific fraction the more bioavailable, in terms of abundance, is the compound for the degrading microbial consortia. It is clear that the bioavailability of a specific compound is not only controlled by its quantitative abundance. Other

factors, such as the compound-specific water solubility also contribute to the availability of a fraction in the water phase, where the metabolic processes take place. This implies that crude oil constituents that are more water soluble are likely also more bioavailable than the less soluble constituents. In this context, it is interesting to note that individual isomers of the same compound, e.g., the three xylenes, are characterised by similar water solubilities. Following PRICE ET AL. (1976) the most water soluble isomer among the three dimethylbenzenes is *ortho*-xylene (167ppm/25°C), whereas *para*-xylene (157ppm/25°C) and *meta*-xylene (134ppm/25°C) are less water soluble. In comparison to the water solubility of the most soluble crude oil constituent benzene (1780ppm/25°C) it becomes clear that the differences of water solubility's for the three xylenes are rather small. However, one might assume that even these slight differences control the bioavailability, and hence, also affect the extent of depletions. If this were the case the order of water solubilities should be reflected in the extent of concentration decreases. Interestingly, this is not obvious for the abundances of dimethylbenzenes in the biodegraded crude oil samples from Angola, because *meta*-xylene the least water soluble isomer, is the most degraded substrate. This implies that water washing is not the main control on the quantitative abundance of the dimethylbenzenes. Additionally, it substantiates the assumption that in samples from Angola the relative biodegradability of individual alkylbenzene isomers is considerably controlled by its quantitative abundance in the crude oil.

Alkylnaphthalenes

In total, 23 individual naphthalenes including the parent hydrocarbon and naphthalenes with attached alkyl groups containing one, two and three carbon atoms were identified. A partial mass chromatogram for the C_0-C_3 alkylnaphthalenes is shown in Figure 23. Summed concentrations for identified alkylnaphthalenes of the different subgroups are given in Figure 78.

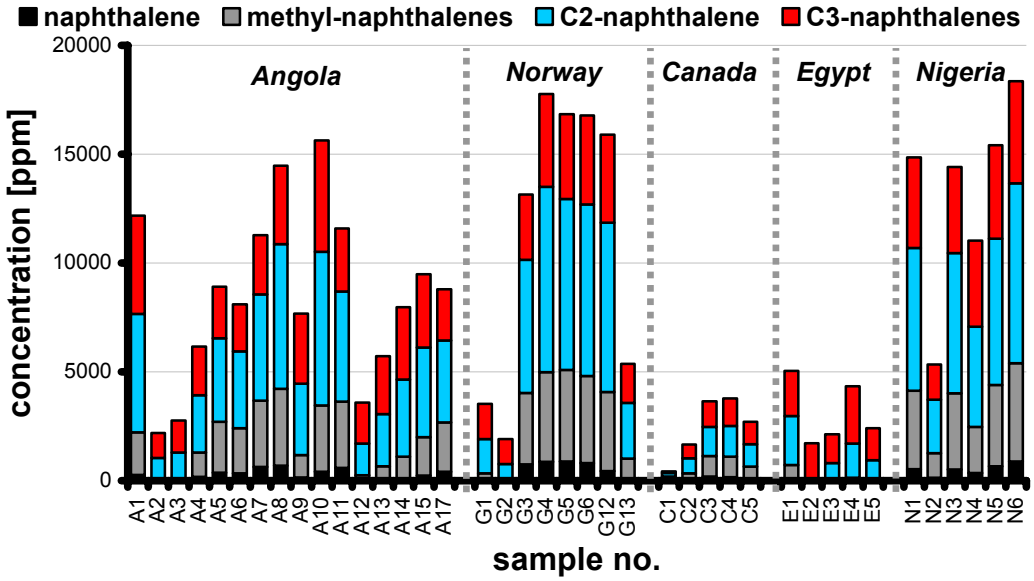

Fig. 78: Summed concentrations for all identified alkylnaphthalenes in crude oils from Angola, Norway, Canada, Egypt and Nigeria. For each sample the concentrations for naphthalene, methylnaphthalenes, C_2- and C_3 -naphthalenes are shown by the stacked bars.

Highest summed alkylnaphthalene concentrations with more than 15,000 ppm were determined for samples A10 from Angola, G4, G5, G6 and G12 from Norway, and for N5 and N6 from Nigeria. All other crude oils have alkylnaphthalene amounts below 15,000 ppm. The lowest concentration of this aromatic compound group with 480 ppm was measured for crude oil C1 from Canada. Each of the five individual sample sets is characterised by a high variability of alkylnaphthalene amounts giving a first indication that this compound class is affected by biodegradation.

This assumption is supported by Figure 79 A-D which illustrates that the variability of alkylnaphthalene concentrations in most of the samples correlates to the extent of biodegradation as indicated by ratios shown on the x-axes. The correlation of the summed alkylnaphthalene concentrations resemble to the results displayed for total aromatic hydrocarbon amounts and alkylbenzene concentrations (Figures 69 A-D and 73 A-D). Again the correlation of concentrations vs. the extent of biodegradation is highest for crude oils from Angola, Canada and Nigeria. In contrast, the alkylnaphthalene concentrations in samples from Norway and Egypt show no clear correlation to the extent of

biodegradation as indicated by the parameters shown on the x-axes in Figure 79 A-D. As mentioned before, this observation is only relevant for the two sample sets with the least variability of API gravities. This raises the question as to whether individual alkylnaphthalenes are biodegraded to different degrees.

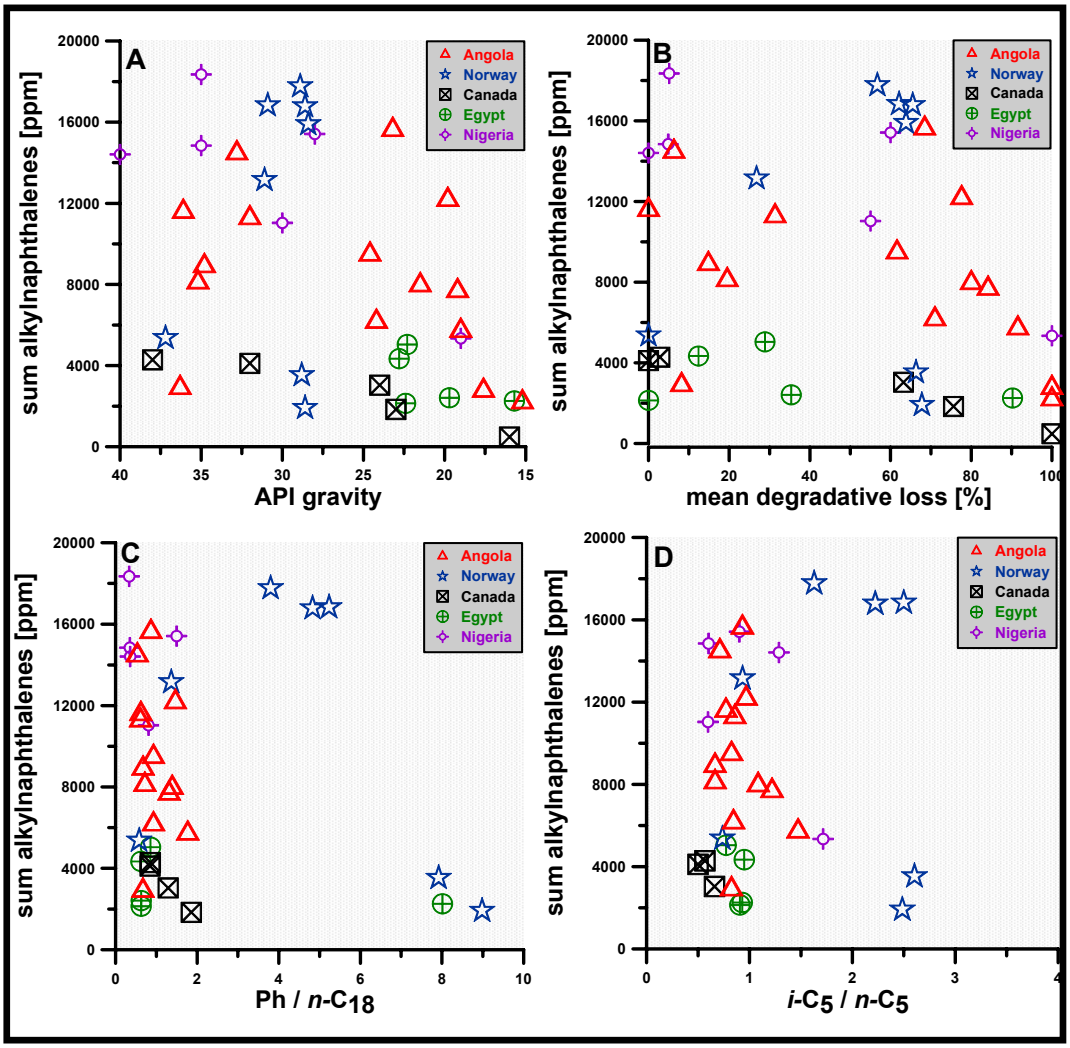

Fig. 79 A-D: The crossplots show summed concentrations of alkylated naphthalenes vs. API gravity, mean degradative loss, Ph/*n*-C_{18} and *i*-C_5/*n*-C_5 ratios which all indicate increasing extents of biodegradation on the x-axis from the left to right.

The triangular plot of Figure 80 clearly illustrates that the relative amounts of C_1-, C_2- and C_3- naphthalenes are highly variable within the five sample sets. According to the assumption of HUANG ET AL., 2004 that compounds with higher number of carbon atoms in the alkylated group are more recalcitrant to biodegradation Figure 80 indicates that C_1- and C_2- alkylnaphthalenes are

relatively depleted and that C_3- alkylnaphthalenes are relatively enriched. This general trend is obvious for samples of each biodegradation sequence and illustrated in Figure 80 by the grey dashed arrow.

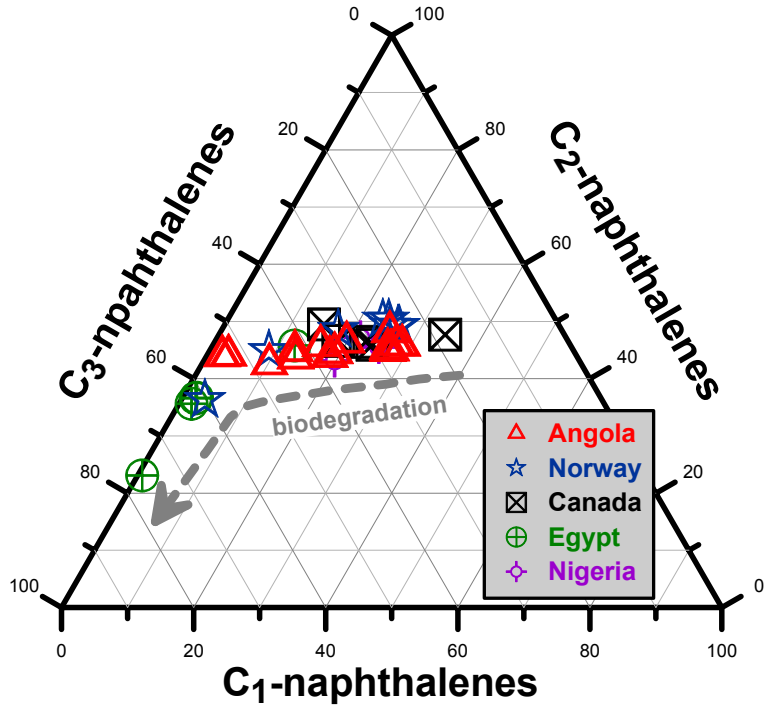

Fig. 80: Triangular plot showing relative abundance of C_1-, C_2- and C_3-alkylnaphthalenes. Obviously, relative amounts of C_1- and C_2-alkylnaphthalenes are clearly depleted within the different petroleum systems. In contrast, relative amounts of C_3-alkylbenzenes apparently increase.

The triangular plot indicates the strongest variability of relative alkylnaphthalene amounts for crude oils from Angola. Within this sample set the relative methylnaphthalene (C_1) concentrations decrease from ~30% to ~5%, whereas C_2-alkylnaphthalenes remain almost constant and C_3- alkylnaphthalenes are relatively enriched from ~25 to ~55%. Based on these relative changes C_1-alkylnaphthalenes are obviously depleted about 83.3% and C_4- alkylnaphthalenes are apparently enriched about 120% relative to least degraded sample.

In contrast to the relative changes that are displayed by the triangular plot, the crossplot of calculated concentrations vs. the mean degradative loss (Figure 81) clearly shows that all alkylnaphthalene subgroups in crude oils from Angola are

significantly depleted. It is noteworthy that the concentrations shown in Figure 81 are displayed on a logarithmic scale, and hence indicate a remarkable depletion of alkylnaphthalenes in Angolan samples within light to moderate levels of biodegradation.

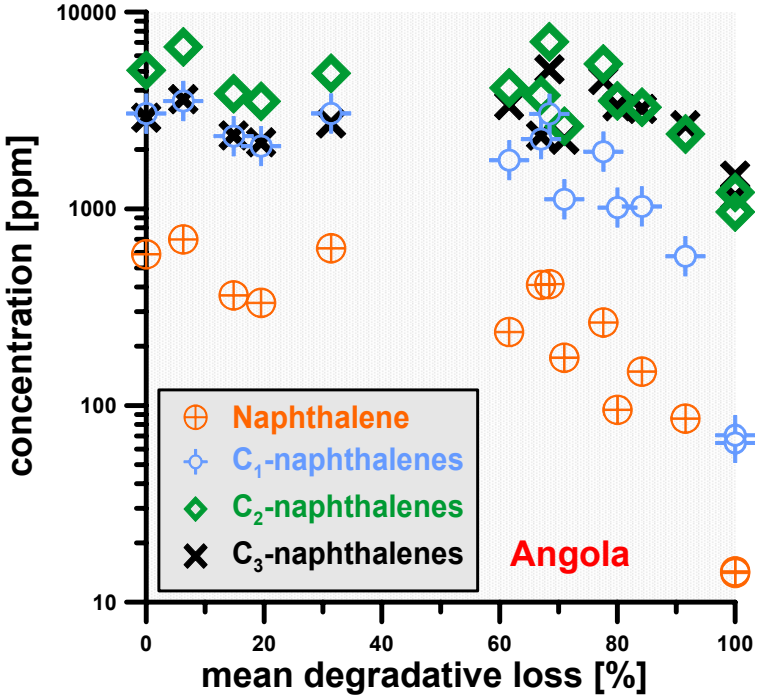

Fig. 81: Crossplot of calculated concentrations for naphthalene, C_1-, C_2- and C_3 alkylnaphthalenes in crude oils from Angola vs. the biodegradation parameter mean degradative loss. The alkylnaphthalene concentrations, displayed on a logarithmic scale, are significantly depleted in light to moderately biodegraded crude oil samples from Angola.

It is shown in Figure 81 that in crude oils from Angola the concentrations of naphthalene decrease from 700 ppm to 14 ppm, whereas C_1- alkylnaphthalene concentration shift from 3500 ppm to 65ppm, which both represents a total depletion of ~98%. Summed concentrations for C_2- alkylnaphthalenes decrease from 7000 ppm to 950 ppm, those for C_3- alkylnaphthalenes shift from 5100 ppm to 1150 ppm, which represent total depletions of 86.4% and 77.4%, respectively. This illustrates that the total amounts of naphthalene and C_1 –naphthalenes are more depleted than the concentrations of C_2- and C_3- naphthalenes, with the latter as the least affected.

It was shown before that the concentrations of C_2-, C_3- and C_4- alkylbenzenes are depleted about 100%, 99.9% and 97.7%, respectively. Hence, in Angolan crude oils the C_2- and C_3- alkylnaphthalenes are less degraded than any of the three alkylbenzene subgroups. This shows that the calculation of compound concentrations obviously enables a better comparison of quantitative changes occurring in biodegraded crude oils than is possible by assessing relative concentration changes. It also illustrates that the individual alkyl subgroups are depleted to different extents, with the higher alkylated compounds being more recalcitrant to biodegradation. While this observation has already been made by FISHER ET AL. (1998) who reported that, e.g., dimethylnaphthalenes are depleted prior to trimethylnaphthalenes, it should be noted that the approach used here is capable to quantify the compositional differences.

In this context it is interesting to note that FISHER ET AL. (1996 and 1998) also reported that individual C_2- alkylnaphthalenes are depleted to different extents. In FISHER ET AL. (1998) the following order from most to least susceptible to biodegradation for individual dimethylnaphthalenes was suggested; 1,6>2,7>1,7~1,3~1,4~1,2~2,6>>1,5>>2,3. Hence, it was postulated that 1,6-dimethylnaphthalene is less recalcitrant to biodegradation than all other dimethylnaphthalenes. It should be noted that these results are based on the analysis of biodegraded sediments that are contaminated with drill mud and thus reflect observations made in a single case study. However, FISHER ET AL. (1998) also investigated the susceptibility of alkylnaphthalenes of crude oils from Australian reservoirs, where a susceptibility for dimethylnaphthalenes of 1,6>>1,5>2,3 was assessed. Another study by WAMMER AND PETERS (2005) is based on laboratory experiments and quantified the biodegradation rates for individual alkylnaphthalenes. The authors attributed differences in the susceptibility to biodegradation of dimethylnaphthalenes to differences in the molecular structure of the individual isomers. Figure 82 shows the numbering system for naphthalene and all dimethylnaphthalenes sorted according to the combination of alkyl substituents position.

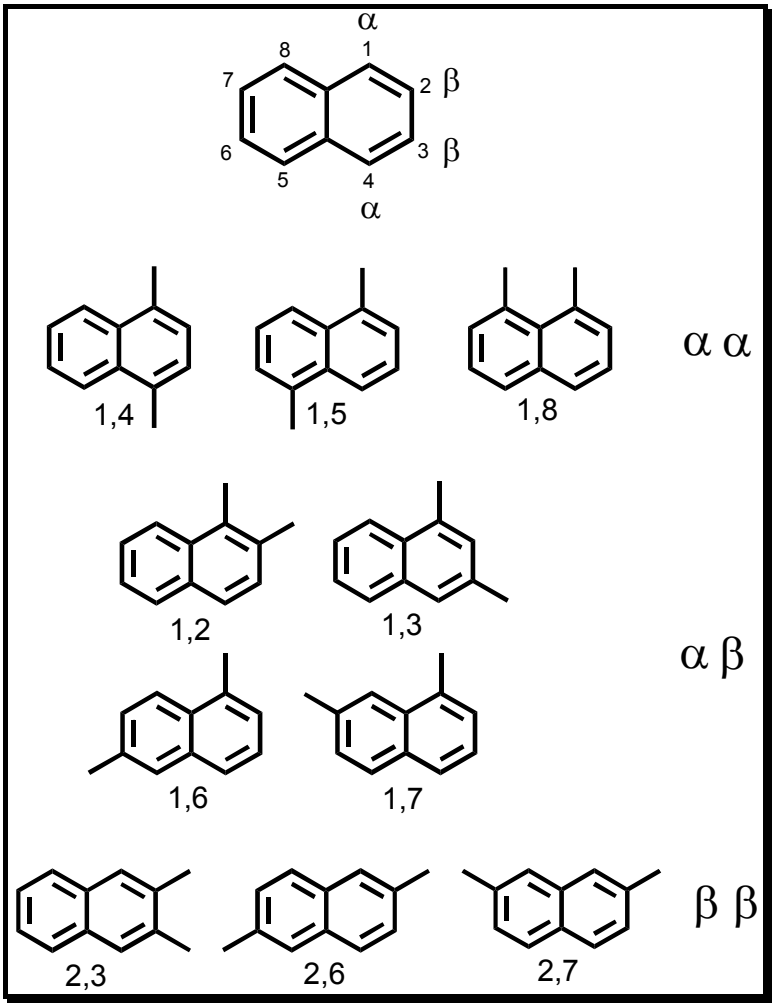

Fig. 82: The figure shows the molecule structure of naphthalene with the numbering system (top) and all isomers of dimethylnaphthalenes sorted according to the three combinations of alkyl substituent positions.

WAMMER AND PETERS (2005) showed that dimethylnaphthalenes with an alkyl substituent in an α position are less susceptible to biodegradation than those with an alkyl substituent in the β position. The authors reported that under laboratory conditions 1,8-DMN is the most recalcitrant dimethylnaphthalene isomer against biodegradation, whereas 2,7-DMN represents the most susceptible isomer. Hence, the results of WAMMER AND PETERS (2005) are contrary to the susceptibilities reported by FISHER ET AL. (1998), who observed that 1,6-DMN is the most susceptible isomer among the dimethylnaphthalenes in crude oils. A simple way to illustrate which of these two isomers is more labile against biodegradation for crude oils under study is to calculate the concentration ratio of 1,6/2,7-DMN. If

increasing extents of biodegradation are accompanied by increasing ratios, 1,6-DMN would be more recalcitrant than the 2,7- isomer, if the ratio decreases 1,6-DMN would be faster depleted. Figure 83 shows the 1,6/2,7 -DMN ratio for crude oil samples from Angola, where the C_2- alkylnaphthalenes are clearly affected (see Figure 81). Also shown are the concentration ratios of 1,6/1,5 -DMN and 2,7/1,8 -DMN, which include the most and least susceptible isomers as suggested by FISHER ET AL. (1998) and WAMMER AND PETERS (2003), respectively. Due to the co-elution of 1,4-DMN with 2,3-DMN, the latter isomer, which was suggested by FISHER ET AL. (1996 AND 1998) to be the most recalcitrant dimethylnaphthalene, is not used in the concentration ratio.

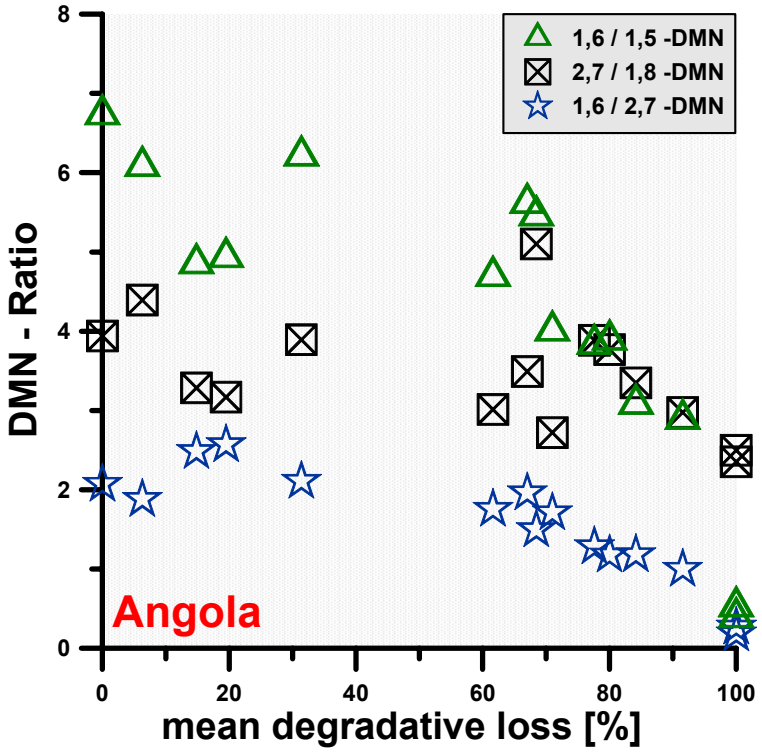

Fig. 83: Crossplot of three dimethylnaphthalene (DMN) ratios versus the biodegradation indicator mean degradative loss. Increasing extents of biodegradation are accompanied by decreasing concentration ratios.

The dimethylnaphthalene (DMN) concentration ratios shown in Figure 83 clearly decrease in the Angolan crude oils samples. This implies that 1,6-DMN is more susceptible to biodegradation than 1,5-DMN, as suggested by FISHER ET AL. (1998). It also fits to the laboratory experiments of WAMMER AND PETERS (2005),

because 1,6-DMN is characterised by an αβ configuration of the alkyl substituents, whereas in 1,5-DMN both methyl substituents are in αα position, and therefore thaught to be more recalcitrant to biodegradation. Figure 83 also shows that the 2,7/1,8 –DMN ratio decreases with ongoing biodegradation, which is in agreement with WAMMER AND PETERS (2005) who reported that dimethylnaphthalenes with an αα configuration of the alkyl substituents (e.g., 1,8-DMN) are more recalcitrant to biodegradation than isomers which have the alkyl substituents in ββ positions (e.g., 2,7-DMN). Interestingly, Figure 83 also shows a clear decrease of the 1,6/2,7 –DMN ratio in the Angolan sample set. This, however, is contrary to the assumption of WAMMER AND PETERS (2005), who proposed that dimethylnaphthalene isomers with alkyl substituents in αβ position (e.g., 1,6-DMN) are more recalcitrant than isomers which have the two substituents in ββ position (e.g., 2,7-DMN). The decrease of the 1,6/2,7 –DMN ratio with increasing biodegradation supports the observation of FISHER ET AL. (1996 AND 1998), who observed that 1,6-DMN is the most susceptible isomer among the dimethylnaphthalenes. However, it should also be noted that WAMMER AND PETERS (2005) investigated the effects of aerobic biodegradation and that is likely not the degradation mechanism most relevant in petroleum reservoirs, which implies that the results obtained from that laboratory study cannot stringently be assigned to the field samples used in this study. Additionally, it is noteworthy that WAMMER AND PETERS (2005) calculated biodegradation rates that are independent of bioavailability limitations.

It is interesting to note again (see chapter 2.5.2.2.1) that in particular the quantitative bioavailability, in terms of abundance, might control the extent of depletions of a specific substrate in a petroleum reservoir. This assumption is supported by Figure 84, because the obviously most depleted 1,6-DMN is the isomer with highest abundances in the least degraded samples. Due to the chromatographic co-elution of 1,4-DMN and 2,3-DMN only the concentrations for eight of the ten isomers are displayed.

Interestingly, Figure 84 illustrates not only that the strongest depletion is obvious for 1,6-dimethylnaphthalene, but also indicates that the slightest decrease can be calculated for 1,8-dimethylnaphthalene. For 1,8-DMN the lowest initial concentrations within the least degraded sample corresponds to the slightest maximum concentration decrease during ongoing biodegradation. This observation, as well as the approximation of concentrations going along with biodegradation was already described for results obtained for alkylbenzenes. Consequently, the concentrations calculated for dimethylnaphthalenes substantiate the results discussed for alkylbenzenes and again suggest that rather the calculated quantities of individual crude oil constituents control the extent of biodegradation.

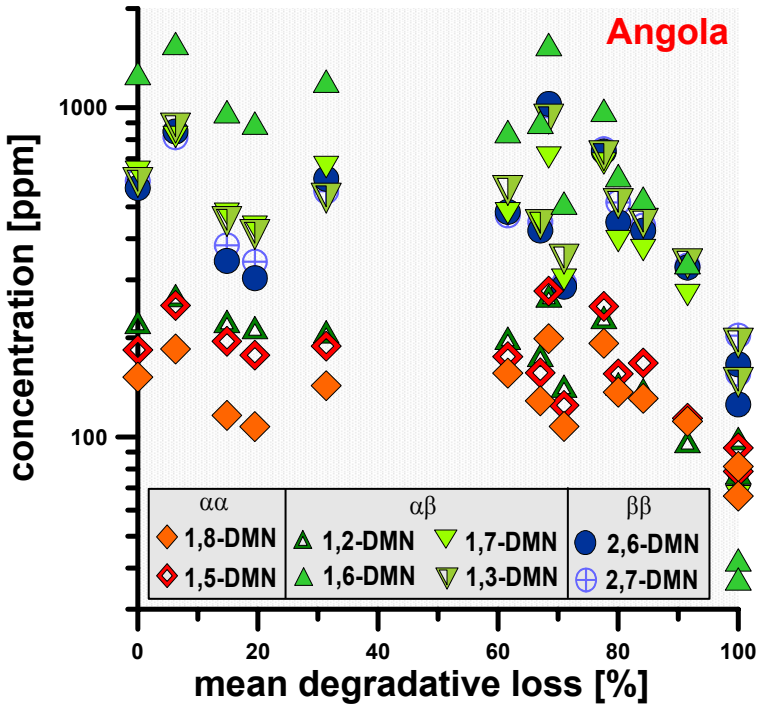

Fig. 84: Crossplot of the concentrations for dimethylnaphthalenes vs. the mean degradative loss that increases during proceeding biodegradation. The plot clearly shows that in Angolan crude oils 1,6-DMN is most depleted among the six displayed isomers.

It appears reasonable that also physical-chemical properties, such as water solubilities and structural characteristics might affect the bioavailability and/or biodegradability of a specific compound. However, Table 5 indicates that both water solubility and the position of the alkyl substituents do not correlate to the

maximum degradative loss of the individual dimethylbenzenes in crude oils from Angola. Table 5 illustrates that, e.g. the most depleted isomer 1,6-DMN is characterised by the lowest water solubility among the dimethylnaphthalenes. This clearly shows that water washing is not a relevant process that affects the abundance of aromatic hydrocarbons in crude oils from Angola. Table 5 also shows that the position of the alkyl substituents do not control the extent of degradation, because 1,6-DMN, as the most depleted compound is characterised by an αβ configuration, which is thought to be less susceptible to biodegradation than the ββ configuration. Interestingly, the maximum degradative losses correlate to the initial compound concentrations in the least degraded sample. Only 1,7-DMN is more strongly degraded than indicated by the initial concentration. This single inconsistency could be attributed to the limited chromatographic separation with 1,3-DMN, as shown in Figure 23. However, for seven of the eight chromatographically separated isomers of dimethylnaphthalenes the maximum degradative loss correlates to the initial concentration in the least affected crude oil. Consequently, the data shown and discussed give rise to the interpretation that the extents of degradative losses are predominantly controlled by the quantitative abundances of the substrates in the petroleum reservoir.

compound	max. degradative loss [%]	biodegradation extent	position of alkyl substituent	initial compound concentration [ppm]	water solubilties [mg/l]
1,6-DMN	97.6	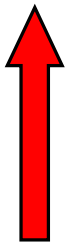	αβ	1515	0.9
1,7-DMN	89.7		αβ	706	n.a.
2,6-DMN	83.8		ββ	1027	1.7
2,7-DMN	80.0		ββ	1014	14.9
1,3-DMN	79.1		αβ	924	8
1,5-DMN	66.6		αα	277	3.1
1,2-DMN	63.0		αβ	261	14.9
1,8-DMN	59.0		αα	199	12.9

Table 5: The table correlates for eight individual dimethylnaphthalenes (DMN) the maximum degradative loss [%], which was suggested earlier in this study, the position of the alkyl substituent, the initial concentration of the compound in the least biodegraded sample and water solubilities, which are adopted from WAMMER AND PETERS (2005). For 1,7-DMN no aqueous solubility was available (n.a.). The red arrow indicates increasing maximum extents of compound-specific degradative losses.

Alkyldibenzothiophenes

In total, 22 individual dibenzothiophenes including the parent compound (dbt) and dibenzothiophenes substituted with alkyl groups containing one (C_1-dbt`s), two ($C_2$-dbt`s) and three (C_3-dbt`s) carbon atoms in the chain were identified. A partial mass chromatogram for the C_0-C_4 alkyldibenzothiophenes is shown in Figure 24. Summed concentrations for all identified alkyldibenzothiophenes in crude oils from the five different biodegradation sequences are shown in Figure 85

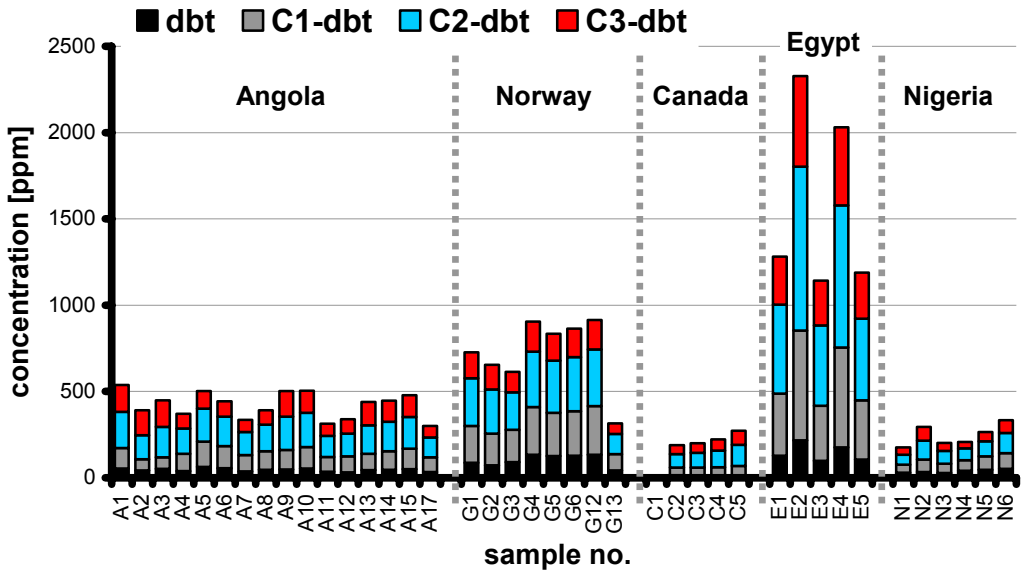

Fig. 85: Summed concentrations for alkyldibenzothiophene subgroups in crude oils from Angola, Norway, Canada, Egypt and Nigeria. Stacked bars indicate concentrations for dibenzothiophene (dbt), methyldibenzothiophenes (C_1-dbt), C_2 and C_3 -dibenzothiophenes. For sample C1 from Canada no alkylated dibenzothiophenes and only traces (5 ppm) for the parent dibenzothiophene were detected.

Highest summed amounts of alkyldibenzothiophenes were determined in crude oils from the Sudr oil field (E1-E5) from Egypt. In these crude oils, which were generated from a sulphur-rich carbonaceous source rock, calculated concentrations of dibenzothiophenes vary between 1140 ppm and 2330 ppm. In all other investigated samples the amounts of these sulphur bearing aromatic compounds are below 1000ppm. The lowest concentrations were measured for the marine sourced crude oils from the Tuktuk oil field in Canada. Relatively high concentrations of dibenzothiophenes were also determined in the crude oils from

the Gullfaks field offshore Norway which were sampled from the Brent Formation (G1-G6 and G12).

Each of the five different sample sets is characterised by only slight variances of alkyldibenzothiophene amounts giving a first indication that this compound class is obviously not strongly affected by initial to moderate biodegradation in the investigated petroleum systems. This assumption is supported by Figure 86 A-D which illustrate that the summed alkyldibenzothiophene concentrations do not systematically decrease with proceeding extents of biodegradation as indicated by the API gravity, the mean degradative loss, the Ph/*n*-C_{18} and *i*-C_5/*n*-C_5 ratios.

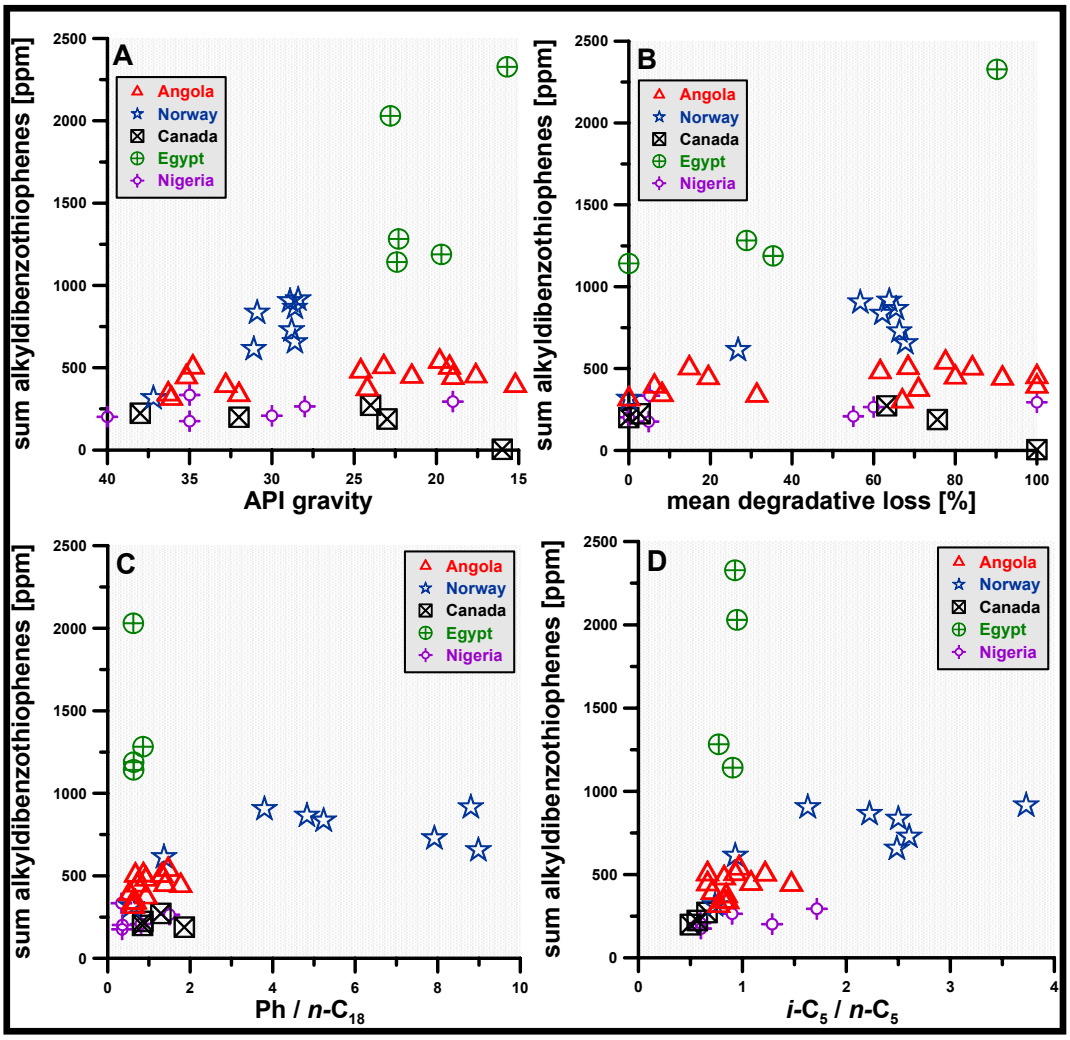

Fig. 86 A-D: The crossplots show the summed concentrations [ppm] of alkyldibenzothiophenes vs. API gravity, mean degradative loss, Phytane / *n*-C_{18} and *i*-C_5 / *n*-C_5 ratios which indicate increasing extents of biodegradation on the x-axis from the left to right.

However, the evaluation of concentrations for individual alkyldibenzothiophene subgroups indicates that individual alkyl subgroups of these aromatic hydrocarbons may be affected by biodegradation. Figure 87 shows that in crude oils from Angola some minor variability in the relative abundances for C_1-C_3 alkyldibenzothiophenes occur.

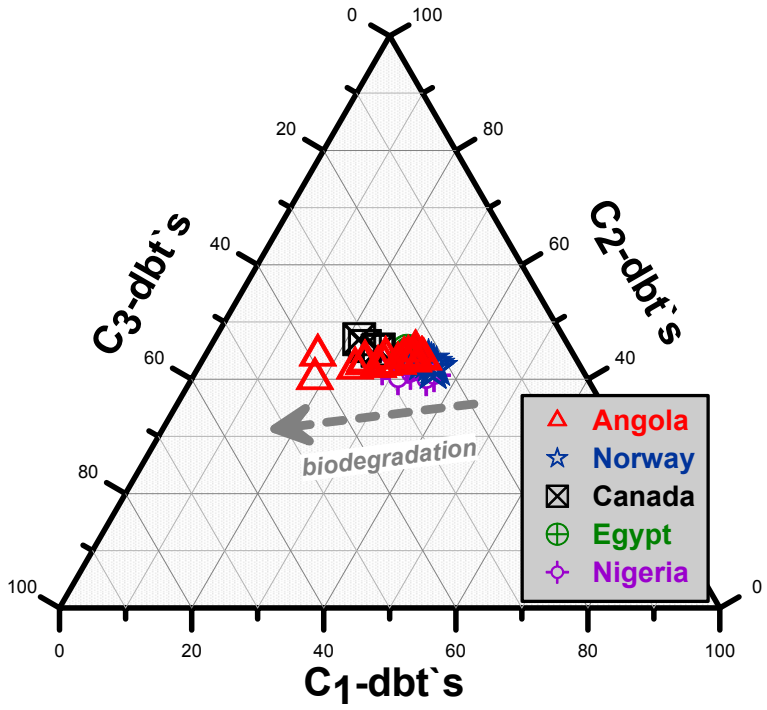

Fig. 87: Triangular plot showing the relative abundances of dibenzothiophenes with one, two and three carbon atoms in the alkyl substituent for crude oils from the five biodegradation sequences. Obviously, only in crude oil samples from Angola slight variances in the abundance of C_1-C_3 alkyldibenzothiophenes occur. The other four sample sets are characterised by invariant dbt- abundances.

Assuming that dibenzothiophenes with higher degree of alkylation are less susceptible to biodegradation, the triangular plot indicates that C_1-dbt`s in samples from Angola are most susceptible to biodegradation among the three displayed subgroups. Figure 87 also illustrates that the relative abundances of $C_2$-dbt`s remain almost constant in Angolan crude oils and that the amount of C_3-dbt`s relatively increases. The grey dashed arrow in the triangular plot indicates the relative compositional changes within the dibenzothiophene subgroups of Angolan crude oil samples. Contrary to the Angolan samples the plot also shows

that in crude oils from the other four petroleum systems almost no variances of relative abundances for alkyldibenzothiophenes occur. In chapter 5.2.1 it was shown that crude oils from Angola are the most biodegraded samples among the five investigated petroleum systems. This together with the invariance of alkyldibenzothiophene amounts in the other four sample sets gives rise to the assumption that this compound class is less affected by biodegradation than alkylbenzenes and alkylnaphthalenes.

This assumption is supported by Figure 88, which shows that in crude oils from Angola only the calculated concentrations of methyldibenzothiophenes are slightly depleted at pronounced degradation above 60% of mean degradative loss. In contrast, the concentrations of the other dibenzothiophene subgroups remain almost constant even at elevated biodegradation levels.

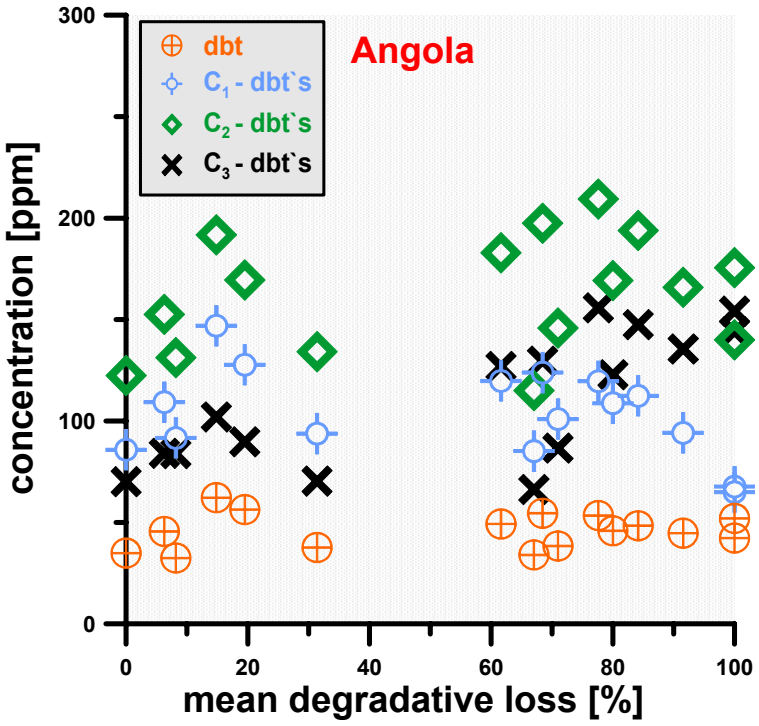

Fig. 88: Crossplot of calculated concentrations for dibenzothiophene (dbt), C_1-, C_2- and C_3- dibenzothiophenes in crude oils from Angola vs. the biodegradation parameter mean degradative loss, which was earlier suggested in this study.

The concentrations of methyldibenzothiophenes in Angolan crude oils vary from 147 ppm to 65 ppm, and thus, represent a maximum depletion of 55.8%. Compared with the maximum depletions for summed amounts of methylnaphthalenes (98%) it becomes evident that methyldibenzothiophenes are clearly less affected by light to moderate extents of biodegradation. The concentration decrease for the C_1-dbt`s amount is accompanied by a slight complementary increase of $C_3$-dbt`s. Assuming that C_3-dbt`s are not formed *de novo* the weak increase can be attributed to a relative enrichment of $C_3$-dbt`s in the crude oils when other compounds, such as the C_1-dbt`s are depleted.

A more detailed consideration of the individual methyldibenzothiophene concentrations for specific isomers (Figure 89) shows that obviously only 4-methyldibenzothiophene is clearly depleted in Angolan crude oils.

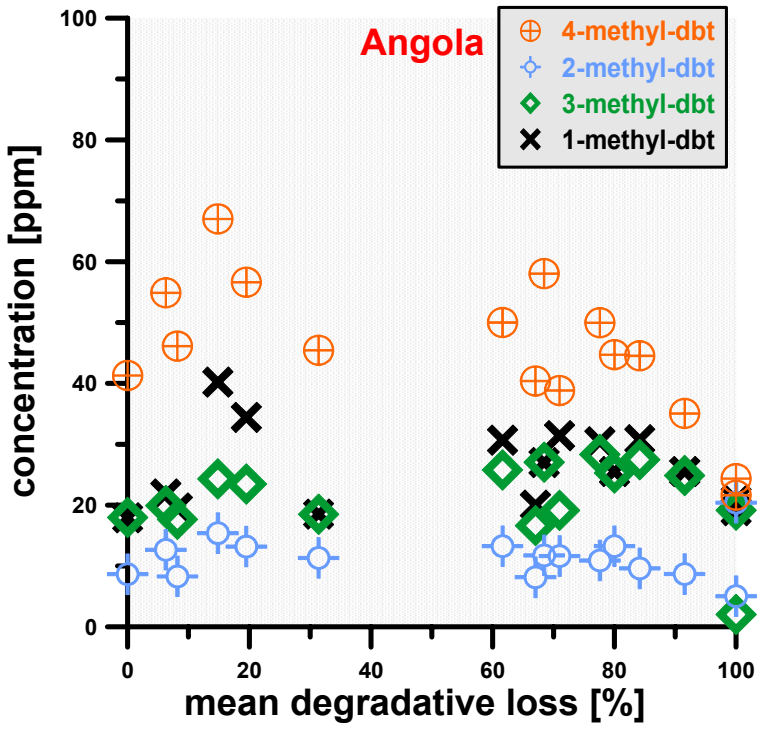

Fig. 89: The plot shows that in crude oils from Angola an increasing extent of biodegradation, as indicated by the mean degradative loss [%], is accompanied by a concentration decrease of 4-methyl-dibenzothiophene. Obviously, the other 3 displayed isomers of methyl-dibenzothiophenes are not affected by initial to moderate biodegradation in samples from Angola.

The calculated concentrations of the other individual methyldibenzothiophenes remain constant. This indicates that in crude oils from Angola these compounds are not affected by light to moderate biodegradation. Interestingly, the slightly depleted 4-methyldibenzothiophene is the C_1-dbt isomer with the highest calculated concentration in the least biodegraded crude oil as shown in Figure 90. This observation was already described for individual alkylbenzenes and alkylnaphthalenes, where relative strongest concentration shifts of specific isomers were detected for the compounds with highest concentrations in the least degraded samples. Hence, this observation again substantiates the assumption that relative degradation rates for specific crude oil constituents depend on the quantitative abundance.

Alkylphenanthrenes

In total, 28 individual phenanthrenes were identified, including the parent phenanthrene and alkylphenanthrenes with one, two and three carbon atoms in the alkyl substituent. A partial mass chromatogram for the C_0-C_3 alkylphenanthrenes is shown in Figure 25. Figure 90 shows the summed concentrations for the four different alkylphenanthrene subgroups in the 40 crude oils from the five different biodegradation sequences.

Highest summed alkylphenanthrene concentrations were determined for samples A1-A3 and A10 from Angola with more than 5000 ppm. All other crude oils have concentrations below 5000 ppm for this compound class. Lowest summed concentrations with less than 2000 ppm were determined for samples C1-C4 from Canada and for N4 from Nigeria. In the heavily biodegraded sample C1 from Canada only minor amounts (26 ppm) of the parent phenanthrene were detected. The highest variability of alkylphenanthrene concentrations within one of the investigated petroleum systems is obvious for crude oils from Angola. Here, the concentrations vary between 6000 ppm and 2350 ppm.

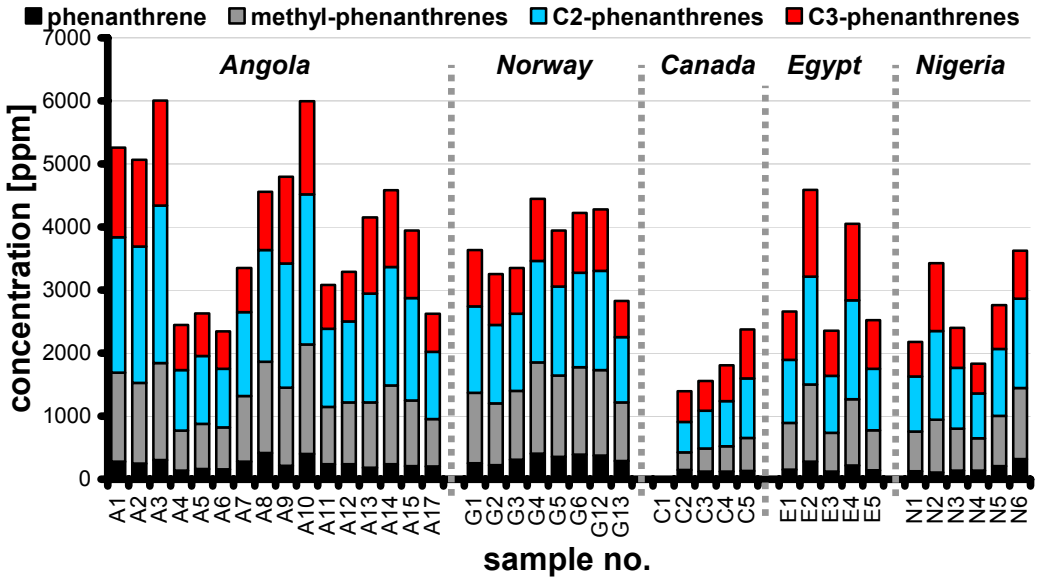

Fig. 90: Summed concentrations for alkylphenanthrene subgroups in samples from the biodegradation sequences. Stacked bars indicate concentrations for phenanthrene (black), methylphenanthrenes (grey), C_2- (blue) and C_3– (red) phenanthrenes.

Interestingly, the lowest summed alkylphenanthrene concentrations in the Angolan sample set were calculated for crude oils A4-A7, A11-A12 and A17, These samples were characterised by the D/(D+R) sterane ratio to be generated from a slightly different source rock lithofacies (see chapter 5.1), which indicates that the calculated concentration variations of alkylphenanthrenes in samples from Angola are rather source dependent than controlled by the extent of biodegradation. This assumption is supported by Figure 91 A-D, which shows no correlation of alkylphenanthrene amounts to the different biodegradation parameters. The plots apparently indicate that in crude oils from Angola ongoing biodegradation is accompanied by an increase of summed concentrations for alkylphenanthrenes. Here, it should be pointed out that the calculation of the concentration refers to 1 gram of crude oil. Therefore, the concentration of a nonbiodegraded oil constituent is relatively enriched if other compounds in this oil are depleted. Assuming that alkylphenanthrenes are not formed *de novo* in a petroleum reservoir the apparent concentration increase of these aromatic hydrocarbons can be assigned to a relative enrichment in the residue. It is clear that also the relative enrichment of a specific substrate does not preclude that the compound is not depleted, but it illustrates that the specific substrate is relatively

slightly depleted compared to the quantitative relevant depletions, and therefore can be assigned to be relatively unaffected.

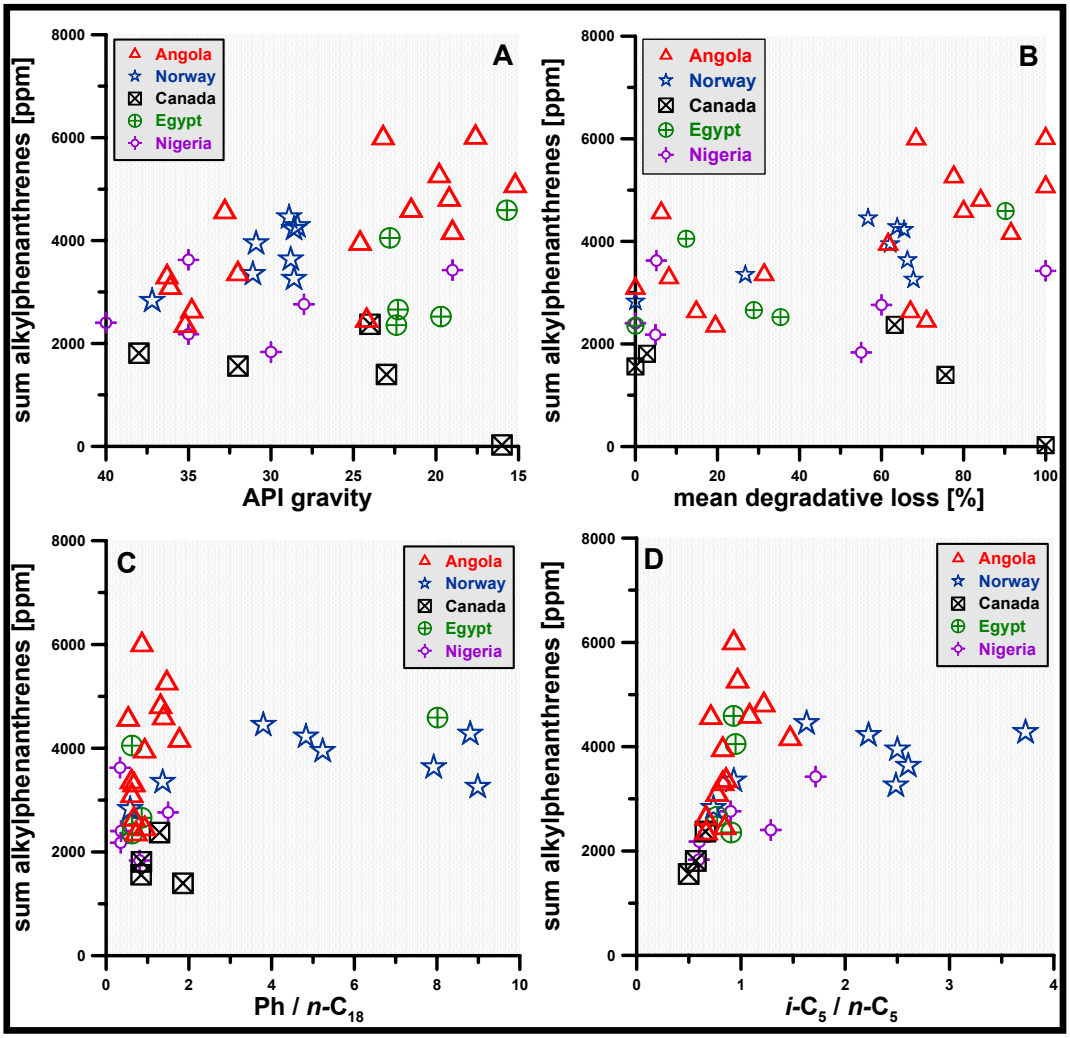

Fig. 91 A-D: The crossplots show the summed concentrations [ppm] of alkyldibenzothiophenes vs. API gravity, mean degradative loss, Phytane / n-C_{18} and i-C_5 / n-C_5 ratios which indicate increasing extents of biodegradation on the x-axis from the left to right.

The assumption that alkylphenanthrenes are not significantly affected by biodegradation is supported by the triangular plot of Figure 92, which illustrates that no clear variations of relative abundances for C_1- to C_3- alkylphenanthrenes occur in four of the five investigated petroleum systems. Only for crude oils from Angola slight differences in the relative abundances of the three displayed alkylphenanthrene subgroups are obvious.

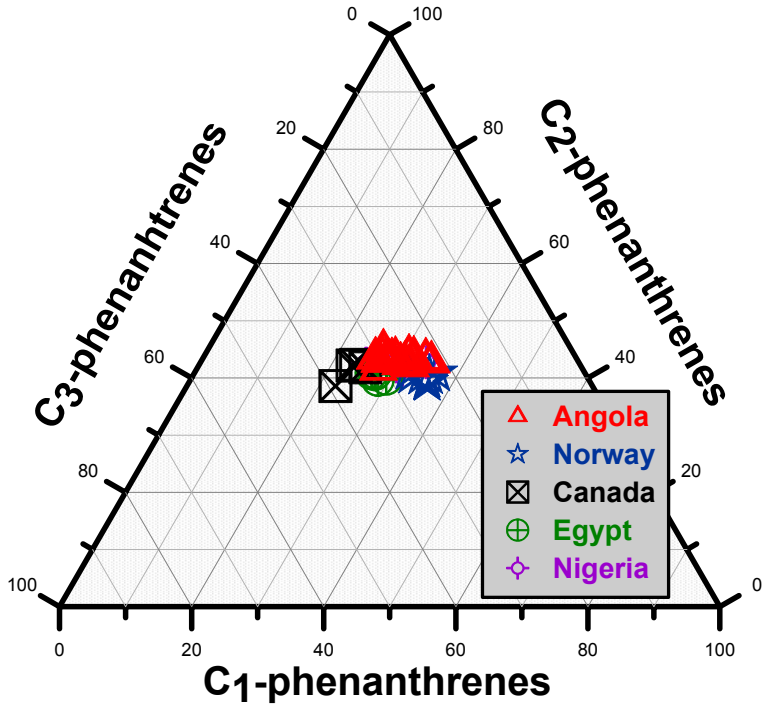

Fig. 92: Triangular plot showing the relative abundance of C_1-, C_2- and C_3-alkylphenanthrenes. Obviously, relative amounts of the individual alkylphenanthrene subgroups are not significantly affected to different extents in the investigated petroleum systems.

Assuming that phenanthrenes with lower degrees of alkylation are more affected by biodegradation, the triangular plot indicates a slight depletion of C_1-alkylphenanthrenes, constant C_2- abundances and a relative enrichment of C_3-alkylphenanthrenes. Here, it should be noted again that the differences in alkylphenanthrene amounts might also be due to the slightly different source rocks, and therefore, cannot be stringently attributed to biodegradation. However, the relative invariance of alkylphenanthrene amounts in comparison to the relative shifts of alkylated benzenes, naphthalenes and dibenzothiophenes as illustrated in Figures 76, 80 and 87, respectively, denotes to a high resistivity of alkylphenanthrenes to biodegradation within light to moderate alteration levels. Because the majority of the samples investigated in this study is characterised by alteration levels between PM 0-3, this invariance of individual alkylphenanthrene amounts is in accordance with HUANG ET AL. (2004) who postulated that biodegradation affects this compound class not prior to PM level 3 to 4.

For crude oils from Angola it was shown before that the concentrations of C_1- and C_2- alkylbenzenes and alkylnaphthalenes decrease systematically within light to moderate biodegradation levels. In contrast, the calculated concentrations of alkylphenanthrenes are not depleted within these biodegradation levels as illustrated by Figure 93 A-D.

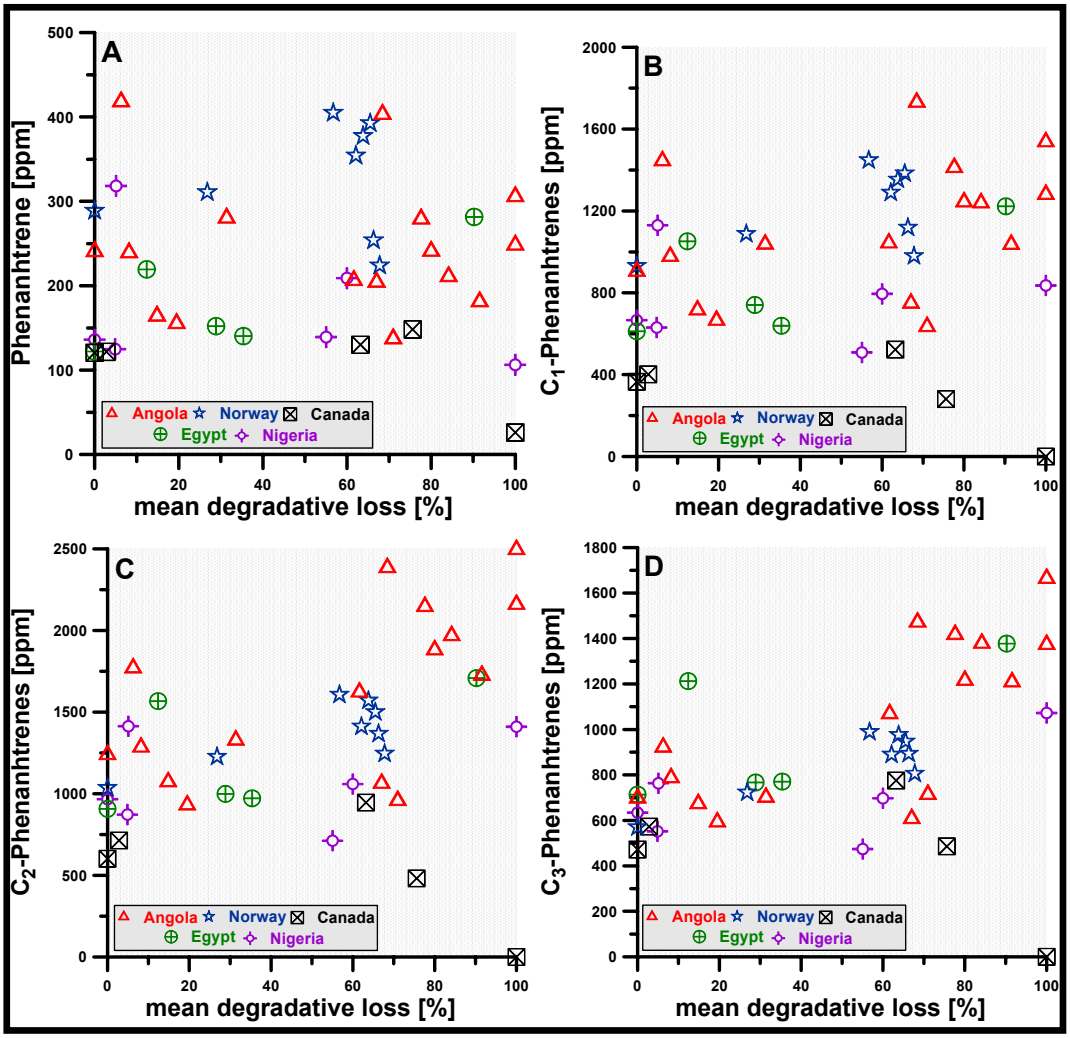

Fig. 93 A-D: Crossplots of calculated concentrations for phenanthrene, C_1-, C_2- and C_3-alkylphenanthrenes in crude oils from the five biodegradation sequences vs. the mean degradative loss.

Neither the parent phenanthrene nor the C_1-, C_2- and C_3- alkylphenanthrene concentrations decrease with increasing extent of biodegradation in any of the five investigated sample sets. Hence, the results of this study again substantiate the general assumption (e.g., HUANG ET AL., 2004) that alkylphenanthrenes are more resistant to biodegradation than alkylated benzenes and naphthalenes.

Figure 93 A-D shows that none of the four alkylphenanthrene subgroups is affected by biodegradation in crude oils under study, hence, it appears also unlikely that individual isomers of methylphenanthrenes are depleted to different extents as it was reported by HUANG ET AL. (2004) for more heavily biodegraded crude oils. The authors observed in Chinese crude oils a relative enrichment of 9-methylphenanthrene within biodegradation levels PM 5-7. The lower susceptibility of 9-methylphenanthrene to biodegradation was also reported by ROWLAND ET AL. (1986) and BUDZINSKI ET AL. (1998), who performed both incubation experiments, where samples were aerobically biodegraded. HUANG ET AL. (2004) reported that above moderate biodegradation levels the following order of susceptibility for individual methylphenanthrene isomers occurs: 2-MP > 1-MP; 3-MP > 9 MP. Figure 94 shows the calculated concentrations for the four methylphenanthrene isomers in Angolan crude oils. Figure 95 shows concentration ratios with 9-MP in the numerator to illustrate possible relative concentration shifts.

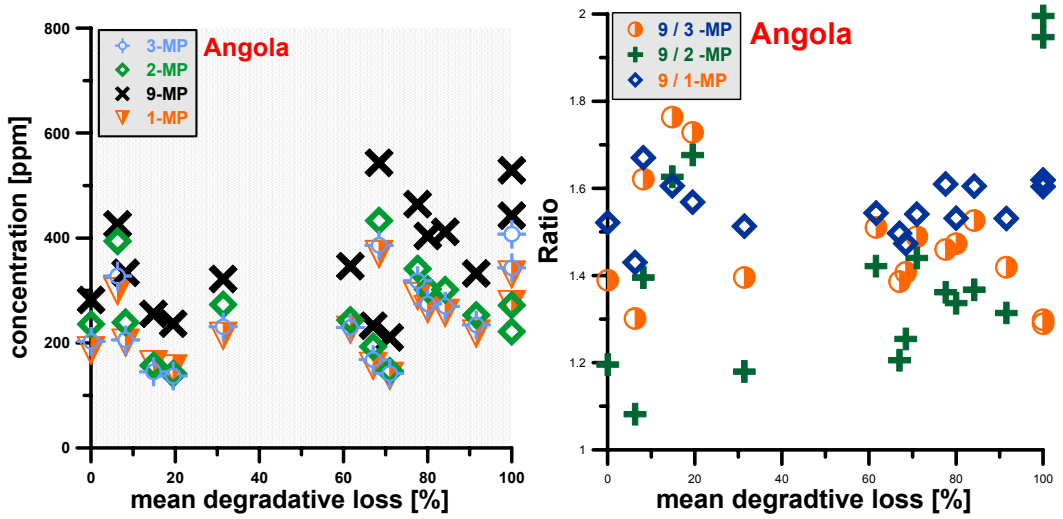

Fig. 94 (left): In crude oils from Angola increasing extents of biodegradation are not accompanied by systematic concentration depletions of individual methylphenanthrene isomers. **Fig. 95 (right):** Concentration ratios including the four methylphenanthrenes with 9-methylphenanthrene (9-MP) in the numerator indicate no systematic trend.

The concentration data shown in Figure 95 indicate that none of the four individual methylphenanthrenes is systematically depleted within light to moderate biodegradation levels. The observed concentration invariance of

methylphenanthrenes denotes to a rather high recalcitrance of these hydrocarbons against light to moderate biodegradation. This assumption is supported by Figure 95, because none of the three concentration ratios with 9-methylphehanthrene (9-MP) in the numerator shows a systematic trend. Hence, the data substantiate previously published results of HUANG ET AL. (2004), who showed that individual isomers of methylphenanthrenes are not depleted by biodegradation within light to moderate stages of biodegradation.

5.2.2.3 Alteration patterns of aromatic hydrocarbons

The aromatic hydrocarbons are in addition to light and saturated hydrocarbons the quantitatively most important compound class in conventional crude oils (PETERS ET AL., 2005). Figure 96 shows the correlation of concentrations for these two hydrocarbon compound classes in the crude oils from the five biodegradation sequences.

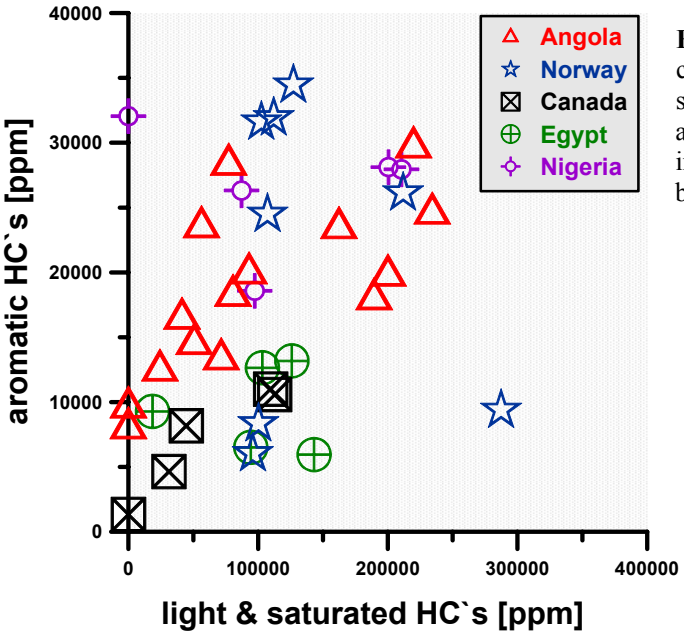

Fig. 96: Correlation of summed concentrations for light and saturated hydrocarbons to summed amounts of aromatic hydrocarbons in crude oils from the five biodegradation sequences.

The crossplot indicates that in Angolan and Canadian crude oils the summed concentrations of aromatic hydrocarbons clearly correlate to the summed amounts

of light and saturated hydrocarbons. Total summed concentrations for aromatic hydrocarbons are roughly one order of magnitude lower than for summed light and saturated hydrocarbons. Interestingly, the observed fair linear correlation between the two volumetrically most relevant hydrocarbon compound classes can not be observed for samples from Norway, Egypt and Nigeria, and therefore denote to different alteration effects occurring in different petroleum systems, as already discussed in chapter 5.2.1. Hence, it is suggested that the concept how to assess alterations for single crude oil constituents, which was introduced in chapter 5.2.1 for light and saturated hydrocarbons can also be applied to compounds of the aromatic hydrocarbon fraction. It was already shown in chapters 5.2.2.1 that in Angolan crude oil samples alkylated benzenes and naphthalenes are significantly depleted within light to moderate biodegradation levels. Figure 97 shows that proceeding biodegradation, as indicated by the mean degradative loss is accompanied by a clear concentration decrease of summed concentrations of alkylbenzenes and alkylnaphthalenes in Angolan samples.

Consequently, this sample set is suitable for illustrating the quantitative effects of biodegradation on individual alkylbenzenes and alkylnaphthalenes. According to the biodegradation assessment concept discussed in chapter 5.2.1, Figure 96 illustrates that in samples from Angola the calculated degradative losses for summed alkylbenzenes and alkylnaphthalenes clearly correlate to increasing extents of biodegradation. Obviously, the extent of depletion, as illustrated by the degradative losses, are higher for summed alkylbenzenes than for alkylnaphthalenes in most of the crude oils from Angola. This indicates a higher susceptibility of the alkylbenzenes, whose molecular structures are based on only one aromatic ring, whereas the apparently more recalcitrant alkylnaphthalenes are based on two condensed aromatic rings. However, the biodegradation assessment concept described in chapter 5.2.1 can also be used to calculate the degradative losses for individual crude oil constituents. Figures 99 and 100 show the degradation patterns for individual alkylbenzenes and alkylnaphthalenes of three selected crude oils from Angola, which represent different biodegradation levels by means of the mean degradative loss.

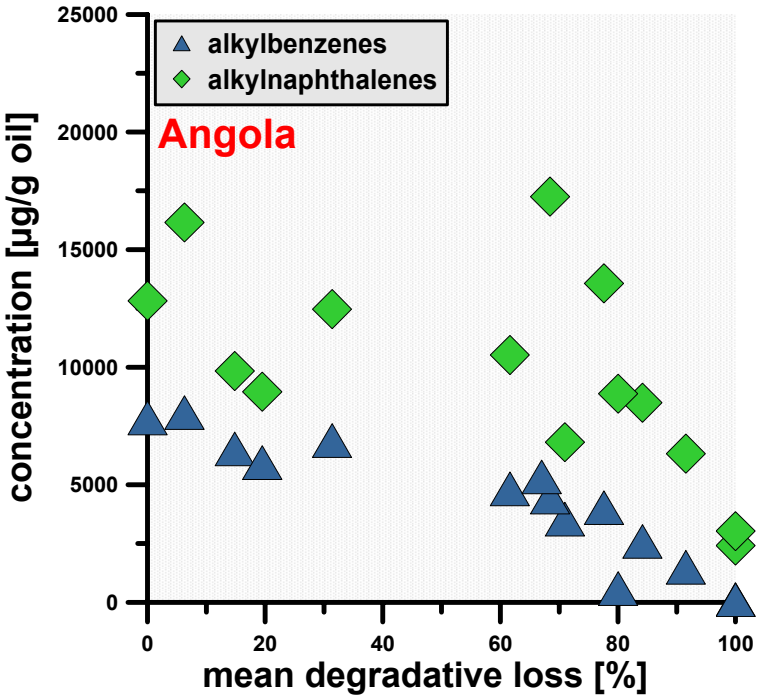

Fig. 97: In crude oils from Angola ongoing biodegradation, as indicated by the mean degradative loss, is accompanied by a clear concentration decrease of alkylated benzenes and naphthalenes.

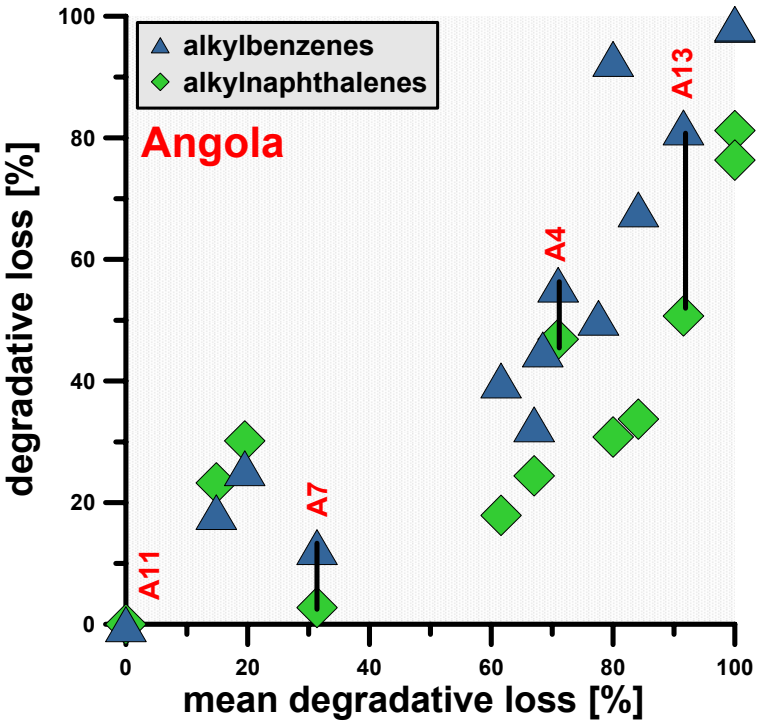

Fig. 98: In crude oils from Angola an increasing extent of biodegradation is accompanied by increasing degradative losses for alkylated benzenes and naphthalenes. Calculated degradative losses for alkylnaphthalenes are less pronounced than for alkylbenzenes in most of the Angolan samples.

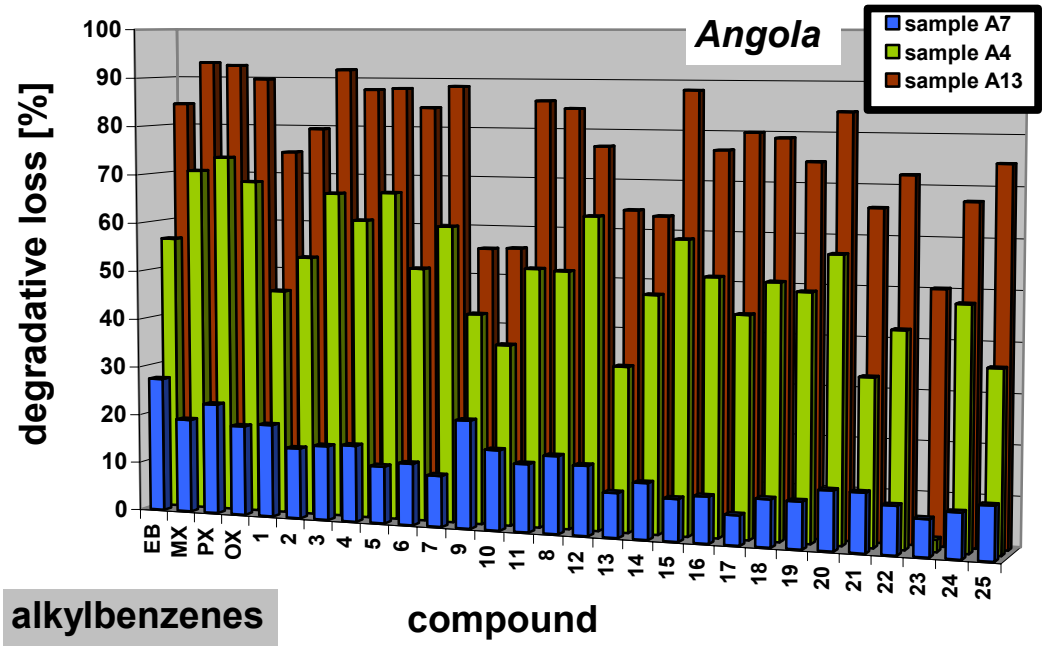

Fig. 99: Degradative losses for individual alkylbenzenes in three selected crude oils from Angola. Degradative losses for each compound were calculated as a percentage relative to the concentration of the respective alkylbenzene in the least biodegraded sample A11. Compound names for the displayed numbers are assigned in Figure 22; EB = ethylbenzene; MX = *meta*-xylene; PX = *para*-xylene; OX = *ortho*-xylene.

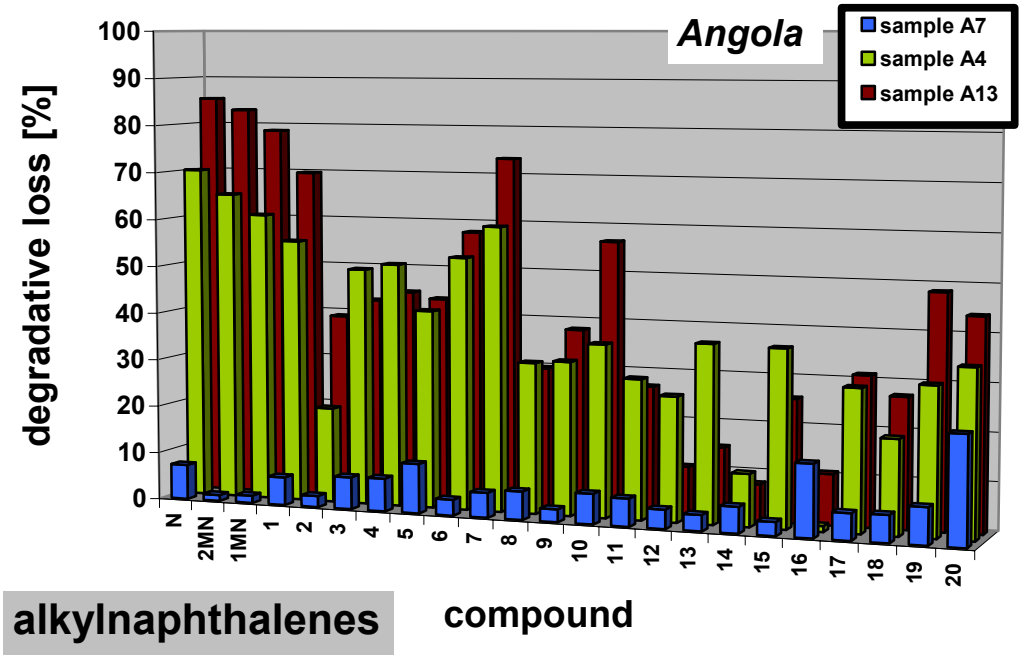

Fig. 100: Degradative losses for individual alkylnaphthalenes in three selected crude oils from Angola. Degradative losses for each compound were calculated as a percentage relative to the concentration of the respective alkylnaphthalene in the least biodegraded sample A11. Compound names for the displayed numbers are assigned in Figure 23; N = naphthalene; 2MN = 2-methylnaphthalene; 1MN = 1-methylnaphthalene.

According to equation (2) which was discussed in chapter 5.2.1., degradative losses for individual aromatic hydrocarbons can be calculated as a percentage relative to the concentration of each respective compound in the least biodegraded sample in each individual biodegradation sequence. Figures 99 and 100 show the degradative losses for the Angolan samples A7, A4 and A13, which are characterised by biodegradation extents of 31.4%, 71.0% and 91.5% mean degradative loss, respectively. These crude oils were already used to illustrate degradation patterns for individual light and saturated hydrocarbons and represent three different alteration levels in terms of light to moderate biodegradation. However, the degradative losses for individual aromatic compounds shown in Figures 99 and 100 clearly illustrate that in samples from Angola alkylbenzenes are stronger affected by biodegradation than alkylnaphthalenes.

Interestingly, the calculated degradative losses show no significant depletion preference for a specific isomer of, e.g. dimethylbenzenes (MX; PX; OX) in one of the three selected samples. This observation appears to be contrary to the results discussed in chapter 5.2.2.1, where it was shown that the total concentration of *meta*-xylene is most strongly depleted among the 3 isomers *meta*-, *para*- and *ortho*-xylene in Angolan crude oils. However, it was also shown in chapter 5.2.2.1 that with increasing extent of biodegradation the total concentrations of dimethylbenzenes progressively approximate to the same value. Here, it should be noted that the calculation of the degradative loss sets the amount of each respective compound in the least biodegraded sample to 100% and therefore neglects any concentration differences in the initial amounts of the different crude oil constituents. Therefore, degradative losses illustrate depletions for individual oil constituents independently of the initial concentration and enable the comparison of relative depletions for different compounds. Additionally, the degradative loss provides the opportunity to compare depletions of the same compound in crude oils from different petroleum systems, where the initial concentrations of the respective compound might be different. In this context, Figure 101 and 102 show degradation patterns for alkylbenzenes and alkylnaphthalenes for three crude oils from Canada.

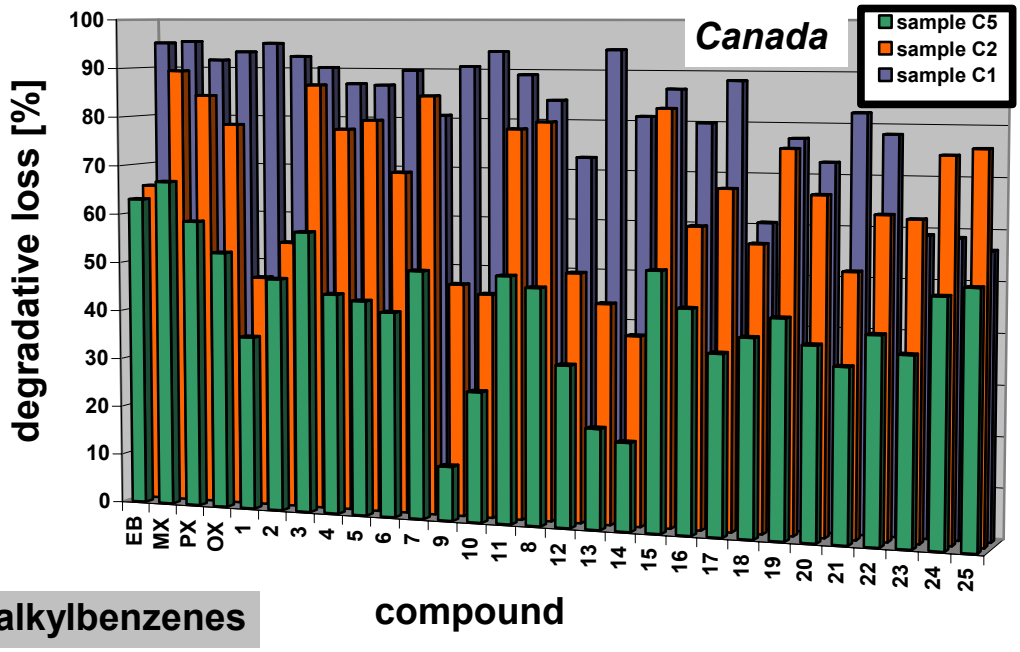

Fig. 101: Degradative losses for individual alkylbenzenes in three selected crude oils from Canada. Degradative losses for each compound were calculated as a percentage relative to the concentration of the respective alkylbenzene in the least biodegraded sample C3. Compound names for the displayed numbers are assigned in Figure 22; EB = ethylbenzene; MX = *meta*-xylene; PX = *para*-xylene; OX = *ortho*-xylene.

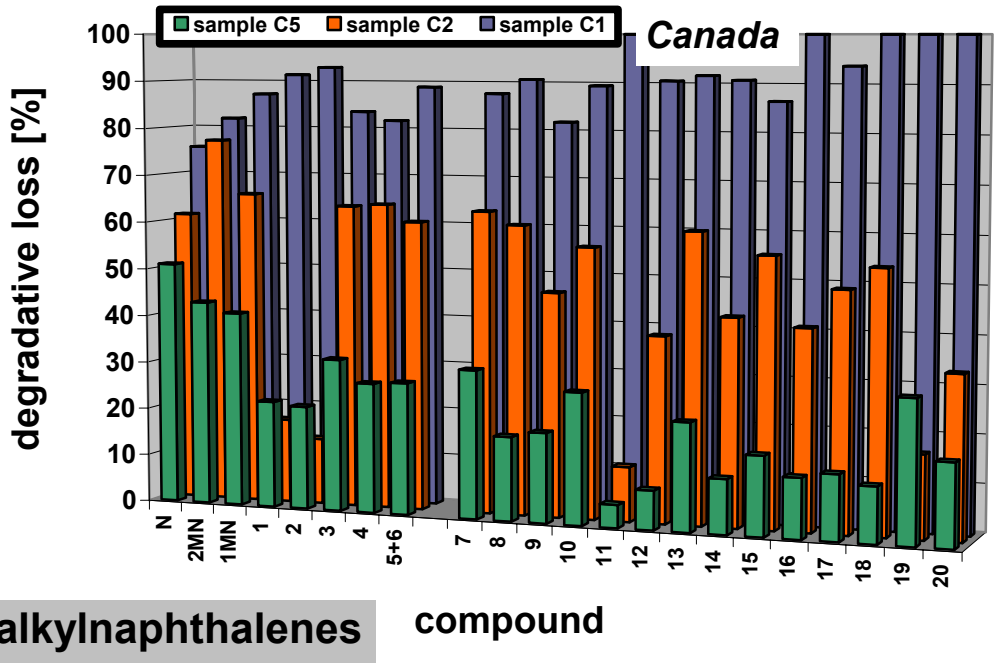

Fig. 102: Degradative losses for individual alkylnaphthalenes in three selected crude oils from Canada. Degradative losses for each compound were calculated as a percentage relative to the concentration of the respective alkylnaphthalene in the least biodegraded sample C3. Compound names for the displayed numbers are assigned in Figure 23; N = naphthalene; 2MN = 2-methylnaphthalene; 1MN = 1-methylnaphthalene. Due to the chromatographic co-elution of 1,3-DMN and 1,7-DMN in samples from Canada only one value for both compounds (5+6) can be given.

It was shown in Figure 96 that beside crude oils from Angola also samples from Canada show a systematic correlation between the concentrations for aromatic hydrocarbons and the amount of light and saturated hydrocarbons. Therefore, the degradation losses for individual alkylated benzenes and naphthalenes for three selected crude oils from Canada are shown in Figures 99 and 100. The degradation patterns suggest that especially the alkylnaphthalenes are relatively stronger depleted in Canadian samples than in crude oils from Angola. However, it also becomes clear, that the degradation patterns of aromatic hydrocarbons, as already shown for light and saturated hydrocarbons, are different in different petroleum systems. This clearly shows that the assessment of biodegradation effects needs to be performed by tools which consider a great variety of different oil constituents. Such an evaluation is possible using the parameters suggested in this study and the application is not only limited to light and saturated hydrocarbons but can also, as shown in this chapter, be applied to the aromatic hydrocarbon fraction. The assessment of biodegradation effects on individual aromatic hydrocarbons showed that alkylbenzenes and alkylnaphthalenes are significantly affected within initial and moderate alteration levels. This leads to the question as to whether the application of molecular parameters that are based on such compounds are still reliable tools for light to moderately biodegraded crude oils. In particular, the application of alkylnaphthalenes, which are often used to assess, e.g., the thermal maturity of crude oils, may lead to misinterpretations if this compound class is affected by biodegradation. Therefore, the following chapter discusses the effects of light to moderate biodegradation on selected geochemical parameters based on aromatic hydrocarbons.

5.2.2.4 Impact of biodegradation on aromatic hydrocarbon parameters

Aromatic hydrocarbons, such as alkylphenanthrenes, alkylnaphthalenes, and alkyldibenzothiophenes are routinely used as crude oil maturity indicators (e.g., ALEXANDER ET AL., 1983, 1985; RADKE AND WELTE, 1981, RADKE ET AL.1982,

1986, RADKE, 1988). Generally, it assumed that these aromatic hydrocarbons are not affected within light to moderate biodegradation levels. However, for this assumption the counterevidence was given is this study, and hence, puts up the question to which extent light to moderate biodegradation potentially influence the maturity proxies.

It was shown earlier that the Angolan samples are characterised by slight differences in thermal maturity. However, it was also already discussed that the quantitatively most important compositional variations in this petroleum system can be mainly traced back to biodegradation. Figure 103 shows for crude oils from Angola the values for two routinely used maturity parameters. The crossplot indicates an almost linear correlation for the MPI-1 and the C_{29}-ββ/(ββ+αα)-cholestane ratio. The latter ratio is based on steranes which are assumed to be affected not prior to heavy levels of biodegradation (PETERS ET AL., 2005), and hence, should be a reliable tool to assess thermal maturity in light to moderately biodegraded samples. The MPI-1 is based on methylphenanthrenes that are also not affected by light to moderate biodegradation, as it was shown before. Hence, both parameters appear to be reliable tools to assess the thermal maturity in light to moderately biodegraded crude oils.

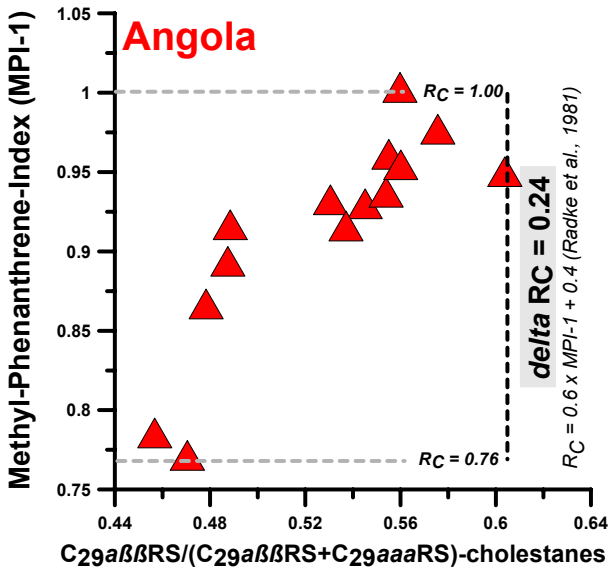

Fig. 103: Correlation of the thermal maturity parameters MPI-1 and C_{29}-cholestane ratio for crude oils from Angola. Both parameters increase with higher thermal stress. The linear correlation suggests that both parameters are only controlled by thermal stress.

The assumption that the MPI-1 is not affected by light to moderate biodegradation is supported by Figures 104 and 105, which illustrate that the biodegradation parameters mean degradative loss and Ph/*n*-C_{18} show no clear linear correlation to the MPI-1. This clearly indicates that light to moderate biodegradation does not significantly affect the MPI-1 in crude oils from Angola. Hence, the MPI-1 can be used as a reliable maturity parameter for the light to moderately biodegraded crude oil samples from Angola.

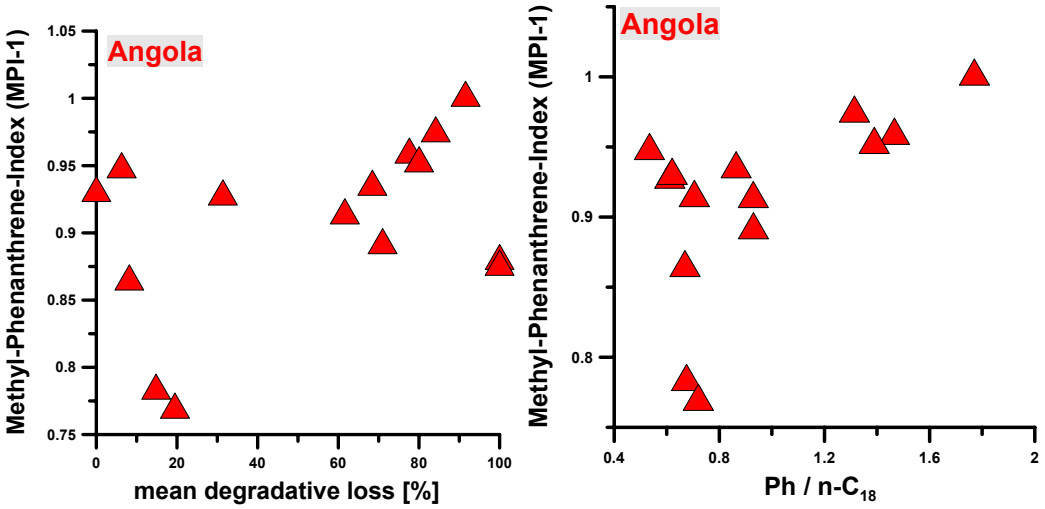

Fig. 104 (left): Correlation of thermal maturity, as indicated by the MPI-1, and the biodegradation parameter mean degradative loss. **Fig. 105 (right): C**orrelation of MPI-1 to the biodegradation parameter Ph/*n*-C_{18}.

Thermal maturities are also routinely assessed by parameters that are based on alkylnaphthalenes. It was shown by RADKE ET AL. (1982) and ALEXANDER ET AL. (1983) that with increasing thermal maturity the abundance of alkylnaphthalene isomers that have alkyl substituents in β positions relatively increase compared to alkylnaphthalene isomers that have alkyl substituents in α positions. Accordingly, both studies suggested concentration ratios with β isomers in the numerator and α isomers in denominator. Hence, the suggested ratios increase with increasing thermal maturity. The authors attributed this effect to the increasing temperature which facilitates chemical reactions that lead to the preferential depletion of the thermally less stable α isomers.

Figure 106 illustrates the maturity parameters MNR and ENR, which were suggested by RADKE ET AL. (1982) in correlation to the Methylphenanthrene Index (MPI-1). It has already been shown that the latter parameter is not affected by light to moderate biodegradation. In Figure 107 the MPI-1 is plotted versus the maturity parameters DNR-1 that was suggested by RADKE ET AL. (1982) and the DNR-2 to DNR-5 ratios, which were suggested by ALEXANDER ET AL. (1985). Obviously, the individual alkylnaphthalene ratios displayed on the x-axes in Figures 106 and 107 show no systematic correlation to the MPI-1. This gives rise to the assumption that in Angolan crude oils the maturity parameters which are based on alkylnaphthalenes are not solely affected by thermal stress.

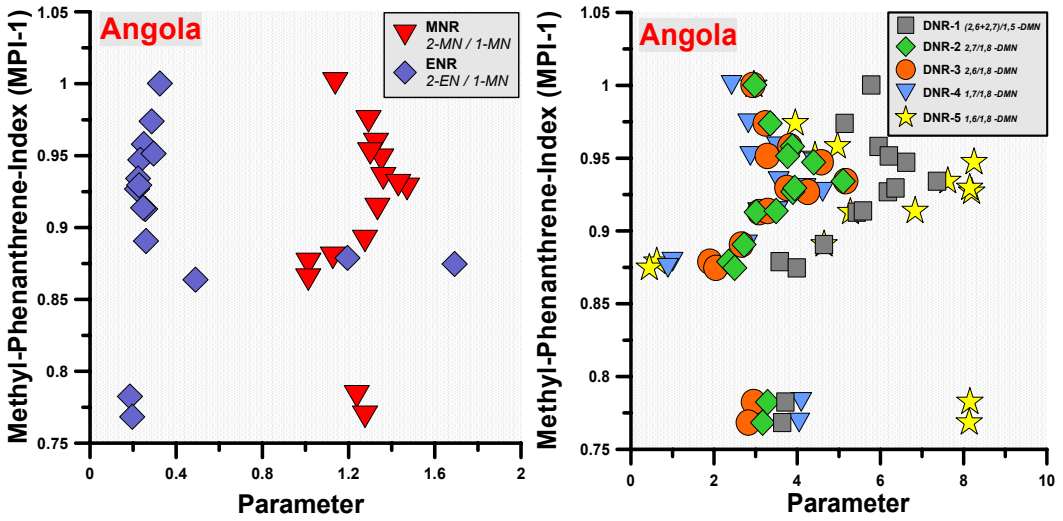

Fig. 106 (left): Methylphenanthrene Index (MPI-1) vs. the methylnaphthalene ratio (MNR) and the ethylnaphthalene ratio (ENR) suggested by RADKE ET AL. (1982). **Fig. 107 (right):** Crossplot of Methylphenanthrene Index (MPI-1) vs. the dimethylnaphthalene ratios DMN-1 suggested by Radke et al. (1982) and the dimethylnaphthalene ratios (DNR 2-5) suggested by ALEXANDER ET AL. (1985). Obviously the MPI-1 does not strictly correlate to the seven displayed maturity parameters that are based on alkylnaphthalenes.

It was already shown in chapter 5.2.2.2 that in crude oils from Angola the concentrations of alkylnaphthalenes decrease significantly with proceeding extents of biodegradation. Figure 108 and 109 display the MNR, ENR and the DNR`s in correlation to the biodegradation parameters mean degradative loss. Here, it is shown that increasing extents of biodegradation obviously have no significant effect on the MNR parameter (Figure 108). Only the two most

biodegraded samples A2 and A3, which are characterised both by 100% mean degradative loss, show clearly elevated concentration ratios of the MNR. This indicates that in these two samples 1-methylnaphthalne is stronger depleted than 2-methylnaphthalene. Interestingly, for samples A2 and A3 inferred vitrinite reflectances of R_C [MPI-1] = 0.93 and 0.92, respectively, were calculated. These values are well within the range of all other R_C -values (0.86-1.00) determined for Angolan crude oils, and hence, illustrates that rather biodegradation than the thermal maturity caused the elevated MNR ratios in these two Angolan samples. Figure 108 also shows that the ENR, which should increase with increasing thermal maturity obviously commence to decrease slightly at 60% mean degradative loss. Assuming that this decrease is due to the increasing extent of biodegradation this implies that 2-ethylnaphthalene is more susceptible to biodegradation than 1-ethylnaphthalene.

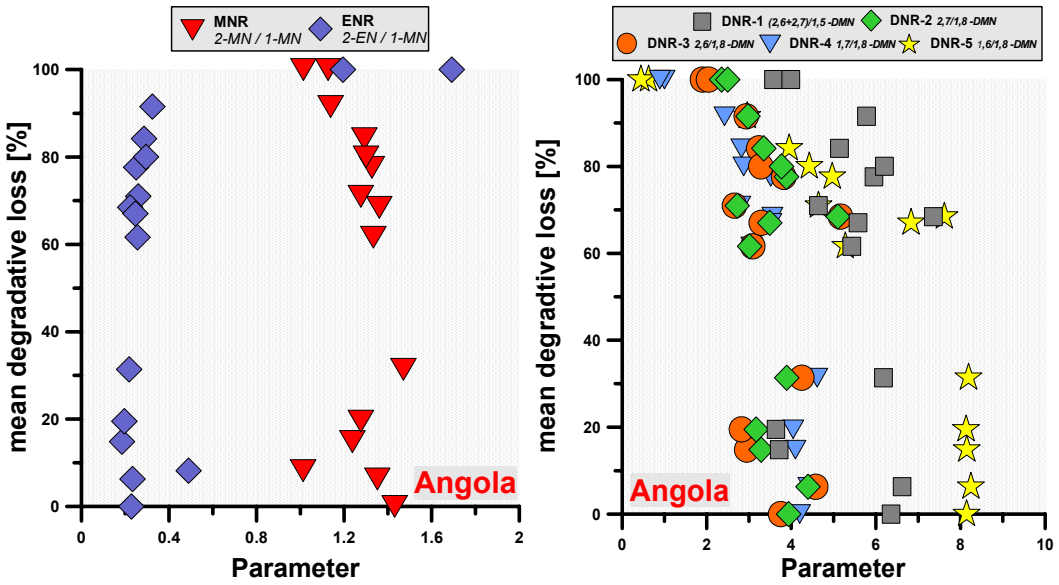

Fig. 108 (left): Correlation of the mean degradative loss to thermal maturity ratios 2-methylnaphthalenes/1-methylnaphthalne (MNR) and 2-ethylnaphthalene and 1-methylnaphthalene (ENR) **Fig. 109 (right):** Correlation of the mean degradative loss to five different thermal maturity ratios that are based on dimethylnaphthalenes (DNR 1-5), which were suggested by RADKE ET AL. (1982) and ALEXANDER ET AL. (1985).

Figure 109 illustrates that in Angolan crude oils increasing mean degradative losses are accompanied by a systematic decrease of the dimethylnaphthalene

ratios. For example the DNR-5 displayed by the yellow stars decreases during biodegradation in crude oils from Angola from 8.1 in the least biodegraded sample A11 to a value of 0.4 in the strongest altered crude oil A3. It is noteworthy that these two samples are characterised by similar thermal maturities, as indicated by the inferred vitrinite reflectances, based on the MPI-1, of R_C=0.96 for sample A11 and 0.92 for sample A3. For the other DNR ratios the same trend, however less pronounced, of decreasing ratios with increasing extent of biodegradation is obvious, which implies that rather biodegradation than the thermal maturity control the dimethylnaphthalene ratios (DNR`s) in Angolan oils. Consequently, the DNR`s must be used with caution when applied to biodegraded crude oils, even for the light to moderate alteration extents.

In addition to the application of alkylphenanthrenes and alkylnaphthalenes as maturity indicators, also specific alkylated dibenzothiophenes are used to assess thermal maturity in crude oils (e.g., RADKE ET AL., 1982, 1986; RADKE AND WILLSCH, 1994; CHAKHMAKHCHEV ET AL., 1997; SANTAMARIA-OROZCO ET AL., 1998). It was shown before that in Angolan crude oils among alkylated dibenzothiophenes only 4-methyldibenzothiophene is clearly affected by light to moderate biodegradation. Therefore, it is reasonable that the various suggested thermal maturity parameters, which are not based on 4-methyldibenzothiophene are reliable proxies even for light to moderately biodegraded crude oils. In contrast, the parameters 4-methyldibenzothiophene/dibenzothiophene (4-MDBT/DBT) and 4-MDBT/(4-MDBT + 1-MDBT), which were suggested by RADKE ET AL. (1982) and RADKE AND WILLSCH (1994), respectively, might be affected by biodegradation. Figure 110 shows both parameters in correlation to the MPI-1 and Figure 111 correlates both parameters with the mean degradative loss.

Figure 110 indicates a good correlation between the MPI-1 and the maturity parameters based on alkyldibenzothiophenes. Only samples A2 and A3 from Angola do not follow the general trend which is obvious for the other crude oils from this petroleum system. As mentioned before these two samples are the most

biodegraded crude oils from Angola. Figure 111 illustrate that ongoing biodegradation, as illustrated by increasing mean degradative losses, is accompanied by decreasing DBT parameters. Interestingly, in Figure 112 samples A2 and A3 are in accordance with the trend obvious for the other oils. This suggests that the slight maturity differences in oils from Angola may override the effects of light to moderate biodegradation on DBT parameters, and that alteration extents above moderate levels, which are relevant for samples A2 and A3, lead to a significant depletion of 4-methyldibenzothiphene, as it is indicated by the clearly decreased DBT ratios. Hence, it appears likely that rather the slight maturity differences (delta R_C = 0.24), which were observed for Angolan crude oils, control the DBT parameters than biodegradation effects within light to moderate alteration levels.

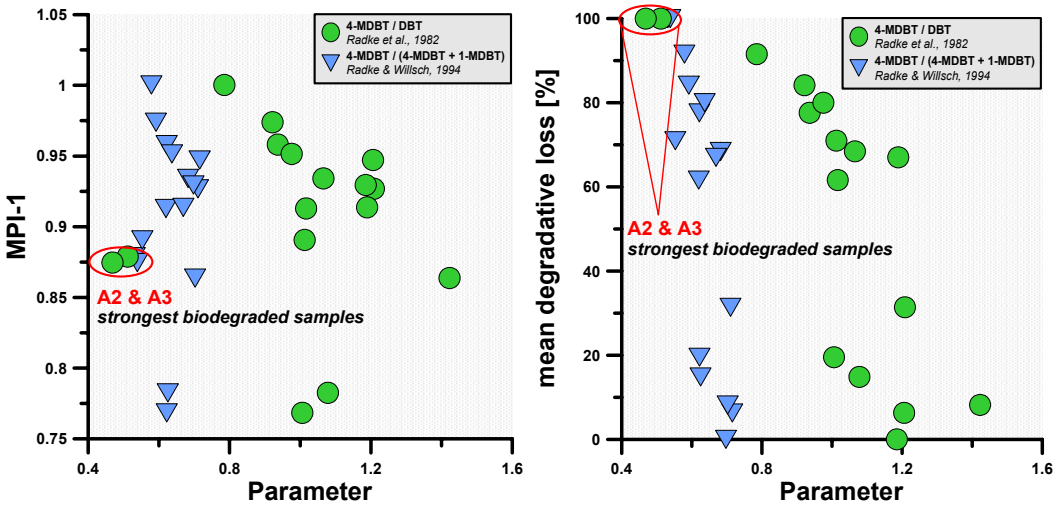

Fig. 110 (left): Correlation of the Methylphenanthrene Index (MPI-1) and maturity parameters, which are based on 4-methyldibenzothiophene. **Fig. 111 (right):** Correlation of the mean degradative loss and maturity parameters, which are based on 4-methyldibenzothiophene.

5.2.2.5 Conclusions

It was shown before that the extent of biodegradation for specific aromatic hydrocarbons seems to be more pronounced for compounds and compound groups which are characterised by higher concentrations. However, it has to be mentioned

that the calculation of concentrations refers to 1g of crude oil, which implies that if a specific substrate fraction is depleted, others are relatively enriched in the residuum. This relative enrichment effect, which is only due to the chosen kind of concentration calculation, is more pronounced the less abundant a relatively unaffected fraction is represented in the crude oil. This implies that crude oil constituents of low concentrations might be slightly depleted but due to a relative enrichment in the residuum their calculated concentration remains constant or even increases. However, the concentrations of aromatic hydrocarbons calculated and discussed in this study clearly illustrate that, as shown for the Angolan crude oils, the extent of biodegradation is higher for alkylbenzenes and alkylnaphthalenes than for alkylated dibenzothiophenes and phenanthrenes. It was also shown that if specific aromatic hydrocarbons are affected by biodegradation a possible impact on widely applied thermal maturity parameters can not be excluded. Especially, the application of maturity parameters that are based on alkylnaphthalenes is restricted to a detailed evaluation of possible biodegradation impacts. The evaluation of individual compound concentrations also clearly showed that biodegradation may results in individual degradation effects within the aromatic hydrocarbon fraction in different petroleum systems, as it was also shown for light and saturated hydrocarbons.

5.3 Part III: Biodegradation effects on compound-specific isotopes

5.3.1 Introduction

Isotopic data are used, together with biomarkers, to determine genetic relationships among oils and bitumens (PETERS ET AL., 2005). In the literature analysis of isotope data is focused on carbon isotopes because carbon is the dominant element in petroleum and can easily be analysed by bulk and compound-specific methods (PETERS ET AL., 2005). The evaluation of compound-specific hydrogen isotope ratios is of increasing interest since the technique to determine compound-specific hydrogen isotope ratios of hydrocarbons became available a few years ago (HILKERT ET AL., 1999). Carbon and hydrogen compound-specific isotope analysis (CSIA) is used for oil - oil and oil - source rock correlation studies (e.g., LI ET AL., 2001; ODDEN ET AL, 2002; SCHIMMELMANN ET AL., 2004, DAWSON, ET AL., 2005, 2007). It is well accepted that biodegradation causes an enrichment of the heavier isotopes in the residual substrate fraction. Therefore, several authors used laboratory experiments to investigate the effects of biodegradation on compound-specific carbon and/or hydrogen isotopic composition of aromatic and chlorinated hydrocarbons (e.g. MANCINI ET AL., 2003; MECKENSTOCK ET AL., 1999; WILKES ET AL., 2000). These observations led to the application of stable carbon and hydrogen isotope ratios to evaluate biodegradation of organic contaminants in groundwater (RICHNOW ET AL., 2003; MECKENSTOCK ET AL., 2004). In contrast, only few studies (GEORGE ET AL., 2002; MASTERSON ET AL., 2001; ROONEY ET AL., 1998; VIETH & WILKES, 2006) have used the carbon isotopic compositions of light hydrocarbons to trace biodegradation of oils in petroleum reservoirs. It was shown by HARRINGTON ET AL. (1999) and SMALLWOOD ET AL. (2002) that other in-reservoir alteration

processes, e.g., water washing and evaporative fractionation have no or only little effect on the carbon isotopic composition making this technique a powerful tool to decipher microbially caused alterations. In contrast, hydrogen isotopic compositions of hydrocarbons are influenced by evaporation (WANG & HUANG, 2003). Additionally, hydrogen isotope ratios could also be affected by equilibrium exchange reactions between water-bound hydrogen and carbon-bound hydrogen over geologic time scales (SESSIONS ET AL., 2004). Recently, the dependence of hydrogen isotopic compositions of different hydrocarbons on the maturity of the organic matter was discussed (DAWSON ET AL., 2005; RADKE ET AL., 2005; PENDENTCHOUK ET AL., 2006; DAWSON ET AL., 2007).

The isotopic compositions of carbon, hydrogen, oxygen, nitrogen and sulphur are often investigated in geochemical studies. Most abundant in organic material, these elements have at least two stable isotopes which can be detected mass spectrometrically (HOEFS, 2004). Isotopic compositions are reported in δ-notations (‰) relative to an international standard. Carbon isotope ratios refer to the Vienna Pee Dee Belemnite standard (V-PDB) and hydrogen isotope ratios are measured relative to the Vienna Standard Mean Ocean Water (V-SMOW) according to the following equations for carbon (1) and hydrogen (2)

$$\delta^{13}C[‰] = \left(\frac{^{13}C/^{12}C_{sample}}{^{13}C/^{12}C_{s\tan dard}} - 1 \right) \times 1000 \qquad \textbf{(1)}$$

$$\delta D[‰] = \left(\frac{D/H_{sample}}{D/H_{s\tan dard}} - 1 \right) \times 1000 \qquad \textbf{(2)}$$

Although the chemical and physical properties of stable isotopes are nearly identical, minor differences exist between the strength of chemical bonds where light and heavy isotopes are involved. Such energy differences in the dissociation

or formation of bonds in the transition state of a chemical reaction control the reactivity of the individual stable isotopes in biological processes and lead to isotope fractionation effects. A chemical bond formed by a lighter isotope (atom) is weaker than one by a heavier isotope (atom). Consequently, the activation energy for the cleavage of a chemical bond formed by a heavier isotope is higher. Therefore, biochemical processes will preferentially utilize molecules containing lighter isotopes. Such a kinetic isotope fractionation can be divided into primary and secondary effects. The primary effect occurs if a heavy isotope (atom) is directly involved in the reaction mechanism. Secondary isotope effects can appear if the heavy isotope is located close to the bond but not directly involved in the reaction. Such secondary isotope effects are commonly one to two orders of magnitude lower than primary isotope effects (MECKENSTOCK ET AL., 2004). The CSIA integrates the isotope signal of the entire molecule. It is evident that the intrinsic isotope effect at the reactive atom(s) of the molecule is higher than the overall isotope fractionation detected by CSIA. Consequently, the detectable isotope fractionation effect decreases with increasing molecular weight, i.e. increasing number of carbon and/or hydrogen atoms. The higher the number of respective "passive" atoms per molecule, the more "diluted" is the extent of fractionation. It was shown by MORASCH ET AL. (2004) that for molecules with more than 12-14 carbon atoms the dilution of the intrinsic isotope fractionation effect is too pronounced for the detection of the expected carbon isotope shift. Additionally, BOREHAM ET AL. (1995) showed that biodegraded *n*-alkanes with more than 12 carbon atoms exhibit no detectable isotopic shifts. Consequently, the carbon isotopic composition of such hydrocarbons is not affected by biodegradation and can still be used as an isotopic marker for, e.g., source or thermal maturities (VIETH & WILKES, 2006).

5.3.2 Stable carbon isotope ratios

It was mentioned before, that carbon isotopic compositions of light hydrocarbons can be used to decipher biodegradation (VIETH AND WILKES, 2006), if differences between oil samples due to variability in the source rock composition and thermal maturity can be excluded. Therefore, only carbon isotope ratios from 40 crude oil samples, which were defined to be mainly affected by biodegradation (for details see chapter 5.1) are shown. Results of CSIA of all crude oils investigated within this study are listed in the Appendix. In some cases, missing values for compounds in individual samples are due to increased standard deviations (>0.5%) for the three replicate measurements, and therefore are not shown. Compared to conventional GC/MS measurements the sensitivity of the CSIA is lower and, hence in some other cases missing values are also due to low compound concentrations in individual samples, which could not be detected or a base line separation was not possible.

Angola

For samples from the Angolan biodegradation sequence compound-specific $\delta^{13}C$ ratios are shown in Figure 112. Crude oils A2, A3 and A13 were far too viscous for injection into the GC-C-IRMS system, hence, no data can be provided for these samples. To highlight possible effects of compositional differences in the two source rock formations (see chapter 5.1.4) on the $\delta^{13}C$ values, individual hydrocarbons in samples derived from source "A" are labelled in Figure 112 with coloured symbols, oils from source "B" are indicated by open grey symbols. Carbon isotopic ratios for the Angolan samples mainly vary between -37.5‰ and -30‰. However, the broadest variabilities of $\delta^{13}C$ values were measured for compounds within the light hydrocarbon range (*i*-C_4 - *n*-C_{10}). Within the light hydrocarbons a maximum difference of $\delta^{13}C$ ratios between the lightest and heaviest carbon isotopic signature of 10.9‰ and 8.4‰ for *n*-butane and *n*-

pentane, respectively was determined. In contrast, $\delta^{13}C$ ratios for mid- and long-chain saturates (> *n*-C_{10}) show lower variability and are mainly in the range from -37.5‰ to –35‰. This may demonstrate that these hydrocarbons are biodegraded to a lesser extent, but it was discussed before that biodegradation does not lead to a detectable isotope fractionation in compounds with more than 12 carbon atoms (MORASCH ET AL., 2004 and BOREHAM ET AL., 1995). The wide range of carbon isotopic ratios within the light hydrocarbon fraction of the investigated crude oils is in accordance with microbial processes leading to the fractionation of carbon isotopes. Hence, this sample set appears to be appropriate to assess biodegradation by $\delta^{13}C$ ratios, as it is discussed in the following chapters.

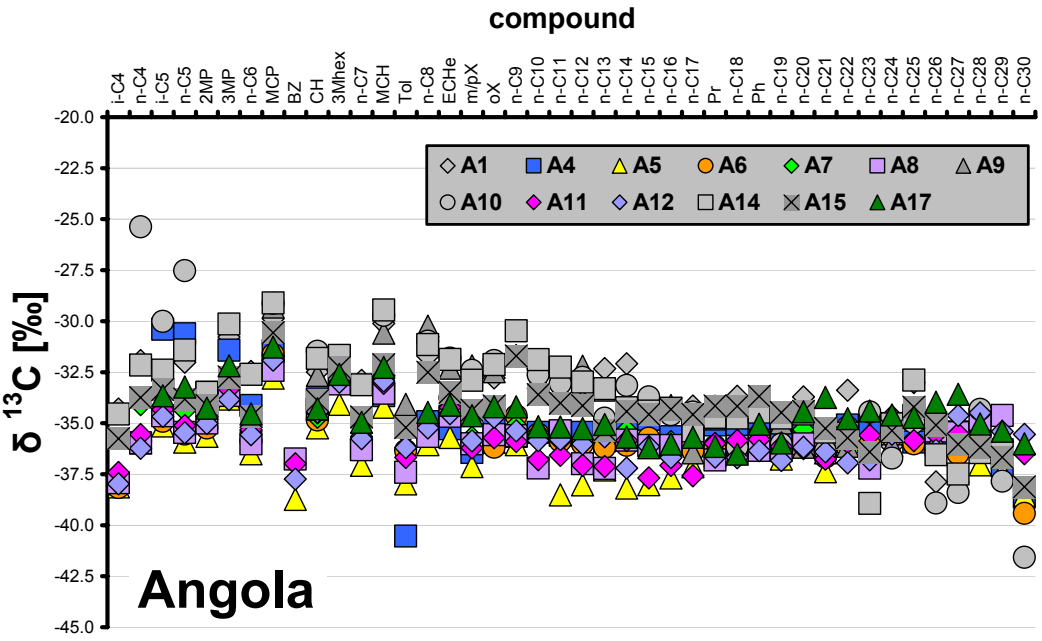

Fig. 112: $\delta^{13}C$ ratios for light and saturated hydrocarbons in crude oil samples from the Angolan biodegradation sequence. Crude oils A2, A3 and A13 were too viscous for injection into the GC-C-IRMS system, hence, no data can be provided for these samples.

Norway

For the Norwegian biodegradation sequence $\delta^{13}C$ ratios are shown in Figure 113. Due to limited sample amount no GC-C-IRMS measurements can be provided for

sample G12. In general, $\delta^{13}C$ ratios in crude oils from Norway differ between -32.5‰ and -25‰, and are thus more enriched in ^{13}C than the samples from Angola. Carbon isotopic ratios tend to shift to lighter $\delta^{13}C$ values with higher molecular weights of the crude oil constituents. However, the carbon isotopic ratios for samples from Norway indicate higher variability within the light hydrocarbon range than for mid- and long-chain saturates, as it was also observed for the crude oils from Angola. Again the highest difference between lightest and heaviest carbon isotopic ratio were calculated for *n*-butane and *n*-pentane with 7.0‰ and 4.5‰, respectively. The changes in $\delta^{13}C$ ratios of the light hydrocarbons in crude oils from the Gullfaks oil field in Norway were already discussed with respect to biodegradation by VIETH AND WILKES (2006). Hence, this sample set is used in the following chapters to illustrate how carbon isotope ratios can be used to assess biodegradation in petroleum reservoirs.

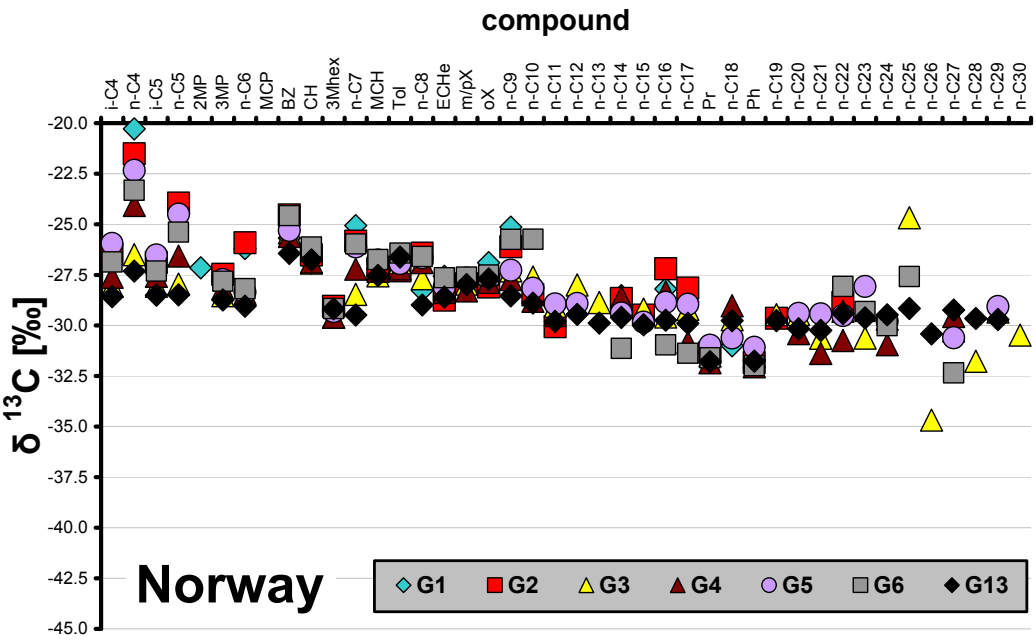

Fig. 113: $\delta^{13}C$ ratios for light and saturated hydrocarbons in crude oil samples from the Norwegian biodegradation sequence. Due to limited sample amounts of G12 no GC-C-IRMS measurements were possible.

Canada

For samples from the Canadian biodegradation sequence compound-specific $\delta^{13}C$ ratios are shown in Figure 114. Sample C1 is too pasty to be injected into the GC-C-IRMS system, hence, no isotopic data are available. Reproducible $\delta^{13}C$ ratios in Canadian crude oils mainly vary between -32.5‰ and 27.5‰ and are thus comparable to the measured ratios in the Norwegian sample set. In accordance with the data for samples from Norway, apparently carbon isotopic ratios shift to lighter $\delta^{13}C$ values with higher molecular weights of the crude oil constituents. However, due to the limited number of $\delta^{13}C$ values for light hydrocarbons, this sample set will not be included into further considerations on the impact of biodegradation on compound-specific $\delta^{13}C$ ratios.

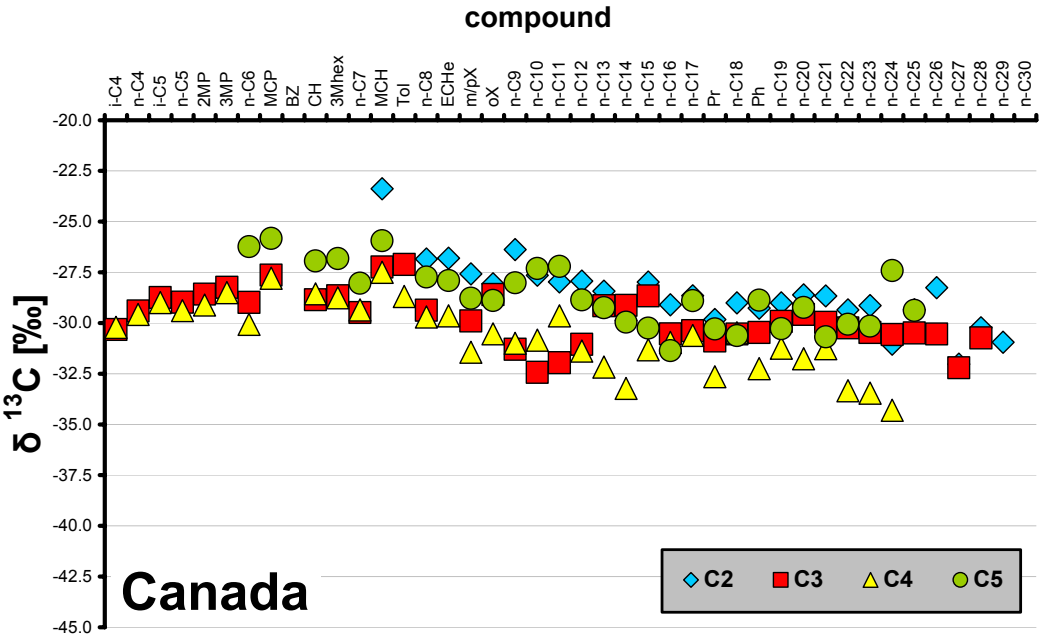

Fig. 114: $\delta^{13}C$ ratios for light and saturated hydrocarbons in crude oil samples from the Canadian biodegradation sequence.

Egypt

For crude oil samples from the Sudr oil field in Egypt compound-specific $\delta^{13}C$ ratios are shown in Figure 115. Due to increased standard deviations (>0.5%) for the three replicate measurements of each sample, only few values in the light hydrocarbon range could be determined. Reliable $\delta^{13}C$ ratios for compounds in Egyptian samples vary between -32.5‰ and -22.5‰ and thus, are comparable to the carbon isotopic composition of crude oil constituents in Norwegian oils. In accordance with the data for samples from Norway and Canada, $\delta^{13}C$ ratios apparently shift to lighter $\delta^{13}C$ values with higher molecular weights of crude oil constituents. Due to the limited number of $\delta^{13}C$ ratios for light hydrocarbons, which might be affected by biodegradation, this samples set is excluded from further considerations.

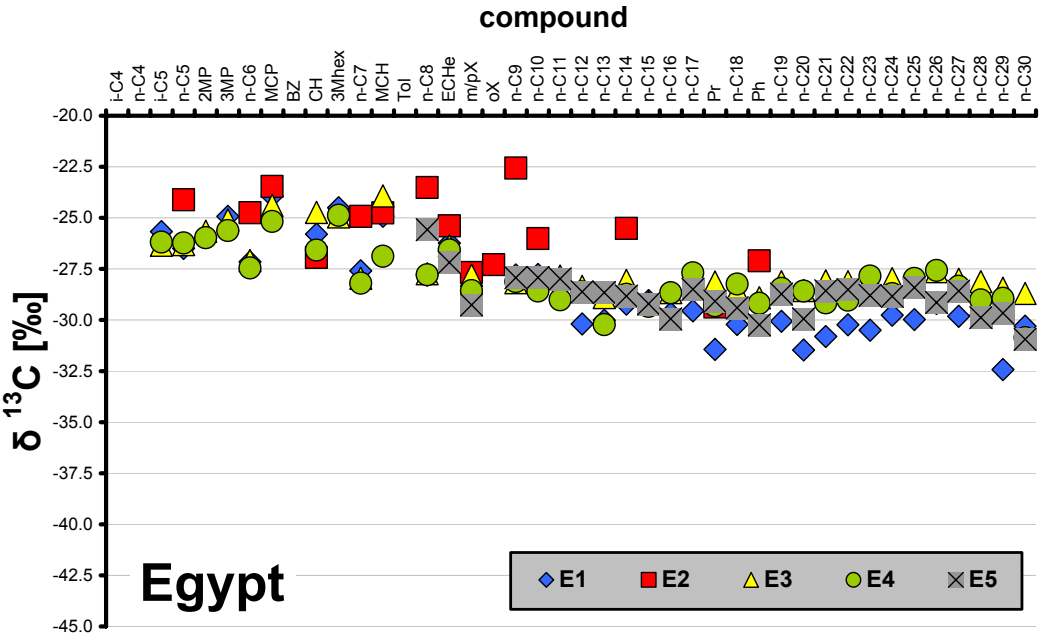

Fig. 115: $\delta^{13}C$ ratios for light and saturated hydrocarbons in crude oil samples from the Egyptian biodegradation sequence.

Nigeria

For crude oil samples from Nigeria compound-specific $\delta^{13}C$ ratios are shown in Figure 116. In general, $\delta^{13}C$ ratios of the investigated compounds in Nigerian

crude oils vary between -40‰ and 30‰, and thus represent the broadest range within all five investigated sample sets. As also described for the other four sample sets carbon isotopic ratios shift to lighter $\delta^{13}C$ values with higher molecular weights of the crude oil constituents. The highest variability of compound-specific $\delta^{13}C$ ratios occur again within the light hydrocarbon range. For low molecular weight hydrocarbons $\Delta\delta^{13}C$ values of 8.2‰ and 7.8‰ for *n*-butane and *n*-pentane, respectively, were calculated.

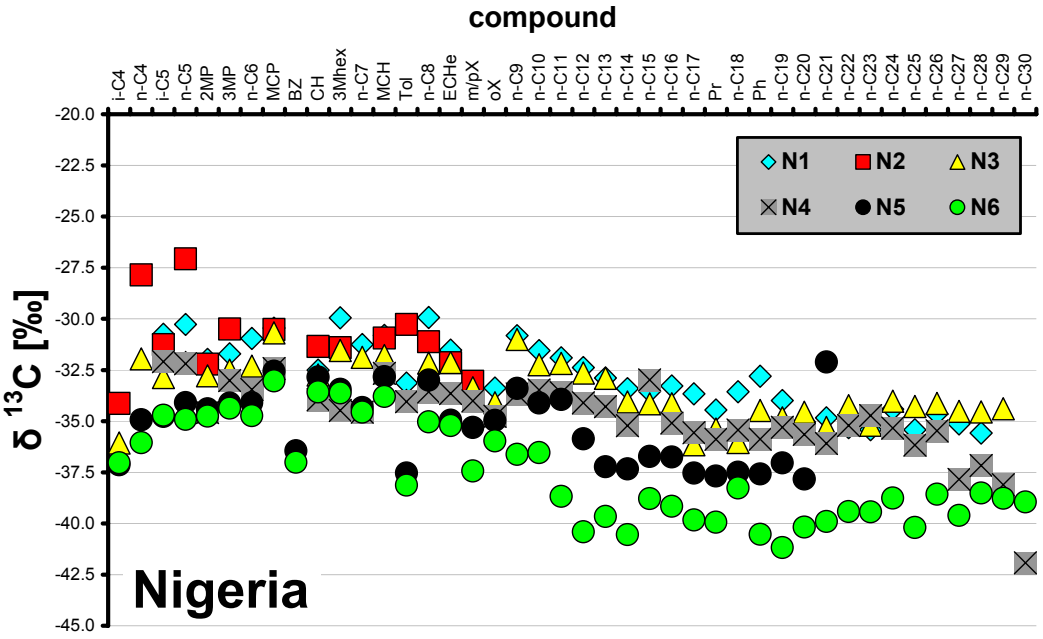

Fig. 116: $\delta^{13}C$ isotopic ratios for light and saturated hydrocarbons in crude oil samples from the Nigerian biodegradation sequence.

5.3.2.1 Effect of source and maturity on $\delta^{13}C$ ratios

Stable carbon isotopic composition of petroleum hydrocarbons are used to determine the geological age of source rocks, their depositional environment and the type of source organic matter (e.g., SOFER, 1984; CHUNG ET AL, 1992,

MURRAY ET AL., 1994; SANTOS NETO AND HAYES, 1999; DAWSON ET AL., 2007). Also the thermal maturation of kerogen and petroleum was reported to affect the stable carbon isotopic compositions (CLAYTON, 1991). Recently, carbon isotope ratios for light hydrocarbons were used to assess petroleum biodegradation (VIETH AND WILKES, 2006). However, the use of carbon isotopic compositions to assess in-reservoir biodegradation is most effective if source rock organofacies and thermal maturity, which may also lead to variabilities in $\delta^{13}C$ ratios of crude oils, are well-constrained. Therefore, this chapter evaluates possible impacts of slight variances in source rock organofacies and thermal maturity on $\delta^{13}C$ ratios.

In the preceding paragraphs $\delta^{13}C$ ratios for crude oil samples from the five biodegradation sequences were shown. Within these sample sets a high similarity for source rock organofacies, depositional environment and thermal maturity was assessed (chapter 5.1). However, it was also shown, that some minor compositional differences exist, which are not due to in-reservoir alteration. Hence, it is appropriate to evaluate possible impacts of the slight variances of source rock organofacies and thermal maturity on compound-specific carbon isotope ratios even within the biodegradation sequences. For this purpose, the carbon isotopic compositions of pristane and phytane are used, because these isoprenoids show no detectable fractionation effect caused by biodegradation, and thus appear to be reliable indicators for effects on $\delta^{13}C$ ratios resulting from differences in source and maturity. Only few compound-specific $\delta^{13}C$ values for the light hydrocarbons in samples from Canada and Egypt are available, therefore only the sample sets from Angola, Norway and Nigeria are used to illustrate source and maturity effects on compound-specific carbon isotope ratios.

In chapter 5.1 it was discussed that samples from Angola show minor variations for few geochemical parameters, such as the X-C_{30}/C_{29}Ts ratio and the D/(D+R) ratio. This may indicate slight variability for the source rock organofacies. Especially, the latter ratio separates the crude oil samples from Angola into two subsets by ratios below and above 0.5. Figure 117 illustrates that the variability of the D/(D+R) ratio correlates to the $\delta^{13}C$ ratios of pristane and phytane. Angolan

crude oil samples, for which D/(D+R) ratios < 0.5 were calculated, are characterised by $\delta^{13}C$ ratios of 34.5‰ to 37‰ for pristane and phytane, respectively. In contrast, for samples with D/(D+R) ratios > 0.5, heavier $\delta^{13}C$ ratios of 34.7‰ to 33.5‰ for the isoprenoids were determined. This indicates that $\delta^{13}C$ ratios of pristane and phytane are related to the slight differences in the source rock composition. Therefore, samples with D/(D+R) ratios < 0.5 are labelled with source "A", and samples with values > 0.5 are marked as source "B".

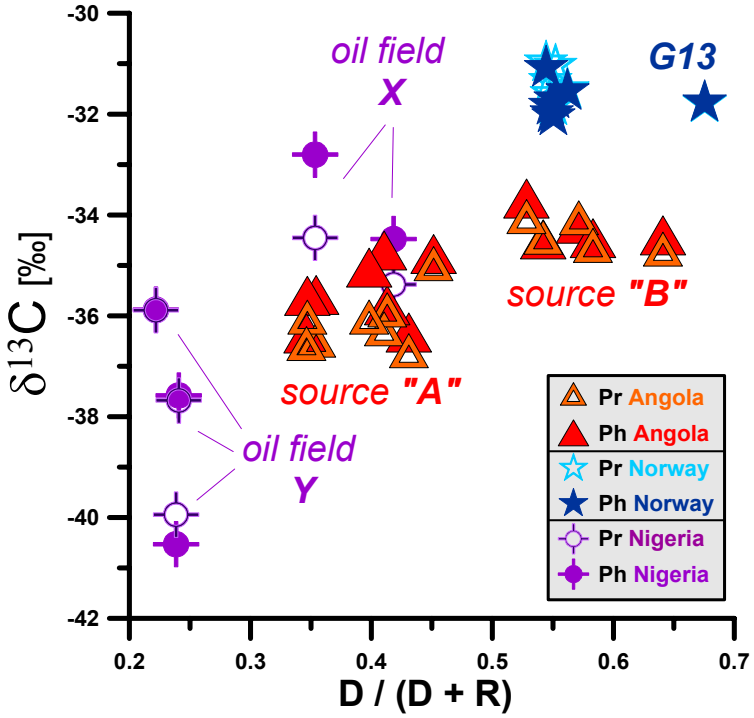

Fig. 117: Plot of $\delta^{13}C$ ratios vs. the dia/(dia+reg) sterane ratio (D/D+R) for crude oils from Angola, Norway and Nigeria.

Interestingly, this observation is in accordance with $\delta^{13}C$ for light hydrocarbons, which are shown in Figure 112. Here it is indicated, that $\delta^{13}C$ ratios for low molecular weight compounds vary slightly depending on the different sources of the oils, as they are assigned in Figure 117. Most investigated crude oil constituents in samples from source "A" are characterised by heavier $\delta^{13}C$ values than samples expelled from source "B". For compounds of crude oils generated from source "A", $\delta^{13}C$ values of light hydrocarbons mainly range from -33‰ to

-30‰. In contrast, compounds in crude oils derived from source "B" are characterised by lighter $\delta^{13}C$ values (-33‰ and -37.5‰). This indicates that $\delta^{13}C$ ratios of light hydrocarbons in crude oils from Angola are influenced by the source rock composition. However, it appears likely that $\delta^{13}C$ ratios of light hydrocarbons in the Angolan oil samples are also affected by biodegradation, but the differentiation of $\delta^{13}C$ ratios of the light hydrocarbons as well as for pristane and phytane in both subsets suggest a high sensitivity of the carbon isotopic composition to even slight differences in the source rock organofacies.

Such a dependence of $\delta^{13}C$ ratios on slight differences in source rock organofacies, as indicated by the D/(D+R) ratios, is also obvious for samples from Nigeria (Figure 117). Nigerian samples with D/(D+R) ratios < 0.3 are derived from oil field X, which are characterised by $\delta^{13}C$ ratios of -36‰ to -32‰ for pristane and phytane. In contrast, $\delta^{13}C$ ratios of -40‰ to -36‰ were determined for pristane and phytane in samples with D/(D+R) ratios > 0.3, which are derived from oil field Y. As already observed for the Angolan crude oils, Nigerian samples with higher D/(D+R) ratios are characterised by heavier $\delta^{13}C$ ratios in pristane and phytane.

This general trend can also be observed for the Norwegian crude oils, because the relatively heavy $\delta^{13}C$ ratios for pristane and phytane (-32‰ to -31‰) in the Gullfaks samples are accompanied by relatively high D/(D+R) ratios > 0.5. However, $\delta^{13}C$ ratios for the isoprenoids in the Norwegian samples are invariant compared to the differences of $\delta^{13}C$ ratios observed in Angolan and Nigerian crude oils, and thus are in accordance with the high similarity of source rock composition, as illustrated by the constant D/(D+R) ratios. Only sample G13 is characterised by an increased D/(D+R) ratio, which can be referred to the charge history, because hydrocarbons of this sample are thought to be generated from two sources (HORSTAD ET AL., 1995). However the stable carbon isotopic composition is identical to that of the other samples derived from the Gullfaks field.

Besides differences in the source rock organofacies, also variances in thermal maturity might affect carbon isotope ratios of crude oils. In chapter 5.1 it was shown that crude oils from Angola, Norway and Nigeria are characterised by only slight variability in thermal maturities. According to CLAYTON (1991) thermal maturity may affect the $\delta^{13}C$ ratio of the bulk organic carbon only in the order of up to 1‰ in crude oils. Nevertheless, it can not be excluded that slight maturity differences are related to larger variations in $\delta^{13}C$ ratios of individual compounds. Figure 118 illustrates that the observed slight differences in thermal maturity, as indicated by the C_{29} [αββ / (αββ + ααα)] sterane parameter, have no clear impact on $\delta^{13}C$ ratios of pristane and phytane.

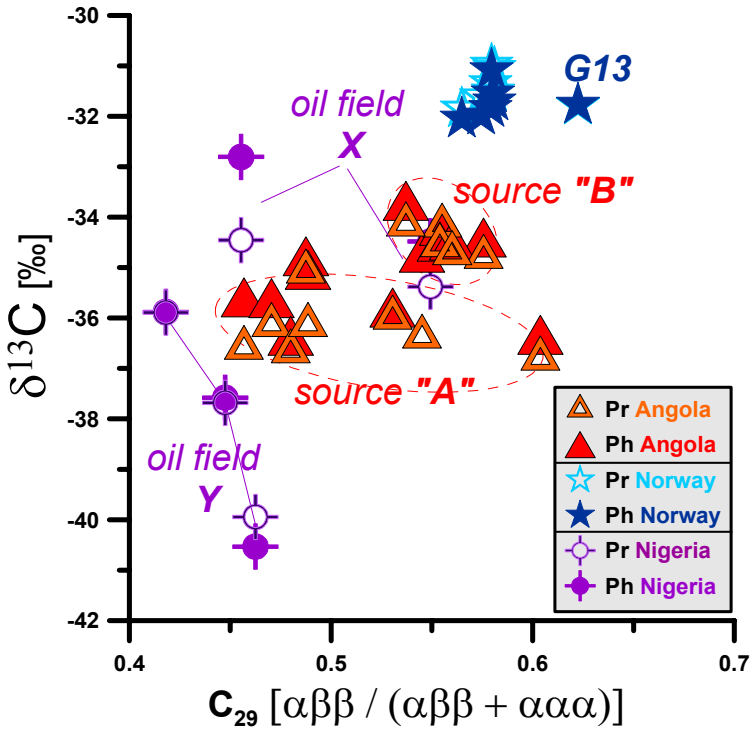

Fig. 118: Plot of $\delta^{13}C$ ratios for pristane and phytane vs. the maturity parameter C_{29} [αββ / (αββ + ααα)] steranes for crude oil samples from Angola, Norway and Nigeria.

Only within each of the two subsets "A" and "B" from Angola, a slightly negative correlation between $\delta^{13}C$ values and the thermal maturity can be observed. The plot denotes that with increasing thermal maturity $\delta^{13}C$ ratios shift to lighter carbon isotopic compositions. The plot also illustrates that Angolan samples from

source “B” are isotopically heavier than those derived from source “A”, but thermal maturities for crude oils from source “B” are within the range of maturities for samples from source “A”. Hence, it appears likely that the source dependence is more pronounced in the compound-specific $\delta^{13}C$ ratios than an effect of thermal maturity. In addition, Nigerian samples, that cover the broadest maturity range among the five investigated sample sets (see chapter 5.1.1), show a slight correlation of thermal maturity to $\delta^{13}C$ ratios for pristane and phytane within the two subsets, which originate from the two oil fields X and Y. The correlation within the two Nigerian subsets is comparable to the Angolan subsets. Again $\delta^{13}C$ values of pristine and phytane become lighter with increasing thermal maturity. Interestingly, the shift in $\delta^{13}C$ ratios of pristane and phytane in crude oils from oil field Y is about 5‰, which would clearly exceed the range which was suggested by CLAYTON (1991). It is clear, that this observation for Nigerian oils is not very robust, because both subsets comprise only two and three data points, respectively. However, the effect of thermal maturity on $\delta^{13}C$ ratios of pristane and phytane in Nigerian crude oils appears to be weaker, than the dependence on source rock characteristics. This can be concluded because the less mature sample from oil field X is characterised by a comparable maturity assessed for crude oils from oils from oil field Y, but characterised by clearly heavier isotopic compositions. The assumption that thermal maturity has no significant effect on $\delta^{13}C$ ratios for pristane and phytane is also indicated by the Norwegian samples. Within the Norwegian samples only sample G13 is slightly more mature, but $\delta^{13}C$ ratios of pristane and phytane are within the range of the other crude oils. Consequently, it is concluded that in crude oils from Angola, Norway and Nigeria, slight differences in thermal maturity have a lesser effect on the $\delta^{13}C$ ratios of pristane and phytane than differences in the source rock composition.

It was mentioned before, that carbon isotopic ratios of the isoprenoids pristane and phytane are not affected to a detectable amount by biodegradation (MORASCH ET AL., 2004). Before it was also shown, that slight differences in thermal maturity obviously have no significant influence on the $\delta^{13}C$ ratios of pristane and phytane. In contrast, $\delta^{13}C$ ratios of pristane and phytane are affected by even slight

differences in source rock organofacies. Hence, it is concluded that the carbon isotopic differences of pristane and phytane which are illustrated in Figure 119 are mainly related to compositional variations in the source rocks.

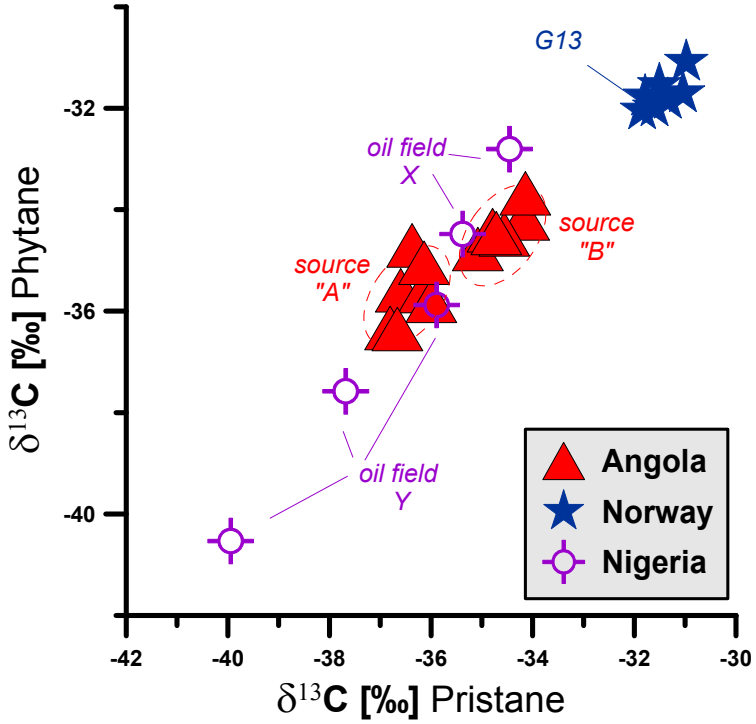

Fig. 119: Plot shows a linear correlation of compound-specific $\delta^{13}C$ ratios for pristane and phytane in crude oil samples from Angola, Norway and Nigeria.

Consequently, the plot shown in Figure 119 enables the homogeneity or inhomogeneity of crude oils to be characterised based on carbon isotopic composition. This correlation tool was already used by COLLISTER ET AL. (1991). Accordingly, the sample set from Norway, which is characterised by the lowest range of $\delta^{13}C$ ratios for pristane and phytane (± 1‰) can be assessed as the most homogeneous sequence among the three investigated sample sets. For crude oils from Angola $\delta^{13}C$ ratios vary in the order of ± 2.1‰ for source "A" samples, and ± 1.1‰ for source "B" samples. Hence, the carbon isotopic and thus also molecular homogeneity for Angolan sourced "B" crude oils is comparable to the Norwegian sample set. The two Nigerian subsets from oil field X and Y are characterised by $\delta^{13}C$ ranges for the isoprenoids of ±2.6‰ and ±4.6‰, respectively, and thus, represent the most inhomogeneous sequences among the three sample sets discussed here.

Therefore, the assessment of biodegradation using compound-specific isotopes of light hydrocarbons, as it will be discussed in the following chapter, is carried out separately for each of the two subsets from Angola. Based on the carbon isotopic composition the Nigerian biodegradation sequence has to be separated into two subsets, which belong to the two oil fields X and Y and comprise only two and three samples, respectively. Due to this limited sample numbers for each of the two Nigerian subsets the assessment of biodegradation using compound-specific carbon isotope ratios is not appropriate. Additionally, sample G13 from the Gullfaks field in Norway, which likely has received a charge contribution from a second source (HORSTAD ET AL., 1995), is excluded from the Norwegian subset. This is done, because carbon isotopic compositions are obviously affected by even slightest variances in the source organic matter, and it cannot be excluded that the $\delta^{13}C$ ratio of this sample is affected by the charge pulse of the second source rock.

5.3.2.2 Assessment of biodegradation by $\delta^{13}C$ ratios

Numerous studies have used the isotope fractionation effect to decipher biodegradation in laboratory experiments (e.g., MANCINI, ET AL., 2003, MECKENSTOCK ET AL., 1999; WILKES ET AL., 2000) and in contaminated aquifers (HUNKELER ET AL., 1999; MANCINI ET AL., 2002; MECKENSTOCK ET AL., 2004; SHERWOOD LOLLAR ET AL., 2001). In recent years an increasing number of studies assessed petroleum biodegradation by isotope fractionation (DAWSON ET AL., 2007; GEORGE ET AL., 2002; MASTERSON ET AL., 2001; ROONEY ET AL., 1998). However, only VIETH & WILKES (2006) quantified biodegradation in petroleum reservoirs using the carbon isotopic composition of crude oils.

In petroleum reservoirs biodegradation leads to an enrichment of ^{13}C in the degraded crude oil constituent. VIETH AND WILKES (2006) showed for crude oils

from the Gullfaks field in Norway that this change in isotopic composition can be related to a decrease in concentration of the respective compound. This correlation of isotopic composition and the decrease in compound concentration is expressed by the Rayleigh equation, which was demonstrated in laboratory and field studies (MECKENSTOCK ET AL., 1999; RICHNOW ET AL., 2003; VIETH ET AL., 2005). This approach was also used by VIETH AND WILKES (2006) to quantify the extent of depletions for specific crude oil constituents in samples from the biodegraded Gullfaks reservoir. The isotope fractionation caused by biodegradation can be described by the Rayleigh equation (Eq. 3)

$$\frac{R}{R_i} = F^{\left(\frac{1}{\alpha}-1\right)} \tag{3}$$

where F is defined as the remaining fraction (C/C_i) of the individual crude oil constituent. R is the isotopic composition of the compound with the respective F, and R_i gives the initial isotopic composition of the crude oil constituent. The isotope fractionation factor (α) relates the changes in isotopic composition and the changes in compound concentration in the crude oil during biodegradation (VIETH AND WILKES, 2006).

Changes in the carbon isotopic composition can be illustrated by calculating the enrichment in $\delta^{13}C$ ratios from the least degraded sample of a biodegradation sequence to the degraded crude oil. Such $\Delta\delta^{13}C$ values for light hydrocarbons in crude oils from the two Angolan subsets and Norway are shown in Figures 120, 121 and 122.

Calculated $\Delta\delta^{13}C$ ratios for light hydrocarbons in Angolan crude oils that were generated from source "A" are shown Figure 120. In this plot calculated differences in the carbon isotopic composition of light hydrocarbons refer to $\delta^{13}C$ ratios of the respective compound in sample A11, which is illustrated by the black triangles and the black horizontal line representing zero values on the y-axis. This sample was characterised by the MEAN DEGRADATIVE LOSS (see chapter 5.2) as

the least degraded crude oil in the entire Angolan sample set. Calculated $\Delta\delta^{13}C$ values of light hydrocarbons for all other crude oils from source "A" are given as the difference to the endmember A11.

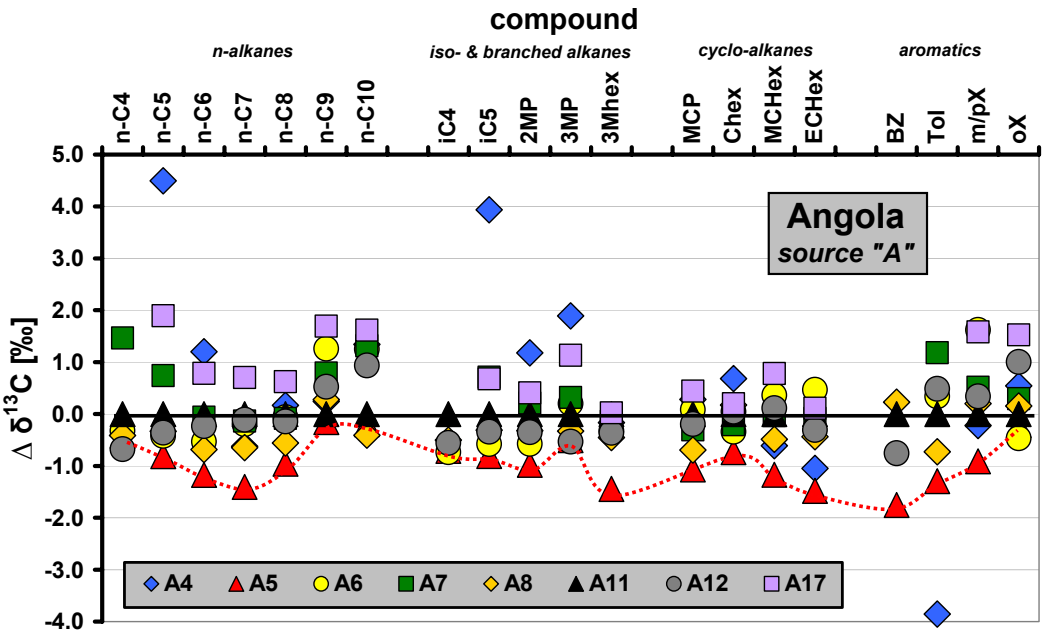

Fig. 120: $\Delta\delta^{13}C$ values for light hydrocarbons in crude oils from Angola, which were generated from source "A". Values are given as difference to the least degraded crude oil A11. Interestingly, the least degraded sample A11, which indicated by the black triangles and the black horizontal line at unity, is not characterised by the lightest carbon isotopic composition. The lightest $\delta^{13}C$ ratios were calculated for sample A5, which is indicated by the red triangles and the red dashed curve.

The least degraded crude oil sample A11 is characterised by the highest concentration of summed light and saturated hydrocarbons and should, according to the Rayleigh model, also show the lightest isotopic composition. However, Figure 120 indicates that sample A11 is not the isotopically lightest sample, because several "negative" enrichments were calculated for light hydrocarbons in crude oils from subset "A". However, most of these calculated negative $\Delta\delta^{13}C$ values are within the standard deviation of isotope measurements (± 0.5‰). Only for sample A5 $\delta^{13}C$ ratios are clearly lighter than in the compositional endmember. In sample A5 lightest $\delta^{13}C$ ratios for 16 of 20 investigated light hydrocarbons in the "A" subset were assigned. In Figure 120 this sample is labelled by the red triangles and the red dashed line. Assuming that source rock

lithofacies, organofacies and thermal maturity are similar in crude oils of the source "A" subset, it is surprising to see that sample A5 shows the lightest carbon isotopic composition although the MEAN DEGRADATIVE LOSS (MDL = 14.8%) indicates a higher extent of biodegradation for this crude oil than for the compositional endmember A11 (MDL = 0%). One might assume that the extent of biodegradation indicated by the MDL, and hence also the summed concentration of light and saturated hydrocarbons, is lower in sample A11, but that the individual concentrations of specific light hydrocarbons are higher in sample A5. In this case it would be reasonable that $\delta^{13}C$ values of several light hydrocarbons in sample A5 are lighter than in A11. However, this is not the case, and hence, the correlation of compound concentration and $\delta^{13}C$ is not given, which precludes the application of the Rayleigh model. Assuming that the composition of the source material in subset "A" is identical and that the observed crude oil maturities are similar within this subset, it has to be considered that processes other than biodegradation, thermal maturity and source rock organofacies have affected the carbon isotopic composition in sample A11. However, the exact mechanisms, which may lead to this anomalous light carbon isotopic composition, cannot be further evaluated, because of limited access to the geological background information of the petroleum system in Angola. Consequently, the assessment of biodegradation by compound-specific isotope ratios for samples from Angolan subset "A" using the Rayleigh model is not appropriate.

In contrast to the $\Delta\delta^{13}C$ values of light hydrocarbons in crude oils from Angolan subset "A", samples from source "B" indicate lightest carbon isotope ratios of low molecular weight components for the least degraded sample (A15). In Figure 121 calculated differences in the carbon isotopic composition ($\Delta\delta^{13}C$) of light hydrocarbons in crude oils from the "B" subset are given relative to the $\delta^{13}C$ ratios of least biodegraded oil sample A15, which is illustrated by the black triangles and the black horizontal line at unity. This crude oil is characterised by highest summed concentration of light and saturated hydrocarbons ((i-C_5 – n-C_{30}),

which defines the MEAN DEGRADATIVE LOSS, and also by the highest concentrations of individual light hydrocarbons (*i*-C_5 – *n*-C_{10}).

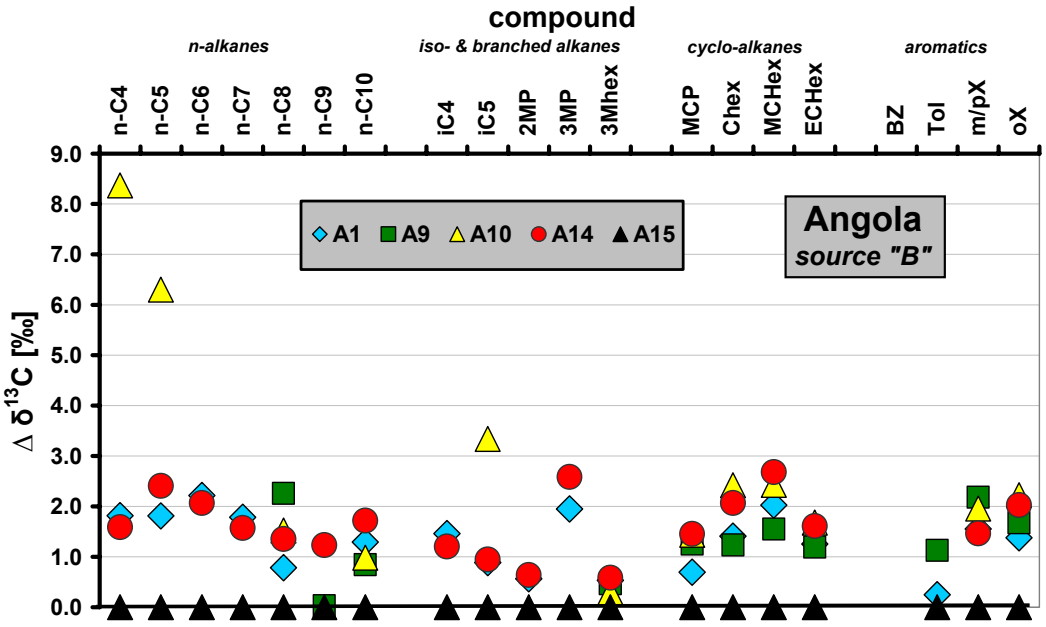

Fig. 121: $\Delta\delta^{13}C$ values for light hydrocarbons in crude oils from Angola, which were generated from source "B". Values are given as difference to the least degraded crude oil A15. Within the "B" subset lightest carbon isotopic compositions of light hydrocarbons were calculated for the least degraded sample A15, as assessed by the MEAN DEGRADATIVE LOSS.

The largest overall variance in ^{13}C was determined for *n*-butane, *n*-pentane and *iso*-pentane in sample A10 with $\Delta\delta^{13}C$ values of 8.4, 6.3 and 3.3 ‰, respectively. Interestingly, by means of the MEAN DEGRADATIVE LOSS, sample A10 is not the most biodegraded crude oil in the Angolan "B" subset. However, calculated individual compound concentrations for *iso*-pentane and *n*-pentane (the concentration of *n*-butane was not determined) are the lowest within the 5 crude oils from the "B" subset analysed for compound-specific carbon isotopes. This clearly shows the correlation of the compound concentration and carbon isotopic composition in this subset and suggests that the Rayleigh-model can be applied for Angolan crude oil samples from source "B".

The successful application of the Rayleigh model to assess biodegradation by carbon isotopic composition was already demonstrated by VIETH AND WILKES (2006) for samples from the Gullfaks field in Norway. These samples are also

used in this study and calculated $\Delta\delta^{13}C$ values of light hydrocarbons are displayed in Figure 122.

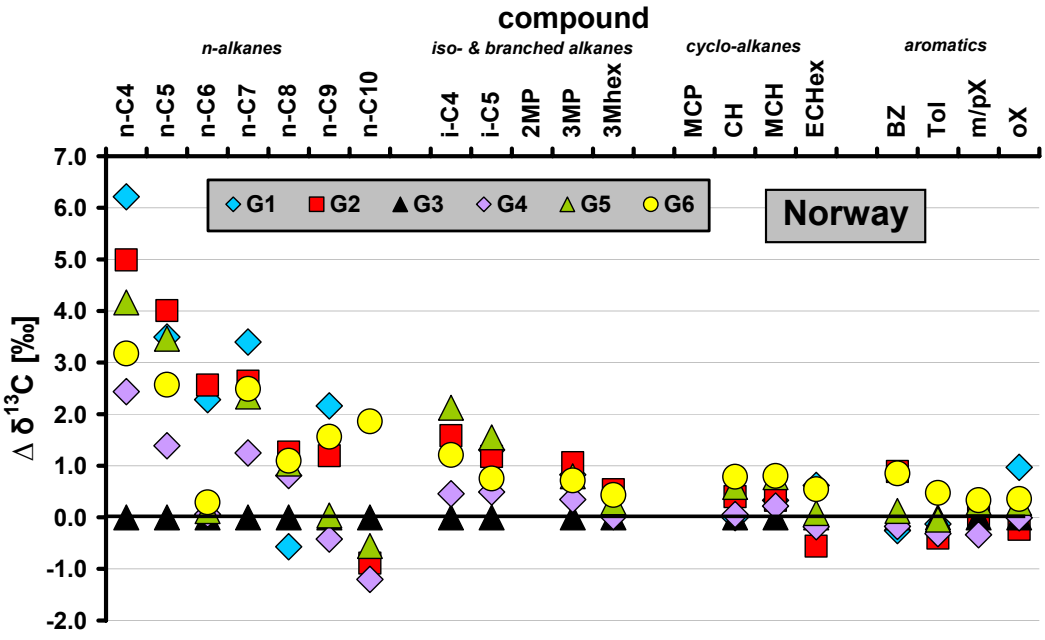

Fig. 122: $\Delta\delta^{13}C$ values for light hydrocarbons in six of the eight crude oils from the Gullfaks field in Norway. Sample A13 was excluded, because this crude oil has likely received a charge contribution from a second source rock. Due to limited sample amounts no isotopic measurements for sample G12 were possible. Carbon isotopic values are given as difference to the least degraded crude oil G3, which is labelled by black triangles and the black horizontal line at unity.

As discussed before, the compositional endmember G13 has received an additional charge from a second source rock, which might have influenced the carbon isotopic composition. Hence, this sample was excluded for the assessment of biodegradation by carbon isotopic compositions. Due to limited sample amount no stable isotopic measurements for sample G12 were possible. Therefore, the assessment of biodegradation by $\delta^{13}C$ ratios is carried out only for six of the eight crude oils from the Gullfaks field. Among these six crude oils, sample G3 is the least biodegraded crude oil by means of the MEAN DEGRADATIVE LOSS. Hence, $\Delta\delta^{13}C$ values shown in Figure 122 were calculated relative to sample G3.

Within the light hydrocarbons of the Norwegian crude oil samples the largest overall difference in ^{13}C is calculated for *n*-butane and *n*-pentane with $\Delta\delta^{13}C$ values of 6.2 and 4.0, respectively. Most calculated $\delta^{13}C$ ratios for short-chain *n*-

alkanes are heaviest in sample G1, which is also the strongest biodegraded crude within the Norwegian biodegradation sequence. The slightly lighter $\delta^{13}C$ ratio of *n*-pentane and *n*-hexane in sample G1 relative to G2 is within the standard deviation of isotopic measurements (± 0.5‰). However, compound concentrations for *n*-C_5 and *n*-C_6 are in both samples the lowest among the six crude oils from the Gullfaks field. Due to the MEAN DEGRADATIVE LOSS, these two crude oils are also the strongest biodegraded samples. Only for *n*-octane an anomalous light $\delta^{13}C$ ratio in sample G1 was calculated, which cannot be referred to an increased compound concentration. However, the good correlation of compound-specific $\delta^{13}C$ ratios and concentrations indicate that the Rayleigh-model can be applied for the assessment of biodegradation in the Norwegian sample set.

Interestingly, the extent of isotopic fractionation seems to decrease with increasing chain-length of the *n*-alkanes. This observation is in agreement with, e.g. BOREHAM ET AL. (1995) who showed that the intrinsic isotopic fractionation effect, which generally is controlled by the reaction of one specific carbon atom within the molecule, decreases with increasing carbon number. Among the short-chain *n*-alkanes the isotopic enrichment reaches from 6.2 to 1.9 ‰ for *n*-butane and *n*-decane, respectively. The decrease in carbon isotopic fractionation can also be observed, however less pronounced, for branched alkanes, with the highest fractionation for *iso*-butane (2.1‰) and the lowest isotopic difference for 3-methylhexane (0.5‰). The investigated cyclic and aromatic light hydrocarbons show only slight differences in $\delta^{13}C$ values (± 1‰) for crude oils from the Gullfaks field, which indicates a high stability of the carbon isotopic composition in these crude oil constituents. However, it should also be pointed out that the concentrations of these compounds are significantly depleted. It appears possible that this incongruity between the depletion of concentration and the relative invariance of $\delta^{13}C$ ratios is related to the different endmembers to which the isotopic (G3) and compositional (G13) calculations refer. However, even when carbon isotopic variabilities are referred to the same endmember (G13) the maximum isotope enrichment for one of the investigated cyclic and aromatic light

hydrocarbons is 2‰ for benzene in sample G2. Based on this theoretical calculation all other investigated cyclic and aromatic light hydrocarbons would also show a maximum carbon isotopic difference of ± 0.5‰, which is within the standard deviation of isotopic measurements, and hence, would again denote to high invariance of the carbon isotopic composition in these crude oil constituents.

In this study, the Rayleigh model can be applied to assess biodegradation for crude oils from Angola (subset B) and Norway, because both sample sets are characterised by a high homogeneity with respect to source rock organic matter and thermal maturity. Also, the systematic correlation of compound concentrations to $\delta^{13}C$ ratios suggests that both sample sets are suitable for assessing microbial degradation processes by using carbon isotopic fractionation. In both sample sets the largest change in $\delta^{13}C$ values has been observed for *iso*-pentane and *n*-pentane. For these two compounds the correlation of $\delta^{13}C$ ratios and compound concentrations is illustrated in Figure 123 and 124 for Angolan and Norwegian samples, respectively. In both plots it is shown that samples with highest concentration of *iso*-pentane and *n*-pentane are characterised by the lightest $\delta^{13}C$ ratio. It is also obvious that with increasing extent of biodegradation, which is indicated by the decrease of compound concentrations, $\delta^{13}C$ ratios of *iso*-pentane and *n*-pentane shift to heavier values. This clearly implies that the isotopic fractionation process can be described by the Rayleigh-equation. Based on the Rayleigh model, equation (4)

$$\ln\left(\frac{R}{R_i}\right) = \left(\frac{1}{\alpha} - 1\right) \times \ln F \qquad \textbf{(4)}$$

can be applied to calculate the isotopic fractionation factor (α), which is the measure of the kinetic isotope fractionation that goes along with biodegradation of a specific substrate. The fractionation factor is determined by the correlation of the natural logarithms of the concentration gradient and the change in $\delta^{13}C$ values

for a defined crude oil constituent. From the slope (y) of the linear regression line he compounds-specific fractionation factor can be calculated.

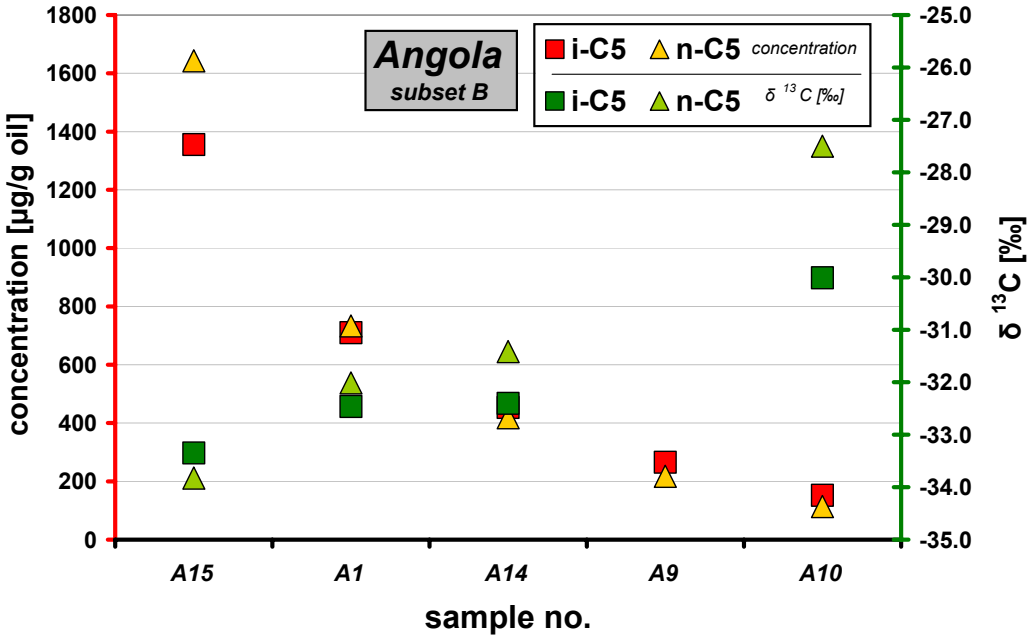

Fig. 123: The plot indicates a good correlation of compound concentration and $\delta^{13}C$ ratios for *iso*-pentane and *n*-pentane in crude oils from the Angolan subset "B". For sample A9 no $\delta^{13}C$ ratios for iso-pentane and n-pentane are available.

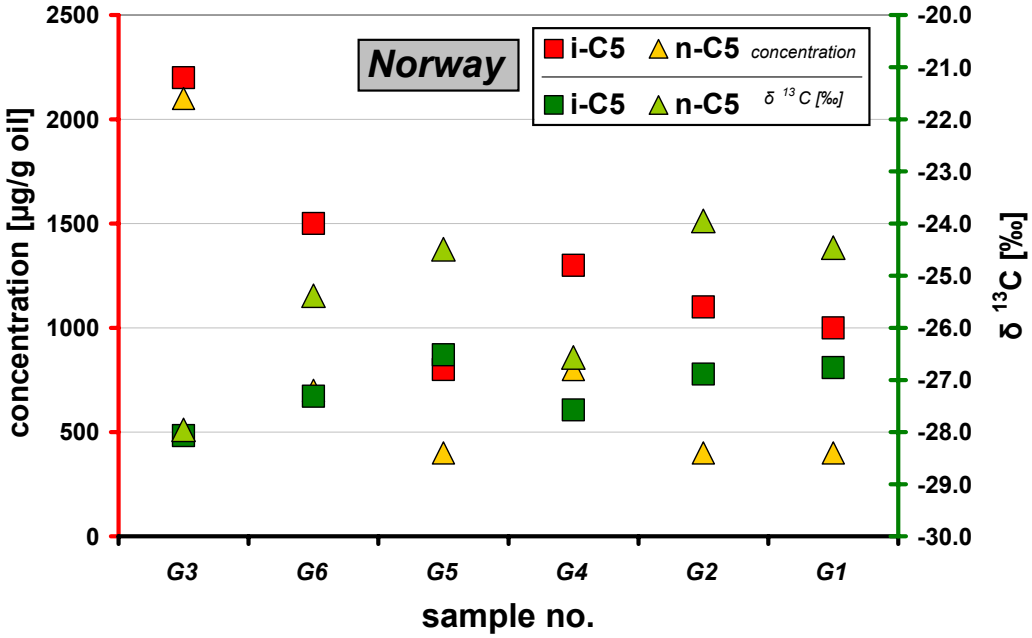

Fig. 124: The plot indicates a good correlation of compound concentration and $\delta^{13}C$ ratios for *iso*-pentane and *n*-pentane in crude oils from the Gullfaks field in Norway. Here, it should be noted that compound concentrations for crude oils from Norway, which were assigned in this study slightly differ to the concentrations published by VIETH AND WILKES (2006). Concentrations shown in this plot were adopted from the cited literature.

For crude oils from the Angolan subset "B" the correlations of compound concentrations and $\delta^{13}C$ ratios for *iso*-pentane and *n*-pentane following the Rayleigh model are illustrated in Figure 125.

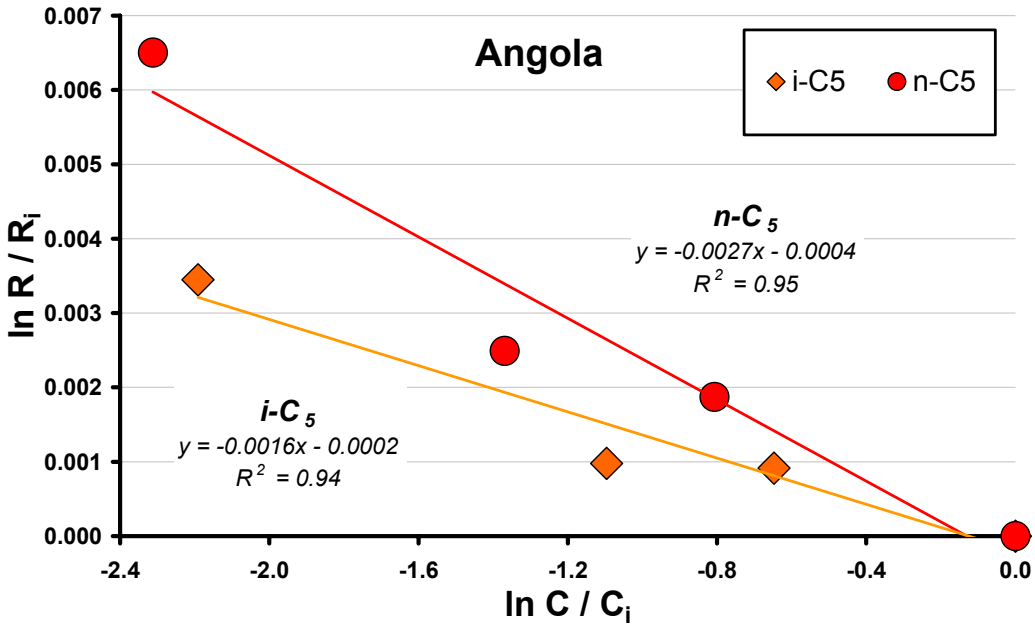

Fig. 125: Concentration and carbon isotope data of *iso*-pentane and *n*-pentane in four crude oil samples from the Angolan subset "B" plotted according to the Rayleigh equation. $\delta^{13}C$ ratios for *iso*-pentane and *n*-pentane in sample A9 were not available.

In crude oil samples from the Angolan subset "B" coefficients of determination for the linear regression lines (R^2), when natural logarithms of R/R_i are plotted over natural logarithms of C/C_i, are 0.94 and 0.95 for *iso*-pentane and *n*-pentane, respectively. This high correlation of compound concentration and $\delta^{13}C$ ratios clearly indicates that the Rayleigh equation can be used to describe kinetic isotope fractionation process that accompanies petroleum biodegradation. In Angolan crude oils the slopes of linear regression lines (y) for *iso*-pentane and *n*-pentane are shown in Figure 125. Based on these slopes individual isotope fractionation factors for *iso*-pentane (α = -1.0016) and *n*-pentane (α = -1.0027) can be calculated.

For the Norwegian samples the slopes of linear regression lines for *iso*-pentane and *n*-pentane are shown in Figure 126. Based on these slopes, fractionation

factors of -1.0016 and -1.0023 for *iso*-pentane and *n*-pentane, respectively, can be calculated. Interestingly, these fraction factors are identical or rather nearly identical to those determined for *iso*-pentane and *n*-pentane in Angolan samples. Hence, it can be concluded that the degradation mechanisms for the two compounds are similar in both petroleum systems.

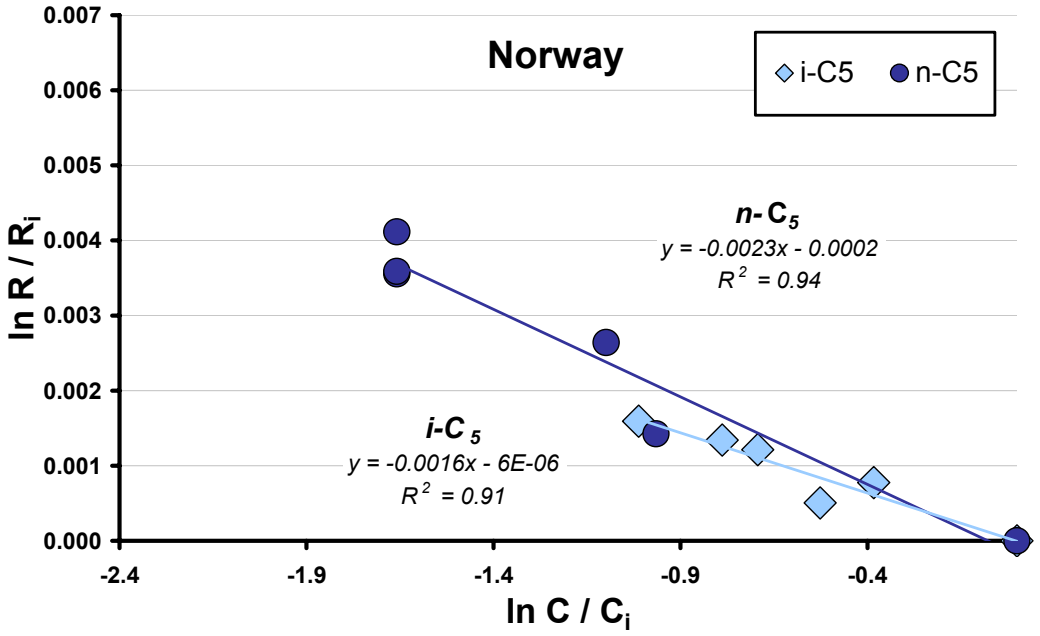

Fig. 126: Concentration and carbon isotope data of *iso*-pentane and *n*-pentane in six crude oil samples from the Gullfaks field in Norway plotted according to the Rayleigh equation. Concentration data used for this plot are adopted from VIETH AND WILKES (2006).

However, it is also obvious that the fractionation factors for *iso*-pentane and *n*-pentane are different. In this context, VIETH AND WILKES (2006) pointed out that *iso*-pentane and *n*-pentane are composed of the same number of carbon atoms, and, therefore it was considered that the different fractionation factors are due to mechanistic differences in the microbial utilisation of these two substrates. In the cited publication it is also stated that the fractionation factors may not only differ due to the different substrates, but also for different enzymatic reactions, as discussed by MORASCH ET AL. (2004) and ZWANK ET AL. (2005). Furthermore, it is elucidated by VIETH AND WILKES (2006) that the different fractionation factors for *iso*-pentane and *n*-pentane in the Gullfaks field are not only due to a relatively more efficient utilisation of the *n*-alkane, but also to a different isotope effect of

the initial activation reaction in the two compounds. However, the different extents of concentration decrease and different shifts of $\delta^{13}C$ ratios indicate that *iso*-pentane is degraded at a relatively lower rate than *n*-pentane, in both petroleum systems.

5.3.2.3 Quantification of biodegradation by compound-specific carbon isotopes

Assuming that in selected petroleum reservoirs the mechanisms of petroleum biodegradation for individual crude oil constituents are comparable and therefore are related to identical compound-specific isotope fractionation factors, the isotopic data can be used to quantify the depletion of a substrate in crude oil sample. It is clear that it has to be excluded that carbon isotope ratios of the individual compounds are influenced by other processes than biodegradation. If so, the extent of degradation in the residual crude oil constituent can be assessed using a known isotope fractionation factor (α) and the isotopic composition of the biodegraded (R) and non- or least biodegraded substrate fraction (R_i). The percentage of depletion (B_i) of a crude oil constituent is calculated using equation (5)

$$B_i = \left[1 - \left(\frac{R}{R_i} \right)^{\left(\frac{1}{\frac{1}{\alpha}-1} \right)} \right] \times 100 \qquad \textbf{(5)}$$

To check, if the percentage depletion that was calculated from the isotopic data correlates to the concentration decrease of the respective compound, the following equation (6)

$$B_c = \left(1 - \frac{C}{C_i}\right) \times 100 \qquad (6)$$

can be used, where B_C is the percentage of degradation of a degraded crude oil constituent whose concentration (C) is calculated relative to the concentration of the same compound in the least degraded crude oil (C_i). This calculation is identical with the assessment of the degradative loss, which was discussed in chapter 5.2. However it is important to note, that the degradative losses calculated in chapter 5.2 refer to different endmembers as those used for isotopic considerations.

The correlation of calculated depletions of *iso*-pentane that are based on the concentration and on the carbon isotopic composition is shown in Figure 127 for crude oil samples from Angola and Norway.

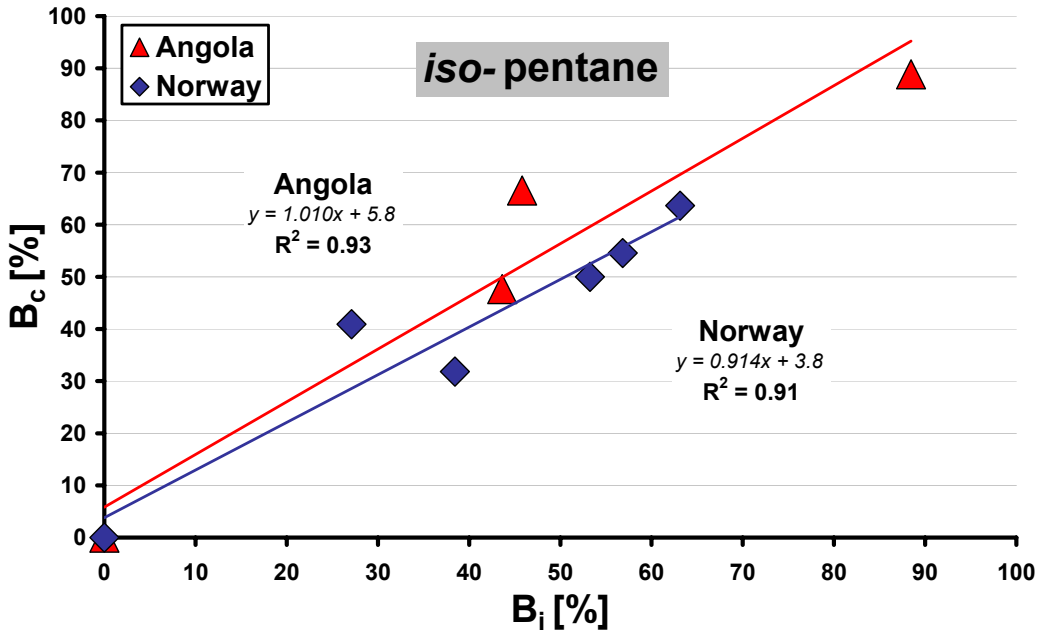

Fig. 127: Correlation of calculated extent of biodegradation given in percent, which is based on the concentration decrease (B_c) and on the carbon isotopic composition (B_i) for *iso*-pentane in crude oil samples from Angola and Norway. For the calculation of B_i the isotope fractionation factor of $\alpha = -1.0016$ was used, as determined for both sample sets.

Here, the coefficients of determination (R^2) of 0.93 and 0.91 for the Angolan and Norwegian samples, respectively, indicate a high correlation, which shows that the isotopic composition can be used to assess the extent of biodegradation of individual crude oil constituents. However, it is clear that the calculation of B_i, which is based on isotopic data, only is feasible when appropriate fractionation factors are available. At best, these fractionation factors should be obtained from independent laboratory experiments, as discussed by VIETH AND WILKES (2006). It was also discussed that carbon isotope fractionation factors being derived from degradation experiments with pure cultures in the laboratory and those calculated from crude oil samples that were collected in petroleum reservoirs can be different. This variance was attributed to the fact that under defined and ideal laboratory conditions the isotopic composition is only influenced by biodegradation, whereas in a petroleum reservoir other factors might affect the enrichment of ^{13}C in crude oil constituents. It was also discussed by VIETH AND WILKES (2006) that different fractionation factors for specific crude oil constituents, e.g., for *iso*-pentane and *n*-pentane could be due to mechanistic differences in the initial reaction of the degradation pathway.

It appears reasonable that isotope fractionation factors may also vary for the same substrate in different petroleum systems, which in this case would denote to differences in the degradation reactions in the reservoir. Hence, the determination of compound-specific isotope fractionation factors from various petroleum systems might lead to the assessment of general fractionation factors, which can be applied for, e.g., all anaerobically biodegraded petroleum reservoirs. In this context it is interesting to note, that the fractionation factors for *iso*-pentane calculated in Angolan and Norwegian crude oils are identical, and therefore suggest that the degradation mechanisms in these two petroleum systems are similar. According to VIETH AND WILKES (2006) who showed that biodegradation in the Gullfaks reservoirs occurs under anaerobic conditions, it might be assumed that biodegradation in the Angolan reservoirs also proceeds under comparable conditions. However, it is clear that similar fractionation factors may also result

from a combination of various mechanisms and therefore cannot stringently be referred to one specific reservoir characteristic.

In contrast to the identical fractionation factors that were calculated for *iso*-pentane (α = 1.0016), those assessed for *n*-pentane are slightly different in samples from Angola (α = -1.0027) and Norway (α = -1.0023). For the calculation of biodegradation extents following equation (5) the averaged fractionation factor (α = -1.0025) was used. Results of the quantification of depletion extents (B_i) shown in Figure 128 indicate a high correlation in both sample sets to the calculated degradative losses, which are based on the compound concentration of *n*-pentane (B_c).

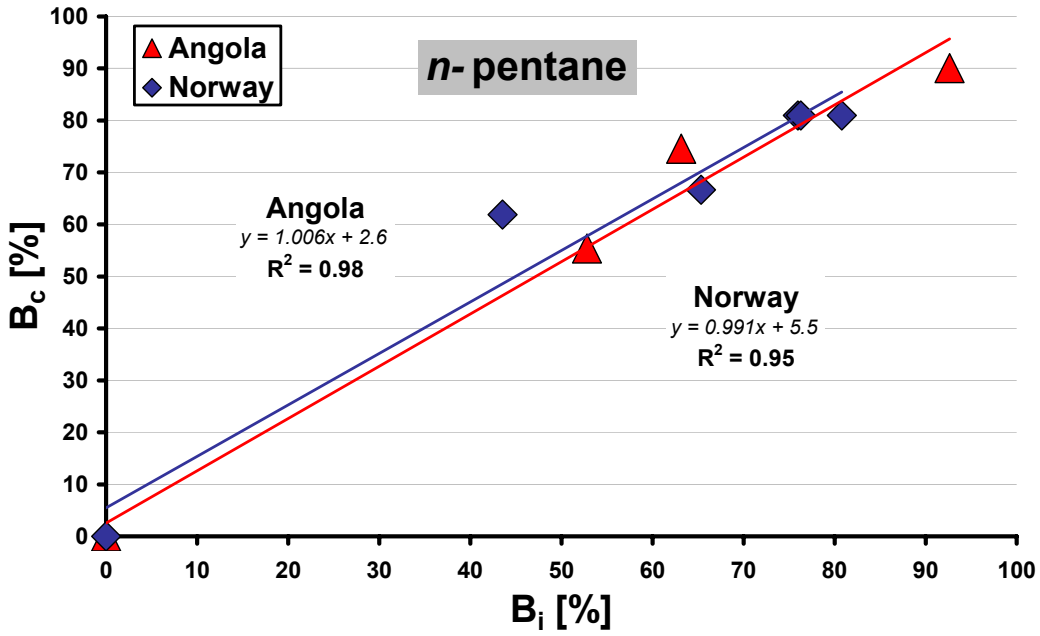

Fig. 128: Correlation of calculated concentration decrease (B_c) to the calculated substrate depletion, which is based on the carbon isotopic composition (B_i) for *n*-pentane in crude oil samples from Angola and Norway. For the calculation of B_i an isotope fractionation factor of α = -1.0025 was used. This is an averaged fractionation factor based on the two slightly different factors calculated for Angolan and Norwegian crude oils.

This high correlation of degradative losses derived from compound concentrations and from isotopic data clearly indicates that the calculated fractionation factors can be used to quantify substrate depletions in biodegraded petroleum reservoirs.

In the current literature, several forms are used to describe the isotope fractionation process during biodegradation. An often used definition is the isotope enrichment factor ε, which is defined as ε = (b1000), with b = (α-1) (MECKENSTOCK ET AL., 2004). This enrichment factor can also be used to illustrate how carbon isotopic compositions can be used to quantify substrate depletions in biodegraded crude oils.

For this approach the activation mechanisms of specific crude oil constituents have to be considered. Figure 129 shows a selected part of the degradation pathway for *n*-hexane during anaerobic biodegradation, as suggested by WILKES ET AL. (2002).

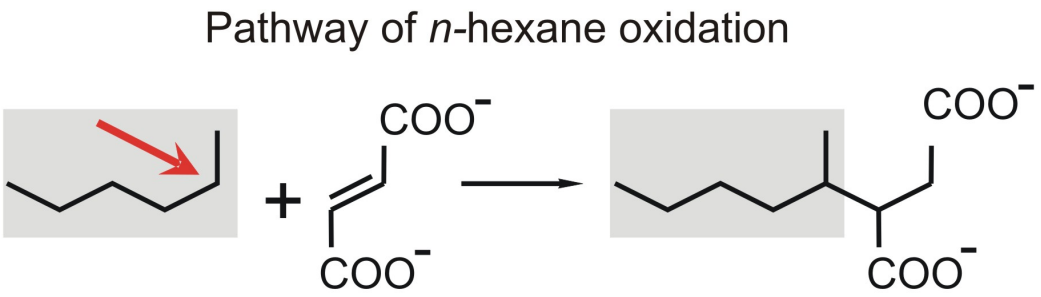

Fig. 129: Selected part of *n*-hexane activation during anaerobic biodegradation as suggested by WILKES ET AL., 2002. The red arrow indicates that only one specific carbon atoms is directly involved in the molecular reaction.

Taking into account that atoms that are directly involved in the molecular reaction are subject to the kinetic isotope fractionation, whereas those that are not involved in the reaction remain isotopically stable, it becomes clear that the measured isotopic enrichment of e.g., a specific *n*-alkane is n-C_X times lower than the intrinsic fractionation at the activated carbon atom. Assuming that the activation mechanisms for all other *n*-alkanes are similar to that suggested by WILKES ET AL. (2002), the intrinsic isotopic enrichment of one carbon atom can be used to calculate the fractionation factors and isotopic enrichment for *n*-alkanes with n-C_X carbon atoms. Hence, the already defined fractionation factors for *iso*-pentane (α = 1.0016) and *n*-pentane (α = -1.0025) in Angolan and Norwegian crude oil samples enable the calculation of the intrinsic isotopic enrichment of one carbon

atom in both molecules. Accordingly, the calculated enrichment factors of the activated carbon atom in *iso*- and *n*-alkanes are ε = 8.0 and ε = 12.5, respectively. These enrichment factors divided by the number of carbon atoms of a given iso- or n-alkane give the enrichment factors for the particular compound and illustrate the dilution of the isotope fractionation effect with increasing chain-length of the molecule. Hereafter, these theoretical enrichment factors can be re-calculated to specific fractionation factors, which can be used to quantify the extent of biodegradation in the respective crude oil constituent. Extrapolated fractionation factors that are based on *iso*-pentane and *n*-pentane are shown in Table 5.

comp.	*i*-C_4	*n*-C_4	comp.	*i*-C_8	*n*-C_8
α	-1.0020	-1.0031	α	-1.0010	-1.0016
comp.	*i*-C_5	*n*-C_5	comp.	*i*-C_9	*n*-C_9
α	-1.0016	-1.0025	α	-1.0009	-1.0014
comp.	*i*-C_6	*n*-C_6	comp.	*i*-C_{10}	*n*-C_{10}
α	-1.0013	-1.0021	α	-1.0008	-1.0013
comp.	*i*-C_7	*n*-C_7	comp.	*i*-C_{15}	*n*-C_{15}
α	-1.0011	-1.0018	α	-1.0005	-0.0008

Table 6: Calculated carbon isotopic fractionation factors for *i*-C_5 and *n*-C_5 and the extrapolated fraction factors for selected *iso*-alkanes and *n*-alkanes

The extrapolated fractionation factors can now be used, together with the respective isotopic composition, to quantify the substrate depletion of the respective compound by the approach discussed before (Equation 5). Figure 130 shows these calculated fraction depletions for some selected *iso*-alkanes and *n*-alkanes. The plot clearly indicates that the higher the number of carbon atoms in per molecule, the more diluted becomes the extent of analysed isotope fractionation. The plot illustrates that for a 4‰ shift in the carbon isotopic composition a substrate depletion of 80% is necessary, and vice versa, a $\delta^{13}C$ enrichment of 4‰ corresponds to a degradative loss of 80% for *n*-pentane. Accordingly, the degradative losses for other *iso*-alkanes and *n*-alkanes can be

assessed. This implies that the analysis of compound-specific carbon isotopic compositions can be used to quantify the extent of individual crude oil constituents.

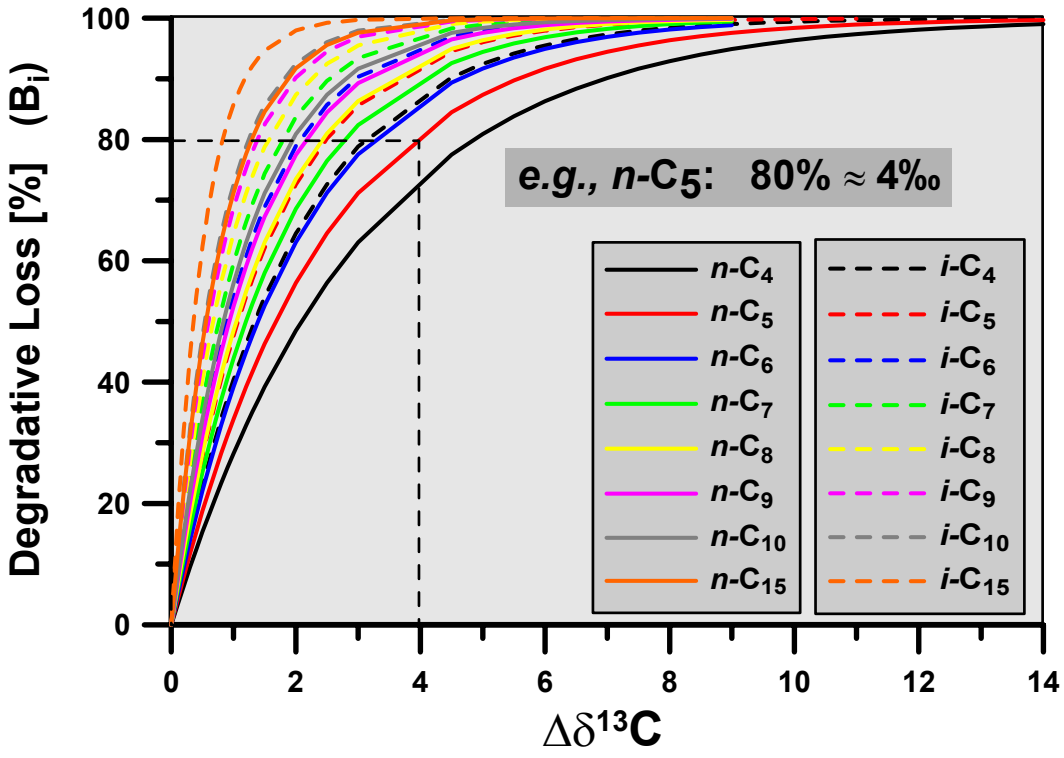

Fig. 130: Degradative losses vs. $\Delta\delta^{13}C$ values. The plot indicates that with increasing molecule chain-length the isotopic dilution effect increases. The more carbon atoms are present in the molecule the more this compound must be degraded to yield an isotopic shift. The plot can be used to asses the extent of degradation that is necessary to yield a compound-specific isotopic enrichment, or vice versa, a specific isotopic enrichment corresponds to a specific degradative loss of the compound.

5.3.2.4 Conclusions

Petroleum biodegradation of individual crude oil constituents can be assessed by compound-specific carbon isotope ratios. However, it is necessary to pre-establish even slightest compositional variances of the source rock organic matter, which

obviously lead to differences in the compound-specific carbon isotopes. Therefore, the use of compound-specific carbon isotopes to assess biodegradation is restricted to crude oil samples, which are characterised by a high compositional homogeneity due to source rock organofacies and source rock lithology. Interestingly, minor variances of the thermal maturity have no significant effect on the compound-specific carbon isotope ratios. Because carbon isotopic composition of crude oils are not significantly affected by other in-reservoir alteration processes, such as evaporative fractionation and water washing (HARRINGTON ET AL., 1999; SMALLWOOD ET AL., 2002), the clear isotopic fractionation of light hydrocarbons in samples from Angola and Norway can solely be attributed to biodegradation. VIETH AND WILKES (2006) already showed that the carbon isotopic fractionation within light hydrocarbons of crude oils from Norway can be correlated to the decrease in compound concentrations, and hence, the Rayleigh model can be applied to assess petroleum biodegradation by carbon isotopic signatures. This approach is most effective if appropriate fractionation factors are available, which should be obtained from laboratory experiments, where defined conditions exclude, that $\delta^{13}C$ signatures are affected by processes other than biodegradation. However, here it was shown that the isotope fractionation factors of specific crude oil constituents in samples from Angola and Norway are similar, and hence, might denote to similar degradation mechanisms. The investigation of isotopic compositions of various petroleum reservoirs therefore may provide the opportunity to assess generalised fractionation factors which are sufficient to decipher specific in-reservoir alteration processes. It was shown that the approach of VIETH AND WILKES (2006) to quantify the mass loss of individual crude oil constituents by compound-specific carbon isotope ratios can also be applied to a subset of crude oil samples from Angola.

5.3.3 Stable hydrogen isotope analysis

Stable hydrogen isotopic ratios of organic compounds preserved in sediments reflect the hydrogen isotopic compositions of ancient meteoric waters (DAWSON ET AL., 2005). Photosynthetic organisms utilize water as their main source of hydrogen and the deuterium/hydrogen (D/H) composition of the source water is reflected in the D/H ratio (δD) of the organisms (SESSIONS ET AL., 1999), which may contribute to the pool of source organic matter for petroleum. Hence, the analysis of compound-specific hydrogen isotopic compositions in crude oils may also provide insights into the D/H composition of the palaeoenvironmental depositional setting and into the D/H composition of the biological precursor compound (type of organic matter). It is also known that post-depositional processes, such as thermal maturation, influence the stable hydrogen isotopic composition (e.g., DAWSON ET AL., 2005 & 2007, LI ET AL., 2001, RADKE ET AL., 2005, PENDENTCHOUK ET AL., 2006). Furthermore, it was shown by WANG AND HUANG (2003) that vaporisation may lead to a progressive deuterium-depletion within low molecular weight constituents of the residuum, indicating a preferential vaporization of D-containing species. SESSIONS ET AL. (2004) showed that equilibrium exchange reactions lead to D/H fractionation between meteoric waters and organic compounds. It was also shown that biodegradation processes affect the hydrogen isotopic compositions (e.g., POND ET AL., 2002, MANCINI ET AL., 2003), leading to an enrichment of the heavier deuterium in the residual substrate fraction. This implies that petroleum biodegradation might be quantified by the assessment of hydrogen isotopic compositions, as it was already discussed for carbon isotopic compositions (chapter 5.3.1). However, most studies that discuss biodegradation effects on D/H ratios are based on laboratory experiments and petroleum contaminations in the environment. In contrast, only few studies discussed the influence of biodegradation on the hydrogen isotopic composition of crude oils (SUN ET AL., 2005).

It was discussed before, that carbon isotopic compositions of light hydrocarbons can be used to assess biodegradation, if differences due to source rock organofacies can be excluded. Accordingly, only crude oil samples, which were defined to be mainly affected by in-reservoir alterations (for details see chapter 5.1) are used to illustrate possible influences of biodegradation on the hydrogen isotopic composition. Compound-specific δD ratios of all investigated crude oils, including the samples which do not belong to the pre-established biodegradation sequences, are listed in the Appendix. Missing values for compounds in individual samples are due to limited baseline separation and increased standard deviations (> 5%) for the three replicate measurements, and therefore are not shown. Compound-specific hydrogen isotopic ratios for crude oils from Canada and Egypt are not available at the moment. Compound-specific δD ratios for crude oils from Angola, Norway and Nigeria are shown in Figure 131, 132 and 133, respectively.

Angola

For crude oil samples from the Angolan biodegradation sequence compound-specific δD ratios are shown in Figure 131. Crude oils A2, A3 and A13 were too viscous for injection into the GC-C-IRMS system, hence, no data can be provided for these samples. In general, hydrogen isotopic ratios (δD) for investigated light and saturated hydrocarbons in the Angolan samples vary between -180‰ and -40‰. Interestingly, δD ratios of compounds in the Angolan samples shift to heavier δD ratios with increasing chain-length of the molecule. This is contrary to the observation made for the carbon isotopic composition ($\delta^{13}C$) in Angolan crude oils, which shifts to lighter values. It is also interesting to note, that the high variability of δD ratios is not restricted to the light hydrocarbon range, as it was observed for the carbon isotopic composition, but is also obvious for the mid- and long-chain *n*-alkanes.

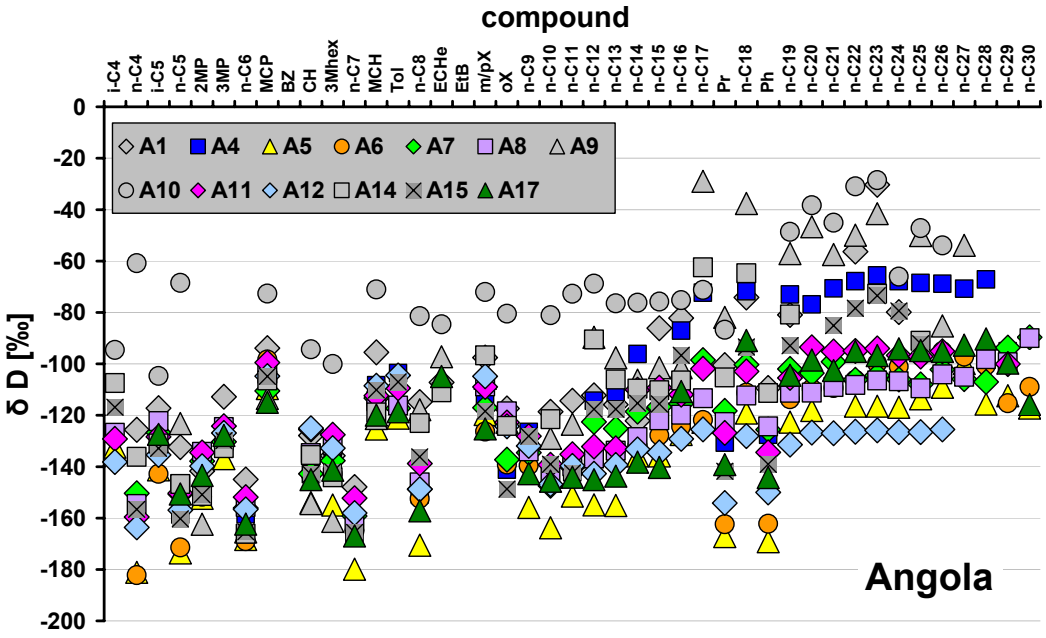

Fig. 131: δD ratios for light and saturated hydrocarbons in crude oil samples from the Angolan biodegradation sequence. Crude oils A2, A3 and A13 were too pasty for injection into the GC-C-IRMS system, hence, no data can be provided for these samples.

Norway

For crude oil samples from the Norwegian biodegradation sequence compound-specific δD ratios are shown in Figure 132. Due to limited sample amount no δD-values can be provided for sample G12. In general, hydrogen isotopic ratios (δD) for investigated light and saturated hydrocarbons in the Norwegian samples vary between -160‰ and -60‰. As already described for the Angolan crude oil samples, δD ratios shift to heavier isotopic compositions with increasing chain-length of the molecule. This observation is contrary to the carbon isotopic composition, which shifts to lighter values. Also comparable with the Angolan sample set is the high varibility of δD ratios for all investigated crude oil constituents in samples G1-G6, which are exclusively sourced from the Draupne Formation. Only sample G13, which was generated from two sources, shows quite similar δD values of mid- to long-chain saturated hydrocarbons (>*n*-C_9), however, pristane and phytane are slightly out of the steady line that shifts to heavier values with increasing chain length.

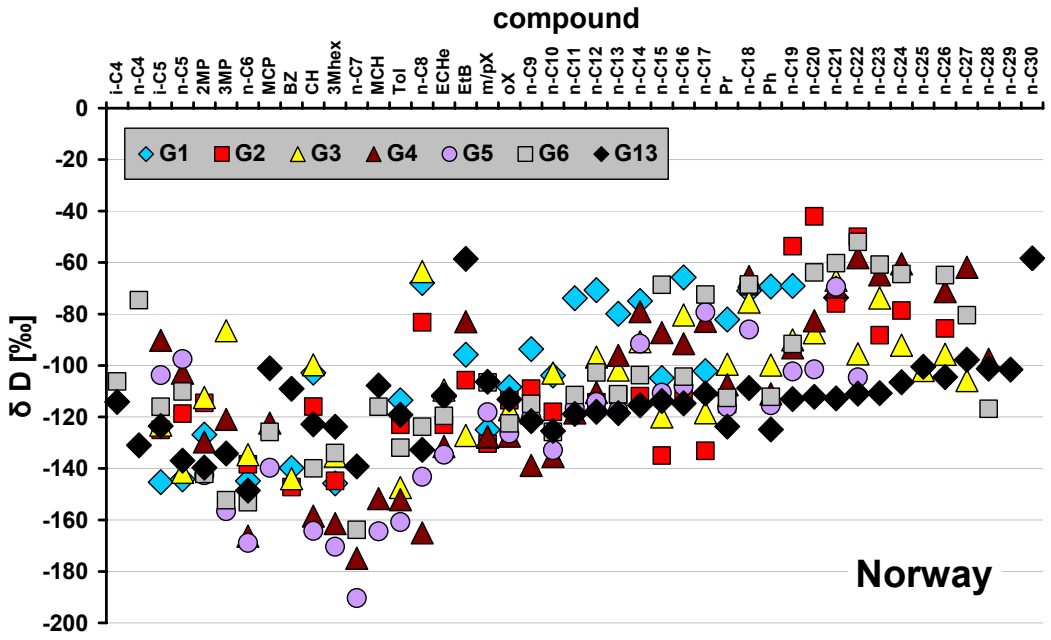

Fig. 132: δD ratios for light and saturated hydrocarbons in crude oil samples from the Gullfaks field in Norway. Due to limited sample amount of G12 no determination of δD-values was possible.

Nigeria

For crude oil samples from Nigeria compound-specific δD ratios are shown in Figure 133. In general, δD ratios vary between -150‰ and -80‰, and thus represent the smallest range of hydrogen isotopic compositions within the three investigated sample sets. The light hydrocarbons are characterised by a relatively larger range of δD ratios than the mid- and long-chain *n*-alkanes. Obviously, δD values for light hydrocarbons become heavier with increasing molecular weight. In contrast, hydrogen isotopic compositions for the mid and long-chain *n*-alkanes obviously shift to slightly lighter δD ratios with increasing molecular weight. The variability of compound-specific δD ratios is rather limited compared to the sample sets from Angola and Norway. Interestingly, in Nigerian samples specific crude oil constituents (methylcyclopentane, benzene, methylcyclohexane and ethylbenzene) are characterised by relatively heavy δD ratios.

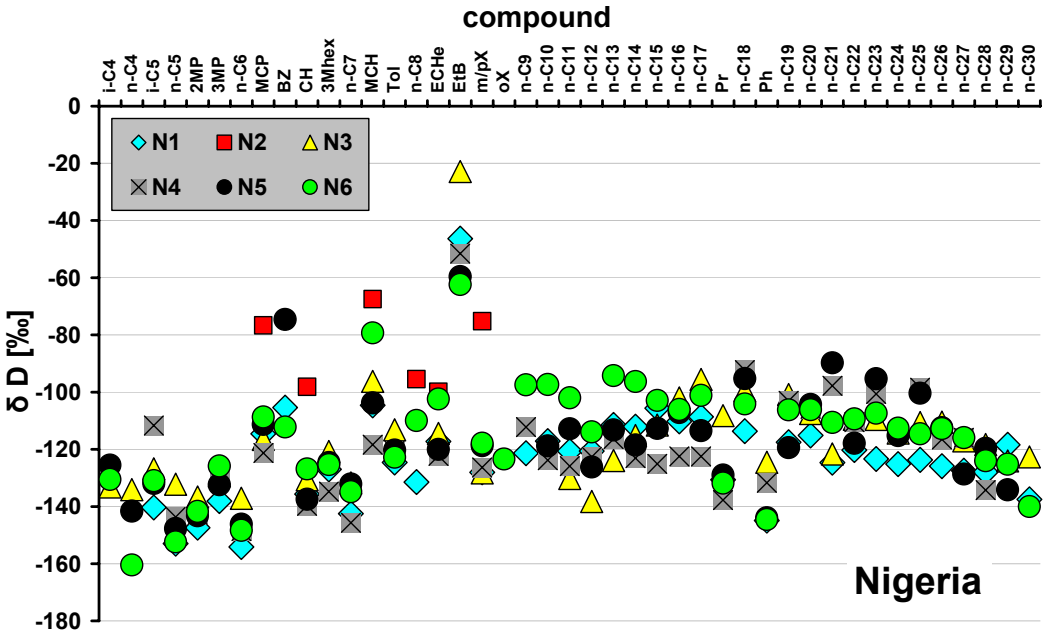

Fig. 133: $\delta^{13}C$ isotopic ratios for light and saturated hydrocarbons in crude oil samples from the Nigerian biodegradation sequence.

5.3.3.1 Source, depositional and maturity effects on δD ratios

In Figures 131, 132 and 133 it was shown that compound-specific hydrogen isotopic compositions significantly vary within the three investigated sample sets from Angola, Norway and Nigeria. As already mentioned, such variations might reflect differences in the source of the organic matter and/or the impact of various post-depositional processes, such as thermal maturation, equilibrium exchange reactions, vaporisation and biodegradation. Hence, it is necessary to decipher these possible influences on the stable hydrogen isotopic composition before δD ratios can be used to assess biodegradation in a petroleum reservoir.

In chapter 5.3.2.1 it was shown that the slight differences in source rock organofacies affected the compound-specific carbon isotopic composition in crude oils from Angola. Hence, it appears likely that also the hydrogen isotopic

composition of these crude oil samples is affected by the slightly different source rocks. With respect to the two Angolan subsets, which are distinguished by the D/(D+R) ratio (see chapter 5.1.3.2) and the carbon isotopic composition (see chapter 5.3.2.1) hydrogen isotopic signatures mainly vary between -180‰ to -60‰ and -160‰ to -40‰ for samples from subset "A" and subset "B", respectively. This slight but systematic shift of ±20‰ between the two subsets suggests that δD ratios, which are shown in Figure 131 by coloured symbols for samples from subset "A" and by grey symbols for crude oils from subset "B", are influenced by the slightly different sources. Interestingly, DAWSON ET AL. (2007) observed deuterium enriched isotopic compositions of mid- and long-chain *n*-alkanes in crude oils, which are characterised by a relatively increased input of terrestrial organic matter. Accordingly, crude oils from Angolan subset "B" would have been generated from a source rock that contains higher amounts of terrestrial organic matter than samples of subset "A". However, it should also be noted that terrestrial organic matter has been shown to display wide variations in δD ratios. SCHIMMELMANN ET AL. (2004) and XIONG ET AL. (2005) observed lighter δD signatures in terrestrially sourced *n*-alkanes than in marine-sourced *n*-alkanes. Generally it is assumed that terrestrially derived organic matter is depleted in deuterium relative to marine-sourced organic matter, because δD ratios of meteoric source waters are typically more negative than ocean waters (CRAIG, 1961). Nevertheless, it is also known that meteoric waters can become significantly enriched in deuterium by, e.g., climatic variances so that the biosynthetic products of aquatic organisms and terrestrial plants are characterised by relatively heavier hydrogen isotopic compositions (DAWSON ET AL., 2007). Hence, the hydrogen isotopic compositions are obviously not unambiguously indicative for a specific depositional environment. However, in Figure 134 the differentiation of the two slightly different Angolan source rock compositions is also indicated by compound-specific hydrogen isotope compositions, because increased D/(D+R) ratios are accompanied by heavier hydrogen isotopic compositions of pristane and phytane.

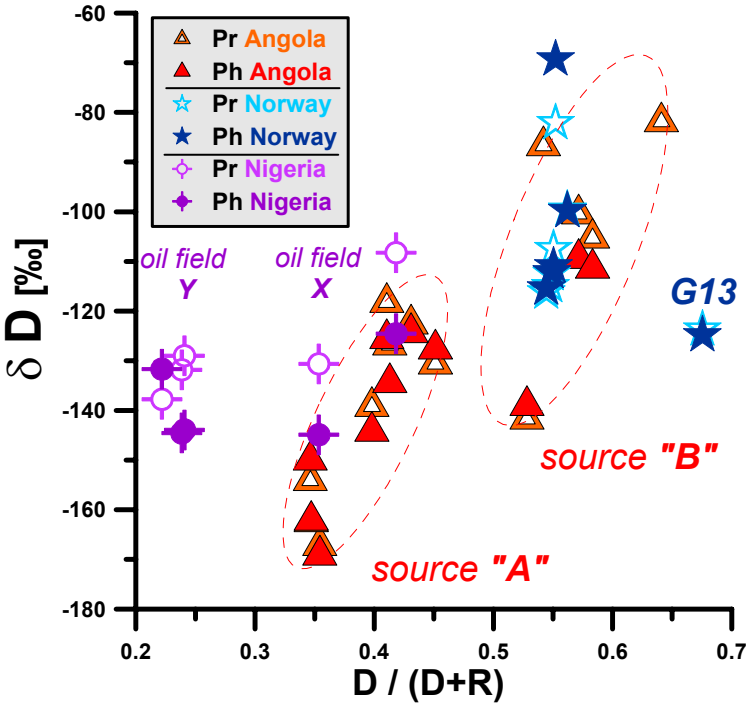

Fig. 134: Plot of δD ratios vs. the D/(D+R) sterane ratio for crude oils from Angola, Norway and Nigeria.

The linear correlation of the source parameter D/(D+R) and the hydrogen isotopic composition within the two subsets also suggests that compositional differences in the source rocks are responsible for differences in the δD ratio of the two isoprenoids in crude oils from Angola. Interestingly, the D/(D+R) ratio is mainly used to distinguish between clay-poor and clay-rich source rocks with higher values for the latter lithofacies. It is interesting to note that clays, e.g. kaolinite [$Al_2Si_2O_5(OH)_4$] are characterised as alumosilicates which bear significant amounts of hydrogen. In this context, it was discussed that diagenetic effects over geological times can result in significant hydrogen isotopic exchange between organic hydrogen and the surrounding environment (e.g., SCHIMMELMANN ET AL., 1999, SESSIONS ET AL., 1999 & 2004). Interestingly, it was already discussed by ALEXANDER ET AL. (1984) and DAWSON ET AL. (2007) that clay surfaces are capable to promote the D/H exchange in the sedimentary environment. Hence, it cannot be excluded that equilibrium exchange reactions within the depositional setting contribute to the measured hydrogen isotopic composition of individual compounds in Angolan crude oils. However, for crude oils from Norway and

Nigeria Figure 134 indicates no systematic correlation between the hydrogen isotopic composition of pristane and phytane and the source parameter D/(D+R). These two samples sets are characterised by relatively constant δD ratios (Nigeria) and invariant D/(D+R) ratios (Norway). However, it is also obvious that in both Angolan subsets, due to the wide overlap of various compound-specific δD ratios (Figure 131), not only equilibrium exchange reactions influence the hydrogen isotopic composition.

In this context, it is also interesting to note that the isoprenoids pristane and phytane in both Angolan subsets are characterised by clearly lighter hydrogen isotopic composition than, e.g. n-C_{17} and n-C_{18}. Based on laboratory experiments, such deviant hydrogen isotopic compositions of isoprenoids and *n*-alkanes are attributed to different D/H fractionation between organic lipids and water for biosynthesized *n*-alkyl and isoprenoid components (SESSIONS ET AL., 1999). Thus, it is assumed that isoprenoid lipids are depleted in deuterium relative to *n*-alkyl lipids in organic matter. The data shown in Figure 131 obviously suggest that this isotopic difference between isoprenoids and *n*-alkanes can be preserved over geological times and during the thermal mobilisation of organic matter from the kerogen to liquid oil and its migration into the petroleum reservoir. In Figures 132 and 134 it is shown that also in crude oil samples from Norway and Nigeria deuterium in pristane and phytane is depleted compared to the *n*-alkanes, however, the extent is less pronounced than in Angola.

In addition to the source-related differences of δD ratios and the discussed diagenetic effects, indigenous hydrogen isotopic compositions are also affected by thermal effects which promote the hydrogen exchange between organically bound hydrogen and water hydrogen of the depositional and reservoir setting. It was clearly shown by, e.g., DAWSON ET AL. 2005 & 2007, RADKE ET AL., 2005, PENDENTCHOUK ET AL., 2006 that thermal maturation leads to an enrichment of deuterium in the sedimentary organic matter. This is thought to result especially from hydrogen exchange between the sedimentary hydrocarbons and deuterium-enriched formation waters (SCHIMMELMANN ET AL., 1999). Figure 135 shows δD

ratios of pristane and phytane in correlation to the sterane maturity parameter C_{29} ββ/(ββ+αα) for crude oil samples from Angola, Norway and Nigeria.

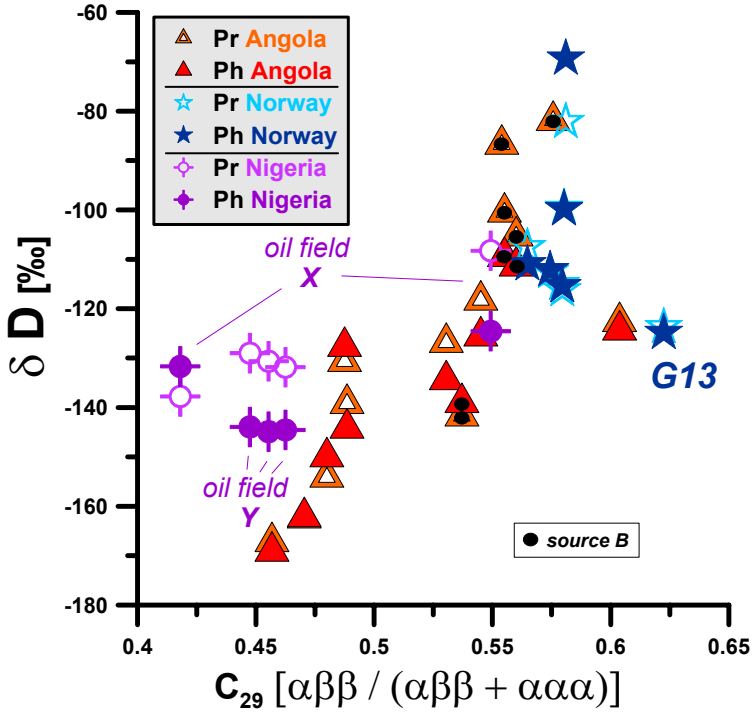

Fig. 135: Plot of δD ratios for pristane and phytane vs. the maturity parameter C_{29} [αββ / (αββ + ααα)] steranes for crude oil samples from Angola, Norway and Nigeria.

Interestingly, the δD ratios of isoprenoids in crude oils from Angola show a systematic correlation to the thermal maturity parameter. In samples from Angola δD ratios systematically shift to heavier isotopic compositions with increasing thermal maturity. Interestingly, in the Angolan samples the clear correlation between the maturity parameter and the hydrogen isotopic composition is also obvious within the two subsets. This suggests that even slight maturity differences may lead to a significant enrichment of deuterium in hydrocarbons. However, it should be noted again, that also slight differences in the lithofacies within the two Angolan subsets may have influenced the hydrogen isotopic composition. For crude oils from Norway and Nigeria Figure 135 indicates no systematic correlation between the hydrogen isotopic composition of pristane and phytane and the thermal maturity. However, these two sample sets are characterised by relatively constant δD ratios (Nigeria) or invariant C_{29} ββ/(ββ+αα) ratios

(Norway). This implies, that in crude oil samples from the Gullfaks field, neither the source rock organofacies nor the thermal maturity controls the wide range of δD ratios, and, that the thermal maturity variations in Nigerian samples obviously have no significant effect on the hydrogen isotopic composition. However, Figure 136 illustrate that in the Gullfaks oils samples δD ratios for pristane and phytane significantly vary (±50‰).

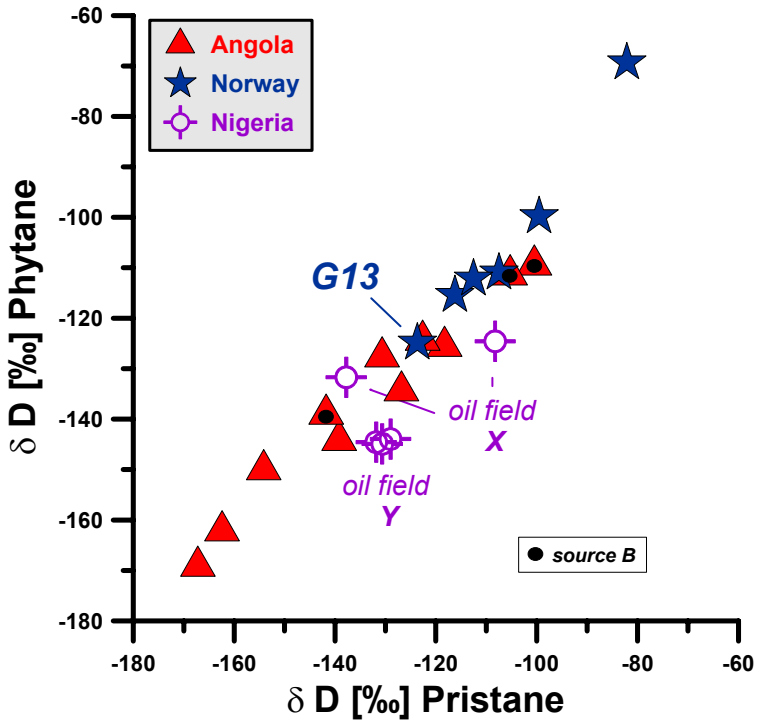

Fig. 136: Plot shows a linear correlation of compound-specific $\delta^{13}C$ ratios for pristane and phytane in crude oil samples from Angola, Norway and Nigeria. Interestingly, δD ratios of pristane and phytane in samples from Norway show a broad range, which cannot be explained by differences in source and maturity and biodegradation.

This pronounced variability cannot be explained by biodegradation, because the dilution effect that was already described for the carbon isotopes is likely also relevant for hydrogen isotopes and hence, anticipates that biodegradation is detectable in pristane and phytane. Hence, it appears likely that besides source, maturity and biodegradation also other impacts, such as the discussed hydrogen exchange reactions, may affect the compound-specific hydrogen isotopic composition of crude oils sampled in petroleum reservoirs.

Based on studies of sedimentary source rocks PENDENTCHOUK ET AL. (2006) and DAWSON ET AL. (2007) showed that with increasing maturity the isoprenoids pristane and phytane become relatively stronger enriched in deuterium than *n*-alkanes. In these studies it was also shown that with increasing thermal exposure the differences of δD ratios between *n*-alkanes and isoprenoids gradually decrease. Hence, the hydrogen isotopic compositions of crude oils, which are expelled during different stages of thermal maturity, may reflect the thermally promoted hydrogen exchanges by varying differences in δD ratios for isoprenoids and *n*-alkanes and, hence, denote to different levels of thermal maturity. Figure 137 shows the sterane maturity parameter C_{29} ββ/(ββ+αα) in correlation to the calculated difference of summed δD ratios for pristane and phytane and the summed δD ratios for *n*-heptadecane (n-C_{17}) and *n*-octadecane (n-C_{18}).

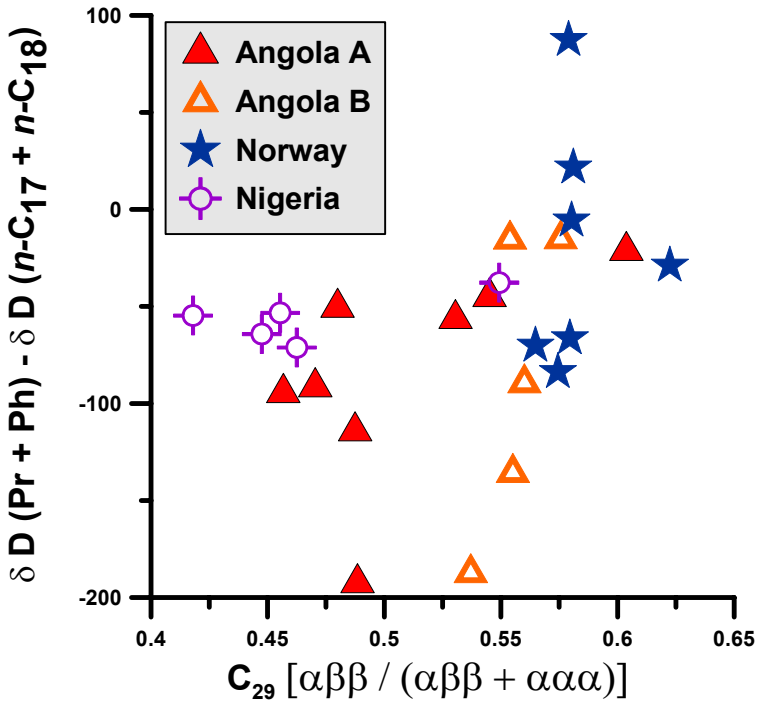

Fig. 137: Plot shows the correlation of the maturity parameter C_{29} ββ/(ββ+αα) to the calculated difference of summed δD values of pristane and phytane and the sum for δD values of *n*-C_{17} and *n*-C_{18}. Following DAWSON ET AL. (2007) the calculated difference should decrease with increasing thermal maturity. Interestingly, this can be observed for crude oils from both Angolan subsets, and, hence indicates that the slight maturity differences in Angolan samples are responsible for the clear enrichment of deuterium.

Following PENDENTCHOUK ET AL. (2006) and DAWSON ET AL. (2007) the calculated difference should decrease with increasing thermal maturity, which is indicated by higher C_{29} ββ/(ββ+αα) ratios. Interestingly, in most samples of both Angolan subsets the increase of maturity is accompanied by a systematic decrease of the calculated difference between δD ratios for isoprenoids and *n*-alkanes. In particular, crude oil samples from Angolan subset "B" show a good correlation of both maturity indicators. This decrease of the calculated difference between δD ratios for isoprenoids and *n*-alkanes cannot be attributed to differences in the source rock lithology. Hence, it can be concluded that the hydrogen isotopic composition of crude oils from Angola is clearly affected by the slight maturity differences, which have no comparable effect on the molecular composition, as it was discussed earlier in this study (see chapter 5.1 and 5.2.2).

5.3.3.2 Implications for the assessment of biodegradation by δD ratios

Based on laboratory experiments and environmental studies it was shown by e.g., POND ET AL., 2002 and MANCINI ET AL., 2003, that biological activity affects the hydrogen isotopic compositions leading to an enrichment of the heavier isotope deuterium in the residual substrate fraction. However, it was also discussed by e.g. DAWSON ET AL. (2005 AND 2007), PENDENTCHOUK ET AL. (2006) and SESSIONS ET AL. (2004) that other factors, such as hydrogen exchange reactions with the depositional environment and thermal maturity may influence the stable hydrogen isotopic composition. In chapter 5.3.3.1 it was clearly shown that for the investigated samples especially increasing thermal maturity leads to an enrichment of deuterium in the crude oils. In particular, for the Angolan samples it appears likely that the hydrogen isotopic composition is affected by exchange reactions due to differences in the lithofacies of the source rocks and by the slight variations in thermal maturity. Crude oil samples from Nigeria are also

characterised by slight to moderate variations in thermal maturity. Therefore, it is not appropriate to assume that δD ratios are only affected by biodegradation, even though a clear correlation of source and maturity to δD ratios is not obvious. In contrast, crude oil samples from the Gullfaks field in Norway are characterised by the highest congruity of thermal maturity and source rock organofacies and therefore appear to be the sample sequence with hydrogen isotopic compositions that are least affected by processes other than biodegradation.

It was shown before that compound concentrations and carbon isotopic compositions of light hydrocarbons are affected by light to moderate biodegradation. Differences in the hydrogen isotopic composition (ΔδD) for light hydrocarbons in the Gullfaks samples from Norway are shown in Figure 138.

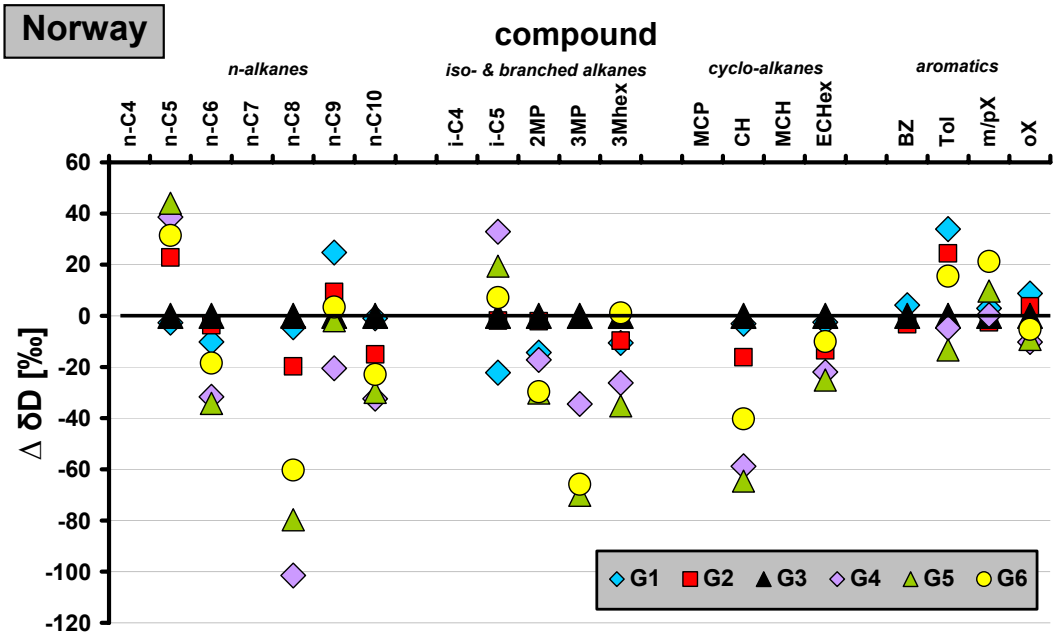

Fig. 138: ΔδD values for light hydrocarbons in six of the eight crude oils from the Gullfaks field in Norway. Sample A13 was excluded, because this crude oil has likely received a charge contribution from a second source rock. Due to limited sample amounts no isotopic measurements for sample G12 were possible. Carbon isotopic values are given as difference to the least degraded crude oil G3 by means of the mean degradative loss. This least degraded crude oil sample is labelled by the black triangles and the black horizontal line at unity.

In this plot ΔδD values for the six crude oil samples (G1 –G6), which were generated from the Draupne Formation are displayed. Due to the high sensitivity

of hydrogen isotopic compositions to differences in source rock organofacies and thermal maturity crude oil sample G13 was excluded from the sample set. This crude oil is characterised by a slightly increased maturity compared to the other six Norwegian crude oils and was likely generated from the Draupne and the Heather Formation, and hence, it appears likely that these maturity and source differences also have affected the hydrogen isotopic composition. In Figure 138 ΔδD values are calculated between the δD ratios of compounds in the least degraded sample G3 and the δD ratio of the respective compound in the degraded crude oil.

Interestingly, Figure 138 illustrates that most light hydrocarbons in the least degraded crude oil sample G3 are not characterised by the lightest hydrogen isotopic composition. Various negative ΔδD values indicate that crude oil constituents in sample G3 are heavier than in the more biodegraded samples. Interestingly the mean degradative loss and the carbon isotopic data indicated that sample G3 is the least degraded crude oil among the six Gullfaks samples, which were sourced from the Draupne Formation. Considering the high compositional congruity of these six Norwegian samples, which indicated almost no variances for source rock organofacies, source lithology and thermal maturity it is interesting to see that ΔδD values show a broad spread. Theoretically, this heterogeneity of ΔδD values may suggest that, e.g., hydrogen isotopic compositions of light hydrocarbons are also affected by exchange reactions, which may occur in the depositional environment, during burial and with oil field waters in the petroleum reservoir. It appears reasonable that such hydrogen exchange reactions are dependent on the time of exposure, e.g. in the petroleum reservoir, and that relative exchange rates are due to the specific molecular structure of the different crude oil constituents. Hence, if compound-specific hydrogen exchange reaction rates would be known, it could be possible to recalculate the storage time of the crude oils in the petroleum reservoir. However, at present it is not known to which exact extent the various processes affect the hydrogen isotopic composition in crude oils, and therefore, it is also not reasonable to assess individual influences, such as the storage time or the extent of

petroleum biodegradation by D/H ratios, even not for crude oil samples which are characterised by high similarities of source rock organofacies, source lithology and thermal maturity. In order to use the δD ratios as effective biodegradation indicators the influence of each individual process on the hydrogen isotopic compositions has to be quantified and extracted from the indigenous D/H composition. For this approach it is necessary to study biodegraded crude oils, which are characterised by a higher similarity of, e.g. thermal maturity and source rock composition than the crude oil samples which were investigated in this study. However, if such samples are available it appears likely that the approach, which was discussed for the compound-specific carbon isotopes, can also be applied for the compound-specific hydrogen isotopic compositions.

5.3.3.3 Conclusions

Compound-specific hydrogen isotopic compositions of crude oils are controlled by numerous fractionation processes that occur prior, during and after the deposition of the organic matter. Source-related differences such as increased terrestrial organic proportions in the source rock could be documented by an enrichment of deuterium in the hydrogen isotopic composition. However, this observation, as carried out for Angolan crude oils, cannot unambiguously be transferred to any sample set, because several factors, such as climatic variations in the area of primary production, can influence the isotopic composition of the hydrogen source. A further pre-depositional, source related impact was discussed concerning different D/H fractionation between organic lipids and water for biosynthesized *n*-alkyl and isoprenoid components, which results in deuterium-enriched *n*-alkanes in sedimentary organic matter. However, here it was shown for Angolan samples that these source-related differences of δD signatures are still detectable in crude oils, and hence, are preserved along the deposition and burial

of the organic matter and along the generation and migration of petroleum. It was also discussed that exchange reactions between the organic hydrogen and the depositional environment may lead to differences in the isotopic composition of crude oils. Such exchange reactions may occur between the organic-bound hydrogen and mineral-bound hydrogen or hydrogen of formation waters. Additionally, hydrogen isotopic compositions are significantly affected by thermal maturity. Increasing thermal stress obviously promotes hydrogen exchange reactions between the organic matter and the depositional environment leading to an enrichment of deuterium in the substrate fraction. In particular, for the crude oil samples from Angola, the impact of thermal maturation on the hydrogen isotopic composition was shown. A further impact on hydrogen isotopic compositions, as it was proven in laboratory experiments, is the fractionation caused by biodegradation. However, due to the great variety of influences that occur in natural systems it is highly challenging to decipher the biologically caused hydrogen fractionation in petroleum reservoirs. To assess the extent of hydrogen fractionation caused by biodegradation it would be necessary to quantify every individual process which affects the hydrogen isotopic composition. Then, biodegradation-related fractionation could be re-calculated and assessed similar to the approach proposed by VIETH AND WILKES (2006), and which was applied in this study in chapter. 5.3.2 Obviously, the assessment of biodegradation by hydrogen isotopic compositions is only possible in ideal petroleum system, where, like under laboratory conditions, all discussed influences are known. Such an ideal petroleum system is likely not existent, and therefore hydrogen isotopic compositions appear to be unsuitable to assess petroleum biodegradation.

5.4 Summary

The main focus of this study is on the assessment and quantification of alteration effects that occur within the early levels of petroleum biodegradation. For this purpose, 55 crude oil samples from petroleum systems in Angola, Norway, Canada, Egypt and Nigeria are investigated.

The organic geochemical characterisation of the crude oils shows that five sample sets differ clearly due to source rock organofacies, lithofacies and thermal maturity exist. However, within each of the five individual sample sets compositional differences are mainly due to in-reservoir biodegradation. These five biodegradation sequences are used to decipher and to quantify the molecular and isotopic differences.

First, main crude oil constituents such as light hydrocarbons and *n*-alkanes are analysed and quantified. The determination of individual compound concentrations enables to assess even the slightest compositional alterations, which would be not obvious if only conventional compound ratios are considered. This study suggests a new molecular biodegradation parameter, the MEAN DEGRADATIVE LOSS (MDL), which can be used to avoid misinterpretations of microbial caused alterations in petroleum reservoirs. For instance, the calculation of the MDL shows that contrary to conventional molecular biodegradation tools, some crude oils from the Norwegian sample set are less biodegraded than various samples from Angola. By use of another molecular parameter that is proposed in this study, the DEGRADATIVE LOSS (DL), it is shown that in each biodegraded petroleum reservoir the degradation patterns are different, which likely reflects the occurrence of different microbial consortia in the subsurface. Additionally, this study denominates the crude oil constituents which are mainly responsible for the observed decrease in API gravity during petroleum biodegradation. It is also demonstrated how the API gravity can be inferred directly from the molecular composition of biodegraded crude oils.

In addition to the description and discussion of the new biodegradation concept, this study also suggests that the quantitative abundance of crude oil constituents affects relative degradation rates during biodegradation. Based on the investigation of aromatic hydrocarbons it is discussed that mainly the compound concentrations of substrates control the bioavailability in terms of abundance. Obviously, other properties such as the water solubility and the molecular structure of the specific compound have less influence on relative biodegradation rates than the quantitative abundance. This leads to the interpretation that dependent on the quantitative availability of a substrate, those microbial communities develop in reservoirs that are capable to degrade the most abundant substrates. Once the crude oil composition changes, it appears reasonable that also the microbial community changes, as it is well-known from common biocenoses. Hence, the degradation patterns in individual petroleum reservoirs will be different in response to the specific petroleum reservoir properties such as the different crude oil compositions.

The study shows that also stable carbon isotopes can be used to quantify individual substrate depletions in crude oils. However, for this purpose it is necessary to pre-establish even the slightest compositional variances of, e.g., the source rock organic matter which obviously leads to differences in the compound-specific carbon isotope ratios. The use of compound-specific carbon isotopes to assess biodegradation is therefore restricted to crude oil samples which are characterised by a high compositional homogeneity due to source rock organofacies and source rock lithology. Interestingly, minor variances of the thermal maturity seem to have no significant effect on the compound-specific carbon isotope ratios. Because carbon isotopic compositions of crude oils are not significantly affected by other in-reservoir alteration processes, such as evaporative fractionation and water washing, the clear carbon isotopic fractionation of light hydrocarbons in samples from Angola and Norway could solely be attributed to biodegradation. This illustrates that the combined evaluation of molecular and isotopic compositions enables a detailed assessment of processes that are active in a petroleum reservoir.

In contrast to the stable carbon isotopes, the compound-specific hydrogen isotopic compositions of crude oils are significantly affected by numerous other fractionation processes than biodegradation. Such fractionation processes occur prior, during and after the deposition of the organic matter. To date, it appears not suitable to assess the extent of biodegradation via δD ratios, because several impacts, such as thermal maturity and hydrogen exchange reactions, on hydrogen isotopic compositions are not yet completly deciphered. However, it would be possible to assess petroleum biodegradation via δD ratios if every individual process that affects the hydrogen isotopic composition can be quantified. Then, biodegradation-related fractionation could be re-calculated and assessed similar to the approach that is discussed here for the carbon isotopic compositions. However, the present study shows how generalised concepts can be used to quantify the various molecular and isotopic alterations occurring in biodegraded petroleum reservoirs.

6 References

AECKERSBERG, F.; BAK, F. WIDDEL, F. (1991): Anaerobic oxidation of saturated hydrocarbons to CO_2 by a new type of sulfate-reducing bacterium. *Achieves of Microbiology, 156, 5-14.*

AITKEN, C.M. JONES, D.M. LARTER, S.R. (2004): Anaerobic hydrocarbon biodegradation in deep subsurface oil reservoirs. *Nature, 431, 291-294.*

ALEXANDER, R., KAGI, R.I., SHEPPARD, P.N. (1983): Relative abundance of dimethylnaphthalene isomers in crude oils. *Journal of Chromatography, 267, 367-372.*

ALEXANDER, R., KAGI, R.I., LARCHER, A.V. (1984): Clay catalysis of alkyl hydrogen exchange reactions – reaction mechanisms. *Organic Geochemistry 6, 755–760.*

ALEXANDER, R.; KAGI, R.I.; ROWLAND, S.J.; SHEPPARD, P.N.; CHIRILA, T.V. (1985): The effects of thermal maturity on distributions of dimethylnaphthalenes and trimethylnaphthalenes in some Ancient sediments and petroleums. *Geochimica et Cosmochimica Acta, 49, 385-395.*

ANNWEILER, E., MATERNA, A., SAFINOWSKI, M., KAPPLER, A., RICHNOW, H.H., MICHAELIS, W., MECKENSTOCK, R.U. (2000): Anaerobic degradation of 2-methylnaphthalene by a sulphate-reducing enrichment culture. *Environmental Microbiology, 66, 5329-5333.*

ANNWEILER, E.; MICHAELIS, W.; MECKENSTOCK, R.U. (2001): Anaerobic cometabolic conversion of benzothiophene by a sulfate-reducing enrichment culture and in a tar-oil-contaminated aquifer. *Applied and Environmental Microbiology., 67, 5077-5083.*

BAILEY, N. JOBSON, A.M., ROGERS, M. (1973): Bacterial degradation of crude oil. Comparison of field and experiment data. *Chemical Geology, 11, 203-221.*

BAKR, M.M.Y. & WILKES, H. (2002): The influence of facies and depositional environment on the occurrence and distribution of carbazoles and

benzocarbazoles in crude oils: a case study from the Golf of Suez, Egypt. *Organic Geochemistry, 33, 561- 580.*

BARSON, D., BACHU, S. & ESSLINGER, P. (2001): Flow systems in the Mannville Group in the east-Central Athabasca area and implications for steam-assisted gravity drainage (SAGD) operations for *in situ* bitumen production. *Bulletin of Canadian Petroleum Geology,* 49, 376–392.

BASKIN, D.K. & JONES, R.W. (1993): Prediction of oil gravity prior to drill-stem testing in Monterey formation reservoirs, offshore California. *American Association of Petroleum Geologists Bulletin, 77/9, 1479-1487.*

BASTIN, E.; GREER, F.; MERRIT, C.; MOULTON, G. (1926): The presence of sulphate reducing bacteria in oil field waters. *Science, 63, 21-24.*

BEHAR, F.; DE BARROS PENTEADO, H.L.; LORANT, F.; BUDZINSKI, H. (2006) : Study of biodegradation processes along the Carnaubais trend, Potiguar Basin (Brasil) – Part 1. *Organic Geochemistry, 37, 1042-1051.*

BEMENT, W.O.; MCNEIL, R.I.; LIPPINCOTT, R.G. (1996): Predicting oil quality from sidewall cores using PFID, TEC and NIR analytical techniques in sandstone reservoirs, Rio Del Rey Basin, Cameroon. *Organic Geochemistry, 24, 1173-1178.*

BLANC, P. & CONNAN, J. (1994): Crude oils in reservoirs: the factors influencing their composition. *American Association of Petroleum Geologists Memoir, 60 237-247.*

BOREHAM, C. J.; DOWLING, L.M.; MURRAY, A.P. (1995): Biodegradation and maturity influences on n-alkane isotopic profiles in terrigeneous sequences. *Organic Geochemistry: Developments and Applications to Energy, Climate, Environment and Human History. Selected Paper of the 7th International Meeting on Organic Geochemistry, 539-541.*

BRICE, S.E., COCHRAN, M.D., PARDO, G., EDWARDS, A.D. (1982): Tectonics and sedimentation of the South Atlantic rift sequence: Cabinda, Angola. In: Watkins, J.S. & Drake, C.L. (Eds.), Studies in continental margin geology, *American Association of Petroleum Geologists Memoir, 34, 5-18.*

BROOKS, P.W. (1986): Unusual biological marker geochemistry of oils and possible source rocks, offshore Beaufort Mackenzie Delta, Canada. *Organic Geochemistry, 10, 401-406.*

BUDZINSKI, H.; GARRIGUES, P.; CONNAN, J.; DEVILLERS, J.; DOMINE, D.; RADKE, M.; OUDIN, J.-L. (1995): Alkylated phenanthrene distributions as maturity and origin indicators in crude oils and rock extracts. *Geochimica et Cosmochimica Acta, 59, 2043-2056.*

BUDZINSKI, H.; RAYMOND, N.; NADALIG, T.; GILEWICZ, M.; GARRIGUES, P.; BERTRAND, J.C.; CAUMETTE, P. (1998): Aerobic biodegradation of alkylated aromatic hydrocarbons by a bacterial community. *Organic Geochemistry, 28, 337-348.*

CHAKHMAKHCHEV, A. & SUZUKI, N. (1995): Aromatic sulphur compounds as maturity indicators for petroleums from the Buzuluk depression, Russia. *Organic Geochemistry, 23, 617-625.*

CHAKHMAKHCHEV, A.; SUZUKI, N.; TAKAYAMA, K. (1997): Distribution of alkylated dibenzothiophenes in petroleum as a tool for maturity assessments. *Organic Geochemistry, 26, 483-490.*

CHUNG, H.M., ROONEY, M.A., TOON, M.B., CLAYPOOL, G.E. (1992): Carbon isotope composition of marine crude oils. AAPG Bulletin, 76, 1000-1007.

CLAYTON, C. J. (1991): Effect of maturity on carbon isotope ratios of oils and condensates. *Organic Geochemistry, 17, 887-899.*

COATES, J.D.; ANDERSON, R.T.; LOVELY, D.R. (1996): Oxidation of polycyclic aromatic hydrocarbons under sulfate-reducing conditions. *Applied and Environmental Microbiology, 62, 1099-1101.*

COATES, J.D.; CHAKRABORTY, R.; MCINERNEY, M.J. (2002): Anaerobic benzene biodegradation – a new era. *Research in Microbiology, 153, 621-628.*

COLE, G.A., REQUEJO, A.G., ORMEROD, D., YU, Z., CLIFFORD, A. (2000): Petroleum Geochemical Assessment of the Lower Congo Basin. *In: Mello, M.R. & Katz, J. (eds.), Petroleum systems of South Atlantic margins. American Association of Petroleum Geologists Mem., 73, 325-339.*

COLLISTER, J.W., SUMMONS, R.E., LICHTFOUSE, E., HAYES, J. M. (1991): An isotopic biogeochemical study of the Green River oil shale. *Organic Geochemistry, 19, 265-276.*

CONNAN, J. (1984): Biodegradation of crude oils in reservoirs. *In : Brooks, J. & Welte, D.H. (Eds.), Advances in Petroleum Geochemistry. Academic Press, London, pp. 299-330.*

CRAIG, H. (1961): Isotopic variations in meteoric waters. *Science, 133, 1702-1703.*

DAVIS, J. & YARBROUGH, H. (1965): Anaerobic oxidation of hydrocarbons by idesulfovibrio desulvuricans. *Chemical Geology, 1, 137-144.*

DAWSON, D., GRICE, K., AND ALEXANDER, R. (2005): Effect of maturation on the indigenous δD signatures of individual hydrocarbons in sediments and crude oils from the Perth Basin (Western Australia). *Organic Geochemistry, 36, 95-104.*

DAWSON, D., GRICE, K., ALEXANDER, R., EDWARDS, D. (2007): The effect of source and maturity on the stable isotopic compositions of individual hydrocarbons in sediments and crude oils from the Vulcan Sub-basin, Timor Sea, Northern Australia. *Organic Geochemistry, 38, 1015-1038.*

DEPAUW, G.A. & FROMENT, G.F. (1997): Molecular analysis of the sulphur components in a light cycle oil of a catalytic cracking unit by gas chromatography with mass spectrometric and atomic emission detection. *Journal of Chromatography A, 761, 231-247.*

DIDYK, B., SIMONEIT, B.R.T., BRASSELL, S.C., EGLINTON, G. (1978): Organic geochemical indicators of palaeoenvironmental conditions of sedimentation. *Nature, 272, 216– 222.*

DIXON, J.; DIETRICH, J.R.; MCNEIL, D.H.; MCINTYRE, D.J.; SNOWDON, L.R.; BROOKS, P. (1985): Geology, biostratigraphy and organic geochemistry of Jurassic to Pleistocene strata, Beaufort-Mackenzie area, northwest Canada. *Course Notes, Canadian Society of Petroleum Geologists, Calgary, 65pp.*

DOUST, H. & OMATSOLA, E. (1990): Niger Delta. *In: Divergent/passive margin basins. (J.D. Edwards & P.A. Santagrossi, Eds.) American Association of Petroleum Geologists Memoir, 48, 239-248.*

FISHER, S.J.; ALEXANDER, R.; KAGI, R.I. (1996): Biodegradation of alkylnaphthalenes in sediments adjacent to an off-shore petroleum production platform. *Polycyclic Aromatic Compounds, 11, 35-42.*

FISHER, S.J.; ALEXANDER, R.; KAGI, R.I.; OLIVER, G.A. (1998): Aromatic hydrocarbons as indicators of petroleum biodegradation in North Western Australian reservoirs. *In: Purcell, P.G. & purcell, R.R. (Eds.): The sedimentary basins of Western Australia 2. Proceedings of Petroleum Exploration Society Symposium, Perth, 185-194.*

FOSSEN, H. & HEESTHAMMER, J. (1998): Structural Geology of the Gullfaks Field, northern North Sea. *In: Coward, M.P., Johnson, H, Daltaban, T.S., Structural geology in reservoir characterization. Geological Society Special Publications, 127, 231-261, London: Geological Society.*

FOSSEN, H. & HEESTHAMMER, J. (2000): Possible absence of small faults in the Gullfaks Field, northern North Sea: implications for downscaling of faults in some porous sandstones. *Journal of Structural Geology, 22, 851-863.*

FRIMMEL, A., OSCHMANN, W., SCHWARK, L. (2004): Chemostratigraphy of the Posidonia Black Shale, SW Germany: I. Influence of sea-level variation on organic facies evolution. *Chemical Geology, 206, 199-230.*

FRITSCHE, W. & HOFRICHTER, M. (2000): Aerobic degradation by microorganisms. *In: Biotechnology, 11b, 146-164, (J. Klein, Ed.), John Wiley & Sons, New York.*

GEORGE, S.C., BOREHAM, C.J., MINIFIE, S.A., TEERMAN, S.C. (2002): The effect of minor to moderate biodegradation on C5 to C9 hydrocarbons in crude oils. *Organic Geochemistry 33, 1293-1317.*

GOODWIN, N.; PARK, P.; RAWLINSON, A. (1981): Crude oil biodegradation under simulated and natural conditions. *Advances in Organic Geochemistry, 650-658.*

GOOSSENS, H., DE LEEUW, J.W., SCHENCK, P.A., BRASSELL, S.C. (1984): Tocopherols as likely precursors of pristane in ancient sediments and crude oils. *Nature, 312, 440– 442.*

GORMLY, J.R., BUCK, S.P., CHUNG, H.M. (1994): Oil-source rock correlation in the North Viking Graben. *Organic Geochemistry, 22, 403-413.*

HALPERN, H. (1995): Development and application of light-hydrocarbons-based star diagrams. *American Association of Petroleum Geologists Bulletin, 79, 801-815.*

HARMS, G.; ZENGLER, K.; RABUS, R.; AECKERSBERG, F.; MINZ, D.; ROSELLO-MORA, R. ET AL. (1999): Anaerobic oxidation of o-xylene, m-xylene, and homologous alkylbenzenes by new types of sulfate-reducing bacteria. *Applied and Environmental Microbiology, 65, 999-1004.*

HARRINGTON, R.R.; POULSON, S.R.; DREVER, J.I.; COLBERG, P.J. S.; KELLY, E.F. (1999): Carbon isotope systematics of monoaromatic hydrocarbons: vaporization and adsorption experiments. *Organic Geochemistry, 30, 765-775.*

HARTGERS, W.A.; SINNINGHE DAMSTE, J.S.; DE LEEUW, J.W. (1992): Identification of C2-C4 alkylated benzenes in flash pyrolysates of kerogens, coals and asphalthenes. *Journal of Chromatography, 606, 211-220.*

HEAD, I.M., JONES, D.M., LARTER, S.R. (2003): Biological activity in the deep subsurface and the origin of heavy oil. *Nature 426, 344-352.*

HEAD, I.M.; JONES, D.M; RÖLING, W.F.M. (2006): Marine microorganisms make a meal of oil. *Nature Reviews Microbiology, 4/3, 173-182.*

HEESTHAMMER, J. & FOSSEN, H. (2001): Structural core analysis from the Gullfaks area, northern North Sea. *Marine and Petroleum Geology, 18, 411-439.*

HEESTHAMMER, J.; LANDRO, M.; FOSSEN, H. (2001): Use and abuse of seismic data in reservoir characterization. *Marine and Petroleum Geology, 18, 635-655.*

HILKERT, A.W.; DOUTHITT, C.B.; SCHLÜTER, H.J.; BRAND, W.A. (1999): Isotope ratio monitoring gas chromatography / mass spectrometry of D/H by high temperature conversion isotope ratio mass spectrometry. *Rapid Communications in Mass Spectrometry, 13, 1226-1230.*

HOEFS, J. (2004): Stable Isotope Geochemistry. 5th Ed., 244 p., Springer.

HORSFIELD, B.; DISKO, U.; LEISTNER, F. (1989): The micro-scale simulation of maturation: outline of a new technique and its potential applications. *Geologische Rundschau, 78/1, 361-374.*

HORSTAD, I.; LARTER, S.R.; DYPVIK, H.; AARGAARD, P.; BJORNVIK, A.M.; JOHANSSEN, P.E.; ERIKSEN, S. (1989): Degradation and maturity controls on oil field petroleum column heterogeneity in the Gullfaks field, Norwegian North Sea. *Organic Geochemistry, 16, 497-510.*

HORSTAD, I.; LARTER, S.R.; MILLS, N. (1992): A quantitative model of biological petroleum degradation within the Brent Group reservoir in the Gullfaks Field, Norwegian North Sea. *Organic Geochemistry, 19, 107-117.*

HORSTAD, I., LARTER, S.R.; MILLS, N. (1995): Migration of hydrocarbons in the Tampen Spur area, Norwegian North Sea: a reservoir geochemical evaluation. In: *The geochemistry of reservoirs (Eds.: Cubitt, J.M. & England, W.A.), 159-183, Geological Society London, Special Publication 86.*

HUANG, H. & MEINSHEIN, W.G. (1979): Sterols as ecological indicators. *Geochimica et Cosmochimica Acta, 43, 739-745.*

HUANG, H. & PEARSON, M.J. (1999): Source rock paleoenvironments and controls on the distribution of dibenzothiophenes in lacustrine crude oils, Bohai Bay Basin, eastern China. *Organic Geochemistry, 30, 1455-1470.*

HUANG, H.; BOWLER, B.F.J.; OLDENBURG, T.B.P.; LARTER, S.R. (2004): The effect of biodegradation on polycyclic aromatic hydrocarbons in reservoired oils from the Liaohe basin, NE China. *Organic Geochemistry, 35, 1619-1634.*

HUGHES, W.B.; HOLBA, A.G.; DZOU, L.I.P. (1995): The ratios of dibenzothiophene to phenanthrene and pristane to phytane as indicators of depositional environment and lithology of petroleum source rocks. *Geochimica et Cosmochimica Acta, 59, 3581-3598.*

HUNKELER, D., ARAVENA, R., BUTLER, B.J. (1999): Monitoring microbial dechlorination of tetrachloroethene (PCE) in groundwater using compound-specific stable carbon isotope ratios: microcosm and field studies. *Environmental Science and Technology, 33, 2733–2738.*

HUNT, J.M.; HUC, A.Y.; WHELAN, J.K. (1980): Generation of light hydrocarbons in sedimentary rocks. *Nature, 288, 688-690.*

KILLOPS, S.D. & KILLOPS, V.J. (2005): An introduction to organic geochemistry - 2nd ed. 393 *p., Blackwell Publishing.*

KOOPMANS, M.P.; LARTER, S.R.; ZHANG, C.; MEI, B.; WU, T.; CHEN, Y. (2002): Biodegradation and mixing of crude oils in Eocene Es3 reservoirs of the Liaohe basin, northeastern China. *American Association of Petroleum Geologists Bulletin, 86/10, 1833-1843.*

LAFARGUE, E. & LE THIEZ, P. (1996): Effect of water washing on light ends compositional heterogeneity. Organic Geochemistry 24, 1141-1150.

LANE, L.S. (2002): Tectonic evolution of the Canadian Beaufort Sea – Mackenzie Delta Region: A brief review. *Geological Survey of Canada, Contribution No. 2001143.*

LARTER, S., WILHELMS, A., HEAD, I., KOOPMANS, M., APLIN, A., DI PRIMIO, R., ZWACH, C., ERDMANN, M., TELNÆS, N. (2003): The controls on the composition of biodegraded oils in the deep subsurface-part 1: biodegradation rates in petroleum reservoirs. *Organic Geochemistry, 34, 601-613.*

LARTER, S., HUANG, H., ADAMS, J., BENNETT, B., JOKANOLA, O., OLDENBURG, T.B.P., JONES, M., HEAD, I., RIEDIGER, C., FOWLER, M. G. (2006): The controls on the composition of biodegraded oils in the deep subsurface: Part II — Geological controls on subsurface biodegradation fluxes and constraints on reservoir-fluid property prediction. *American Association of Petroleum Geologists Bulletin, 90/6, 921-938.*

LI, M.; HUANG, Y.; OBERMAJER, M.; JIANG, C.; SNOWDON, L.R.; FOWLER, M.G. (2001): Hydrogen isotopic compositions of individual alkanes as a new approach to petroleum correlation. Case studies from the Western Canada Sedimentary basin. *Organic Geochemistry, 32, 1387-1399.*

MAGOT, M., OLLIVIER, B., PATEL, B.K.C. (2000): Microbiology of petroleum reservoirs. *Antonie van Leeuwenhoek International Journal of General and Molecular Microbiology, 77, 103-116.*

MANCINI, S.A., LACRAMPE-COULOUME, G., JONKER, H., VAN BREUKELEN, B.M., GROEN, J., VOLKERING, F., SHERWOOD LOLLAR, B. (2002): Hydrogen isotopic enrichment: an indicator of biodegradation at a petroleum hydrocarbon contaminated field site. *Environmental Science and Technology, 36, 2464–2470.*

MANCINI, S.A.; ULRICH, A.C.; LACRAMPE-COULOUME, G.; SLEEP, B.; EDWARDS, E.A.; LOLLAR, B.S. (2003): Carbon and hydrogen isotopic fractionation during anaerobic biodegradation of benzene. *Applied and Environmental Microbiology., 69, 191-198.*

MANGO (1987): An invariance in the isoheptanes of petroleum. *Science 273, 514-517.*

MANGO, F.D. (1990A): The origin of light cycloalkanes in petroleum. *Geochimica et Cosmochimica Acta, 54, 23-27.*

MANGO, F.D. (1990B): The origin of light hydrocarbons in petroleum: A kinetic test of the steady-state catalytic hypothesis. *Geochimica et Cosmochimica Acta, 54, 1315-1323.*

MANSUY, L., PHILP, R.P., ALLEN, J. (1997): Source identification of oil spills based on the isotopic composition of individual components in weathered oil samples. *Environmental Science and Technology, 31, 3417-3425.*

MASTERSON, W.D.; DZOU, L.I.P.; HOLBA, A.G.; FINCANNON, A.L.; ELLIS, L. (2001): Evidence of biodegradation and evaporative fractionation in West Sak, Kuparuk and Prudhoe Bay field areas, North Slope, Alaska. *Organic Geochemistry, 32, 411-441.*

MCHARGUE, T.R. (1990): Stratigraphic Development of Proto-South Atlantic Rifting in Cabinda, Angola – A petroliferous Lake Basin. In: Katz, B.J. (ed.), Lacustrine basin exploration case studies and modern analogs. *American Association of Petroleum Geologists Memoir, 50, 307-326.*

MECKENSTOCK, R.U.; MORASCH, B.; WARTHMANN, R.; SCHINK, B.; ANNWEILER, E.; MICHAELIS, W.; RICHNOW, H.H. (1999): $^{13}C/^{12}C$ isotope fractionation of aromatic hydrocarbons during microbial degradation. *Environmental Microbiology, 5, 409-414.*

MECKENSTOCK, R.U.; MORASCH, B.; GRIEBLER, C.; RICHNOW, H.H. (2004): Stable isotope fractionation analysis as a tool to monitor biodegradation in contaminated aquifers. *Journal of Contaminant Hydrology, 75, 215-255.*

MILNER, C. W. D.; ROGERS, M.A.; EVANS, C.R. (1977): Petroleum transformations in reservoirs. *Journal of Geochemical Exploration, 7, 101–153.*

MÖSSNER, S.G.; LOPEZ DE ALDA, M.J.; SANDER, L.C.; LEE, M.L.; WISE, S.A. (1999): Gas chromatographic retention behaviour of polycyclic aromatic sulphur heterocyclic compounds, (dibenzothiophene, naphtho[b]thiophenes, benzo[b]naphthothiophenes and alkylsubstituted derivatives) on stationary phases of different selectivity. *Journal of Chromatography A, 841, 207-228.*

MOLDOWAN, J.M.; SEIFERT, W.K.; GALLEGOS, E.J. (1985): Relationship between petroleum composition and depositional environment of petroleum source rocks. A*merican Association of Petroleum Geologists Bulletin, 69, 1255-1268.*

MORASCH, B.; RICHNOW, H.H.; VIETH, A.; SCHINK, B.; MECKENSTOCK, R.U. (2004): Stable isotope fractionation caused by glycyl radical enzymes during bacterial degradation of aromatic compounds. *Applied and Environmental Microbiology, 70, 2935-2940.*

MURRAY, A.P., SUMMONS, R.E., BOREHAM, C.J., DOWLING, L.M. (1994): Biomarkers and n-alkane isotope profiles for Tertiary oils: relationship to source rock depositional setting. *Organic Geochemistry, 22, 521-542.*

NOVELLI, G. & ZOBELL, C. (1944): Assimilation of petroleum hydrocarbons by sulfate-reducing bacteria. *Journal of Bacteriology, 47, 447-448.*

ODDEN, W.; PATIENCE, R.L.; VAN GRAAS, G.W. (1998): Application of light hydrocarbons (C4-C13) to oil/source rock correlations: a study of light hydrocarbon compositions of source rocks and test fluids from offshore Mid-Norway. *Organic Geochemistry, 28, 823-847.*

ODDEN, W.; BARTH, T.;TALBOT, M. R. (2002): Compound-specific carbon isotope analysis of natural and artificially generated hydrocarbons in source rocks and petroleum fluids from offshore Mid-Norway. *Organic Geochemistry, 33, 47-65.*

OLAUSSEN, S. BECK, L., FALT, L. M., GRAUE, E., JACOBSEN, K. G., MALM, O. A. SOUTH, D. (1992): Gullfaks Field - Norway, East Shetland Basin, northern North Sea. *In: Foster, N. H. & Beaumont, E. A. (eds.): Structural traps; VI, 55-83.*

OLDENBURG, T.B.P., WILKES, H., HORSFIELD, B., VAN DUIN, A.C.T., STODDART, D., WILHELMS, A. (2002): Xanthones - novel aromatic oxygen-containing compounds in crude oils. *Organic Geochemistry, 33, 595-609.*

OWOYEMI, A., O. & WILLIS, B. J. (2006): Depositional patterns across syndepositional normal faults, Niger Delta, Nigeria. *Journal of Sedimentary Research, 76, 346-363.*

PALMER, S.E. (1993): Effect of biodegradation and water washing on crude oil composition. *In: Engel, M.H. & Macko, S.A. (Eds.), Organic Geochemistry. Plenum Press, New York, pp. 511-533.*

PATTON, T.L., MOUSTAFA, A.R.; NELSON, R.A., ABDINE, A.S. (1994): Tectonic evolution and structural setting of the Gulf of Suez Rift. *In: Landon, S.M. (Ed.), Interior Rift Basins, American Association of Petroleum Geologists Memoir, 59, 9-56.*

PENDENTCHOUK, N.; FREEMAN, K.H.; HARRIS, N.B.; CLIFFORD, D.J.; GRICE, K. (2004): Sources of alkylbenzenes in Lower Cretaceous lacustrine source rocks, West African rift basin. *Organic Geochemistry, 35, 33-45.*

PENDENTCHOUK, N., FREEMAN, K.H., AND HARRIS, N.B. (2006): Different response of dD values of n-alkanes, isoprenoids, and kerogen during thermal maturation. *Geochimica et Cosmochimica Acta, 70: 2063-2072.*

PETERS, K.E. & MOLDOWAN, J.M. (1993): The Biomarker Guide: interpreting molecular fossils in petroleum and ancient sediments. - *363 p., New Jersey (Prentice Hall).*

PETERS, K.E., MOLDOWAN, J.M., MCCAFFREY, M.A., FAGO, F.J. (1996): Selective biodegradation of extended hopanes to 25-norhopanes in petroleum reservoirs. Insights from molecular mechanics. *Organic Geochemistry 24, 765-783.*

PETERS, K.E.; FRASER, T.H.; AMRIS, W.; RUSTANO, B.; HERMANTO, E. (1999): Geochemistry of Crude Oils from Eastern Indonesia. *The American Association of Petroleum Geologists Bulletin, 83, 1927-1942.*

PETERS, K.E.; WALTERS, C.C.; MOLDOWAN, J.M. (2005): The Biomarker Guide - 2nd ed. *1155 p., Cambridge University Press.*

PHILP, R.P. & GILBERT, T.D. (1986): Biomarker distributions in oils predominantly derived from terrigeneous source material. *In: Advances in Organic Geochemistry 1985, Eds. Leythaeuser, D. & Rullkötter, J., Pergamon Press, 73-84.*

POND, K.L., HUANG, Y., WANG, Y., KULPA, C.F. (2002): Hydrogen Isotopic Composition of Individual n-Alkanes as an Intrinsic Tracer for Bioremediation and Source Identification of Petroleum Contamination. *Environmental Science and Technology, 36, 724-728.*

PRICE, L.C. (1976): Aqueous solubility of Petroleum as applied to its origin and primary migration. *American Association of Petroleum Geologists Bulletin, 60, 213-244.*

RABUS, R.; FUKUI, M.; WILKES, H.; WIDDEL, F. (1996): Degradative capacities and 16S rRNA-targeted whole-cell hybridization of sulphate reducing bacteria in an anaerobic enrichment culture utilizing alkylbenzenes from crude oil. *Applied and Environmental Microbiology, 62, 3605-3613.*

RADKE, M.; WILLSCH, H.; WELTE, D.H. (1980): Preparative Hydrocarbon Group Type Determination by Automated Medium Pressure Liquid Chromatography. *Analytical Chemistry, 52, 406-411.*

RADKE, M. & WELTE, D.H.(1981): The Methylphenanthrene Index (MPI): A maturity para- meter based on aromatic hydrocarbons. *In: Advances in Organic Geochemistry (Bjorey, M. et al., eds.) 504-512, J. Wiley 8 Sons, Chichester (1983).*

RADKE, R.; WELTE, D.H.; WILLSCH, H. (1982): Geochemical study on a well in the Western Canada Basin: Relation of aromatic distribution pattern to maturity of organic matter. *Geochimica et Cosmochimica Acta, 46, 1-10.*

RADKE, M: WELTE, D.H.; WILLSCH, H. (1986): Maturity parameters based on aromatic hydrocarbons: Influence of the organic matter type. *Organic Geochemistry, 10, 51-63.*

RADKE, M. (1988): Application of aromatic compounds as maturity indicators in source rocks and crude oils. *Marine and Petroleum Geology, 5, 224-236*

RADKE, M. & WILLSCH, H. (1994): Extractable alkyldibenzothiophenes in Posidonia Shale (Toarcian) source rocks: relationship of yields to

petroleum formation and expulsion. *Geochimica et Cosmochimica Acta, 58, 5223-5244.*

RADKE, J., BECHTEL, A., GAUPP, R., PUTTMANN, W., SCHWARK, L., SACHSE, D., AND GLEIXNER, G. (2005): Correlation between hydrogen isotope ratios of lipid biomarkers and sediment maturity. *Geochimica et Cosmochimica Acta, 69, 5517-5530.*

RICHNOW, H.H.; ANNWEILER, E.; MICHAELIS, W.; MECKENSTOCK, R.U. (2003): Microbial in situ degradation of aromatic hydrocarbons in a contaminated aquifer monitored by carbon isotope fractionation. *Journal of Contaminant Hydrology, 65, 101-120.*

ROADIFER, R.E. (1987): Size distributions of the world's largest known oil and tar accumulations, in R. F. Meyer, ed., Exploration for heavy crude oil and natural bitumen. *American Association of Petroleum Geologists Studies in Geology, 25, 3-23.*

ROBERTS, A.M.; YIELDING, G., BADLEY, M.E. (1990): A kinematic model for the orthogonal opening of the Late Jurassic North Sea rift system, Denmark-Mid Norway. *In: Blundell, D.J. & Gibbs, A.D., Tectonic evolution of the North Sea rifts, 180-199, Oxford, Clarendon Press.*

ROBISON, V.D. (1995): Source rock characterisation of the Late Cretaceous Brown Limestone of Egypt. *In: Katz, B. (Ed.), Petroleum Source Rocks. Springer, Heidelberg, 265-281.*

ROONEY, M.A.; VULETICH, R.; GRIFFITH, C.E. (1998): Compound-specific isotope analysis as a tool for characterizing mixed oils: an example from the West of Shetlands area. *Organic Geochemistry, 29, 241-254.*

ROSENFELD, W. (1947): Anaerobic oxidation of hydrocarbons by sulfate-reducing bacteria. *Journal of Bacteriology, 54, 664-665.*

ROWLAND, S.J.; ALEXANDER, R.; KAGI, R.I.; JONES, D.M.; DOUGLAS, A.G. (1986): Microbial degradation of aromatic components of crude oils: A comparison of laboratory and field observations. *Organic Geochemistry, 9, 153-161.*

RULLKÖTTER, J.; MEYERS, P.A.; SCHAEFER, R.G.; DUNHAM, K.W. (1986): Oil generation in the Michigan Basin: A biological marker carbon and isotope approach. *Organic Geochemistry, 10, 359-375.*

SANTAMARIA-OROZCO, D.; HORSFIELD, B.; DI PRIMIO, R.; WELTE, D.H. (1998): Influence of maturity on distributions of benzo- and dibenzothiophenes in Tithonian source rocks and crude oils, Sonda de Campeche, Mexico. *Organic Geochemistry, 28, 423-439.*

SANTOS NETO, E.V. & HAYES, J.M. (1999): Use of hydrogen and carbon stable isotopes characterising oils from the Potiguar Basin (onshore), Northeastern Brazil. *American Association of Petroleum Geologists Bulletin, 83, 496-518.*

SCHIMMELMANN, A., LEWAN, M.D., WINTSCH, R.P. (1999): D/H isotope ratios of kerogen, bitumen, oil, and water in hydrous pyrolysis of source rocks containing kerogen types I, II, IIS, and III. *Geochimica et Cosmochimica Acta 63, 3751–3766.*

SCHIMMELMANN, A.; SESSIONS, A.L.;BOREHAM, C.J.; EDWARDS, D.S.; LOGAN, G.A.; SUMMONS, R.E. (2004): D/H ratios in terrestrially sourced petroleum systems. *Organic Geochemistry, 35, 1169-1195.*

SCHOELLKOPF, N.B. & PATTERSON, B.A. (2000): Petroleum Systems of Offshore Cabinda, Angola. In: Mello, M.R. & Katz, J. (eds.), Petroleum systems of South Atlantic margins. *American Association of Petroleum Geologists Memoir, 73, 361-376.*

SCHULTZ, K.I. (1994): Structure and stratigraphy of the Gulf of Suez, Egypt. In: Landon, S.M. (Ed.), Interior Rift Basins, *American Association of Petroleum Geologists Memoir Memoir, 59, 57-96.*

SESSIONS, A.L., BURGOYNE, T.W., SCHIMMELMANN, A., HAYES, J.M. (1999): Fractionation of hydrogen isotopes in lipid biosynthesis. *Organic Geochemistry 30, 1193–1200.*

SESSIONS, A.L., SYLVA, S.P., SUMMONS, R.E., AND HAYES, J.M. (2004): Isotopic exchange of carbon-bound hydrogen over geologic timescales. *Geochimica et Cosmochimica Acta, 68, 1545-1559.*

SHAHIN, A.N. & SHEHAB, M.M. (1984): Petroleum generation, migration and occurrence in the Gulf of Suez, offshore South Sinai. *In: EGPC 7th Exploration and Production Conference, Cairo, Egypt, 121-153.*

SHAHIN, A.N.; HASSOUBA, A.H.; SHARAF, L.M. (1994): Assessment of petroleum potential in the northern Gulf of Suez. *In: EGPC 12th Exploration and Production Conference, Cairo, Egypt, 152-161.*

SHERWOOD LOLLAR, B., SLATER, G.F., SLEEP, B., WITT, M., KLECKA, G.M., HARKNESS, M., SPIVACK, J. (2001): Stable carbon isotope evidence for intrinsic bioremediation of tetrachloroethene and trichloroethene at area 6, Dover Air Force Base. *Environmental Science and Technology, 35, 261–269.*

SMALLWOOD, B.J.; PAUL PHILP, R.; ALLEN, J.D. (2002): Stable carbon isotopic composition of gasolines determined by isotope ratio monitoring gas chromatography mass spectrometry. *Organic Geochemistry, 33, 149-159.*

SNOWDON, L.R. (1987): Organic properties and source rock potential of two early Tertiary shales, Beaufort-Mackenzie Basin. *Bulletin of Canadian Petroleum Geology, 35, 212-232.*

SOFER, Z. (1984): Carbon Isotope Compostions of Crude Oils: Application to Source Depositional Environments and Petroleum Alteration. *American Association of Petroleum Geologists Bulletin, 68, 31-49.*

SOFER, Z.; REGAN, D.R.; MULLER, D.S. (1993): Sterane isomerization ratios of oils as maturity indicators and their use as an exploration tool, Neuquen Basin Argentina. In: *Actas del XII. Congreso de Geologico Argentino y Il Congreso de Exploracion de Hidrocarburos, Actas T°1, 407-411.*

SUN, Y., CHEN, Z., XU, S., CAI, P. (2005): Stable carbon and hydrogen isotopic fractionation of individual n-alkanes accompanying biodegradation: evidence from a group of progressively biodegraded oils. *Organic Geochemistry, 36, 225-238.*

TALUKDAR, S.C. & DOW, W.G. (1990): Geochemistry off oils provides optimism for deeper exploration in atlantic off Trinidad. *Oil and Gas Journal, 12, 118-122.*

TANG, J. & LERCHE, I. (1992): Analysis of the Beaufort-Mackenzie Basin, Canada: burial, thermal and hydrocarbon histories. *Marine and Petroleum Geology, 9, 510-525.*

TEN HAVEN, H.L., DE LEEUW, J.W., RULLKÖTTER, J. SINNINGHE DAMSTE, J.S. (1987): Restricted utility of the pristane/phytane ratio as a palaeoenvironmental indicator. *Nature, 330, 641-643.*

TEN HAVEN, H.L. (1996): Applications and limitations of Mango`s light hydrocarbon parameters in petroleum correlation studies. *Organic Geochemistry, 24, 957-976*

TISSOT, B.P. & WELTE, D.H. (1984): Petroleum Formation and Occurrence. *p. 699, Springer-Verlag, Berlin.*

THOMPSON, K.F.M. (1978): Light hydrocarbons in subsurface sediments. *Geochimica et Cosmochimica Acta, 43, 657-672.*

THOMPSON, K.F.M. (1983): Classification and thermal history of petroleum based on light hydrocarbons. *Geochimica et Cosmochimica Acta, 47, 303-316.*

THOMPSON, K.F.M. (1988): Gas-condensate migration and oil-fractionation in deltaic systems. *Marine and Petroleum Geology, 5, 237-245.*

VALLE, P.J., GJELBERG, J.G., HELLAND-HANSEN, W. (2001): Tectonostratigraphic development in the eastern Lower Congo Basin, offshore Angola, West Africa. *Marine and Petroleum Geology, 18, 909-927.*

VAN AARSSEN, B.G.K.; BASTOW, T.P.; ALEXANDER, R.; KAGI, R.I. (1999): Distributions of methylated naphthalenes in crude oils: indicators of maturity, biodegradation and mixing. *Organic Geochemistry, 30, 1213-1227.*

VIETH, A., KÄSTNER, M., SCHIRMER, M., WEISS, H., GÖDEKE, S., MECKENSTOCK, R.U., RICHNOW, H.H. (2005): Monitoring in-situ biodegradation of benzene and toluene by stable carbon isotope fractionation. *Environmental Toxicology and Chemistry, 24, 51–60.*

VIETH, A. & WILKES, H. (2006): Deciphering biodegradation effects on light hydrocarbons in crude oils using their stable carbon isotopic composition: a case study from the Gullfaks oil field, offshore Norway. *Geochimica et Cosmochimica Acta, 70, 651-665.*

VOLKMAN, J.K.; ALEXANDER, R.; KAGI, R.I.; ROWLAND, S.J.; SHEPPARD,, P.N. (1984): Biodegradation of aromatic hydrocarbons in crude oils from the Barrow Subbasin of western Australia. *Organic Geochemistry, 6, 619-632.*

WAMMER, K.H., PETERS, C.A. (2005): Polycyclic Aromatic Hydrocarbon Biodegradation Rates: A Structure-Based Study. *Environmental Science and Technology, 39, 2571-2578.*

WANG, Y., AND HUANG, Y. (2003): Hydrogen isotopic fractionation of petroleum hydrocarbons during vaporization: implications for assessing artificial and natural remediation of petroleum contamination. *Applied Geochemistry, 18, 1641-1651.*

WELTE, D.H.; KRATOCHVIL, H.; RULLKÖTTER, J.; LADWEIN, H.; SCHAEFER, R.G. (1982): Organic Geochemistry of crude oils from the Vienna Basin and an assessment of their origin. *Chemical Geology, 35, 33-68.*

WENGER, L.M., DAVIS, C.L., ISAKSEN, G.H. (2001): Multiple controls on petroleum biodegradation and impact on oil quality. *Society of Petroleum Engineers Paper 71450.*

WEVER, H.E. (2000): Petroleum and source rock characterization based on C_7 star plots: Examples from Egypt. *American Association of Petroleum Geologists Bulletin 84, 1041-1054.*

WIDDEL, F. & RABUS, R. (2001): Anaerobic biodegradation of saturated and aromatic hydrocarbons. *Current Opinion in Biotechnology, 12, 259-276*

WILKES, H., CLEGG, H., DISKO, U., WILLSCH, H., HORSFIELD, B. (1998): Fluoren-9-ones and carbazoles in the Posidonia Shale, Hils Syncline, northwest Germany. *Fuel, 77, 657-668.*

WILKES, H., BOREHAM, C., HARMS, G., ZENGLER, K., RABUS, R. (2000): Anaerobic degradation and carbon isotopic fractionation of alkylbenzenes in crude oil by sulphate-reducing bacteria. *Organic Geochemistry 31, 101-115.*

WILKES, H., RABUS, R., FISCHER, T., ARMSTROFF, A., BEHRENDS, A., WIDDEL, F. (2002): Anaerobic degradation of *n*-hexane in a denitrifying bacterium: Further degradation of the initial intermediate (1-methylpentyl)succinate via C-skeleton rearrangement. *Archives of Microbiology 177, 235-243.*

XIONG, Y., GENG, A., PAN, C., LIU, D., PENG, P. (2005): Characterization of the hydrogen isotopic composition of individual *n*-alkanes in terrestrial source rocks. *Applied Geochemistry, 20, 455–464.*

YU, A.; Cole, G.; Grubitz, G. (2002): How to predict biodegradation risk and reservoir fluid quality. *World Oil, 223/4, 1-5.*

ZENGLER, K.; RICHNOW, H.H.; ROSSELLÓ-MORA, R.; MICHAELIS, W.; WIDDEL, F. (1999): Methane formation from long-chain alkanes by anaerobic microorganisms. *Nature, 401, 266-269.*

ZIEGLER, T. (2003): Geological overview of the Gulf of Guinea and prospectivity of the JDZ. Presentation on the Nigeria - São Tomé and Príncipe 2003 JDZ Licensing Round. Online-publication: http://www.nigeriasaotomejda.com/PDFs/Roadshow%20Presentations/Regional%20Geology.pdf

ZWANK, L., BERG, M., ELSNER, M., SCHMIDT, T.C., SCHWARZENBACH, R.P., HADERLEIN, S.B. (2005): New evaluation scheme for two-dimensional isotope analysis to decipher biodegradation processes: application to groundwater contamination by MTBE. *Environmental Science and Technology, 39, 1018–1029.*

7 Appendix

no.	compound	abbreviation	no.	compound	abbreviation
1	*iso*-pentane	*i*-C_5	34	2-methylheptane	2-mhep
2	*n*-pentane	*n*-C_5	35	3-methylheptane	3-mhep
3	2,2-dimethylbutane	2,2-dmb	36	*n*-octane	*n*-C_8
4	cyclopentane	cp	37	ethylcyclohexane	echex
5	2,3-dimethylbutane	2,3-dmb	38	meta+para -xylene	m+p-xylene
6	2-methylpentane	2-mp	39	2+4-methyloctane	2+4-mo
7	3-methylpentane	3-mp	40	3-methyloctane	3-mo
8	*n*-hexane	*n*-C_6	41	ortho-xylene	o-xylene
9	2,2-dimethylpentane	2,2-dmp	42	*n*-nonane	*n*-C_9
10	methylcyclopentane	mcp	43	*n*-decane	*n*-C_{10}
11	2,4-dimethylpentane	2,4-dmp	44	*n*-undecane	*n*-C_{11}
12	2,2,3 trimethylbutane	2,2,3-tmb	45	*n*-dodecane	*n*-C_{12}
13	benzene	b	46	*n*-tridecane	*n*-C_{13}
14	3,3-dimethylpentene	3,3-dmp	47	*n*-tetradecane	*n*-C_{14}
15	cyclohexane	chex	48	*n*-pentadecane	*n*-C_{15}
16	2-methylhexane	2-mhex	49	*n*-hexadecane	*n*-C_{16}
17	2,3-dimethylpentane	2,3-dmp	50	*n*-heptadecane	*n*-C_{17}
18	1,1 dimethylpentane	1,1-dmcp	51	pristane	Pr
19	3-methylhexane	3-mhex	52	*iso*-octadecane	*i*-C_{18}
20	*1,cis*,3-dimethylcyclopentane	c-1,3-dmcp	53	*n*-octadecane	*n*-C_{18}
21	*1, trans*,3-dimethylcyclopentane	t-1,3-dmcp	54	phytane	Ph
22	*1, trans*,2-dimethylcyclopentane	t-1,2-dmcp	55	*n*-nonadecane	*n*-C_{19}
23	*n*-heptane	*n*-C_7	56	*n*-icosane	*n*-C_{20}
24	methylcyclohexane	mchex	57	*n*-henicosane	*n*-C_{21}
25	1-*trans*-1,3-trimethylcyclopentane	1,1,3-tmcp	58	*n*-docosane	*n*-C_{22}
26	ethylcyclopentane	ecp	59	*n*-tricosane	*n*-C_{23}
27	2,5-dimethylhexane	2,5-dmhex	60	*n*-tetracosane	*n*-C_{24}
28	2,4-dimethylhexane	2,4-dmhex	61	*n*-pentacosane	*n*-C_{25}
29	1-*trans*-2,4-trimethylcyclopentane	1,2,4 tmcp	62	*n*-hexacosane	*n*-C_{26}
30	3,3-dimethylhexane	3,3-dmhex	63	*n*-heptacosane	*n*-C_{27}
31	1-*trans*-2,3-trimethylcyclopentane	1,2,3-tmcp	64	*n*-octacosane	*n*-C_{28}
32	2,3,4-trimethylpentane	2,3,4-tmp	65	*n*-nonacosane	*n*-C_{29}
33	toluene	t	66	*n*-tricontane	*n*-C_{30}

Table X- 1.: List of 66 light and saturated hydrocarbons, which were identified by thermovaporisation gas chromatography. Also given are abbreviations used in the chromatogram that is shown in Figure 20.

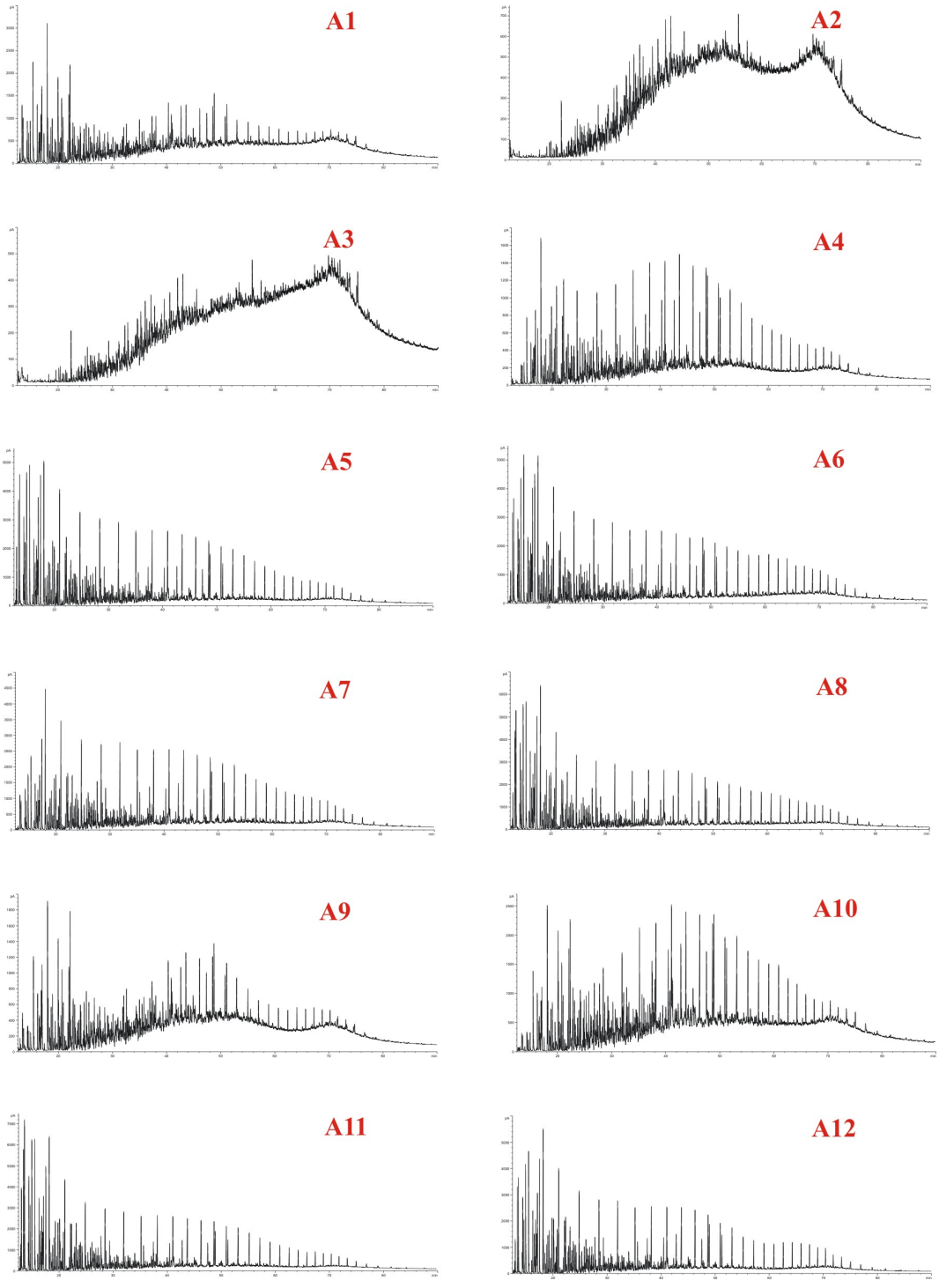

Fig. X- 1: Thermovaporisation chromatograms for crude oils A1 – A12 from Angola.

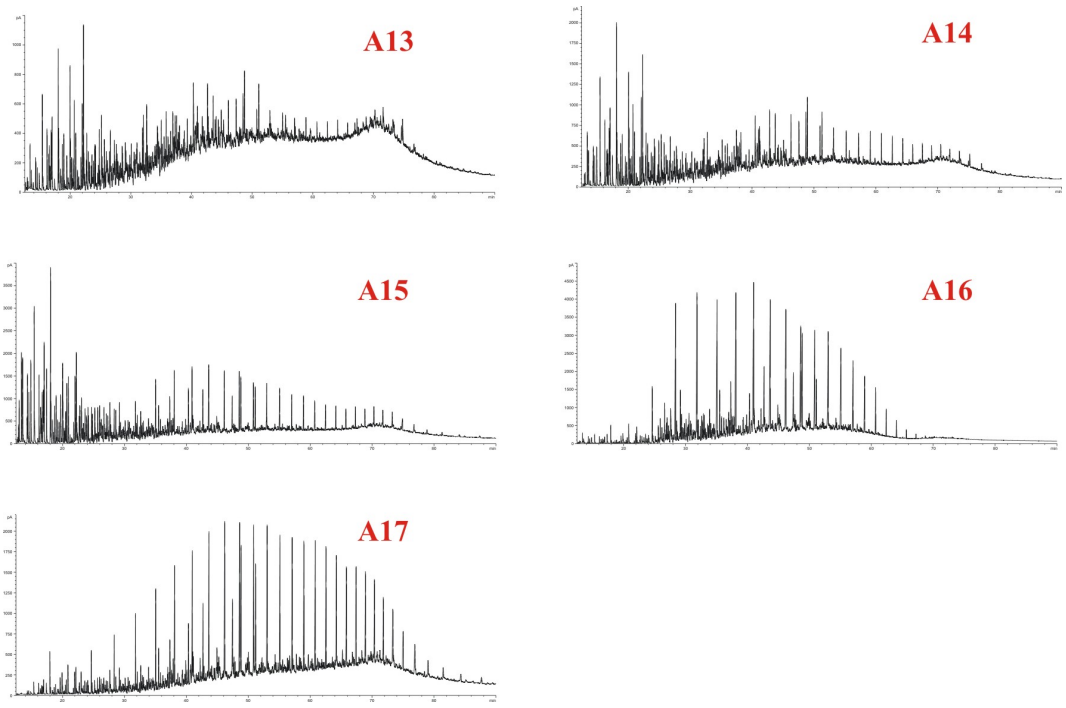

Fig. X- 2: Thermovaporisation chromatograms for crude oils A13 – A17 from Angola.

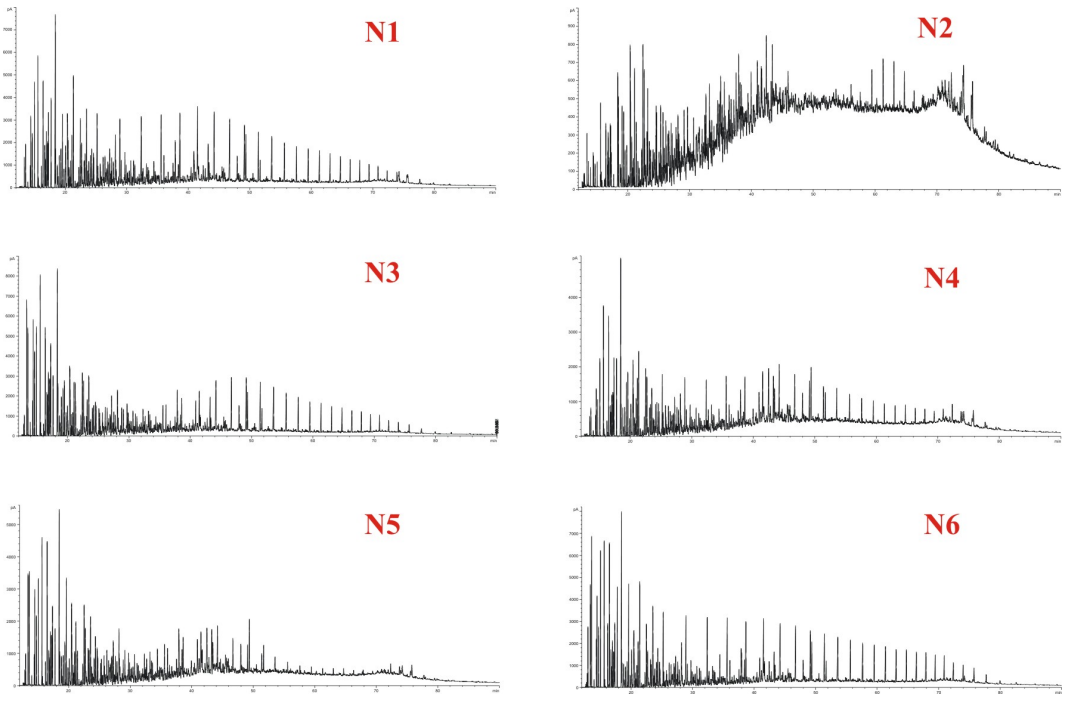

Fig. X- 3: Thermovaporisation chromatograms for crude oils N1 – N6 from Nigeria.

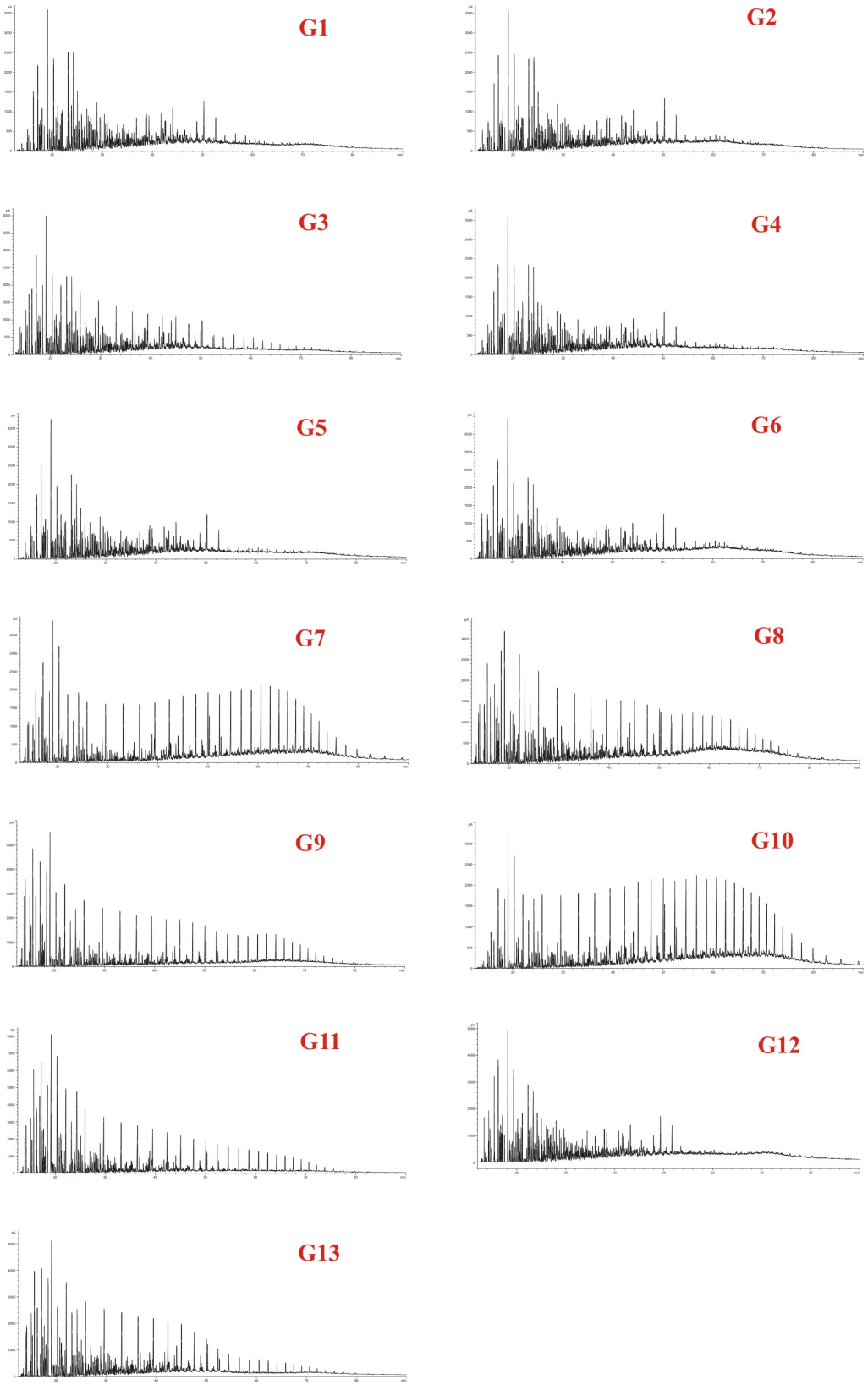

Fig. X- 4: Thermovaporisation chromatograms for crude oils G1 – G13 from Norway.

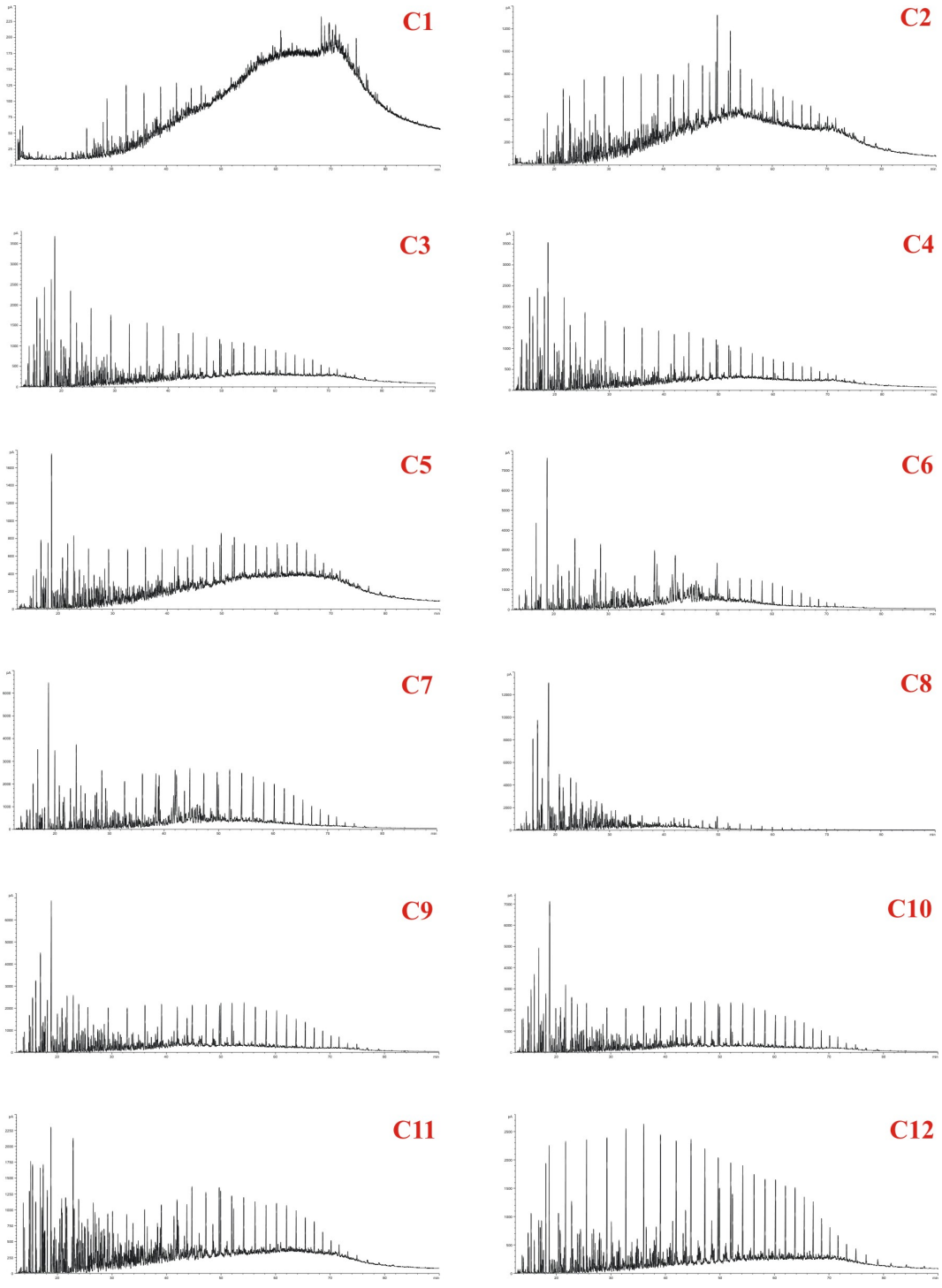

Fig. X- 5: Thermovaporisation chromatograms for crude oils C1 – C12 from Canada.

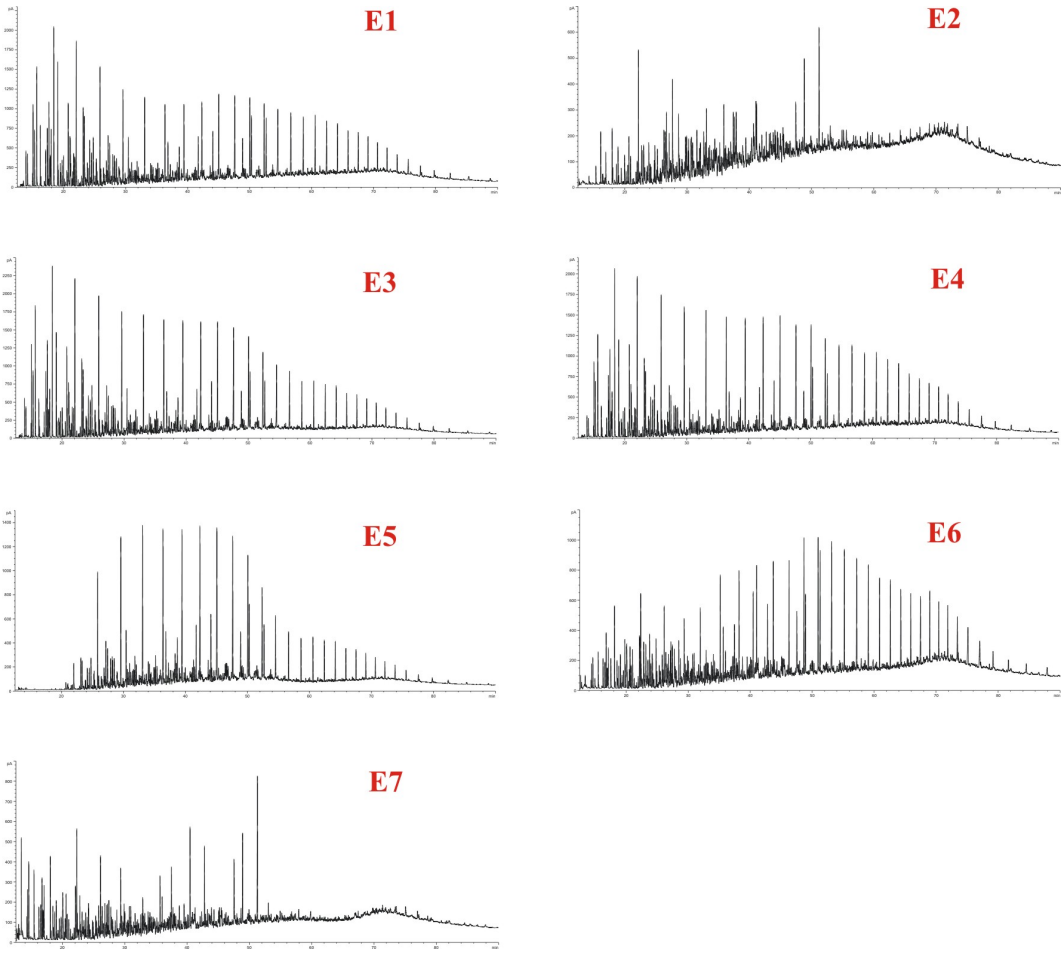

Fig. X- 6: Thermovaporisation chromatograms for crude oils E1 – E7 from Egypt.

compound	*i*-C5	*n*C5	2,2 dmb	cp	2,3 dmb	2 mp	3 mp	*n*C6	2,2 dmp	mcp	2,4 dmp	2,2,3 tmb	b
sample													
A1	710	733	61	210	298	556	516	782	55	1946	170	13	29
A2	0	0	0	0	0	0	0	0	0	0	0	0	0
A3	0	0	0	0	0	0	0	0	0	0	0	0	0
A4	55	66	3	32	48	205	220	326	14	919	52	2	40
A5	2935	4414	30	902	388	3041	2429	5243	15	5739	1013	465	569
A6	2366	3551	32	707	298	2699	2297	5132	9	6195	327	13	464
A7	817	952	30	286	167	1267	1027	2168	31	2878	153	10	450
A8	3558	4995	80	800	597	3509	2781	6366	56	7315	467	28	1144
A9	265	217	30	129	173	215	177	199	30	1041	119	8	12
A10	152	163	40	144	201	164	139	253	59	1211	116	19	32
A11	5752	7456	95	1133	696	4618	3253	7737	61	8169	661	31	1047
A12	3184	3861	61	678	523	3184	2583	5724	55	6807	346	12	711
A13	167	113	28	56	143	127	115	133	28	564	63	12	7
A14	453	418	46	149	270	426	368	537	58	1701	220	28	44
A15	1356	1643	46	416	364	1299	1128	2021	49	3689	303	31	169
A16	178	108	5	27	21	156	107	215	5	262	18	1	8
A17	7	6	1	10	3	42	44	56	4	169	14	1	30
G1	228	88	59	282	330	815	615	513	119	2715	308	17	130
G2	610	246	93	439	400	1101	803	669	116	3044	344	26	190
G3	1704	1828	202	762	853	3259	2237	5117	274	5677	662	46	1505
G4	599	368	100	488	429	1441	1052	1415	173	3629	410	27	419
G5	717	287	115	464	492	1568	1084	1126	165	3510	412	35	274
G6	1441	648	152	630	541	1812	1228	1152	151	3534	404	36	342
G7	1082	1618	96	314	311	1333	837	2864	66	1872	135	33	3310
G8	1156	1477	61	350	267	1744	1316	3398	61	2352	222	19	126
G9	3045	4172	234	522	793	3757	2396	7324	170	4423	393	52	1201
G10	121	277	25	121	137	643	442	1675	43	1205	100	16	2841
G11	2568	4171	287	699	1007	5111	3305	10677	249	7016	671	90	9624
G12	1134	304	137	660	389	1712	1174	567	165	3564	466	89	134
G13	2661	3614	292	885	819	4792	3244	9008	285	6074	575	48	2409
C1	0	0	0	0	0	0	0	0	0	0	0	0	0
C2	0	0	0	0	0	0	0	26	3	26	8	2	23
C3	454	910	44	350	170	1091	737	2611	52	2198	188	27	248
C4	627	1107	47	432	191	1207	811	2651	63	2316	179	29	256
C5	66	20	6	29	28	131	116	428	29	544	76	21	28
C6	526	28	96	154	287	968	728	179	102	1929	172	50	503
C7	428	281	71	276	207	833	586	929	66	2359	124	40	943
C8	586	432	792	1328	2289	839	578	982	79	18135	1537	326	145
C9	559	869	99	431	373	1908	1367	3201	109	4676	285	61	398
C10	1369	1528	157	562	514	2441	1736	3763	152	5418	327	59	649
C11	931	544	75	185	398	1324	1902	1820	141	1306	464	40	52
C12	231	269	52	52	124	744	485	1209	75	719	172	24	72
E1	508	658	22	55	240	1462	1050	2513	41	1223	200	10	144
E2	5	0	6	69	12	0	14	20	8	146	13	4	15
E3	714	787	35	40	289	2067	1509	3421	63	961	267	12	168
E4	400	421	21	13	180	1386	1048	2287	44	672	199	10	83
E5	0	0	0	0	0	0	0	0	0	0	0	0	0
E6	71	30	3	53	20	207	268	129	6	368	29	3	34
E7	554	39	5	58	150	336	581	30	4	599	47	3	23
N1	585	972	133	548	357	2029	1664	3488	137	5117	314	76	822
N2	*n.a*	*n.a*	*n.a*	*n.a*	*n.a*	*n.a*	*n.a*	*n.a*	*n.a*	*n.a*	*n.a*	*n.a*	*n.a*
N3	3614	2810	430	1105	723	3973	3052	4451	249	8016	530	88	522
N4	238	399	81	361	187	856	713	1554	89	2982	151	39	345
N5	1456	1615	157	500	292	1647	1284	2072	102	3341	184	45	560
N6	2249	3292	182	1290	366	2577	1826	4670	116	5649	237	35	2294

Table X- 2: Concentrations [µg/g oil] for light hydrocarbons (*iso*-pentane to benzene).

compound	3,3 dmp	chex	2 mhex	2,3 dmp	1,1 dmcp	3 mhex	c-1,3 dmcp	t-1,3 dmcp	t-1,2 dmcp	*n* C7
sample										
A1	43	1122	351	669	639	620	1051	1190	1835	768
A2	0	0	0	0	0	0	0	0	0	0
A3	0	0	0	0	0	0	0	0	0	0
A4	14	605	292	350	222	616	614	690	1372	1129
A5	39	3158	1838	1192	622	2935	2199	2460	5228	7133
A6	72	2943	1752	1231	644	2707	2275	2480	5250	6470
A7	34	1931	967	649	568	1804	1268	1229	2767	4202
A8	34	4496	2530	1161	1211	3381	2410	2581	4381	7956
A9	26	709	92	403	431	267	765	843	1205	109
A10	43	1048	119	559	671	286	904	1071	1222	266
A11	93	4607	2944	1013	1207	3713	2637	2705	4822	8230
A12	52	3629	2332	1076	1036	3240	2403	2415	4633	7456
A13	25	406	66	260	326	165	430	405	527	106
A14	57	1114	262	590	616	519	951	971	1467	594
A15	46	1820	774	844	674	1434	1507	1597	2861	2134
A16	5	202	94	71	45	147	112	119	217	422
A17	12	145	70	58	43	129	105	116	227	256
G1	107	4365	1343	1032	754	1462	1328	1294	2106	1296
G2	71	4557	1258	1078	711	1439	1239	1190	1983	1160
G3	282	8891	3142	1819	1350	3655	2127	2091	3328	7072
G4	117	5541	1702	1330	905	1965	1580	1477	2390	2644
G5	140	5582	1553	1187	858	1854	1538	1472	2389	1831
G6	119	5377	1432	1141	794	1732	1386	1286	2082	1673
G7	63	4614	963	332	255	1056	449	432	770	3668
G8	55	2925	1759	705	372	2152	854	819	1466	4969
G9	205	7427	2778	685	580	2850	1035	942	1568	8610
G10	56	3508	831	271	220	946	378	375	688	3410
G11	317	15079	5235	1253	1142	5200	1795	1787	2807	15546
G12	141	5047	1498	1181	776	1795	1450	1522	2266	1448
G13	205	10716	4087	1302	1131	4848	1660	1625	2948	12163
C1	0	0	0	0	0	0	0	0	0	0
C2	6	97	59	56	33	115	48	48	64	324
C3	54	3556	1306	582	452	1692	749	743	1298	4569
C4	52	3531	1165	550	438	1500	679	662	1191	3939
C5	34	1031	319	315	232	505	332	326	497	1096
C6	97	6196	617	427	554	1001	882	846	1726	73
C7	66	4964	797	291	380	884	701	698	1280	1450
C8	607	28970	740	4105	2868	977	6109	5851	11136	1530
C9	109	7857	1987	731	595	2253	1466	1473	2634	4634
C10	122	8708	2200	794	630	2428	1612	1592	2852	5542
C11	107	2105	1578	1209	755	2429	842	901	892	1821
C12	56	1251	1113	404	210	1320	336	323	580	3086
E1	32	772	1280	749	158	1886	697	690	1331	4096
E2	11	390	9	74	71	25	53	49	273	29
E3	46	670	1864	995	169	2574	742	645	1314	5681
E4	32	448	1383	850	140	2051	586	562	1029	4484
E5	0	0	0	0	0	0	0	0	0	17
E6	7	295	244	269	39	605	224	217	469	383
E7	6	301	157	325	39	576	273	274	498	37
N1	187	4685	2093	710	1112	2629	2041	2005	3422	5020
N2	*n.a.*	*n.a.*	*n.a.*	*n.a.*	*n.a.*	*n.a.*	*n.a.*	*n.a.*	*n.a.*	*n.a.*
N3	204	5850	2768	946	2000	3649	3296	3274	5407	3528
N4	94	3076	855	455	592	1092	1200	1193	2156	2261
N5	101	3835	959	517	665	1408	1320	1271	2113	1589
N6	102	6704	1705	515	781	1883	1456	1449	2615	5528

Table X- 3: Concentrations [µg/g oil] for light hydrocarbons (3,3-dimethyplpentane to *n*-heptane).

compound	mchex	1,1,3 tmcp	ecp	2,5 dmhex	2,4 dmhex	1,2,4 tmcp	3,3 dmhex	1,2,3 tmcp	2,3,4 tmp
sample									
A1	3691	1001	363	138	258	772	88	964	85
A2	0	0	0	0	0	0	0	0	0
A3	0	0	0	0	0	0	0	0	0
A4	2831	548	305	149	173	553	6	791	87
A5	8778	1050	1165	339	430	1351	43	2050	260
A6	8528	1168	1098	361	418	1398	38	2095	242
A7	7288	1144	571	291	338	982	75	1335	156
A8	12041	1731	933	434	532	1512	143	1951	218
A9	2223	732	290	85	172	616	18	743	99
A10	3070	989	356	136	288	882	33	903	122
A11	12614	1719	1021	456	584	1610	136	2094	224
A12	11347	1624	1061	393	534	1647	55	2221	283
A13	1212	523	154	8	112	374	23	445	76
A14	3112	940	340	153	257	785	63	905	132
A15	5887	1119	567	249	321	1004	73	1304	158
A16	728	96	50	30	37	95	7	127	26
A17	702	122	63	29	37	109	9	157	19
G1	10513	924	1092	397	684	1015	145	1205	219
G2	10076	810	1059	340	634	881	132	1056	173
G3	18552	1530	1539	684	1148	1612	271	1850	339
G4	12263	1102	1223	430	814	1209	215	1390	226
G5	11809	1019	1158	398	735	1141	165	1322	230
G6	10602	887	1135	260	684	985	164	1142	179
G7	9251	265	413	118	210	232	69	225	39
G8	6850	544	707	308	406	710	101	862	177
G9	15735	528	663	333	459	496	140	432	58
G10	8102	277	353	135	202	246	54	245	39
G11	32571	902	1130	775	1030	1008	267	785	63
G12	10304	889	1086	407	664	1001	158	1180	219
G13	21135	1268	1085	610	952	1111	221	1101	137
C1	0	0	0	0	0	0	0	0	0
C2	507	93	59	33	79	111	15	126	39
C3	7943	502	600	248	429	538	86	580	143
C4	7419	482	580	193	400	504	75	555	145
C5	2977	319	268	90	222	296	52	330	113
C6	22088	436	744	135	290	493	111	517	18
C7	17586	323	637	126	216	377	72	384	20
C8	83695	2977	4162	574	2353	4479	872	4328	187
C9	22720	687	1246	248	508	1004	139	1003	66
C10	24113	745	1254	340	553	1060	180	1069	82
C11	3998	986	332	459	807	1061	139	775	271
C12	4082	363	207	262	381	364	79	371	107
E1	3298	403	533	278	347	615	96	762	197
E2	517	145	32	4	16	168	22	324	72
E3	3373	482	545	360	447	762	40	927	223
E4	2609	416	468	272	374	647	52	763	189
E5	38	7	11	11	5	16	3	24	10
E6	1046	82	317	110	118	262	13	409	57
E7	906	81	314	113	134	278	20	402	59
N1	13862	1664	961	338	542	1505	187	1926	137
N2	*n.a.*	*n.a.*	*n.a.*	*n.a.*	*n.a.*	*n.a.*	*n.a.*	*n.a.*	*n.a.*
N3	17193	2635	1020	489	743	2263	237	2796	201
N4	7660	850	774	143	275	808	92	1611	95
N5	7550	870	814	152	270	857	86	1286	117
N6	13622	892	915	158	272	854	97	1164	72

Table X- 4: Concentrations [µg/g oil] for light hydrocarbons (methylcyclohexane to 2,3,4-trimethylpentane).

compound	t	2 mhep	3 mhep	*n* C8	echex	m/p-xylene	2+4 mo	3 mo	o-xylene	*n* C9	*n* C10	*n* C11
sample												
A1	272	487	2990	1398	1812	1299	257	634	502	606	601	515
A2	0	0	0	0	0	0	0	0	0	0	0	0
A3	0	0	0	0	0	0	0	0	0	0	0	0
A4	387	907	2078	2092	1416	1450	508	766	498	1761	1843	1805
A5	2255	4003	2563	8285	3381	4340	1727	2025	1522	7120	6548	6259
A6	2233	3751	2327	7675	4303	4018	1605	1967	1407	6579	5702	5434
A7	2150	2847	1577	6108	2913	4777	1413	1733	1479	5716	5560	5366
A8	3728	4168	2929	8709	3728	6568	1939	2296	2047	7168	6520	6178
A9	239	61	1953	809	1320	879	344	358	405	273	500	855
A10	205	179	3169	1373	2379	1499	179	583	913	827	1914	2003
A11	3380	4534	3074	8923	4097	6046	2103	2299	1944	7406	6541	6029
A12	2856	4252	2802	8828	4162	5201	1839	2120	1308	7467	6634	6308
A13	45	92	1224	573	769	397	20	280	295	184	321	486
A14	257	403	2850	1373	1937	1080	145	520	615	576	466	593
A15	874	1555	1232	2323	2388	1392	709	1162	695	1239	1169	1340
A16	73	293	142	923	392	433	290	459	184	2582	9815	11703
A17	110	276	151	658	535	609	170	249	217	825	1076	1440
G1	6161	2078	1397	2571	7586	9261	2168	1643	3803	2486	2261	1337
G2	6359	1901	1468	1969	6792	8762	1943	1417	3535	1443	1607	1008
G3	9833	4098	2803	9900	10650	12556	3717	2605	5024	8689	7962	6446
G4	7201	2422	1909	4111	8235	9933	2534	1836	3986	4027	3761	2603
G5	5721	1735	1333	2595	7592	8333	1780	1231	3753	2682	2687	1913
G6	5113	1487	1268	2233	6455	7338	1559	1184	3396	2301	2307	1652
G7	8093	1184	787	4341	2534	6231	1145	711	2018	4087	4241	4405
G8	2464	2399	1597	6219	4663	3633	2248	1465	1130	5227	4754	4341
G9	7056	2905	2202	9115	4313	7957	2396	1575	2128	8228	7390	6913
G10	7189	1353	879	4805	2923	5351	1313	900	2187	4873	5379	5854
G11	29636	6254	5080	18014	9076	23859	4810	3004	5687	15364	13746	12133
G12	6750	2139	1902	3687	6868	8319	2088	1671	3647	3108	2095	1478
G13	8627	5295	3498	14478	8974	11139	4469	3028	4183	13414	12660	11796
C1	0	0	0	0	0	0	0	0	0	0	0	0
C2	139	293	188	976	915	572	352	261	461	1000	1133	1071
C3	1973	1913	1155	5241	3488	3672	1527	1007	1391	4560	4450	3823
C4	1922	1755	1056	4932	3442	3793	1478	984	1412	4195	4237	3655
C5	380	576	365	1328	1730	1389	508	400	659	1247	1346	1280
C6	1816	129	1204	1771	3956	13101	157	254	4517	375	603	1065
C7	7215	942	920	3452	3676	14278	987	725	4245	3316	4376	5304
C8	2922	1495	19298	9734	22467	18388	2751	2141	5705	2806	5003	3139
C9	3304	2707	2718	6471	6749	6777	2449	1758	1918	5337	5885	5938
C10	3904	2957	3256	7780	6783	7243	2532	1828	2063	6377	6337	5817
C11	364	1695	1496	2511	4627	2948	1532	1196	834	1685	2287	1732
C12	332	2107	1275	5236	2827	1323	2008	1351	166	6251	7124	7946
E1	159	2337	1248	4636	2766	1278	1521	1321	344	3933	3188	2724
E2	11	20	360	336	226	520	136	177	487	255	127	300
E3	56	3324	1573	6548	3411	1452	1972	1736	243	6204	5787	5583
E4	19	2722	1447	5411	2869	1156	1687	1485	241	5137	4789	4616
E5	3	192	132	866	1087	664	1043	975	158	4116	5657	6272
E6	207	580	472	635	1317	792	596	648	315	739	704	997
E7	131	128	221	269	1151	406	253	243	185	238	365	368
N1	4167	3030	4084	7370	5103	7567	2565	2237	2521	6090	5820	5682
N2	*n.a*	*n.a*	*n.a*	*n.a*	*n.a*	*n.a*	*n.a*	*n.a*	*n.a*	*n.a*	*0*	0
N3	3498	3131	4597	4702	5917	7258	1877	2307	2433	2393	2110	1938
N4	1994	1192	4541	3400	2959	2959	882	991	1164	2516	2405	2287
N5	3909	998	998	2092	3405	4274	759	826	1740	953	964	1261
N6	6508	2293	2082	7009	4117	6889	1444	1488	2271	5995	5822	5820

Table X- 5: Concentrations [µg/g oil] for light hydrocarbons (toluene to *n*-undecane).

compound	*n*C12	*n*C13	*n*C14	*n*C15	*n*C16	*i*-C18	*n*C17	pristane	*n*C18	phytane	*n*C19	*n*C20	*n*C21
sample													
A1	1285	894	1024	1170	1186	1074	1141	1742	952	1396	837	832	660
A2	0	0	0	0	0	0	0	0	0	0	0	0	0
A3	0	0	0	0	0	0	0	0	0	0	0	0	0
A4	2414	2479	2470	2442	2295	1324	2274	2215	1997	1857	1950	1807	1677
A5	6021	5608	5500	5426	5016	2096	4866	3457	4246	2869	4104	3684	3364
A6	5418	5230	4922	4936	4622	2020	4601	3521	4033	2905	3847	3511	3275
A7	5752	5395	5440	5404	5117	2159	5042	3648	4426	2708	4271	3894	3579
A8	6069	5463	5621	5443	5094	2032	5047	3404	4488	2398	4511	3891	3626
A9	928	545	633	1064	1017	811	962	1364	832	1094	790	765	631
A10	2866	2961	3551	3073	2895	1879	2780	3293	2354	2035	2254	2033	1813
A11	6081	5817	5562	5593	5194	2116	5093	3716	4360	2707	4360	3872	3585
A12	6488	6337	5584	5225	4952	2168	4955	3804	4289	2871	4410	3946	3619
A13	643	282	361	436	442	474	408	743	353	625	306	332	234
A14	1061	867	960	967	1026	968	990	1607	901	1252	828	755	586
A15	2303	2246	2479	2621	2434	1382	2386	2343	1970	1831	1799	1668	1385
A16	11872	11740	13455	11286	9868	3290	8979	7015	7680	2829	7835	6799	6344
A17	2074	2635	2903	5124	4810	2129	4745	3751	4100	2890	4052	3615	3359
G1	1340	2024	581	492	497	1528	306	3369	291	2300	358	301	213
G2	1048	1956	433	525	550	1736	313	3859	286	2573	265	235	133
G3	5749	4612	4388	2061	1871	1433	1597	2980	1442	1969	1347	1230	1007
G4	2249	1989	1301	1051	921	1517	702	3324	601	2283	622	648	495
G5	1628	2048	2532	768	712	1448	511	3332	429	2243	352	501	363
G6	1473	872	805	802	729	1444	537	3318	460	2223	433	468	378
G7	4613	4773	5351	5535	6014	1412	6576	3642	6942	1645	7767	7836	7935
G8	4181	3993	3762	3656	3493	1514	3230	3262	2821	2282	2454	2304	1893
G9	6534	6253	5877	5231	4935	1263	4665	2666	4171	1300	4063	3758	3440
G10	6299	6596	6967	7561	8091	1998	8575	5029	8628	2718	9633	9095	8712
G11	11393	10215	8991	8501	7572	1898	6951	3771	6100	1968	5600	5080	4481
G12	984	792	694	633	583	1764	365	3952	303	2664	278	372	204
G13	11155	10232	9144	5355	4868	1877	4323	3602	3697	2136	3379	3018	2492
C1	0	0	0	0	0	0	0	0	0	0	0	0	0
C2	1134	1175	853	910	906	901	870	1796	829	1539	786	737	680
C3	3956	3462	2852	2732	2478	1083	2336	2105	2029	1716	1944	1779	1653
C4	3837	3391	2801	2625	2421	1097	2297	2119	2034	1733	1908	1780	1598
C5	1169	1326	1003	1023	1025	728	1027	1443	981	1265	879	858	801
C6	984	668	876	1291	1754	1728	2331	6202	2827	1469	3632	4097	4718
C7	6617	6546	7000	8238	8286	1587	8356	5085	7892	1217	7673	6833	6355
C8	3757	3700	2391	1935	1814	1097	1765	3773	1542	805	1398	1193	1085
C9	6453	6227	6068	5947	6106	2146	7007	6839	6796	1791	6776	6174	5943
C10	6635	6108	6252	6900	7511	2054	7829	6193	7354	1768	7099	6357	5913
C11	2077	2315	2164	2384	2498	1291	2417	2515	2142	1655	2034	1943	1795
C12	8729	8431	7888	8064	7235	2089	6616	3875	5790	3515	5376	4981	4640
E1	2701	2689	2868	2939	3059	1510	2998	2460	2819	2416	2602	2407	2207
E2	379	633	595	73	183	659	128	1172	212	1697	486	222	148
E3	5701	5773	5529	4611	4610	1582	4290	2611	3925	2466	3679	3337	2982
E4	4736	4731	4685	4691	4618	1572	4270	2600	3913	2434	3638	3312	3039
E5	6460	6639	6691	4350	4309	1454	3993	2421	3673	2313	3511	3183	2846
E6	1558	1649	1484	1573	1746	1004	2153	1313	2272	2294	2187	2086	1928
E7	190	265	282	77	171	896	159	1299	120	2394	338	141	39
N1	6766	7374	7744	6612	5835	1775	5230	4078	4517	1583	4166	3532	3202
N2	0	0	0	0	0	0	0	0	0	0	0	0	0
N3	2350	3058	3794	4873	5629	2117	6058	3858	5532	1989	5350	4783	4374
N4	2943	2856	2670	2554	2017	1244	1840	2856	1616	1305	1384	1222	1095
N5	1926	2171	2055	2052	1424	1303	1140	2978	888	1329	681	534	364
N6	6044	5772	5503	5271	4895	1523	4813	3452	4369	1465	4331	3906	3686

Table X- 6: Concentrations [µg/g oil] for normal and isoprenoid alkanes (n-docecane to n-henicosane).

compound	*n*C22	*n*C23	*n*C24	*n*C25	*n*C26	*n*C27	*n*C28	*n*C29	*n*C30
sample									
A1	662	590	490	496	414	409	340	335	271
A2	0	0	0	0	0	0	0	0	0
A3	0	0	0	0	0	0	0	0	0
A4	1624	1532	1325	1279	1078	1089	916	884	726
A5	3184	2953	2544	2342	1982	1984	1659	1557	1245
A6	3122	2899	2577	2314	2000	1937	1690	1568	1271
A7	3400	3145	2763	2527	2227	2136	1780	1637	1258
A8	3400	3102	2735	2466	2127	2059	1749	1575	1247
A9	650	612	563	577	472	462	387	392	303
A10	1643	1453	1129	948	680	568	443	427	339
A11	3405	3126	2786	2597	2307	2259	1920	1802	1419
A12	3461	3185	2897	2755	2439	2474	2072	2000	1559
A13	255	228	203	232	175	170	149	167	277
A14	590	517	458	460	377	381	314	311	277
A15	1328	1150	1006	943	819	839	735	722	612
A16	5239	4426	2533	1551	725	392	191	139	72
A17	3197	2950	2672	2459	2176	2132	1752	1646	1275
G1	236	176	185	173	154	148	116	87	57
G2	133	131	140	140	125	114	88	55	50
G3	944	820	797	670	624	522	416	326	264
G4	479	409	412	362	323	311	240	194	149
G5	360	303	300	276	232	234	182	148	140
G6	377	320	287	259	208	207	172	126	118
G7	8330	8360	7834	7499	6336	5845	4679	4096	2888
G8	1876	1651	1535	1291	1161	1069	874	749	599
G9	3312	3155	2917	2599	2337	2081	1661	1356	953
G10	8840	8586	8093	7452	6603	6014	4937	4329	3224
G11	4179	3806	3357	2980	2490	2176	1753	1297	814
G12	257	181	172	167	145	136	100	84	71
G13	2315	2032	1825	1580	1343	1191	930	762	572
C1	0	0	0	0	0	0	0	0	0
C2	669	593	575	492	477	350	277	212	158
C3	1577	1371	1286	1049	1018	693	543	417	293
C4	1542	1335	1284	1031	1034	713	540	414	313
C5	750	664	640	538	515	345	260	180	139
C6	4682	4317	3204	2613	1718	1410	811	629	261
C7	5663	4981	3908	3293	2413	2125	1277	1126	522
C8	955	866	686	618	450	418	283	257	138
C9	5378	5027	4174	3769	2760	2622	1739	1539	896
C10	5356	5052	4091	3685	2770	2554	1729	1563	888
C11	1787	1554	1488	1216	1106	747	524	396	258
C12	4685	3995	4053	3176	3233	2120	1682	1249	958
E1	2195	1941	1800	1509	1410	1200	1062	897	820
E2	185	159	174	188	160	149	132	110	109
E3	2961	2611	2477	2023	1879	1578	1342	1119	1034
E4	2984	2601	2473	2045	1882	1591	1367	1166	1037
E5	2831	2436	2332	1927	1773	1494	1284	1090	1009
E6	1846	1593	1514	1262	1232	1098	1163	924	925
E7	78	58	64	75	94	92	63	54	67
N1	2782	2529	2142	1904	1625	1550	1200	1106	776
N2	0	0	0	0	0	0	0	0	0
N3	3912	3525	2949	2582	2181	2084	1717	1508	1128
N4	944	871	776	728	629	653	590	608	455
N5	301	285	302	291	213	211	200	215	188
N6	3468	3263	2893	2742	2452	2469	2084	1930	1441

Table X- 7: Concentrations [µg/g oil] for normal alkanes (*n*-docosane to *n*-tricontane).

compound	ethyl-b	1,3-dm-b	1,4-dm-b	1,2-dm-b	isopropyl-b	n-propyl-b	1-m-3-ethyl-b
sample							
A1	23	78	30	59	61	18	158
A2	1	1	1	1	2	1	2
A3	0	0	0	0	1	0	0
A4	26	106	33	63	54	19	193
A5	50	209	62	138	105	38	406
A6	47	186	63	127	100	34	371
A7	43	293	97	164	81	36	488
A8	44	381	102	195	89	37	580
A9	15	41	18	36	38	17	95
A10	24	59	33	64	58	22	115
A11	60	363	125	201	100	42	576
A12	0	0	0	0	0	0	2
A13	9	25	9	21	25	9	48
A14	0	0	0	0	0	0	4
A15	31	121	40	80	72	26	255
A16	3	28	4	12	8	6	83
A17	32	215	46	113	65	28	340
G1	0	1	0	1	0	0	2
G2	0	1	0	1	1	1	2
G3	56	397	61	216	128	64	543
G4	84	477	55	266	164	86	657
G5	71	336	74	234	150	77	543
G6	75	381	49	233	145	71	485
G7	36	345	90	148	40	25	289
G8	43	197	51	107	92	51	384
G9	84	826	226	286	117	59	823
G10	63	637	157	335	80	41	643
G11	214	1703	740	940	252	131	1647
G12	0	1	0	1	3	3	29
G13	0	1	0	0	0	0	4
C1	2	9	6	10	3	3	30
C2	11	20	12	31	37	18	40
C3	32	190	77	143	69	39	306
C4	34	210	70	150	73	43	329
C5	12	63	32	68	45	21	131
C6	105	982	426	474	157	67	1356
C7	109	1339	375	550	145	66	1570
C8	155	1124	488	601	577	134	1856
C9	78	464	145	179	147	52	975
C10	93	612	189	232	158	54	1039
C11	28	78	24	71	134	54	176
C12	5	35	12	18	15	8	60
E1	9	27	10	17	30	19	177
E2	0	0	0	0	0	0	0
E3	0	2	1	1	1	0	5
E4	2	8	2	4	19	14	125
E5	0	0	0	0	1	1	4
E6	29	49	32	46	30	18	176
E7	17	49	35	25	14	104	85
N1	61	469	84	204	89	32	582
N2	14	11	7	15	28	10	15
N3	49	436	58	175	78	30	589
N4	42	202	31	111	81	20	247
N5	60	285	52	162	100	30	355
N6	63	457	93	202	101	35	520

Table X- 8: Concentrations [µg/g oil] for alkylbenzenes. b = benzene, m = methyl, dm-b = dimethylbenzene.

compound	1-m-4-ethyl-b	1,3,5-tm-b	1-m-2-ethyl-b	1,2,4-tm-b	isobutyl-b	sec.-butyl-b
sample						
A1	91	147	118	601	7	68
A2	1	2	1	5	1	6
A3	0	0	1	1	2	7
A4	98	130	119	606	5	48
A5	185	211	282	1106	5	74
A6	169	187	253	1027	5	72
A7	212	347	215	1367	6	63
A8	252	443	248	1543	7	70
A9	57	81	78	348	5	46
A10	90	186	121	684	7	70
A11	251	392	246	1526	8	75
A12	1	2	2	8	0	1
A13	31	47	39	176	4	33
A14	2	7	5	28	0	6
A15	127	179	157	829	6	65
A16	55	146	58	604	2	16
A17	159	263	170	1064	5	53
G1	0	1	1	4	0	1
G2	1	1	1	4	0	0
G3	218	353	289	1093	15	144
G4	283	395	368	1320	15	183
G5	257	383	335	1199	14	172
G6	246	358	310	1108	10	162
G7	98	284	94	551	7	31
G8	146	221	198	690	8	125
G9	314	673	243	1387	13	104
G10	194	612	213	1176	11	80
G11	805	1945	525	2652	33	208
G12	13	31	26	113	2	22
G13	1	6	3	15	0	3
C1	16	27	18	132	1	7
C2	27	41	55	104	4	59
C3	122	205	179	682	7	107
C4	124	212	186	683	8	115
C5	67	116	105	341	7	79
C6	712	2135	536	3245	25	126
C7	670	1896	521	2899	22	108
C8	1074	1765	831	2787	38	443
C9	355	660	272	1439	13	127
C10	399	787	316	1553	15	130
C11	84	140	128	482	10	216
C12	21	48	23	100	2	29
E1	94	92	111	267	3	48
E2	0	0	0	0	0	0
E3	2	3	4	8	0	2
E4	59	60	67	44	3	50
E5	2	3	3	3	0	3
E6	117	60	139	289	2	24
E7	38	119	217	2	23	28
N1	230	705	192	1829	10	63
N2	15	27	19	86	3	23
N3	241	655	199	1881	8	62
N4	104	266	111	641	7	51
N5	162	398	154	1124	10	64
N6	203	564	170	1476	9	67

Table X- 9: Concentrations [µg/g oil] for alkylbenzenes. b = benzene, m = methyl, tm = trimethyl

compound	1-m-3-isopropyl-b	1,2,3-tm-b	1-m-4-isopropyl-b	1-m-2-isopropyl-b	1,3-diethyl-b
sample					
A1	55	391	58	12	63
A2	1	3	1	0	1
A3	0	1	0	0	1
A4	63	397	33	10	38
A5	130	773	93	17	55
A6	114	680	112	16	50
A7	113	698	102	13	64
A8	135	780	139	14	69
A9	37	241	49	8	39
A10	48	370	59	12	69
A11	132	828	89	15	73
A12	2	6	3	0	1
A13	19	131	21	5	27
A14	6	31	5	2	10
A15	85	484	97	13	54
A16	41	412	63	6	26
A17	93	524	91	11	52
G1	1	3	0	0	1
G2	1	1	1	0	0
G3	144	468	82	30	105
G4	179	579	99	37	129
G5	161	562	93	35	125
G6	146	494	102	33	115
G7	62	159	36	14	28
G8	138	239	86	29	86
G9	166	353	101	30	71
G10	133	448	72	29	64
G11	397	908	182	55	160
G12	28	77	20	7	29
G13	4	10	2	1	3
C1	10	44	25	1	12
C2	20	55	46	12	39
C3	94	276	92	22	63
C4	97	273	93	23	60
C5	47	145	62	17	52
C6	385	1287	344	72	251
C7	384	1234	246	63	220
C8	725	1182	895	112	606
C9	260	455	301	42	198
C10	287	557	319	46	213
C11	69	420	93	19	105
C12	28	30	27	4	17
E1	79	147	69	11	56
E2	0	0	0	0	0
E3	3	5	2	0	2
E4	85	57	76	10	61
E5	5	4	4	1	4
E6	34	182	31	5	43
E7	165	24	5	34	73
N1	122	689	84	17	88
N2	6	128	15	3	27
N3	129	815	79	14	81
N4	61	397	39	12	66
N5	85	506	72	15	68
N6	106	574	39	14	66

Table X- 10: Concentrations [µg/g oil] for alkylbenzenes. b = benzene, m = methyl, tm-b = trimethylbenzene

compound	1-m-3-propyl-b	1-m-2-propyl-b	1,4-dm-2-ethyl-b	1,3-dm-4-ethyl-b	1,2-dm-4-ethyl-b
sample					
A1	124	88	89	155	126
A2	1	1	1	2	2
A3	0	0	0	1	1
A4	138	84	75	112	121
A5	299	196	147	202	213
A6	260	169	129	179	192
A7	307	143	139	200	247
A8	378	164	165	237	307
A9	77	57	57	99	83
A10	130	94	116	196	143
A11	335	152	154	221	280
A12	4	3	4	4	5
A13	40	31	32	57	44
A14	15	15	18	31	25
A15	191	111	106	158	171
A16	123	61	69	117	128
A17	237	120	113	163	193
G1	2	2	1	2	2
G2	2	1	1	1	1
G3	422	266	143	210	225
G4	525	352	183	263	281
G5	460	322	175	261	260
G6	411	288	159	236	230
G7	141	56	55	66	97
G8	356	225	123	172	187
G9	427	164	133	167	215
G10	376	166	125	156	198
G11	993	325	312	375	592
G12	99	79	51	76	81
G13	13	10	7	9	12
C1	39	23	49	29	43
C2	49	64	54	31	52
C3	285	197	124	127	157
C4	291	204	115	122	147
C5	138	126	76	72	97
C6	907	277	578	716	929
C7	858	247	499	614	806
C8	1105	391	578	890	957
C9	482	147	234	332	417
C10	552	169	264	369	470
C11	202	171	101	224	138
C12	73	38	39	29	35
E1	239	193	115	167	148
E2	0	0	0	0	0
E3	9	8	5	7	6
E4	289	188	92	131	95
E5	15	12	7	10	8
E6	96	94	69	112	101
E7	115	88	61	101	89
N1	289	97	167	243	320
N2	13	12	14	69	22
N3	328	117	175	242	362
N4	120	54	74	131	129
N5	190	77	106	169	192
N6	245	84	123	174	238

Table X- 11: Concentrations [µg/g oil] for alkylbenzenes. b = benzene, m = methyl, tm-b = trimethylbenzene

compound	1,3-dm-2-ethyl-b	1,2-dm-3-ethyl-b	1,2,4,5-tem-b	1,2,3,5-tem-b	1,2,3,4-tem-b
sample					
A1	54	63	348	247	430
A2	1	2	23	4	4
A3	1	1	28	2	2
A4	43	54	147	141	363
A5	75	102	107	228	652
A6	69	90	95	198	630
A7	56	86	133	246	507
A8	54	98	152	303	591
A9	38	46	279	145	278
A10	57	63	347	360	569
A11	64	95	144	271	568
A12	2	3	5	12	24
A13	22	26	216	89	144
A14	12	16	98	73	134
A15	59	75	221	222	491
A16	72	53	117	202	586
A17	53	73	107	194	425
G1	1	2	2	4	5
G2	0	1	1	1	2
G3	71	116	123	236	228
G4	86	146	145	287	293
G5	85	145	141	284	283
G6	77	130	129	254	255
G7	41	49	48	80	80
G8	49	86	70	137	157
G9	43	70	98	168	108
G10	65	81	108	199	142
G11	80	132	264	484	189
G12	28	52	56	115	134
G13	4	7	11	19	20
C1	8	16	35	65	77
C2	21	26	32	40	42
C3	43	71	84	158	175
C4	43	70	68	125	132
C5	28	42	53	81	87
C6	250	301	654	1117	789
C7	217	262	566	967	662
C8	276	310	374	646	544
C9	110	127	152	251	260
C10	121	143	175	304	322
C11	64	115	103	218	246
C12	10	16	15	29	23
E1	47	85	60	159	302
E2	0	0	0	0	0
E3	3	5	3	12	18
E4	42	74	37	156	160
E5	4	7	4	17	22
E6	34	67	29	81	189
E7	32	65	28	71	168
N1	68	92	273	416	469
N2	22	28	139	105	174
N3	64	97	228	414	545
N4	66	63	155	191	339
N5	69	77	174	258	413
N6	57	72	162	281	411

Table X- 12: Concentrations [µg/g oil] for alkylbenzenes. b = benzene, dm-b = dimethylbenzene, tem-b = tetramethylbenzene

compound	naphthalene	2-mn	1-mn	2-en	1-en	2,6-dmn	2,7-dmn	1,3-dmn	1,7-dmn
sample									
A1	264	1112	838	210	92	735	748	714	677
A2	14	37	33	40	29	126	156	146	66
A3	14	32	32	54	36	166	203	193	72
A4	175	626	491	128	70	286	293	346	300
A5	363	1294	1046	194	112	343	382	451	476
A6	332	1168	915	179	101	303	341	412	435
A7	630	1817	1235	270	86	608	557	531	660
A8	698	2028	1501	350	100	847	813	867	815
A9	149	580	449	128	67	423	439	445	369
A10	414	1751	1287	287	98	1027	1014	924	706
A11	587	1794	1254	287	88	570	599	593	638
A12	15	119	118	58	26	125	141	166	182
A13	86	305	268	87	54	327	331	336	270
A14	95	573	441	130	60	449	516	511	393
A15	236	1010	757	194	92	482	471	560	478
A16	258	1241	714	181	74	574	516	512	456
A17	410	1399	861	212	78	423	449	442	454
G1	19	164	150	76	46	126	119	180	205
G2	6	34	34	25	14	46	53	74	87
G3	744	1858	1435	396	218	560	584	813	800
G4	866	2266	1856	546	293	786	786	1137	1110
G5	879	2323	1882	503	279	736	753	1061	1028
G6	815	2218	1782	503	275	747	734	1091	994
G7	1133	2586	2030	344	173	650	725	952	783
G8	243	814	730	222	143	243	254	390	383
G9	581	1743	1011	238	104	407	425	445	476
G10	1489	2642	2375	415	220	733	740	1163	1007
G11	1232	3528	2371	614	121	1774	1819	1438	1642
G12	443	1992	1638	482	257	727	716	1107	962
G13	82	503	428	125	75	231	225	308	359
C1	46	92	57	11	7	22	28	52	
C2	73	115	151	108	79	49	55	183	
C3	188	504	442	131	91	136	154	466	
C4	166	493	448	138	91	137	160	497	
C5	92	287	261	102	72	92	112	337	
C6	1473	4701	3954	1696	787	3377	3235	6964	
C7	1332	4195	3576	1595	696	2978	3031	6299	
C8	269	796	463	150	73	143	171	506	
C9	188	841	511	215	95	178	237	735	
C10	321	1273	812	299	132	289	326	987	
C11	174	993	907	225	126	277	336	1120	
C12	31	89	70	28	11	34	37	98	
E1	103	331	281	175	71	190	214	278	241
E2	0	6	9	16	12	29	35	39	59
E3	11	20	20	49	14	66	54	79	98
E4	51	41	45	111	28	146	110	213	175
E5	11	25	28	58	17	77	63	113	100
E6	107	290	262	105	50	104	111	133	97
E7	127	290	238	108	59	97	91	101	89
N1	535	2108	1486	318	130	722	813	803	977
N2	134	715	414	137	65	215	219	273	387
N3	511	2046	1451	337	117	680	748	780	894
N4	355	1281	830	235	120	457	561	496	673
N5	668	2215	1513	339	154	722	794	847	865
N6	875	2604	1917	415	154	929	1092	1188	933

Table X- 13: Concentrations [µg/g oil] for alkylnaphthalenes. mn = methylnaphthalene, en = ethylnaphthalene, dmn = dimethylnaphthalene

compound	1,3+1,7-dmn	1,6-dmn	1,4+2,3-dmn	1,5-dmn	1,2-dmn	1,8-dmn	1,3,7-tmn	1,3,6-tmn
sample								
A1	1391	956	651	249	225	193	737	966
A2	213	41	139	79	76	66	195	165
A3	265	36	180	93	96	81	251	220
A4	647	500	334	125	139	108	298	413
A5	927	947	414	195	219	116	299	461
A6	847	875	380	177	209	108	272	421
A7	1191	1173	459	189	203	143	386	634
A8	1682	1526	626	251	262	185	554	859
A9	814	517	461	168	136	131	527	688
A10	1630	1515	751	277	261	199	857	1198
A11	1231	1238	488	184	217	152	402	656
A12	348	349	169	80	87	74	247	411
A13	606	330	343	114	94	111	444	559
A14	904	606	438	156	141	137	536	718
A15	1038	824	489	175	194	156	520	707
A16	968	1448	424	178	182	120	470	1005
A17	895	879	373	156	172	129	343	521
G1	385	314	184	114	115	99	213	277
G2	161	133	89	53	61	57	143	187
G3	1613	1191	626	339	331	251	426	567
G4	2247	1653	876	483	478	359	628	784
G5	2088	1516	801	424	421	331	604	720
G6	2085	1518	827	434	436	319	602	747
G7	1735	1327	674	262	284	180	472	547
G8	773	632	321	182	183	186	265	291
G9	921	700	334	162	160	134	271	307
G10	2170	1600	829	330	353	231	674	773
G11	3080	2002	970	333	207	266	826	962
G12	2069	1505	819	441	436	327	589	744
G13	668	530	275	163	157	118	286	334
C1	52	39	17	22	8	0	16	19
C2	183	115	71	65	32	118	100	89
C3	466	313	180	123	73	134	164	224
C4	497	331	190	133	81	155	183	245
C5	337	216	148	100	53	140	150	173
C6	6964	4504	3111	1504	1625	906	2795	2754
C7	6299	4140	2868	1375	1577	865	2655	2562
C8	506	320	205	96	47	94	148	172
C9	735	472	320	143	82	168	281	327
C10	987	648	407	172	126	214	333	419
C11	1120	823	341	241	172	221	349	525
C12	98	63	31	32	14	43	65	78
E1	519	373	243	148	182	146	222	386
E2	98	112	60	40	61	55	191	302
E3	176	46	102	82	87	82	166	219
E4	388	84	211	159	174	157	295	479
E5	213	53	117	93	100	89	179	247
E6	230	228	105	65	117	61	106	131
E7	190	179	95	53	119	68	88	99
N1	1781	1341	720	246	313	179	617	813
N2	660	480	289	135	137	122	231	276
N3	1674	1494	668	233	312	183	592	815
N4	1169	945	542	169	244	168	615	800
N5	1713	1526	685	257	324	202	615	875
N6	2121	1909	798	283	353	212	709	1000

Table X- 14: Concentrations [µg/g oil] for alkylnaphthalenes. dmn = dimethylnaphthalene; tmn = trimethylnaphthalene

compound	1,4,6+1,3,5-tmn	2,3,6-tmn	1,2,7-tmn	1,6,7-tmn	1,2,6-tmn	1,2,4-tmn	1,2,5-tmn
sample							
A1	789	595	206	404	428	145	241
A2	241	115	56	90	112	73	103
A3	310	152	74	113	135	86	135
A4	422	259	134	204	252	100	163
A5	442	312	124	243	212	94	174
A6	397	287	125	219	197	84	173
A7	448	397	115	273	199	71	193
A8	591	555	134	364	250	81	217
A9	609	366	142	253	330	117	187
A10	868	745	193	431	446	121	257
A11	474	409	135	289	211	76	248
A12	306	260	96	201	137	57	166
A13	510	304	121	200	267	113	140
A14	589	445	145	291	321	103	174
A15	608	431	166	297	323	109	203
A16	609	521	121	318	330	104	304
A17	384	326	125	219	181	65	191
G1	320	176	79	174	124	67	194
G2	224	125	55	120	91	52	151
G3	620	335	124	324	201	103	305
G4	869	466	181	449	307	142	448
G5	792	420	180	371	259	137	415
G6	829	447	186	418	291	137	437
G7	524	380	103	347	191	79	301
G8	377	170	82	184	131	79	196
G9	296	197	59	171	100	47	174
G10	735	479	137	450	250	96	357
G11	608	672	90	352	137	54	122
G12	826	437	183	421	272	140	437
G13	357	212	77	196	119	55	152
C1	19	15	0	9	0	0	0
C2	119	49	43	74	39	40	74
C3	209	111	74	147	84	48	112
C4	229	114	77	150	90	57	120
C5	185	93	65	127	74	62	93
C6	3095	2169	1550	1882	1519	525	2476
C7	2856	2025	1446	1761	1429	493	2302
C8	151	62	66	92	50	31	124
C9	303	127	181	189	111	72	351
C10	380	182	200	236	136	83	434
C11	442	192	109	240	140	68	173
C12	63	36	18	32	26	15	23
E1	360	240	118	186	198	109	243
E2	272	198	94	149	188	95	232
E3	237	146	74	133	114	76	165
E4	481	290	144	249	229	147	320
E5	270	161	76	143	132	81	180
E6	123	86	50	51	87	54	92
E7	96	76	49	46	79	55	93
N1	686	543	300	378	352	118	349
N2	303	173	122	125	154	98	139
N3	655	558	229	388	323	104	294
N4	639	422	264	329	372	133	386
N5	720	504	298	397	355	138	404
N6	762	624	276	429	382	113	393

Table X- 15: Concentrations [µg/g oil] for alkylnaphthalenes. tmn = trimethylnaphthalene.

compound	phenanthrene	3-mp	2-mp	9-mp	1-mp	3-ep	9,2,1-ep	3,6-dmp	3,5+2,6-dmp	2,7-dmp
sample										
A1	279	318	341	464	289	63	61	84	141	86
A2	248	343	222	442	273	58	39	101	167	114
A3	306	407	272	529	330	68	56	105	200	131
A4	137	141	146	211	137	33	27	43	54	30
A5	164	145	157	255	159	24	24	42	57	33
A6	155	137	141	237	151	26	22	40	47	25
A7	280	231	273	322	213	39	33	56	94	53
A8	418	327	394	426	298	45	46	68	134	72
A9	211	270	301	412	257	53	44	81	126	73
A10	403	386	433	543	369	64	67	91	166	101
A11	241	203	236	282	185	32	39	49	93	53
A12	239	206	239	334	200	46	25	54	86	58
A13	181	234	253	332	217	56	39	81	120	69
A14	241	274	302	404	264	57	51	65	131	80
A15	206	229	244	346	224	50	41	69	104	58
A16	426	288	343	483	307	40	36	76	118	65
A17	204	168	193	233	156	29	23	50	75	42
G1	254	218	244	383	274	51	45	56	87	53
G2	224	191	217	333	238	39	41	50	74	39
G3	311	216	249	366	257	42	41	55	76	43
G4	405	289	320	494	346	53	56	67	99	64
G5	354	259	289	440	302	44	52	62	92	49
G6	393	284	305	465	330	50	58	64	96	53
G7	566	285	344	435	297	52	50	80	125	70
G8	112	109	117	181	117	28	25	35	40	21
G9	146	125	140	161	113	25	21	33	57	30
G10	861	329	410	656	457	54	54	91	149	82
G11	840	666	816	662	408	64	71	108	244	139
G12	377	270	298	456	330	63	56	72	99	56
G13	289	182	211	318	220	31	32	48	72	38
C1	26	0	0	0	0	0	0	0	0	0
C2	148	66	53	83	79	28	17	21	23	18
C3	121	99	81	98	87	25	21	29	32	21
C4	122	117	86	111	88	38	28	35	37	25
C5	130	179	122	121	100	41	38	35	53	34
C6	463	367	502	424	314	73	76	104	177	76
C7	449	376	458	409	293	70	82	100	165	74
C8	28	7	7	15	8	2	0	0	0	0
C9	71	25	44	61	36	13	16	10	11	7
C10	75	24	50	64	41	16	15	4	12	0
C11	90	86	94	122	83	33	30	35	33	21
C12	26	28	36	42	32	16	16	15	24	12
E1	152	161	185	233	161	31	31	40	68	24
E2	282	252	302	384	285	43	40	64	118	46
E3	122	140	152	189	131	26	26	36	60	26
E4	219	235	260	334	222	31	41	56	105	42
E5	140	142	159	200	138	21	29	36	64	26
E6	56	64	67	74	68	20	8	11	28	5
E7	65	55	55	57	55	25	4	7	28	3
N1	125	143	154	201	132	27	23	38	62	33
N2	106	167	197	320	151	47	28	67	92	52
N3	136	155	165	211	135	30	24	37	71	38
N4	139	117	119	161	112	27	15	32	48	21
N5	209	182	187	260	165	37	23	48	83	47
N6	318	254	277	364	234	40	33	64	114	62

Table X- 16: Concentrations [µg/g oil] for alkylphenanthrenes. mp = methylphenanthrene, ep = ethylphenanthrene, dmp = dimethylphenanthrene

compound	1,3+3,9+2,10+3,10-dmp	2,5+2,9+1,6-dmp	1,7-dmp	2,3-dmp	1,9+4,9+4,10-dmp
sample					
A1	795	287	257	129	118
A2	787	285	224	131	130
A3	932	317	258	140	151
A4	317	130	114	49	63
A5	357	168	126	56	79
A6	316	147	110	49	67
A7	460	206	159	71	75
A8	634	256	198	99	93
A9	700	264	243	122	92
A10	852	323	305	138	131
A11	425	174	141	67	73
A12	449	199	149	68	79
A13	614	229	203	92	109
A14	665	244	226	115	114
A15	587	221	189	91	102
A16	571	195	307	85	95
A17	354	154	119	58	56
G1	448	191	165	74	105
G2	420	173	155	70	95
G3	409	169	148	60	103
G4	546	211	190	73	137
G5	481	191	172	73	111
G6	514	203	181	87	99
G7	463	188	157	71	111
G8	212	82	77	34	56
G9	226	93	68	35	47
G10	677	290	238	92	164
G11	744	317	211	114	105
G12	505	212	188	88	120
G13	357	151	117	47	85
C1	0	0	0	0	0
C2	166	66	34	29	44
C3	186	105	57	32	57
C4	220	110	65	48	62
C5	305	166	72	56	92
C6	586	285	279	105	103
C7	567	272	283	99	119
C8	0	0	0	0	0
C9	51	24	15	9	5
C10	39	14	19	8	6
C11	196	93	64	36	59
C12	121	59	42	20	41
E1	327	152	136	47	57
E2	526	264	265	84	117
E3	291	136	124	40	61
E4	526	240	211	74	96
E5	307	157	128	50	64
E6	103	56	39	14	21
E7	81	51	29	12	20
N1	311	119	103	51	50
N2	528	177	145	94	91
N3	354	126	113	62	51
N4	250	91	90	47	37
N5	370	136	124	64	64
N6	493	208	159	76	80

Table X- 17: Concentrations [µg/g oil] for alkylphenanthrenes. dmp = dimethylphenanthrene.

compound	1,8-dmp	1,2-dmp	1,3,6+1,3,10 +2,6,10-tmp	1,3,7+2,6,9 +7e-1mp-tmp	1,3,9+2,3,6-tmp	1,6,9+1,7,9+2,3,7-tmp
sample						
A1	75	52	258	318	64	209
A2	66	57	280	327	71	215
A3	83	55	333	405	81	245
A4	45	54	113	135	31	97
A5	46	62	106	150	31	98
A6	42	41	93	135	27	86
A7	47	36	130	196	32	107
A8	60	65	172	253	43	143
A9	75	96	253	326	68	201
A10	87	60	282	347	67	223
A11	46	47	127	185	31	105
A12	49	22	128	208	31	109
A13	68	48	228	269	57	182
A14	72	61	232	264	60	187
A15	64	48	195	236	48	164
A16	67	46	195	240	40	143
A17	40	64	109	161	29	89
G1	56	36	126	249	48	115
G2	56	33	122	230	42	101
G3	51	30	108	198	39	93
G4	69	42	146	277	51	123
G5	50	35	129	250	42	109
G6	58	38	143	265	47	119
G7	48	26	120	239	42	110
G8	32	20	67	136	25	58
G9	24	33	62	108	20	53
G10	88	53	190	356	67	182
G11	43	21	156	221	35	107
G12	67	43	139	263	49	114
G13	38	20	97	150	34	85
C1	0	0	0	0	0	0
C2	24	12	60	99	22	47
C3	23	14	60	108	18	44
C4	32	16	75	132	25	60
C5	32	23	95	182	38	85
C6	39	28	189	359	53	140
C7	46	35	173	333	45	132
C8	0	0	2	3	1	1
C9	32	2	6	27	3	6
C10	14	2	5	25	1	4
C11	26	11	62	101	27	52
C12	20	7	48	75	21	39
E1	43	44	108	164	24	85
E2	67	75	165	306	45	139
E3	37	44	102	155	21	76
E4	73	73	162	267	46	136
E5	46	44	106	178	29	82
E6	17	26	31	36	59	24
E7	13	30	40	20	7	35
N1	34	19	97	129	31	88
N2	57	32	200	246	57	154
N3	39	21	116	151	28	94
N4	37	17	84	108	22	68
N5	40	22	116	159	31	99
N6	55	28	136	193	36	116

Table X- 18: Concentrations [µg/g oil] for alkylphenanthrenes. dmp = dimethylphenanthrene, tmp = trimethylphenanthrene.

compound	1,3,8-tmp	2,3,10-tmp	tmp (unknown)	1,6,7-tmp	1,2,6-tmp	1,2,7+1,2,9-tmp	1,2,8-tmp
sample							
A1	36	55	81	73	94	68	161
A2	30	56	88	74	76	57	98
A3	32	63	107	93	105	80	120
A4	14	27	41	42	36	27	150
A5	17	32	35	33	23	25	124
A6	14	22	30	28	18	24	116
A7	20	27	38	34	24	24	71
A8	26	41	50	45	34	31	85
A9	27	58	79	71	72	53	170
A10	42	63	88	73	78	54	155
A11	22	28	36	38	28	25	74
A12	16	40	48	57	45	33	71
A13	27	49	78	56	67	49	147
A14	27	51	72	64	72	48	139
A15	21	38	68	47	57	46	151
A16	32	32	62	53	53	38	194
A17	15	20	32	38	21	22	72
G1	22	23	48	35	126	49	52
G2	20	18	42	25	117	45	44
G3	13	18	40	41	97	39	37
G4	19	25	55	47	148	49	51
G5	22	20	50	51	127	47	44
G6	23	26	52	46	127	49	50
G7	18	27	61	50	107	52	22
G8	7	10	21	25	80	26	26
G9	9	13	29	30	49	19	9
G10	28	39	71	73	119	56	39
G11	16	27	58	59	31	48	6
G12	20	27	51	49	155	52	55
G13	14	21	35	35	48	29	22
C1	0	0	0	0	0	0	0
C2	19	13	20	12	141	25	27
C3	19	7	13	11	145	18	29
C4	19	4	23	15	161	27	32
C5	30	16	34	21	189	49	37
C6	27	19	37	38	201	59	47
C7	23	17	34	30	200	52	41
C8	1	1	1	1	13	1	1
C9	0	0	0	0	72	0	2
C10	0	0	0	0	71	0	5
C11	11	6	8	12	53	21	17
C12	11	4	14	7	0	22	18
E1	18	24	40	31	32	34	207
E2	27	41	73	80	85	55	361
E3	23	23	35	31	33	35	179
E4	32	35	56	51	48	52	328
E5	22	23	35	39	33	34	191
E6	6	7	9	9	9	13	65
E7	6	3	6	3	16	11	58
N1	15	24	30	33	37	24	44
N2	17	41	65	58	74	52	109
N3	14	26	39	38	38	27	62
N4	9	17	28	19	28	18	74
N5	13	25	45	43	52	35	77
N6	14	29	43	46	49	32	69

Table X- 19: Concentrations [µg/g oil] for alkylphenanthrenes. tmp = trimethylphenanthrene.

compound	dibenzothiophene	4-m-dbt	2-m-dbt	3-m-dbt	1-m-dbt	1-e-dbt	4,6-dm-dbt	2,4-dm-dbt
sample								
A1	53	50	11	28	30	17	33	20
A2	42	22	5	19	19	12	29	15
A3	52	24	20	2	21	14	33	21
A4	38	39	12	19	31	12	21	13
A5	62	67	15	24	40	11	29	18
A6	56	57	13	23	34	9	26	16
A7	38	45	11	18	19	10	22	14
A8	46	55	13	20	22	8	28	17
A9	48	45	10	27	31	16	30	22
A10	54	58	12	27	27	14	34	22
A11	35	41	9	18	18	7	22	13
A12	32	46	8	18	20	9	23	15
A13	45	35	9	25	26	15	27	17
A14	46	45	13	25	26	12	27	20
A15	49	50	13	26	31	15	30	19
A16	35	33	7	20	16	7	14	12
A17	34	40	8	17	20	8	19	13
G1	87	112	30	33	39	17	51	24
G2	73	94	26	28	36	16	47	23
G3	91	96	26	28	36	15	43	20
G4	134	146	38	42	50	20	63	27
G5	126	131	34	37	49	20	57	28
G6	128	134	35	41	48	22	59	29
G7	60	46	11	13	12	6	22	13
G8	44	57	17	20	25	12	28	14
G9	17	20	4	6	6	3	13	8
G10	118	88	14	20	26	8	42	21
G11	41	69	12	15	6	5	33	19
G12	134	145	43	41	53	21	61	30
G13	43	52	9	15	17	7	25	13
C1	5	0	0	0	0	0	0	0
C2	15	18	5	5	16	5	16	8
C3	12	28	4	5	11	6	18	11
C4	11	27	6	6	12	6	20	10
C5	11	28	5	6	18	8	23	14
C6	58	52	21	20	17	4	21	20
C7	54	53	21	15	15	0	19	20
C8	3	0	0	0	0	0	0	0
C9	17	0	0	0	0	0	0	0
C10	10	6	1	2	1	0	0	0
C11	11	25	4	6	8	7	18	8
C12	8	11	3	4	4	5	12	5
E1	128	151	43	66	99	29	70	34
E2	216	265	66	114	191	55	120	56
E3	98	135	33	59	93	25	64	31
E4	175	254	67	94	164	49	116	51
E5	106	146	40	58	98	29	67	30
E6	79	82	25	39	53	21	45	17
E7	82	76	25	35	54	22	36	15
N1	30	20	5	13	8	3	9	8
N2	34	25	9	21	18	12	15	13
N3	27	23	7	15	10	6	12	9
N4	41	21	7	20	13	6	10	9
N5	46	31	10	21	16	8	13	12
N6	52	41	15	20	15	7	17	15

Table X- 20: Concentrations [µg/g oil] for alkyldibenzothiophenes. m-dbt = methyldibenzothiophene, e-dbt = ethyldibenzothiophenes, dm-dbt = dimethyldibenzothiophene

compound	2-et+2,6-dm-dbt	3,6-dm-dbt	2,7+2,8+3,7-dm-dbt	1,4+1,6+1,8-dm-dbt	1,3-dm-dbt
sample					
A1	18	29	14	43	9
A2	8	13	12	32	5
A3	12	17	14	37	9
A4	12	21	9	34	7
A5	17	31	12	46	7
A6	17	26	11	39	8
A7	13	23	10	26	5
A8	15	29	10	26	6
A9	17	28	13	40	9
A10	19	33	13	37	7
A11	11	22	9	24	4
A12	13	24	8	25	5
A13	12	21	13	34	9
A14	15	26	11	35	8
A15	13	27	12	39	8
A16	7	19	7	11	2
A17	10	20	7	24	4
G1	33	41	20	55	10
G2	32	39	19	48	8
G3	24	32	14	41	8
G4	35	48	23	63	13
G5	36	44	22	57	10
G6	36	49	20	62	12
G7	12	14	7	13	1
G8	19	24	13	33	7
G9	6	8	3	8	1
G10	18	27	11	28	1
G11	19	21	7	9	1
G12	36	49	24	64	12
G13	13	18	7	23	2
C1	0	0	0	0	0
C2	7	8	4	21	3
C3	8	11	3	20	1
C4	10	12	5	23	3
C5	11	12	8	32	2
C6	22	12	20	13	3
C7	17	13	23	17	6
C8	0	0	0	0	0
C9	0	0	0	0	0
C10	0	0	0	0	0
C11	8	11	2	14	1
C12	6	9	5	11	1
E1	45	97	40	114	33
E2	73	179	67	220	75
E3	41	87	31	109	27
E4	66	163	62	192	51
E5	40	89	32	109	31
E6	26	56	23	54	18
E7	26	46	28	54	14
N1	6	9	5	10	2
N2	11	18	9	16	3
N3	8	14	6	11	3
N4	7	9	6	10	1
N5	10	13	9	13	2
N6	13	19	10	15	4

Table X- 21: Concentrations [µg/g oil] for alkyldibenzothiophenes. e = ethyl, dm-dbt = dimethyldibenzothiophene.

compound	3,4-dm-dbt	1,7-dm-dbt	1	2	3	4	5	6	7
sample									
A1	13	12	13	17	38	30	22	20	15
A2	8	7	12	12	36	36	18	16	13
A3	10	8	14	15	40	37	18	15	15
A4	7	9	7	10	22	14	13	11	10
A5	10	9	9	11	21	19	17	13	13
A6	9	8	8	10	22	13	14	13	10
A7	6	4	6	7	18	13	10	9	7
A8	7	6	7	8	22	16	11	11	8
A9	8	10	11	16	35	30	19	20	15
A10	11	7	12	12	33	26	16	17	13
A11	6	5	6	7	19	14	10	8	6
A12	6	4	7	7	21	18	12	12	7
A13	9	9	12	15	33	26	19	17	14
A14	8	7	11	13	30	22	18	16	13
A15	10	9	11	14	32	23	18	16	13
A16	4	3	7	5	13	7	3	5	6
A17	6	4	6	7	17	13	9	7	7
G1	14	11	16	19	38	25	21	18	14
G2	14	9	15	18	34	22	21	18	15
G3	10	8	13	15	28	19	17	15	11
G4	17	11	17	21	42	31	26	22	15
G5	15	11	17	21	39	21	24	22	13
G6	14	11	17	21	39	25	24	22	16
G7	8	2	6	6	18	13	11	10	5
G8	6	6	11	14	21	12	12	10	9
G9	4	1	3	4	11	5	4	5	2
G10	18	4	9	12	33	20	17	17	14
G11	9	1	5	6	21	20	9	12	6
G12	17	13	19	24	45	22	25	21	15
G13	7	2	6	7	16	5	10	11	6
C1	0	0	0	0	0	0	0	0	0
C2	3	3	7	9	14	5	6	5	5
C3	2	3	7	7	13	5	8	8	7
C4	2	6	7	10	17	9	9	8	5
C5	4	7	8	9	19	11	14	12	9
C6	1	9	8	9	25	15	11	12	10
C7	2	10	8	7	25	17	14	10	9
C8	0	0	0	0	0	0	0	0	0
C9	0	0	0	0	21	5	0	0	0
C10	0	0	0	0	19	6	0	0	0
C11	1	2	5	7	14	6	8	5	4
C12	1	2	5	5	12	6	6	5	5
E1	28	26	24	43	61	47	42	34	28
E2	50	54	42	79	108	85	79	78	55
E3	22	26	25	37	54	44	41	32	26
E4	29	46	39	62	95	77	67	63	48
E5	17	29	25	39	58	43	39	35	26
E6	14	17	15	34	40	34	26	27	18
E7	14	16	14	32	36	27	21	27	15
N1	5	2	4	4	11	10	4	5	4
N2	7	5	5	5	21	18	10	10	9
N3	4	3	3	3	12	11	6	6	5
N4	3	7	5	3	10	9	6	3	3
N5	4	4	5	4	12	12	6	8	6
N6	12	5	8	6	16	19	10	8	7

Table X- 22: Concentrations [µg/g oil] for alkyldibenzothiophenes. dm-dbt = dimethyldibenzothiophene, 1-7 = unknown isomers of trimethyldibenzothiophenes.

compound	1	2	3	4	5	6	7	8	9	10	11	12	13
sample													
A1	12	10	10	16	17	24	68	13	115	28	25	25	17
A2	12	10	7	9	15	17	47	12	77	17	21	17	11
A3	13	10	8	10	16	19	54	10	90	23	23	19	13
A4	8	6	6	11	14	20	56	8	92	22	22	20	13
A5	5	4	4	6	8	11	28	4	45	12	11	11	8
A6	5	4	4	6	7	10	27	4	44	12	10	10	7
A7	5	4	3	3	5	6	15	3	24	6	6	5	6
A8	6	4	3	2	3	4	11	2	18	4	5	4	3
A9	12	12	11	19	21	31	81	13	135	34	28	29	21
A10	9	8	7	10	11	16	43	6	72	20	18	18	12
A11	6	3	3	3	5	5	16	3	24	6	7	5	4
A12	0	0	0	6	7	10	24	5	41	13	11	9	8
A13	12	10	9	17	20	29	75	11	126	32	28	29	19
A14	9	8	9	13	14	21	54	9	90	24	21	20	12
A15	10	9	8	15	16	23	63	10	101	24	22	23	16
A16	7	6	5	5	8	10	29	6	44	10	11	9	6
A17	5	3	3	3	5	7	19	4	31	9	9	6	4
G1	7	7	4	4	10	12	27	5	37	7	11	6	0
G2	7	6	3	4	10	11	25	5	36	8	12	5	0
G3	6	6	3	2	8	9	18	3	26	5	8	4	0
G4	8	7	3	4	11	12	26	5	40	8	13	6	0
G5	8	6	3	4	10	12	27	5	36	7	12	5	0
G6	9	7	5	4	12	12	28	5	39	7	13	5	0
G7	3	3	2	1	3	5	10	3	13	5	5	3	3
G8	8	7	4	3	11	13	29	6	44	10	13	7	0
G9	2	2	1	0	2	2	5	2	8	2	3	1	0
G10	5	4	3	1	4	4	11	5	15	4	5	4	2
G11	0	0	0	0	0	0	0	0	0	0	0	0	0
G12	9	7	4	4	11	13	28	4	38	8	14	7	0
G13	3	3	1	0	2	3	5	1	7	1	2	2	0
C1	13	10	8	6	16	19	62	12	80	16	19	11	0
C2	10	8	5	3	11	13	42	8	49	10	12	5	0
C3	7	6	4	2	6	8	22	5	30	4	5	3	0
C4	8	7	4	2	8	8	24	6	32	7	8	5	0
C5	10	8	5	3	8	9	26	6	32	7	7	3	0
C6	0	0	0	0	0	0	0	0	0	0	0	0	0
C7	0	0	0	0	0	0	0	0	0	0	0	0	0
C8	0	0	0	0	0	0	0	0	0	0	0	0	0
C9	4	3	5	1	4	4	13	4	26	7	11	5	3
C10	6	4	4	2	5	5	15	4	29	7	12	3	4
C11	6	6	3	1	4	5	16	3	18	3	3	2	0
C12	6	5	2	1	5	5	17	3	19	1	4	1	0
E1	8	6	3	2	8	8	23	5	30	5	10	5	0
E2	12	10	9	4	13	15	46	7	64	7	14	10	5
E3	7	4	3	2	6	7	19	5	25	3	8	3	2
E4	11	8	4	3	10	12	32	7	42	6	14	6	5
E5	6	5	3	2	7	7	20	4	27	4	9	4	2
E6	7	10	8	29	10	32	90	5	140	22	26	26	9
E7	9	15	12	46	17	51	145	7	234	32	38	40	16
N1	5	3	3	5	3	6	18	1	33	10	7	8	7
N2	14	9	8	11	9	16	43	5	71	21	15	18	12
N3	5	3	3	2	2	3	10	1	17	5	4	3	3
N4	6	5	5	12	6	14	45	6	84	26	20	22	15
N5	6	5	4	9	6	12	35	5	64	19	14	17	10
N6	4	3	3	5	4	6	19	2	33	9	8	9	5

Table X- 23: Concentrations [µg/g oil] for triaromatic steroids. Compound names for numbers used here are shown in Figure 27.

compound	1	2	3a	3b	4	5	6	7	9	8	10
sample											
A1	49	39	12	10	66	214	126	112	45	131	16
A2	33	29	6	6	48	158	105	87	39	109	17
A3	42	38	11	8	58	195	130	101	43	132	22
A4	29	25	7	8	53	184	104	98	39	108	16
A5	25	21	4	3	30	101	60	55	22	64	8
A6	23	19	4	4	32	101	60	53	22	64	7
A7	23	15	4	3	17	57	39	32	14	36	8
A8	26	18	3	2	12	40	30	22	11	31	6
A9	50	43	10	8	77	268	148	135	50	155	19
A10	38	30	9	6	43	135	79	72	28	80	11
A11	20	16	4	3	16	53	36	28	13	37	18
A12	20	17	3	3	29	89	63	44	21	62	30
A13	45	39	10	7	73	245	138	128	47	140	19
A14	39	32	9	6	56	179	105	95	38	106	15
A15	40	35	10	8	63	201	112	104	41	116	17
A16	5	10	4	3	28	96	62	55	24	65	11
A17	19	14	4	3	23	78	50	43	17	51	12
G1	25	27	5	4	16	62	43	40	26	41	10
G2	23	24	5	5	15	62	39	40	23	39	11
G3	20	20	4	3	13	47	30	29	18	30	7
G4	26	28	5	5	18	70	44	44	28	48	12
G5	24	25	5	4	16	66	43	38	25	45	10
G6	27	27	4	3	17	70	44	44	26	47	13
G7	15	16	2	1	8	26	22	13	10	19	0
G8	16	18	4	4	14	61	41	39	24	42	11
G9	8	8	0	0	3	9	9	4	3	9	1
G10	25	25	3	4	7	29	23	13	9	19	3
G11	0	0	0	0	0	0	0	0	0	0	0
G12	25	28	6	5	18	70	46	42	26	46	12
G13	13	13	0	0	5	13	11	8	5	9	3
C1	0	0	0	0	26	138	72	91	50	75	28
C2	15	19	5	4	20	99	51	70	38	54	20
C3	14	16	3	4	10	52	28	34	20	30	14
C4	17	20	4	3	12	57	30	37	19	29	10
C5	20	26	5	4	12	60	32	41	22	33	10
C6	13	7	0	0	0	9	14	0	0	11	0
C7	11	7	0	0	0	6	13	0	0	8	0
C8	0	0	0	0	0	0	0	0	0	0	0
C9	5	2	0	0	0	17	22	0	0	16	5
C10	5	0	0	0	5	18	20	9	3	13	4
C11	14	16	0	0	6	35	17	21	8	16	6
C12	13	19	0	0	6	45	23	33	12	22	9
E1	30	26	7	6	16	113	63	83	28	71	9
E2	62	53	17	13	27	260	112	188	50	123	14
E3	30	23	7	6	14	96	53	70	22	56	5
E4	50	39	10	8	21	166	87	120	34	96	8
E5	32	26	6	4	14	106	57	75	26	62	6
E6	16	15	5	5	17	97	41	71	20	44	7
E7	19	15	6	5	23	121	50	83	23	54	7
N1	13	8	0	0	16	46	34	23	9	33	4
N2	34	25	6	6	45	132	82	66	30	84	10
N3	16	9	0	0	11	29	21	17	7	19	1
N4	12	9	0	0	27	78	55	39	18	53	7
N5	14	11	0	0	24	65	48	32	13	45	5
N6	13	8	0	0	15	41	29	21	8	28	4

Table X- 24: Concentrations [µg/g oil] for monoaromatic steroids. Compound names for numbers used here are shown in Figure 26.

compound	1	2	3	4	5	6	7
sample							
A1	1366466238	1092943869	2910283293	1150136282	605429542	404996067	4130190642
A2	1171134071	954071274	2127727286	1032012754	561762785	428090275	2234736480
A3	1260107624	1005643656	2300024786	1116720361	583745430	520342687	2454886702
A4	871624925	849390407	2920621939	939820616	469461890	192231661	2080897257
A5	634329999	597406675	2511635482	800559536	306827668	127599852	1098375401
A6	694288928	601303123	2924564766	801705654	357905382	126639218	1406415057
A7	617647868	571972104	2329504471	573275189	307692445	140911879	901813893
A8	607320582	446421093	1757424474	539090482	228524096	133869753	716586081
A9	1284326917	1112395686	2551511534	1017280035	547118784	378447372	4232647728
A10	817054732	563154826	1551720918	641511876	311514290	261678345	2366913351
A11	684533004	563355420	2351587257	647268554	292894328	160813679	1191604375
A12	658581626	661931286	2746090076	756580273	377011243	139645661	1425626697
A13	1442498029	1215255999	2534600723	1135379858	551608980	472631813	4765118838
A14	1302531106	920995988	2440488990	907556765	498257169	365397684	3991483186
A15	1001533909	799244599	2195139116	913346279	411869294	246512941	3176552648
A16	466287957	417733770	229748626	188252671	128636130	219677321	733489561
A17	477991688	528446477	2121111246	531224881	310862143	111007729	833543002
G1	525791389	344042513	1031658911	502813265	146592448	219968643	0
G2	414486225	270954610	849453493	393941197	117725430	156176310	0
G3	417332983	265728986	771414703	375025339	95890201	163429070	0
G4	429332035	269830441	877822730	392653971	104530367	199899713	0
G5	410089656	272608398	836850458	322985400	104648309	171256502	0
G6	531826664	357025854	1137099188	483423733	147286279	200003414	0
G7	303665482	201553151	648144424	233605181	86825934	168479056	0
G8	356475026	267410982	864923071	327563009	117671706	119603607	0
G9	250178230	112753911	305083337	165620371	72828024	163086361	0
G10	517853019	227444453	803758391	380171363	92826167	228711141	0
G11	46681189	2713707	5978144	15823702	0	36177053	0
G12	567513264	378342958	1130631112	536779356	147676231	241860977	0
G13	304897362	120637300	384447609	230373809	67143871	180325317	0
C1	523974311	436698645	911856853	742059179	407076378	345636743	0
C2	272056572	280738428	1171033806	435790313	217196013	326324080	179065798
C3	232369734	173176518	1059488818	362721641	173267368	135062509	119485214
C4	269748836	198664519	1138144557	410922241	208364615	157276693	147656268
C5	290732764	193743598	1214666725	442279944	221479838	164114125	117988046
C6	223246423	324836084	1526474021	322979138	234295312	278676342	440147030
C7	130220349	194069003	910305048	213067147	125908610	163510167	275290323
C8	53977947	76021372	396642692	111148461	49590483	94930404	232558993
C9	406303890	550214879	2763908337	762371568	353725165	627619247	1743607302
C10	423917169	563752603	2873273945	892305880	360962151	694304780	1869796378
C11	170099878	94774064	441207288	279788629	149852417	88623436	86957415
C12	154838579	106478374	608315261	256211630	114413727	60785820	48293711
E1	267750935	463593058	1448464517	282539562	124364493	63947697	0
E2	317226078	565437646	1817622889	318346761	136953722	57747982	0
E3	238072615	425140526	1274198385	253186675	92984439	59314378	0
E4	215645942	376521368	1167940820	200740818	95151318	58150777	0
E5	309991228	517119264	1548019339	343418398	125456937	72736177	0
E6	153688906	473206042	1604716829	137005076	104147245	22712498	74588915
E7	157853071	444086941	1524513249	135661744	99923725	21323854	67518720
N1	1433896595	1377057232	4276426536	1219874043	791870129	0	12732862894
N2	2243566142	2120908961	4052175597	1513288149	891682506	0	5712763866
N3	678874148	459237744	1665217124	410707432	282423443	124566862	2655716062
N4	2555754841	3051352884	7249515992	1418304140	1471251009	277086954	4835922649
N5	1835168199	2129751129	5376933443	1209181623	996777811	174969079	3830588309
N6	1379565450	1340753848	4066600455	809348990	688514448	132595432	2696338057

Table X- 25: Relative abundances (peak areas) for hopanes. Compound names for numbers used here are listed in Table 2.

compound	8	9	10	11	12	13
sample						
A1	4496594734	504983387	1487874684	1050884237	838573104	578780611
A2	3402833771	456023241	1106757811	800576531	700297907	494617095
A3	3646566049	502728257	1172579496	829680871	787810065	536256673
A4	4118707094	492079106	1492428160	1103032698	793854535	648439098
A5	4236545119	400493046	1385452189	970856885	714306904	484492378
A6	4725614826	441513501	1584539769	1106743377	786855922	554586534
A7	3920725413	354199147	1171614854	826763907	673713263	469636081
A8	3271483530	263608115	1001765696	716227502	557398543	375521777
A9	3776362295	466016662	1265838227	874188118	707112268	505869133
A10	2632521015	295084510	887930293	608606351	492615137	344169196
A11	3960199901	324337621	1209716313	848973422	687291041	478957730
A12	4563152213	418472348	1345235602	955841769	732639210	534692493
A13	4070152261	457279060	1390443982	975912996	773482231	553171031
A14	3890848898	424479478	1255418798	902865948	735744415	489979212
A15	3845768741	421620499	1227840844	850079403	691590629	505850053
A16	295347957	67828882	102880901	78259734	60915235	41056624
A17	3523974287	316344584	1045058045	744091297	563282512	397307573
G1	2442935145	160745988	953464739	660860775	593065717	414226017
G2	1914768191	145600189	783021809	548366527	503720471	334786503
G3	1804331913	118105079	737403698	518488222	450001591	305929373
G4	2136386749	130977534	827043347	583618872	511667533	354382739
G5	1883221079	128666114	746702845	539460551	460089336	312252230
G6	2589952856	179309364	1023109245	710873514	626593037	420382199
G7	1273058215	107137948	461576284	315277036	281616672	185405334
G8	1925170662	127678388	781411637	552908558	471610469	315761499
G9	782354820	75059513	274400836	209673513	184383566	124734903
G10	1699062450	139012746	575058835	385783682	376400470	223642673
G11	20891709	0	6903312	3343306	0	0
G12	2689516291	177734865	1062571504	749005681	657028071	461012116
G13	994018885	77359366	342395463	245309760	223975085	138310579
C1	115718425	84456749	78298528	80585801	47856358	34963035
C2	2696123467	252585233	1134580775	776421854	761831848	522256052
C3	2801698140	194840123	1032286869	725204987	672821926	431730577
C4	3169627097	211043482	1158775005	845964403	761731826	520101497
C5	3274736659	235788604	1243351958	870252200	781849223	548666749
C6	2519806066	284776006	701134304	600829604	297192342	208830982
C7	1466607127	154244128	407499943	313577166	167615712	123972423
C8	700678816	82468536	184426519	139427139	81245901	61425749
C9	4923246901	567252157	1341403758	1021550577	561515093	416645597
C10	5216888986	664537282	1388047089	1064852824	565296575	413201052
C11	1366644901	100693631	483526871	363949701	331504441	239930397
C12	1708711634	108635771	735089503	499111703	458862617	318405032
E1	1860525009	109425441	875708764	622903547	527936016	339116168
E2	2016195789	120596242	952313887	697854139	560446713	375217749
E3	1603364299	94367887	758308862	548617828	439510997	302128482
E4	1465534810	82554403	701983615	507951180	411332123	275741912
E5	2024741322	113680825	950253292	681837756	550984151	373454594
E6	1692565182	75564041	1000413633	728305650	593838733	388223158
E7	1707315549	82883613	1065692936	766673539	623688387	408986817
N1	5892733320	845955965	1425512447	1067232642	636284439	452271656
N2	5136636893	751971120	1507178410	1024499495	846022363	594520806
N3	2635570187	282664424	603694500	446988893	319187710	226715467
N4	8290897767	1030953068	2041675568	1424862287	1048496373	791771951
N5	6250769869	656659342	1509349347	1035360601	757349849	533159497
N6	5144220054	484354810	1194965512	882584787	599191588	426465582

Table X- 26: Relative abundances (peak areas) for hopanes. Compound names for numbers used here are listed in Table 2.

compound	14	15	16	17	18	19
sample						
A1	631299445	419377806	373312048	235406204	237054836	151846839
A2	550675941	393331634	324319778	216996457	203134682	138208291
A3	605888249	406065094	356720797	228191245	225566165	154606042
A4	642486382	448840532	372777237	254163635	239258330	177574762
A5	501038451	348951610	272053116	190005666	159089770	125047459
A6	561649633	384294199	303230112	219559927	167268596	139260723
A7	462706353	328151765	242262298	175257621	154750134	116240919
A8	374495679	270422935	207389526	145649167	113792133	87883837
A9	542012719	347701787	333863613	190773181	191775168	126352326
A10	355117588	240795748	207049290	121025102	120075952	85405220
A11	487887608	342685125	258568867	170563694	154748059	123394551
A12	522053035	371716695	291273606	186104066	178221173	144809848
A13	601416907	381177217	386722406	218554296	228578421	147475396
A14	529888945	346624785	314724807	192179399	180253156	123245101
A15	493197484	332293239	284099586	192438946	177591561	123781164
A16	47755668	28328752	25442667	8831049	10649870	5350897
A17	414088572	297947876	213636040	148989466	134651774	100278692
G1	408287592	283988570	215876829	142000585	193661820	124490245
G2	351887024	231484791	196815826	131228473	166168336	112451537
G3	309102730	215455416	175038516	121407163	147037802	99784629
G4	354393692	241191866	192318801	125636023	167465381	108761339
G5	322153741	221702735	175245228	122596668	154673909	94747358
G6	419453302	286337488	232106446	154250946	197301152	127008520
G7	187746438	123709518	94351671	71331803	67912923	47386406
G8	320334053	217328068	185113184	125035916	147724953	106642362
G9	103878910	77683213	63048308	46764837	58177488	36661628
G10	256255542	171183612	129383762	81232491	90319919	69774911
G11	0	0	0	0	0	0
G12	464989429	312757999	244326792	169533790	216571875	142518165
G13	142278621	99091961	88485279	65143778	75608464	46905318
C1	44878724	38577252	38968578	16606604	52053742	40419733
C2	483268616	327867323	294139557	177650860	284966300	201956727
C3	419388973	291633680	230039467	149110012	197295252	138224869
C4	478637283	325234712	262118415	175064489	214595700	145328519
C5	497790804	352190310	254011041	183928645	220949078	144173842
C6	129431091	94896528	50885946	37183354	20919518	18729209
C7	77543898	54304309	29318328	20253444	10618791	6752809
C8	41503193	29174316	18900336	11516362	7291533	6152904
C9	288933889	211468836	117381936	84078258	47145466	35556256
C10	278693105	200396331	110041923	78764970	44852362	35311030
C11	196220727	143579169	115201934	76908963	94260229	64276640
C12	287381036	191078487	153650884	112579316	137998118	100063821
E1	283327428	193362210	182394816	116776225	165165316	114973074
E2	324490703	214227163	218239511	148458836	204482389	132862707
E3	247057828	171325295	159415632	110613587	138292706	98185664
E4	228723284	158541874	147657441	98276289	132609254	91691317
E5	312803373	214176171	204815558	133484793	180790300	133775051
E6	344589987	220711412	202454107	134367876	268046472	172276335
E7	375318241	247502487	232989975	146483295	305150986	203498652
N1	330737168	227129367	145955787	99549567	58094346	40345609
N2	520814967	336796173	283241874	178127991	127486852	98106129
N3	156186459	115092061	76656556	53603857	27240758	20500900
N4	540912997	376748655	261595584	187392569	119441778	91161284
N5	408336001	279777805	202225925	136818831	92957014	71734873
N6	320596562	220431669	144888152	99961705	70338295	44133061

Table X- 27: Relative abundances (peak areas) for hopanes. Compound names for numbers used here are listed in Table 2.

compound	A1	A2	A3	A4	A5	A6	A7	A8
sample								
A1	1802487544	1287423179	431410147	594098372	935741943	593460596	487315311	915999361
A2	1881385923	1344244664	523955233	692649195	676122448	384947344	283541097	506068520
A3	1923670931	1334955776	554705800	718748058	749642257	396184689	329912943	550937670
A4	1411391453	994155595	289049024	406759480	1192447300	656982077	514473373	1175196409
A5	1075178226	774079071	247570209	366226149	1201484664	788134203	656625651	1439079517
A6	1078050307	788032052	240010409	329673866	1278102019	853978936	703673218	1476687361
A7	957406108	667029337	205233502	281423393	803560898	656395053	562216859	817236087
A8	853180365	585222071	173193131	254116041	595660290	601372707	511664471	556316795
A9	1689921002	1233635312	404422813	585159382	655360348	398566057	342609478	640070088
A10	1042132758	720071406	239123261	305829254	543047221	417668482	326793334	511666003
A11	980413487	685174088	213529885	301959450	792687748	665355419	539902024	799019773
A12	884448639	618265174	197573803	252838944	997734228	688611168	573352027	1124677915
A13	1908298061	1372939136	473771238	677114232	779857005	456082096	380773386	702679472
A14	1601392594	1108078922	363725711	522709679	773051591	519804589	408301156	715978223
A15	1265037688	920752596	309550634	438863535	757965653	490390829	401085829	787585485
A16	306076415	233588603	235284542	300742304	88752204	57374549	33824266	66630003
A17	827111623	571658817	173274499	252894600	764374274	550405968	451603420	797813968
G1	1688965175	1140937246	346589655	519377911	722041058	752020752	621666173	699924818
G2	1322692099	920340477	267772268	392496991	603881533	613516141	517071665	529533693
G3	1250881689	863907279	251211234	351196614	532272883	543465246	481434004	472249221
G4	1420252513	981311505	277364209	422298023	617600589	622482567	549883410	574737803
G5	1235627428	796818540	238383724	344038002	557829270	591047785	494803125	482213103
G6	1651024452	1120034359	330929832	495178942	737846617	769597270	647897479	677381220
G7	667576736	426896247	128763005	192853509	272532226	298541003	249514578	232537688
G8	1109181746	768435527	230123013	336026533	580518494	603589920	502420156	539950913
G9	577290573	390124059	117236192	176593142	113523265	131796924	116539376	97332779
G10	1271333694	834485549	222947089	330028484	401168450	493109747	388116150	349502138
G11	209013423	144343940	45627305	59784199	37911497	46776771	31572366	34838164
G12	1657635466	1153082883	357941609	529662193	792049376	801405070	692226233	714048149
G13	835330100	571894969	176898695	230227829	221331589	244955980	198794548	179894212
C1	4351534440	2899887938	886374941	1235190749	212299216	0	0	0
C2	2458228161	1699053106	460829234	701546182	894116445	882310037	738717055	701577485
C3	1987700048	1360389158	398306452	575262718	734500788	796584827	693430973	634403057
C4	2324976812	1585798562	484566563	710017089	867000577	913605091	802053734	736193837
C5	2463979119	1649642308	509936543	698516055	862897289	963453008	814522901	754695215
C6	309740034	211813505	65147718	87669602	106343330	93938378	71598483	104273046
C7	164895785	118563394	38406215	51195941	52498191	45365167	38131148	53293633
C8	72109724	51744503	15726326	20835011	31103954	20183420	21245903	35914717
C9	525024787	345962197	113362304	137699747	215733055	166355431	141426452	241976071
C10	582004732	412876323	130463263	175235150	245321061	176901456	148120331	277009471
C11	1642894288	1170965083	381588370	513941616	468652374	524155571	432683885	380053011
C12	1700825136	1157391973	345164945	505462052	627518953	720060627	626146941	536432326
E1	648753937	462506948	134897450	200034336	464060214	505281763	426035041	405956626
E2	502596650	365394364	111133445	153933372	468398684	520956994	441361363	461207177
E3	549900511	389448915	122672905	183827383	411627886	430109996	377405077	353417463
E4	523843186	374923618	112404275	172487168	363110478	421600825	344368825	331000610
E5	695449016	507982491	136102301	215399855	510202590	570286002	460313445	445204054
E6	271979469	228747763	60314831	84208245	457519640	518756366	440854806	452803104
E7	311773465	229622879	60275919	93447187	466131584	511339229	446448613	463370867
N1	317537389	232186950	86158559	113772142	341431022	184319725	141036399	541629611
N2	1247179583	861163336	286208464	373137828	556299235	403779603	335876800	541891482
N3	331930978	228591616	66568704	95630340	238820673	205754331	163304153	266228370
N4	434443673	307664447	106140854	126919188	975041484	391932052	305825386	1442026926
N5	325576144	249280671	65885123	102465417	666427282	319061005	251029076	867043191
N6	236272834	185197307	54966072	81003028	476396706	243978138	204431577	631583395

Table X- 28: Relative abundances (peak areas) for C_{27} -steranes. Compound names for numbers used here are listed in Table 3.

compound	B1	B2	B3	B4	B5	B6	B7	B8
sample								
A1	1814898453	1169736608	377089646	555071544	278014602	735925930	485242433	783241772
A2	2402578985	1578063953	515106576	651793426	215838532	447496614	319236961	435819751
A3	2551293994	1597880084	548000046	756327033	244344638	477136000	373640254	485226751
A4	1316676811	853360914	303816424	416314519	350322193	860605202	536237348	1033780000
A5	1042513684	662563464	240352439	315356716	449862971	979880802	724906663	1278468700
A6	989165488	673027917	219128022	317847908	410555086	905262847	747142961	1289759513
A7	1036671903	654461818	221039965	282058028	303564210	827763519	662848661	756364419
A8	928024563	560995664	206433829	258629983	261162511	770602981	594161612	545708168
A9	1716820242	1167543892	427824776	524225530	186216823	482383893	349209288	561655242
A10	1016930502	657304960	214023332	313695215	177808304	509413260	375297830	447154965
A11	1008211676	660451850	226757667	301722549	293351006	787291543	650317828	756940917
A12	860207368	573217957	199561113	272467270	333298127	872743101	649487334	988514299
A13	2014288316	1290462302	450770072	632369987	251285517	642990662	468739063	602470723
A14	1587973492	1037279407	362992951	495652994	251417966	633631321	477389419	623963900
A15	1299199290	858218970	302478593	385057478	257188650	601393660	452202656	699644562
A16	1384170292	900031384	315426381	403165820	0	0	0	0
A17	860521352	556484737	190608763	240486784	266129149	709678913	518349682	747579937
G1	1495645695	934027604	298883722	441131749	262696036	765449843	677298022	594018180
G2	1234948526	766598838	235138995	336708097	211347299	612167439	502634379	484392699
G3	1113287862	701108186	243619297	317044801	173459854	518799910	473947345	417099654
G4	1242919170	791641919	267269638	358030552	210016447	645510987	548322837	508011915
G5	1107989785	697132720	232025469	313807268	177957465	551207329	471162738	456299786
G6	1473487157	891141104	326574697	422160973	236016041	723459590	643403994	600542959
G7	663012738	415764903	124313645	187982580	100353960	351012805	288022388	233163321
G8	1010000120	622187237	202542639	313417552	185403510	570090578	474937388	482714883
G9	566649082	368355905	114033101	160477349	31851297	132039074	126619321	80125375
G10	1217820946	773980844	232064383	325623404	153891286	539748270	461684536	310430165
G11	194254904	135241656	44217406	45866487	11009335	43595408	44191983	17638449
G12	1517717439	928024160	339370506	445858014	261516078	810276909	700782468	629886077
G13	792581827	519712545	164718424	231447560	70604577	263658604	233210968	167594602
C1	5958350535	3811211463	1257447254	1648261896	0	0	0	0
C2	3184379718	2062553706	678203893	924651845	803670757	1262432680	1006675561	816057692
C3	2564482126	1631925435	563749324	744698704	675785931	1104581257	904582773	728307279
C4	3029561351	1938538900	699469573	866529212	837305802	1359026489	1123401593	899027139
C5	3281539872	2063050743	675334417	899483922	867394760	1348323219	1109783759	891557931
C6	411023109	277281657	95846296	117747292	105934570	136896595	115596149	152287316
C7	229101448	156194561	56403158	61187411	67220241	71060436	64265436	77723966
C8	83848410	61509128	19403445	22832038	11914300	35298708	25731603	43224019
C9	579408656	398886402	134506163	167629307	197950542	243872246	188700562	282029650
C10	672784976	469367069	147851652	194380373	208910385	272754691	197432420	300578985
C11	2471968620	1590769655	579579466	711806754	476220452	714082347	609444267	470070484
C12	2365903978	1555086587	531558264	670735995	627076199	1005298407	852254293	636406682
E1	695326651	461314778	153289961	197357559	164601728	521721037	433438205	368525599
E2	512282942	338380736	121993795	169311114	157242834	524152516	435450083	393392800
E3	626212803	405205834	139509453	185561970	142954020	429731592	372363361	304588354
E4	602437405	386095225	132996856	170720746	140216473	417669915	357600381	286112530
E5	777400279	516718035	180502367	225009153	177375437	571625168	486169959	381576790
E6	267124039	158643743	49832785	78785307	141987678	506634815	421915156	385027825
E7	280811654	172230518	57434184	90110637	159602934	540951570	446782704	394530402
N1	357524275	220849175	82323081	111064519	93249671	259956022	181546010	528471621
N2	1244306312	724685084	262499303	343911104	165513069	523825247	358600563	495334659
N3	292396904	196866053	66829826	84280299	80421640	225444315	179122107	229325289
N4	446146030	330038046	123065551	147882577	313470854	703084401	400907112	1488060695
N5	339748754	209501187	78321213	117879744	196986635	463928531	313512091	922208528
N6	251456141	162192791	64517837	77733145	175365452	375213229	254367976	634939219

Table X- 29: Relative abundances (peak areas) for C_{28} -steranes. Compound names for numbers used here are listed in Table 3.

compound	C1	C2	C3	C4	C5	C6	C7	C8
sample								
A1	1337339974	975400951	302406104	474715642	537151101	1021975652	713621590	853847813
A2	1865897581	1311615502	401004881	611703005	407586209	734975063	516351774	474256891
A3	1968773702	1410471448	427106027	656268373	449138135	809886650	562138253	578125306
A4	1014204100	732527753	228457987	358875483	763311406	1095299777	757867771	1184946417
A5	759283336	534761966	207960442	295014018	931812754	1152657040	840445217	1438755884
A6	745326590	521660610	195934053	267247836	888914247	1179095490	847152432	1391965060
A7	691362532	493299799	157893259	230302224	560927689	950824232	712921844	827518540
A8	644239627	414240502	139098272	191972534	422208278	822966148	651919567	545586335
A9	1308390637	919742536	307580979	464394353	429545089	812949027	571393030	590965021
A10	763911860	548122284	166924836	249430901	373377963	636270342	450330330	501743745
A11	688247871	484306746	163388766	240922809	652663577	963746082	720897564	838150798
A12	636672552	443891190	198240380	243291716	825121620	1093403371	785738758	1224440762
A13	1519925500	1130267565	364433722	508491474	532495393	913132543	622550333	675399335
A14	1234096570	861624104	298291184	435585317	468540828	855413169	645275440	710236587
A15	968239156	716586957	237001399	346530975	527371455	846569124	626247978	742059778
A16	1041610039	759827192	259346375	348731778	0	0	0	0
A17	592757706	453682339	152501281	204629499	606550563	813389929	588943513	861751719
G1	1534385853	1060757491	342847097	441997069	597300935	1061086935	807904551	750551984
G2	1208716238	833299097	278753917	386848830	502358062	878642060	673131720	625907094
G3	1131683073	768290968	245504134	365307694	438399298	772503391	568265916	531456003
G4	1245789101	892506758	282906188	386602684	547000512	878864124	658833479	637859687
G5	1120945120	767009887	236735626	348293325	459821094	799107097	618232760	568376662
G6	1522427643	1046877694	331017710	489710912	614881333	1070593955	804207635	774227872
G7	788866313	530220138	167870443	227321106	261009007	528568640	414395722	304318757
G8	1042087419	739859472	254440199	332095644	464453332	843659568	667455288	615167106
G9	598771238	426738573	157719521	194924376	91504061	207352882	135068583	122745551
G10	1239934464	842764448	232729452	365655090	364501785	779422765	601634732	404745507
G11	191392948	130108831	36971708	46219241	21645783	61180526	47780521	27965472
G12	1614955760	1114957080	384342338	502313771	636077245	1171432579	881588845	872331325
G13	749773566	532854949	178700630	234901291	153421528	332974680	244827865	197121393
C1	3403436739	2466127144	854317489	1105226207	0	0	0	0
C2	1838222970	1358191527	498107096	613714183	713330617	1213458980	1047313909	779544782
C3	1491215468	1067868856	336182390	460121693	591458445	1052401859	827828262	702985930
C4	1679053342	1202045727	436573390	544053128	630134393	1188893056	961211102	806933760
C5	1753465688	1314247950	440701702	590965479	718089630	1250672844	992946047	778382104
C6	1125476022	721442804	262351969	303746375	462967399	713214797	422820023	688449383
C7	638870264	422354474	155970327	179370532	280020054	409303641	245662807	400896517
C8	168080557	107904975	40973485	48405002	75350191	119720250	60436616	141874606
C9	1171178531	800153691	279053582	361986393	516295474	798442873	404394970	988052569
C10	1317444042	881672857	333724537	396747865	562605083	847711597	422975875	1018498155
C11	1156009771	836868096	270054409	377301332	308940768	635054208	456043912	389335016
C12	1180065133	824356889	269592754	385428117	448304057	824076497	705649029	489179861
E1	464244277	325098907	100517371	155917700	369150901	606267441	485760523	402357664
E2	351180240	263053418	89868918	122752225	341239772	610575803	491541484	407146539
E3	396677916	285589940	98535555	146850420	294626128	518870565	430843371	344308743
E4	373217397	263486074	102096620	136996946	263500534	481648861	419831110	315134754
E5	494217562	359567601	113883917	172931951	367813734	650303773	546576642	425852656
E6	179549550	124068214	44033889	63021339	323935174	559630678	511115117	404491936
E7	208251831	161735405	50499320	86644051	344117759	586263834	507385163	433709759
N1	325703229	217297750	73085874	115451867	286754650	560931488	281185658	720408616
N2	915617996	609890250	202982593	293314820	389263134	797280409	570351990	590138645
N3	220296635	155949763	50639078	72022544	175640650	322414548	227329913	275466355
N4	386533899	276851243	71271289	121910268	721206520	1167718638	535452899	1649884201
N5	308447157	220942486	53474487	97051838	509592302	826096829	443627979	1058041228
N6	219513700	149269015	46150852	77367201	382794137	599711086	385437226	762115147

Table X- 30: Relative abundances (peak areas) for C_{29} -steranes. Compound names for numbers used here are listed in Table 3.

compound	D1	D2	D3	D4	D5	D6	D7	D8
sample								
A1	128518129	107912713	66555097	34086351	110319225	61312882	117038630	103825414
A2	212272170	164424584	72165294	58690936	97439276	52377727	101324819	80457875
A3	216291712	175463790	72076791	53016951	106984882	55562229	101845403	86930804
A4	98687250	77438030	49044108	31127753	119906765	69352066	128984058	139528581
A5	83129415	57821333	29336716	17797707	127165551	85398823	125318631	140702204
A6	75794688	48142641	8346080	14551146	118406472	66028370	108202323	150392226
A7	87596253	60282519	18576386	20562575	101922348	89763557	124266017	96821810
A8	71585127	44795753	27982569	21212269	80379909	87132045	103116498	70519068
A9	106242645	88883682	38922581	34207693	89001615	46840622	90531020	82274674
A10	70750053	51489817	34672679	24553679	59141377	44057585	67468119	59522326
A11	82130015	54456597	24500038	27180919	94455457	78295035	107045799	93423643
A12	61700981	47507126	18686862	23303266	96110806	71472450	115168140	110833330
A13	131673919	107629176	70990623	49910144	95881451	60127864	111218979	93133538
A14	114680293	93722775	63837318	32832910	97941945	58492062	109828776	86383612
A15	93594511	61906040	53021307	34251125	97746163	65760032	92413230	94194285
A16	125507083	89345688	42277903	44456471	0	0	0	0
A17	72684270	48935380	18881446	24549247	87300798	76595281	98639164	93484073
G1	392707235	282319792	100174496	115453272	239444421	220892569	290910391	220609579
G2	315203087	225485701	77411298	91546078	206491343	189174892	242615889	185474014
G3	294949712	208149178	69540305	86929865	182387643	171978308	223131841	157970002
G4	331659015	236262436	83575987	87842354	191759739	185666269	245993113	199804922
G5	301816244	196726887	71109562	81164007	179514072	165277283	205558915	165086238
G6	397977624	287413618	100298317	105968448	236282817	229419091	286817969	228223266
G7	158921462	120854043	40665067	45241049	109830771	132740510	144221829	105138585
G8	267013352	185723294	73255299	86764866	190166825	186584141	233162572	186306118
G9	154599339	108125634	34241783	43837717	36541748	44418546	56185458	34690009
G10	298403003	201267426	76442537	81213242	156897303	181054684	219571123	133839810
G11	43737038	31709453	5959086	11081047	14877685	18529322	16433707	8570474
G12	410580725	295354472	106803990	127049021	251831570	258507926	291607489	247338980
G13	222076836	157035621	53460016	61596962	68045059	79144325	101564223	66512494
C1	1323329012	1042559257	407604638	374602948	0	0	0	0
C2	754497729	537586354	215317926	220343947	394965194	336506994	466641566	315236104
C3	558496320	394598432	157471613	170581086	297491305	282478093	356434710	253277653
C4	645246874	486370444	203607419	199499666	329431917	325658177	400674880	288696132
C5	707590081	503438624	171085038	208977061	333845037	327259688	404725470	302161881
C6	53640354	35236245	20349725	17033929	16854150	21291384	20288733	15557079
C7	34004656	22156737	5905330	10680265	9723901	11460175	11278975	8500471
C8	11751346	8687184	1100941	6302471	7045733	4695740	7037323	9144999
C9	87731687	62107934	4436075	30137470	50917391	47347573	57895713	49334375
C10	98389285	64456983	14170132	26957763	47128584	47359946	70009366	57553090
C11	425285185	292745011	69079464	128960421	148444011	178439232	199444208	129635277
C12	488584006	332256548	75397271	141653180	219603949	245517458	303764720	199635046
E1	58251548	43200174	10526579	20433957	43101343	61445611	66480529	45618540
E2	39971853	29598021	11038193	29583295	49815223	51105255	73847587	45326648
E3	51384776	31420433	10781395	16809970	43094111	49459575	62391830	42232763
E4	48726433	28333958	9492714	17801437	38863737	45041624	59555209	35342259
E5	59682446	40167613	17684380	17163046	50207465	61282103	73422678	47786757
E6	16692491	0	0	0	39456089	46078002	53593747	36728973
E7	17534745	0	0	0	40369496	46275378	60787516	36365188
N1	19795714	19482479	19726353	9155022	51929334	30864809	57630858	35645349
N2	69156816	0	0	0	95955011	56571338	62533737	60055386
N3	13932768	0	0	0	23929847	24017858	30704907	22743503
N4	0	0	0	0	70469377	35420645	66275176	133134437
N5	0	0	0	0	55275575	25204260	36814865	73474842
N6	0	0	0	0	44848278	28458885	43816208	56029230

Table X- 31: Relative abundances (peak areas) for C_{30} -steranes. Compound names for numbers used here are listed in Table 3.

compound	*i*-C_4	*n*-C_4	*i*-C5	*n*-C_5	2MP	3MP	*n*-C_6	MCP	BZ	CH	3Mhex	*n*-C_7	MCH	Tol
sample														
A1	-34.3	-31.9	-32.5	-32.0	-33.6	-30.8	-32.5	-29.9		-32.5	-31.7	-32.9	-30.1	-35.0
A2														
A3														
A4			-30.4	-30.6	-33.5	-31.4	-34.1	-31.4		-33.8	-32.8	-36.3	-33.7	-40.5
A5	-38.1	-36.0	-35.1	-35.9	-35.6	-33.8	-36.5	-32.8	-38.7	-35.2	-34.1	-37.1	-34.2	-38.0
A6	-38.2	-35.9	-34.9	-35.5	-35.2	-33.1	-35.9	-31.6		-34.8	-33.0	-35.9	-32.7	-36.3
A7		-34.1	-33.6	-34.4	-34.5	-33.0	-35.4	-32.0		-34.7	-32.8	-35.8	-33.1	-35.5
A8	-37.9	-36.0	-34.6	-35.4	-35.0	-33.6	-36.0	-32.4	-36.8	-34.3	-33.1	-36.3	-33.5	-37.4
A9								-29.3		-32.7	-31.8		-30.6	-34.1
A10		-25.4	-30.0	-27.5				-29.1		-31.5	-32.0		-29.7	
A11	-37.4	-35.6	-34.3	-35.1	-34.7	-33.3	-35.3	-31.7	-37.0	-34.5	-32.6	-35.7	-33.0	-36.7
A12	-38.0	-36.2	-34.7	-35.5	-35.0	-33.9	-35.6	-31.9	-37.7	-34.5	-33.0	-35.8	-32.9	-36.2
A13														
A14	-34.6	-32.2	-32.4	-31.4	-33.5	-30.1	-32.6	-29.1		-31.8	-31.7	-33.1	-29.5	
A15	-35.8	-33.7	-33.3	-33.8	-34.1	-32.7	-34.7	-30.6		-33.9	-32.3	-34.7	-32.1	-35.2
A16	-35.5	-34.4	-33.3	-33.9	-33.6	-32.3	-34.1	-31.2		-33.2	-31.2	-34.8	-32.9	
A17			-33.7	-33.2	-34.3	-32.2	-34.5	-31.3		-34.3	-32.6	-35.0	-32.3	
G1		-20.3	-26.8	-24.5	-27.1	-27.7	-26.2		-25.7	-26.9		-25.1	-27.2	-27.0
G2	-26.5	-21.5	-26.9	-23.9		-27.5	-25.9		-24.5	-26.5	-29.1	-25.8	-27.2	-27.3
G3	-28.1	-26.5	-28.1	-28.0		-28.5	-28.5		-25.4	-26.9	-29.6	-28.5	-27.5	-26.9
G4	-27.6	-24.1	-27.6	-26.6		-28.2	-28.4		-25.6	-26.9	-29.6	-27.2	-27.3	-27.2
G5	-25.9	-22.3	-26.5	-24.5		-27.7	-28.4		-25.3	-26.3	-29.3	-26.1	-26.8	-26.9
G6	-26.9	-23.3	-27.3	-25.4		-27.8	-28.2		-24.6	-26.1	-29.2	-26.0	-26.7	-26.4
G7		-24.8	-25.5	-26.2	-26.1	-26.6	-27.4		-26.0	-26.5	-27.1	-28.3	-27.0	-28.0
G8	-28.7	-27.8	-28.8	-29.3	-29.6	-28.9	-30.4			-28.4	-29.8	-30.5	-28.6	
G9	-25.7	-25.1	-26.0	-26.0	-26.4	-26.4	-26.6		-27.6	-25.2	-27.6	-27.7	-26.5	-30.9
G10			-24.1	-25.1	-26.0	-26.3	-26.8		-25.1	-25.6	-26.9	-27.8	-26.5	
G11	-26.2	-25.3	-27.1	-26.6	-27.6	-27.7	-27.7		-28.4	-25.5		-29.2	-28.2	-29.3
G12														
G13	-28.6	-27.3	-28.5	-28.5		-28.7	-29.0		-26.4	-26.8	-29.2	-29.5	-27.5	-26.6
C1														
C2													-23.4	
C3	-30.3	-29.4	-28.7	-29.0	-28.6	-28.2	-29.0	-27.6		-28.9	-28.7	-29.5	-27.2	-27.1
C4	-30.2	-29.6	-29.0	-29.4	-29.1	-28.5	-30.1	-27.8		-28.6	-28.8	-29.4	-27.5	-28.7
C5							-26.2	-25.8		-26.9	-26.8	-28.0	-25.9	
C6													-24.2	
C7													-21.7	
C8										-23.4			-22.3	
C9			-25.3	-24.4	-25.3	-24.7	-24.1	-24.8		-25.0	-23.7	-24.7	-23.6	
C10														
C11	-28.9	-25.5	-27.4	-27.1	-27.0	-27.3	-24.6	-24.7		-25.2	-26.2		-24.4	-26.2
C12										-25.2		-26.5	-22.5	
E1			-25.7	-26.5	-26.0	-24.9	-27.2	-23.9		-25.8	-24.5	-27.6	-24.9	
E2				-24.1			-24.8	-23.5		-26.9		-24.9	-24.8	
E3			-26.3	-26.3	-25.7	-25.1	-27.1	-24.4		-24.7	-25.0	-28.0	-23.9	
E4			-26.2	-26.2	-26.0	-25.6	-27.5	-25.2		-26.6	-24.9	-28.2	-26.9	
E5														
E6														
E7														
N1			-30.7	-30.3	-32.0	-31.7	-31.0	-30.4		-32.5	-29.9	-31.3	-30.8	-33.1
N2	-34.1	-27.9	-31.3	-27.1	-32.2	-30.5		-30.5		-31.4	-31.4		-30.9	-30.3
N3	-36.1	-32.0	-32.9	-32.1	-32.8	-32.5	-32.3	-30.7		-32.7	-31.5	-31.9	-31.8	-34.0
N4			-32.1	-32.2	-34.6	-33.0	-33.5	-32.4		-34.0	-34.5	-34.6	-32.7	-34.1
N5	-37.1	-34.9	-34.8	-34.1	-34.4	-34.1	-34.1	-32.6	-36.5	-32.8	-33.4	-34.3	-32.8	-37.5
N6	-37.0	-36.0	-34.7	-34.9	-34.8	-34.4	-34.7	-33.0	-37.0	-33.6	-33.6	-34.6	-33.8	-38.1

Table X- 32: $\delta^{13}C$ ratios [‰] for i-C_4 - toluene in all crude oil samples. Samples A2, A3, A13, C1 were too pasty for injection into the GC-IRMS, hence, no data can be provided.

compound	*n*-C_8	ECHex	m/pX	oX	*n*-C_9	*n*-C_{10}	*n*-C_{11}	*n*-C_{12}	*n*-C_{13}	*n*-C_{14}	*n*-C_{15}	*n*-C_{16}	*n*-C_{17}	Pr
sample														
A1	-31.7	-32.2	-32.8	-32.8		-32.3	-32.6	-33.1	-32.3	-32.1	-34.1	-34.5	-34.2	-34.2
A2														
A3														
A4	-34.9	-35.3	-36.4	-35.2	-35.7	-35.5	-35.6	-35.5	-35.9	-35.4	-34.8	-35.7	-35.3	-35.1
A5	-36.1	-35.7	-37.1	-35.9	-36.1	-37.0	-38.5	-38.0	-37.3	-38.2	-38.0	-37.7	-37.1	-36.6
A6	-35.2	-33.8	-34.6	-36.2	-34.6	-35.5	-35.9	-36.0	-36.2	-36.1	-35.7	-36.4	-36.4	-36.1
A7	-35.2	-34.3	-35.7	-35.4	-35.1	-35.5	-35.9	-35.9	-35.6	-35.3	-36.1	-35.9	-34.5	-36.4
A8	-35.7	-34.7	-36.0	-35.6	-35.6	-37.2	-35.4	-37.0	-37.2	-35.8	-36.1	-36.1	-35.6	-36.8
A9	-30.2	-32.3	-32.2	-32.5	-31.7	-32.8	0.0	-32.2	-33.4	-34.4	-34.3	-34.1	-36.5	-34.8
A10	-31.0	-31.8	-32.4	-31.9	0.0	-32.6	-33.1	-32.7	-34.8	-33.2	-33.7	-34.6	-34.5	-34.6
A11	-35.1	-34.2	-36.2	-35.7	-35.9	-36.8	-36.6	-37.1	-37.1	-35.9	-37.7	-37.1	-37.6	-36.0
A12	-35.2	-34.5	-35.9	-34.7	-35.4	-35.9	-35.8	-36.0	-35.7	-37.2	-36.1	-36.7	-34.8	-36.7
A13														
A14	-31.1	-31.9	-32.9	-32.1	-30.5	-31.9	-32.3	-33.0	-33.3	-34.2	-34.4	-34.3	-35.4	-34.7
A15	-32.5	-33.5	-34.4	-34.2	-31.7	-33.6	-34.0	-34.1	-35.3	-34.4	-34.6	-34.3	-34.6	-34.1
A16	-34.4	-33.6	-33.6	-34.3	-34.5	-33.9	-33.9	-34.1	-34.7	-33.8	-34.4	-35.0	-35.3	-35.2
A17	-34.5	-34.1	-34.6	-34.2	-34.2	-35.2	-35.2	-35.3	-35.1	-35.7	-36.2	-36.0	-35.7	-36.1
G1	-28.3	-27.6		-26.9	-25.1		-29.1			-28.5	-29.6	-28.2	-28.8	-31.0
G2	-26.4	-28.7	-27.9	-28.1	-26.1	-28.5	-30.1			-28.7	-29.5	-27.2	-28.1	-31.3
G3	-27.7	-28.2	-28.0	-27.9	-27.3	-27.6	-29.1	-28.0	-28.9	-28.7	-29.2	-29.6	-29.2	-31.5
G4	-26.9	-28.4	-28.3	-27.9	-27.7	-28.8	-29.5			-28.6		-28.3	-30.8	-31.8
G5	-26.7	-28.1	-27.7	-27.6	-27.3	-28.2	-28.9	-28.9		-29.4	-29.8	-28.9	-29.0	-31.0
G6	-26.6	-27.6	-27.6	-27.5	-25.7	-25.7				-31.1		-31.0	-31.4	-31.6
G7	-28.1	-27.9	-28.8	-28.0		-29.9	-30.4	-30.0	-29.7		-29.6	-30.1	-30.0	-29.4
G8		-28.7		-30.2	-30.2	-31.2	-31.6	-32.2	-31.8	-32.1	-31.5	-31.9	-31.4	-32.4
G9	-28.2	-27.1	-27.4	-26.8	-29.4	-29.9	-30.2	-30.2	-30.1	-29.8	-29.9	-29.1	-30.6	-30.3
G10	-28.8						-28.4	-28.5	-28.7	-28.8	-29.1	-29.1	-29.6	-29.8
G11	-28.8	-27.1			-29.0	-29.4	-30.0	-30.2	-29.8	-29.8	-30.2	-30.2	-30.2	-30.8
G12														
G13	-29.0	-28.6	-28.0	-27.7	-28.5	-28.9	-29.8	-29.5	-29.9	-29.6	-30.0	-29.7	-29.9	-31.8
C1														
C2	-26.8	-26.8	-27.6	-28.1	-26.4	-27.6	-28.0	-27.9	-28.4	-29.9	-28.0	-29.1	-28.7	-29.8
C3	-29.4		-29.9	-28.6	-31.3	-32.4	-32.0	-31.1	-29.1	-29.1	-28.7	-30.5	-30.4	-30.9
C4	-29.7	-29.6	-31.4	-30.5	-31.0	-30.8	-29.6	-31.4	-32.2	-33.2	-31.3	-31.0	-30.6	-32.6
C5	-27.7	-27.9	-28.8	-28.9	-28.0	-27.3	-27.2	-28.9	-29.2	-30.0	-30.3	-31.4	-28.9	-30.3
C6	-25.0	-25.4	-25.1	-26.1		-26.9	-27.0	-27.2	-26.8	-27.5		-28.0	-28.7	-20.8
C7	-23.5	-24.3	-24.1	-25.0	-24.7	-25.1	-25.7	-26.3	-28.5	-27.3	-26.0	-27.4	-25.6	-27.4
C8	-23.0	-23.8	-24.3	-25.8	-24.7	-27.7	-27.8	-28.0	-25.2	-28.5	-28.9	-29.5	-26.4	-29.9
C9	-24.4	-24.7	-24.6	-26.1	-24.5	-25.7	-25.6	-26.0	-26.8	-28.0	-27.7	-27.1	-30.3	-28.9
C10		-27.2	-21.8		-24.5	-24.7	-25.6	-25.7	-25.6	-26.1	-25.6	-27.2	-28.0	-28.3
C11	-27.7				-26.9	-26.6	-28.0	-27.8	-27.9	-28.2	-28.7	-29.0	-28.2	-29.2
C12	-27.6				-26.8	-28.3	-28.4	-28.3	-28.5	-28.6	-29.2	-28.8	-28.9	-29.0
E1	-27.8	-26.2	-27.9		-27.8	-27.8	-28.2	-30.2	-30.0	-29.2	-29.0	-29.7	-29.6	-31.4
E2	-23.5	-25.4	-27.7	-27.3	-22.6	-26.0				-25.5				-29.4
E3	-27.7	-26.4	-27.8		-28.2	-28.0	-27.8	-28.4	-28.9	-28.1	-29.2	-28.7	-28.2	-28.1
E4	-27.8	-26.6	-28.6		-28.1	-28.6	-29.0	-28.6	-30.2	-28.8	-29.3	-28.7	-27.7	-29.3
E5	-25.6	-27.2	-29.3		-27.9	-27.9	-28.0	-28.6	-28.7	-28.8	-29.2	-29.9	-28.5	-29.1
E6														
E7														
N1	-29.9	-31.5		-33.4	-30.8	-31.6	-31.9	-32.4	-32.9	-33.4	-33.5	-33.3	-33.7	-34.5
N2	-31.1	-32.1	-33.1											
N3	-32.2	-32.1	-33.4	-34.1	-31.0	-32.2	-32.2	-32.7	-32.9	-34.1	-34.2	-34.1	-36.2	-35.4
N4	-33.6	-33.6	-34.0	-34.8	-33.7	-33.5	-33.6	-34.1	-34.3	-35.2	-33.0	-35.1	-35.6	-35.9
N5	-33.0	-35.0	-35.3	-35.0	-33.4	-34.1	-33.9	-35.9	-37.2	-37.3	-36.7	-36.8	-37.5	-37.7
N6	-35.0	-35.2	-37.4	-36.0	-36.6	-36.5	-38.7	-40.4	-39.7	-40.5	-38.8	-39.2	-39.8	-39.9

Table X- 33: $\delta^{13}C$ ratios [‰] for *n*-C_8 - pristane in all crude oil samples. Samples A2, A3, A13, C1 were too pasty for injection into the GC-IRMS, hence, no data can be provided.

compound	*n*-C_{18}	Ph	*n*-C_{19}	*n*-C_{20}	*n*-C_{21}	*n*-C_{22}	*n*-C_{23}	*n*-C_{24}	*n*-C_{25}	*n*-C_{26}	*n*-C_{27}	*n*-C_{28}	*n*-C_{29}	*n*-C_{30}
sample														
A1	-33.7	-34.2	-34.6	-33.7	-36.3	-33.4	-35.2	-36.1	-35.9	-37.9	-37.9			
A2														
A3														
A4	-35.3	-34.8	-35.2	-35.0	-35.4	-35.1	-35.1	-35.0	-35.9	-35.5	-35.4	-35.9	-37.1	-38.6
A5	-36.4	-35.6	-36.8	-35.7	-37.4	-35.9	-35.5	-35.5	-35.6	-35.0	-35.4	-37.0	-37.4	-38.5
A6	-36.4	-35.6	-36.1	-35.8	-36.7	-35.4	-36.1	-35.6	-36.0	-36.5	-36.5	-35.8	-36.7	-39.4
A7	-36.2	-34.7	-35.3	-35.3	-35.7	-35.6	-36.6	-35.1	-34.4	-34.7	0.0	0.0	0.0	0.0
A8	-36.1	-36.3	-36.3	-36.0	-36.1	-35.7	-37.2	-35.4	-34.6	-35.4	-35.5	-34.8	-34.6	0.0
A9	-36.0	-34.4	-35.0	-36.2	-36.5	-36.1	-36.3	-36.1	-34.8	-35.9	0.0	0.0	0.0	0.0
A10	-36.2	-34.5	-36.0	-34.5	-36.4	-35.2	-34.5	-36.7	-35.0	-38.9	-38.4	-34.3	-37.8	-41.6
A11	-35.8	-35.8	-36.1	-36.3	-36.8	-36.0	-35.6	-34.7	-35.9	-35.5	-35.5	-36.2	-35.9	-36.5
A12	-36.7	-36.4	-36.8	-36.2	-36.4	-36.9	-36.8	-35.5	-33.0	-36.3	-34.6	-34.5	-35.4	-35.5
A13														
A14	-34.8	-34.5	-34.8	-34.6	-35.4	-35.5	-38.9	-35.0	-32.9	-36.6	-37.5	-36.4	-36.3	0.0
A15	-34.2	-33.7	-34.5	-34.4	-35.3	-35.7	-36.4	-35.4	-34.2	-35.1	-36.0	-36.2	-36.7	-38.1
A16	-35.4	-34.8	-36.6	-36.7	-36.9	-36.3	-36.9	-36.0	-35.3	-35.2	0.0	0.0	0.0	0.0
A17	-36.5	-35.0	-36.0	-34.4	-33.7	-34.8	-34.4	-34.6	-34.7	-34.0	-33.6	-35.0	-35.4	-36.0
G1	-31.0	-31.7												
G2		-31.8	-29.6			-28.9								
G3	-29.7	-31.5	-29.5	-29.5	-30.6	-29.3	-30.6	-29.7	-24.7	-34.7	-30.3	-31.8	-29.3	-30.5
G4	-29.0	-32.0		-30.4	-31.4	-30.7		-31.0			-29.6			
G5	-30.6	-31.1		-29.4	-29.4	-29.5	-28.1	-29.8			-30.6		-29.1	
G6		-32.0				-28.1	-29.3	-30.0	-27.6		-32.3			
G7	-29.6	-29.8	-29.9	-29.8	-30.8	-29.9	-30.1	-29.6	-30.4	-30.6	-30.9	-31.4	-31.7	-32.6
G8	-31.4	-32.8	-31.8	-31.2	-31.7	-31.5	-31.4	-32.8	-31.6	-31.5	-30.7	-31.6	-32.7	-32.2
G9	-30.0	-30.3	-29.4	-29.6	-29.2	-30.1	-29.2	-28.8	-29.1	-29.0	-29.5	-30.2	-31.2	-30.7
G10	-29.8	-29.9	-30.1	-30.6	-29.9	-30.0	-29.7	-29.4	-30.0	-29.7	-30.2	-30.2	-30.1	-30.2
G11	-29.9	-30.4	-29.8	-30.7	-30.3	-29.8	-30.0	-30.4	-30.0	-30.4	-31.0	-30.5	-30.4	-31.6
G12														
G13	-29.8	-31.8	-29.8	-30.2	-30.2	-29.4	-29.6	-29.5	-29.2	-30.4	-29.2	-29.7	-29.7	
C1														
C2	-29.0	-29.3	-29.0	-28.6	-28.7	-29.4	-29.1	-31.0	-29.3	-28.3	-32.0	-30.2	-30.9	
C3	-30.5	-30.5	-29.9	-29.6	-30.0	-30.2	-30.5	-30.6	-30.5	-30.5	-32.2	-30.7		
C4	-30.5	-32.3	-31.2	-31.8	-31.3	-33.3	-33.5	-34.3						
C5	-30.6	-28.9	-30.3	-29.2	-30.7	-30.1	-30.2	-27.4	-29.4					
C6	-29.1	-30.3	-28.7	-29.1	-29.3	-28.4	-29.1	-29.7	-28.6	-29.6	-30.6	-30.4	-30.0	
C7	-26.5	-26.2	-26.7	-27.9	-28.1	-28.2	-30.2	-29.5	-31.7	-28.8	-32.3	-31.2		
C8	-28.9	-30.2	-29.1	-28.4	-28.1	-27.8	-28.5	-28.1		-29.9	-30.3	-27.7		
C9	-27.2	-27.4	-27.2	-26.8	-28.3	-28.6	-29.0	-30.6	-29.4	-29.0	-31.2	-30.4	-31.6	-33.2
C10	-28.1	-26.2	-27.6	-26.7	-28.1	-27.4	-27.5	-27.2	-27.9	-28.0	-25.1	-28.0	-28.1	-28.4
C11	-28.6	-28.6	-28.0	-27.9	-28.9	-29.9	-28.3	-26.2	-28.7	-28.5	-28.8	-28.6	-30.0	-28.6
C12	-29.2	-28.6	-28.2	-29.8	-29.1	-29.8	-29.9	-29.9	-33.3	-29.4	-28.8	-27.6	-29.6	-27.1
E1	-30.2	-30.1	-30.1	-31.5	-30.8	-30.2	-30.5	-29.8	-30.0	-29.2	-29.8	-29.8	-32.4	-30.3
E2	0.0	-27.1												
E3	-28.6	-28.9	-28.1	-28.6	-28.1	-28.1	-27.9	-28.0	-28.2	-27.6	-28.0	-28.1	-28.4	-28.7
E4	-28.2	-29.2	-28.5	-28.6	-29.2	-29.0	-27.8	-28.7	-28.0	-27.6	-28.4	-29.0	-28.9	-30.9
E5	-29.4	-30.2	-28.7	-29.9	-28.6	-28.5	-28.8	-28.8	-28.4	-29.2	-28.6	-29.9	-29.7	-30.9
E6														
E7														
N1	-33.6	-32.8	-34.0	-35.0	-34.8	-35.3	-35.4	-34.4	-35.4	-34.6	-35.1	-35.6		
N2														
N3	-36.0	-34.5	-34.8	-34.6	-35.3	-34.2	-35.2	-34.0	-34.3	-34.1	-34.5	-34.6	-34.4	
N4	-35.4	-35.9	-35.3	-35.6	-36.1	-35.2	-34.7	-35.3	-36.2	-35.5	-37.9	-37.2	-38.1	-41.9
N5	-37.5	-37.6	-37.0	-37.8	-32.1									
N6	-38.3	-40.5	-41.2	-40.2	-39.9	-39.4	-39.4	-38.8	-40.2	-38.6	-39.6	-38.5	-38.8	-38.9

Table X- 34: $\delta^{13}C$ ratios [‰] for *n*-C_{18} – *n*-C_{30} in all crude oil samples. Samples A2, A3, A13, C1 were too pasty for injection into the GC-IRMS, hence, no data can be provided.

compound	i-C_4	n-C_4	i-C_5	n-C_5	2MP	3MP	n-C_6	MCP	BZ	CH	3Mhex	n-C_7
sample												
A1		-125.7	-117.2	-132.4	-141.7	-112.8	-145.0	-93.8		-127.9	-135.7	-147.9
A2												
A3												
A4				-158.7	-149.9	-129.7	-158.6	-102.5		-142.9	-138.9	-166.3
A5	-132.3	-181.1	-141.2	-173.5	-152.3	-136.9	-168.3	-109.6		-153.9	-154.9	-179.9
A6		-182.1	-142.8	-171.4	-151.7	-132.6	-169.0	-98.3		-143.1	-142.8	-165.1
A7		-150.4	-126.8	-150.7	-137.8	-130.4	-156.1	-110.6		-142.8	-137.7	-159.2
A8	-126.8	-154.6	-122.3	-146.9	-134.2	-124.5	-155.6	-103.8		-134.7	-131.6	-161.4
A9				-123.2	-162.4		-165.4	-113.4		-154.3	-161.3	
A10	-94.5	-60.8	-104.7	-68.5				-72.6		-94.3	-100.0	
A11	-129.2	-159.6	-128.4	-150.3	-134.5	-124.2	-151.9	-99.5		-125.5	-127.5	-152.2
A12	-138.2	-163.6	-135.4	-156.9	-139.8	-126.9	-156.6	-104.7		-125.1	-132.8	-158.0
A13												
A14	-107.5	-136.2	-131.0	-146.7	-151.4	-132.8	-166.1	-106.4		-135.5	-144.1	
A15	-116.9	-156.6	-132.9	-160.2	-150.9	-129.9	-165.3	-104.8		-143.0	-142.0	-165.6
A16		-103.2	-115.9	-139.3	-125.0		-164.9	-122.9		-159.5		-172.1
A17			-127.4	-150.6	-143.4	-127.8	-162.3	-114.9		-145.0	-141.4	-166.9

compound	i-C_4	n-C_4	i-C_5	n-C_5	2MP	3MP	n-C_6	MCP	BZ	CH	3Mhex	n-C_7
sample												
G1			-145.3	-144.2	-126.8		-144.8		-139.8	-102.8	-145.8	
G2			-125.0	-118.7	-114.5		-138.4		-147.2	-115.9	-144.8	
G3			-123.1	-141.5	-112.5	-86.5	-134.7		-144.0	-99.7	-135.2	
G4			-90.2	-102.9	-129.7	-120.9	-166.3	-122.4		-158.5	-161.4	-174.8
G5			-103.8	-97.5	-142.6	-156.6	-168.9	-139.7		-164.3	-170.3	-190.3
G6	-106.2	-74.6	-116.0	-110.1	-142.1	-152.3	-153.1	-125.8		-140.0	-134.0	-163.9
G7		-123.5	-111.0	-131.3	-133.8	-121.7	-147.2	-114.2	-124.7	-133.6	-131.7	-156.7
G8	-131.1	-126.9	-127.2	-136.8	-140.0	-134.2	-149.7	-121.3		-138.3	-144.0	-158.5
G9	-120.1	-126.3	-120.5	-123.4	-125.5	-116.2	-128.4	-95.4	-94.3	-107.7	-111.2	-124.2
G10					-132.6	-126.8	-165.0	-116.5	-123.1	-132.3	-138.9	-172.5
G11	-99.1	-118.3	-124.0	-128.0	-132.1	-121.6	-129.7	-95.0	-116.3	-103.6	-109.0	-116.6
G12												
G13	-114.1	-131.0	-123.5	-136.9	-139.7	-134.2	-148.6	-101.1	-109.1	-122.8	-123.8	-139.2

compound	i-C_4	n-C_4	i-C_5	n-C_5	2MP	3MP	n-C_6	MCP	BZ	CH	3Mhex	n-C_7
sample												
N1	0.0	0.0	-140.3	-153.0	-147.4	-138.1	-154.1	-114.6	-105.4	-135.6	-127.0	-142.5
N2	0.0	0.0	0.0	0.0	0.0	0.0	0.0	-76.7	0.0	-98.2	0.0	0.0
N3	-133.1	-134.1	-126.8	-132.2	-136.6	-129.3	-137.1	-116.6	0.0	-130.7	-120.7	-131.8
N4	0.0	0.0	-111.7	-143.7	-142.9	-130.4	-148.6	-121.3	0.0	-139.8	-134.8	-145.7
N5	-125.5	-141.6	-132.0	-147.7	-143.3	-132.4	-146.2	-111.3	-74.6	-137.4	-124.6	-132.1
N6	-130.5	-160.4	-131.0	-152.4	-141.8	-125.8	-148.3	-108.7	-112.2	-126.8	-125.4	-134.8

Table X- 35: δD ratios [‰] for *i*-C_4 to *n*-C_7 in crude oils from Angola, Norway and Nigeria. Samples A2, A3 and A13 were too pasty for injection into the GC-C-IRMS, hence, no data can be provided. Due to limited sample amounts of G12 no GC-C-IRMS measurements for hydrogen isotopic compositions were possible.

compound	MCH	Tol	n-C_8	ECHex	EtB	m/pX	oX	n-C_9	n-C_{10}	n-C_{11}	n-C_{12}	n-C_{13}
sample												
A1	-95.5		-114.9	-107.2		-97.6	-117.3		-118.7	-114.4	-112.3	-115.9
A2												
A3												
A4	-108.3	-103.6	-150.8			-114.9	-141.2	-126.5	-141.8	-142.1	-114.4	-111.0
A5	-125.4	-121.1	-170.5			-119.7	-122.7	-155.8	-163.7	-151.4	-154.8	-155.1
A6	-115.4	-115.5	-152.4			-126.4	-139.2	-139.6	-139.4	-137.7	-137.9	-133.7
A7	-113.4	-117.3	-148.7			-117.1	-137.3	-134.6	-147.4	-140.2	-122.6	-125.2
A8	-114.5	-116.2	-146.2			-108.8	-118.5	-134.1	-143.7	-139.8	-136.8	-133.8
A9	-121.2		-117.8	-97.2		-105.6			-129.0	-123.5	-89.6	-97.6
A10	-71.0		-81.4	-84.6		-72.0	-80.5		-81.1	-72.7	-68.8	-76.5
A11	-112.3	-109.5	-138.8			-109.0	-122.8	-128.2	-139.3	-135.1	-132.2	-132.8
A12	-108.5	-104.5	-148.8			-104.8	-124.3	-131.9	-146.9	-139.7	-142.7	-139.4
A13												
A14	-118.9		-123.1	-111.1		-96.7	-124.2		-121.5		-90.5	-106.1
A15	-110.1	-107.0	-136.2			-118.4	-148.7	-128.1	-139.0	-142.4	-117.6	-117.6
A16	-129.9		-132.6	-97.0		-109.6		-107.1	-106.2	-100.0	-95.9	-100.3
A17	-119.9	-118.6	-157.1	-104.9		-125.3		-142.7	-145.7	-144.0	-145.0	-143.7

compound	MCH	Tol	n-C_8	ECHex	EtB	m/pX	oX	n-C_9	n-C_{10}	n-C_{11}	n-C_{12}	n-C_{13}
sample												
G1		-113.5	-67.9	-112.0	-95.8	-124.9	-108.4	-93.6	-103.9	-73.8	-70.7	-79.9
G2		-123.0	-83.2	-123.0	-105.7	-130.4	-113.5	-109.0	-118.0		-114.3	-111.5
G3		-147.4	-63.5	-109.5	-127.1	-127.8	-117.2	-118.3	-102.9		-96.7	-101.8
G4	-151.7	-152.1	-165.0	-131.5	-83.0	-127.6	-127.4	-138.8	-135.3	-118.4	-110.5	-96.1
G5	-164.4	-160.8	-143.2	-134.6		-118.2	-126.4	-120.2	-132.9	-116.4	-114.2	-117.4
G6	-116.0	-131.9	-123.8	-119.6		-106.6	-122.5	-114.9	-125.8	-111.5	-102.7	-111.1
G7	-130.1	-140.9	-148.8	-115.8	-75.8	-131.2	-127.8	-132.4	-129.3	-124.8	-122.3	-119.2
G8	-122.5	-128.9	-140.4	-112.7	-57.5	-115.6	-128.0	-122.1	-123.8	-119.0	-118.3	-118.1
G9	-93.0	-119.5	-116.5	-102.4	-57.6	-114.1	-116.7	-108.2	-122.3	-117.6	-119.3	-118.8
G10	-134.4	-137.9	-145.1	-114.9	-76.4	-125.8	-123.1	-130.4	-132.4	-127.1	-125.4	-119.6
G11	-101.0	-119.3	-117.4	-99.3	-39.8	-117.0	-122.4	-101.7	-106.7	-99.7	-102.5	-96.9
G12												
G13	-107.7	-119.1	-132.8	-111.5	-58.6	-106.3	-113.2	-121.6	-125.4	-118.8	-118.0	-118.5

compound	MCH	Tol	n-C_8	ECHex	EtB	m/pX	oX	n-C_9	n-C_{10}	n-C_{11}	n-C_{12}	n-C_{13}
sample												
N1	-104.6	-124.6	-131.4	-117.3	-46.3	-128.0	0.0	-121.4	-117.1	-120.6	-120.7	-111.5
N2	-67.5	0.0	-95.4	-99.9	0.0	-75.2	0.0	0.0	0.0	0.0	0.0	0.0
N3	-96.2	-113.1	0.0	-114.4	-22.9	-128.2	0.0	0.0	0.0	-130.2	-138.2	-124.0
N4	-118.4	-120.5	0.0	-122.3	-51.5	-126.3	0.0	-112.2	-123.8	-125.9	-122.7	-116.4
N5	-103.8	-120.3	0.0	-120.0	-59.6	-118.7	0.0	0.0	-118.8	-112.8	-126.2	-113.2
N6	-79.3	-122.7	-110.0	-102.4	-62.4	-117.9	-123.4	-97.4	-97.3	-102.0	-113.9	-94.2

Table X- 36: δD ratios [‰] for methylcyclohexane (MCH) to *n*-C_{13} in crude oils from Angola, Norway and Nigeria. Samples A2, A3 and A13 were too pasty for injection into the GC-C-IRMS, hence, no data can be provided. Due to limited sample amounts of G12 no GC-C-IRMS measurements for hydrogen isotopic compositions were possible.

compound	n-C_{14}	n-C_{15}	n-C_{16}	n-C_{17}	Pr	n-C_{18}	Ph	n-C_{19}	n-C_{20}	n-C_{21}	n-C_{22}	n-C_{23}
sample												
A1	-122.2	-86.1	-82.2		-100.5	-74.2	-109.4	-80.9			-56.3	-30.4
A2												
A3												
A4	-96.2		-87.0	-72.3	-130.7	-71.8	-127.7	-73.0	-76.9	-70.6	-67.8	-65.6
A5	-135.8	-135.8	-127.5	-122.7	-167.2	-119.1	-169.2	-122.7	-118.1		-116.4	-116.5
A6	-131.9	-127.8	-124.4	-121.8	-162.4	-111.2	-162.2	-113.8	-109.7	-109.4	-106.2	-99.8
A7	-118.6	-116.6	-115.5	-98.5	-118.3	-100.3	-125.6	-102.0	-103.6	-99.2	-106.2	-104.6
A8	-128.5	-122.0	-119.8	-113.4	-122.6	-112.3	-124.3	-111.3	-111.2	-109.0	-108.2	-106.5
A9	-106.4	-101.5	-101.5	-29.0	-81.9	-37.6		-57.1	-46.7	-57.5	-49.9	-41.5
A10	-76.2	-75.8	-75.3	-71.2	-86.7			-48.6	-38.3	-45.1	-30.9	-28.5
A11	-110.1	-109.3	-112.0	-101.9	-126.8	-102.9	-134.4	-105.5	-93.5	-95.1	-95.0	-94.0
A12	-133.3	-134.5	-129.2	-125.5	-154.1	-128.1	-150.0	-131.4	-126.7	-127.0	-126.4	-125.9
A13												
A14	-109.7	-110.2	-106.5	-62.5	-105.3	-64.8	-111.4	-80.8				-72.7
A15	-115.3	-115.6	-96.7		-141.8	-93.4	-139.0	-93.0		-85.1	-78.4	-73.4
A16		-99.4	-55.6	-35.7	-88.9	-45.0	-79.7	-48.4	-46.2	-40.1	-45.0	-43.2
A17	-138.2	-140.3	-110.7		-139.2	-90.9	-144.2	-104.4	-98.5	-102.6	-95.2	-96.7

compound	n-C_{14}	n-C_{15}	n-C_{16}	n-C_{17}	Pr	n-C_{18}	Ph	n-C_{19}	n-C_{20}	n-C_{21}	n-C_{22}	n-C_{23}
sample												
G1	-74.9	-104.8	-65.8	-102.1	-82.1	-71.0	-69.3	-69.1		-73.6		
G2	-111.9	-135.0	-110.5	-133.2	-115.0	-69.2		-53.7	-42.1	-75.9	-50.0	-88.3
G3	-90.8	-120.0	-80.4	-118.3	-99.5	-75.4	-99.8	-90.0	-87.3	-66.9	-95.4	-73.8
G4	-79.1	-87.2	-91.5	-82.9	-107.5	-65.4	-111.0	-93.2	-82.6	-69.5	-58.1	-64.7
G5	-91.5	-110.6	-108.1	-79.3	-116.2	-86.0	-115.4	-102.3	-101.5	-69.4	-104.6	
G6	-103.7	-68.6	-104.3	-72.4	-112.5	-68.5	-112.2	-91.7	-63.8	-60.2	-52.0	-60.8
G7	-116.4	-114.8	-112.3	-90.7	-119.6	-86.6	-118.4	-83.9	-83.2	-79.9	-79.6	-79.9
G8	-114.1	-117.0	-104.0	-85.2	-127.6	-83.0	-123.9	-89.9	-86.9	-87.3	-86.2	-87.2
G9	-111.0	-109.4	-110.0	-109.9	-118.2	-110.4	-123.4	-111.1	-96.7	-98.9	-90.6	-94.5
G10	-119.1	-105.2	-112.8	-99.0	-123.8	-96.3	-119.5	-95.0	-96.0	-89.6	-87.1	-70.0
G11	-95.7	-92.7	-90.9	-86.5	-106.8	-89.3	-108.8	-89.4	-75.3	-74.6	-80.4	-78.4
G12												
G13	-115.4	-113.8	-114.7	-110.9	-123.7	-108.7	-124.9	-113.0	-112.1	-112.7	-110.9	-110.8

compound	n-C_{14}	n-C_{15}	n-C_{16}	n-C_{17}	Pr	n-C_{18}	Ph	n-C_{19}	n-C_{20}	n-C_{21}	n-C_{22}	n-C_{23}
sample												
N1	-112.1	-105.6	-110.3	-108.6	-130.6	-113.6	-144.9	-117.5	-115.1	-124.7	-120.3	-123.4
N2	0.0	0.0	0.0	0.0	0.0	0.0	0.0	0.0	0.0	0.0	0.0	0.0
N3	-115.2	-111.5	-102.1	-95.6	-108.3	-99.6	-124.6	-100.8	-107.5	-121.6	-109.5	-109.6
N4	-123.1	-125.1	-122.5	-122.5	-137.8	-92.3	-131.7	-103.0	-105.8	-97.8	-110.5	-100.6
N5	-118.5	-112.7	-107.1	-113.5	-129.0	-95.3	-143.9	-119.4	-104.3	-89.8	-117.9	-95.3
N6	-96.3	-102.9	-106.1	-101.1	-131.8	-104.1	-144.6	-106.2	-106.1	-110.6	-109.4	-107.3

Table X- 37: δD ratios [‰] for *n*-C_{14} to *n*-C_{23} in crude oils from Angola, Norway and Nigeria. Samples A2, A3 and A13 were too pasty for injection into the GC-C-IRMS, hence, no data can be provided. Due to limited sample amounts of G12 no GC-C-IRMS measurements for hydrogen isotopic compositions were possible.

compound	n-C_{24}	n-C_{25}	n-C_{26}	n-C_{27}	n-C_{28}	n-C_{29}	n-C_{30}
sample							
A1	-79.8						
A2							
A3							
A4	-67.9	-68.5	-68.8	-70.8	-67.1	-95.1	
A5	-116.9	-113.6	-109.1	-99.8	-115.7	-112.4	-117.2
A6	-101.1	-96.9	-95.1	-97.2	-100.7	-115.3	-109.0
A7	-106.1	-108.1	-102.3	-105.9	-107.0	-93.7	-89.7
A8	-106.8	-109.5	-104.1	-105.0	-98.2	-99.4	-90.0
A9		-50.0	-85.2	-53.9			
A10	-66.1	-47.2	-54.0				
A11	-96.7	-97.2	-95.1			-100.1	
A12	-126.6	-126.6	-125.5				
A13							
A14		-91.0					
A15	-79.4	-92.2					
A16	-51.1	-53.3					
A17	-94.2	-94.8	-95.1	-92.7	-90.3	-99.7	-115.8

compound	n-C_{24}	n-C_{25}	n-C_{26}	n-C_{27}	n-C_{28}	n-C_{29}	n-C_{30}
sample							
G1							
G2	-78.7		-85.6				
G3	-92.1	-102.0	-95.6	-105.8			
G4	-60.5		-71.3	-61.8	-97.6		
G5							
G6	-64.5		-64.9	-80.4	-116.9	-189.9	
G7	-91.2	-86.6	-68.5	-63.7	-73.8	-86.6	-89.2
G8	-88.7	-82.8	-74.0	-77.7	-96.6	-101.3	
G9	-84.8	-82.5	-80.7	-80.5	-81.2	-83.2	
G10	-73.6	-73.3	-73.8	-74.7	-80.3	-87.8	-88.5
G11	-76.6	-80.9	-75.2	-84.1	-87.7	-66.5	
G12							
G13	-106.5	-100.5	-104.5	-97.7	-101.2	-101.6	-58.4

compound	n-C_{24}	n-C_{25}	n-C_{26}	n-C_{27}	n-C_{28}	n-C_{29}	n-C_{30}
sample							
N1	-125.1	-123.7	-125.9	-127.5	-127.9	-118.5	-137.5
N2	0.0	0.0	0.0	0.0	0.0	0.0	0.0
N3	-114.3	-110.6	-110.5	-117.0	-118.3	-124.1	-122.6
N4	-114.1	-98.5	-116.5	-116.0	-134.3	0.0	0.0
N5	-115.2	-100.4	-112.4	-128.6	-119.7	-134.2	-160.7
N6	-112.6	-114.6	-112.7	-115.9	-124.0	-125.2	-140.0

Table X- 38: δD ratios [‰] for *n*-C_{24} to *n*-C_{30} in crude oils from Angola, Norway and Nigeria. Samples A2, A3 and A13 were too pasty for injection into the GC-C-IRMS, hence, no data can be provided. Due to limited sample amounts of G12 no GC-C-IRMS measurements for hydrogen isotopic compositions were possible.